Extrinsic and intrinsic factors governing bacterial biofilms

DISSERTATION
To fulfill the
Requirements for the Degree
Doctor of Philosophy (PhD)

Submitted to the Council of the Faculty of Biology and Pharmacy of the Friedrich Schiller University Jena

By
M.Sc. Eisha Mhatre
Born on 7th August, 1989 in Mumbai, India

Das Promotionsgesuch wurde eingereicht und bewilligt am:

Gutachter:
1) Dr. Ákos T. Kovács, Institute of Microbiology, Friedrich-Schiller-Universität, Jena, Germany
2) Prof. Stefan Schuster, Department of Bioinformatics, Friedrich-Schiller-Universität, Jena, Germany
3) Prof. Nicola Stanley-Wall, College of Life Sciences, University of Dundee, Scotland, UK

Das Promotionskolloquium wurde abgelegt am: 31st March, 2017

Table of Contents

Overview of Manuscripts

Overview of Manuscripts

This thesis is based on the following manuscripts.

Author abbreviations:
Eisha Mhatre (EM), Ramses Gallegos-Monterrosa (RGM), Theresa Hölscher (TH), Ákos T. Kovács (ATK), Oscar P. Kuipers (OPK), Agnieszka Troszok (AT), Stefanie Lindstaedt (SL), Anandaroopan Sundaram (AS), Benjamin Bartels (BB1), Mike Mühlstädt (MM), Jörg Bossert (JB), Gergely Maróti (GM), Balázs Bálint (BB2).

1. ***From environmental signals to regulators: modulation of biofilm development in Gram-positive bacteria***
   Authors: Eisha Mhatre, Ramses Gallegos-Monterrosa, and Ákos T. Kovács
   Published in: Journal of Basic Microbiology (2014) Volume-54, Pages- 616-32.
   doi: 10.1002/jobm.201400175
   Presented as: Part of Introduction
   Author Contribution

Conceived the paper	EM (40%), RGM (40%), ATK (20%)
Wrote the manuscript	EM (40%), RGM (40%), ATK (20%)

2. ***Specific Bacillus subtilis 168 variants do form biofilms on nutrient rich medium***
   Authors: Ramses Gallegos-Monterrosa, Eisha Mhatre, Ákos T. Kovács
   Accepted in: Microbiology (2016) doi: 10.1099/mic.0.000371
   Presented as: Chapter 1
   Author Contribution

Conceived the project	ATK (100%)
Designed the experiments	RGM (40%), EM (40%), ATK (70%)
Constructed the bacterial strains	RGM (70%), EM (30%)
Performed the experiments	RGM (60%), EM (40%)
Analyzed experimental data	RGM (60%), EM (30%), ATK (10%)
Wrote the manuscript	RGM (80%), EM (10%), ATK (10%)

3. *The impact of manganese on biofilm development of Bacillus subtilis*

Authors: Eisha Mhatre, Agnieszka Troszok, Ramses Gallegos-Monterrosa , Stefanie Lindstaedt, Theresa Hölscher , Oscar P. Kuipers, Ákos T. Kovács

Published in: Microbiology (2016) Volume-162, Pages- 1468-1478

doi: 10.1099/mic.0.000320

Presented as: Chapter 2

Author Contribution

Conceived the project	ATK (100%)
Designed the experiments	EM (30%), ATK (70%)
Constructed the bacterial strains	EM (70%), RGM (10%), SL (10%), TH (10%)
Performed the experiments	EM (70%), ATK (30%)
Analyzed experimental data	EM (60%), ATK (40%)
Contributed methodology	OPK (100%)
Wrote the manuscript	EM (80%), ATK (20%)

4. *Presence of calcium maintains rugose biofilm structure of Bacillus subtilis*

Authors: Eisha Mhatre, Anandaroopan Sundaram, Theresa Hölscher, Mike Mühlstädt, Jörg Bossert, Ákos T. Kovács

Under review: Journal of Bacteriology (2016) Manuscript number- JB00747-16

Presented as: Chapter 3

Author Contribution

Conceived the project	EM (50%), ATK (50%)
Designed the experiments	EM (60%), AS (20%), ATK (20%)
Constructed the bacterial strains	AS (80%), TH (20%)
Performed the experiments	EM (20%), AS (60%), TH (20%)
Analyzed experimental data	EM (40%), AS (40%), TH (10%), ATK (10%)
Assisted surface tension measurements	MM (80%), JB (20%)
Wrote the manuscript	EM (80%), ATK (20%)

5. *Spatially structured environment facilitates the emergence of yield strategists*

Authors: Eisha Mhatre, Benjamin Bartels, Gergely Maróti, Balázs Bálint, Ákos T. Kovács

To be submitted in: Nature/Nature Communications (2016)

Presented as: Chapter 4

Author Contribution

Conceived the project	ATK (100%)
Designed the experiments	EM (50%), BB1 (20%), ATK (30%)
Constructed the bacterial strains	EM (100%)
Performed the experiments	EM (80%), BB1 (20%)
Analyzed experimental data	EM (80%), ATK (20%)
Re-sequenced genomes	GM (50%), BB2 (50%)
Wrote the manuscript	EM (50%), ATK (50%)

6. *Taking the road less travelled: emergence of rare strategies and metabolic interactions in spatially structured environments*

Authors: Eisha Mhatre, Ákos T. Kovács

To be submitted in: NPJ Biofilms and Microbiomes (2016)

Presented as: part of Introduction and General Discussion

Author Contribution

Conceived the project	EM (50%), ATK (50%)
Wrote the manuscript	EM (80%), ATK (20%)

Glossary

1. ***Adaptive radiation***- it is an aftermath of a change in the environment (eg: availability of a new resource) where the population diversifies rapidly from the ancestral species, into the multitudes of new forms that can adapt to a divergent environment.
2. ***Antagonistic pleiotrophy*** – It is a state when one gene controls for more than one trait where at least one of these traits is advantageous and contributes to the organism's fitness and the other is detrimental to the fitness.
3. ***Bistability***- it is the presence of two stable phenotypes within a genetically clonal population, under homogenous condition.
4. ***Black Queen Hypothesis***- It is the theory stating that some microorganisms lose certain costly essential functions and relies on another microbes or the environment to survive efficiently. This theory explains evolution of dependencies in the natural environments and its concept is based on the black Queen card in the game of Hearts, which the players often look out to lose or get rid of.
5. ***Competitive exclusion***- A principle that states that two strains or species competing for the same resource or niche can never coexist and one is always favored, thus leading to the extinction or exclusion of the other species or strain.
6. ***Diazotrophs***- Bacteria or archea that are able to fix the atmospheric nitrogen to a more usable form such as ammonia.
7. ***Ecotypes***- Genetically distinct variety, population or race within species, which is adapted to a particular environmental condition or can be isolated from the same geographical area. *Also see Pherotypes.*
8. ***Efficient metabolism***- A metabolism that coverts the substrate proficiently into the products and metabolic energy without accumulation of energy spilling products such as acids. The substrate energy is converted into biomass and usable energy in form of ATP. Contrary to this, is the inefficient metabolism that is rapid metabolism of the substrate, leading to the accumulation of overflowing metabolites at the expense of biomass. *Also see Overflow metabolism.*
9. ***Fitness landscapes***- a visual, ecological representation of the relationship between the genotype and its reproductive success (fitness).
10. ***Genetic drift***- It is an event in a small population when the occurrence of variant forms of a gene, called alleles, increases or decreases by a chance event over a time resulting in a genetically distinct population compared to the original.

11. ***Metabolic precursors***- a metabolite that participates in a reaction to produce a product. (Eg: pyruvate, acetyl-CoA, etc.)
12. ***Metabolic specialization***- Emerging subpopulation of cells that evolve and adapt specific capabilities to metabolize the nutrients in the surroundings. *Also see Niche specialization.*
13. ***Morphs***- A morphological or functional difference between organisms of distinct populations in a species.
14. ***Mutation event***- a process induced by mutagens or allelic recombinations where there is a change in the nucleotide sequence of the genome of an organism.
15. ***Niche differentiation***- the process by which competing species use the environment differently in a way that helps them to coexist.
16. ***Niche specialization***- Evolution of distinct individuals in the population by natural selection, enabling the adaptation to a particular environmental condition in time or space.
17. ***Niche***- A hyper-volume in the multidimensional space of ecological variables, within which a species can maintain a viable population.
18. ***Peripathetic***- The nomadic lifestyle where the population is never restricted to a particular space.
19. ***Persistence***- a phenotype caused due to an epigenetic trait where the subpopulation, particularly microbial, are viable but in metabolically dormant form leading to a halt in its cell division.
20. ***Phagocytosis***- A process where a cell engulfs a solid particle and forms internal vesicle or a phagosome.
21. ***Phenotypes***- *sees Morphs.*
22. ***Quorum***- The threshold requires to precedent an important event or a stimulus.
23. ***Scavengers***-The population that feeds on the unwanted, waste products or the cell debris.
24. ***Selective coefficient***- the representation of relative advantage or disadvantage of a specific trait with respect to survival and reproductive success.
25. ***Spatial structure***- A set of constraints or patterns that are constant in space but can modify in time. On hindsight, a structure where all its components are arranged locally and hence not uniformly distributed.
26. ***Synthetic communities***- A defined population system, which is less in complexity as compared to the natural population.
27. ***Catabolic repressor***- a mechanism where in presence of a preferred substrate the pathways required to catabolize other substrates is repressed. When the preferred nutrient source is exhausted, the other pathways are depressed and thus organisms can shift their growth on other nutrients.

28. ***Batch culture***- a setup where the limited nutrients are provided to grow the microbial culture. Once the nutrients are utilized the cell density declines.
29. ***Chemostat***- A system where continues supply of resource is available at limiting concentration promoting a continuous growing culture. The rate of nutrient supply can be monitored and defines the rate of fermentation product formation.
30. ***Overflow metabolism***-The incomplete oxidation of the growth substrate instead of using an energetically efficient pathway, leading to the large pool of intermediates that are excreted in the environment causing energy spillage.
31. ***Copiotrophs***- Organisms that grow in organic, carbon rich environments. They are contrary to oligotrophs that usually grow in nutrient limiting conditions and have low rates of metabolism.
32. ***TCA cycle***- It is tri-carboxylic metabolic cell cycle in all aerobic organisms that converts the tri-carbonated, glycolytic products- pyruvate and acetyl-CoA through series of reactions to generate energy and intermediates that play role in biosynthesis of cellular products such as proteins, sugars, nucleotides and fatty acids.
33. ***Pherotypes***-The genotypic ally differentiated variants of a species, which have limited gene flow (mediated by horizontal gene transfer in bacteria) between them.
34. ***Paracrine signaling***- Process where cells produce a signaling molecule or a paracrine factor that induce the cellular processes and differentiation in the neighboring cells.
35. ***Sporulation***- The process involved in bacteria involving the formation of a dormant spore, containing the genomic DNA and resists the starvation and desiccation for long periods in unfavorable environment.

Summary

Bacterial biofilm lifestyle is unique and complex as compared to its free-living state. Due to the abundance of biofilm associations in natural communities, recent studies have focused on various methods to study these multicellular communities- from the laboratory suited biofilm set-ups such as colonies or the air-liquid surface microcosm called pellicles, to the advanced imaging and microscopic techniques to observe the interactions at cellular level. There are specific model microrganisms that have been extensively studied for their biofilm strategies and community behavior. To illustrate few, the host associated infections causing *Staphylococcus* and *Salmonella* spps, marine symbiotic associations and other interactions exhibiting bacteria belonging to the genus Vibrio or various species from the genera, Bacillus and Pseudomonads that dominate the soil bacterial multicellular communities. The observations obtained through these studies, are applied in various ecological, medical and industrial settings. This dissertation focuses on biofilm formation in *Bacillus subtilis* with respect to the environmental and the intrinsic metabolic factors that influence the cellular behavior in communities.

Expression of genes responsible for biofilm formation and media components influence biofilm morphology in colonies and pellicles.

The first study described in this Thesis comprehends the differences between the laboratory and the undomesticated strain with respect to their biofilm forming abilities. Although, the biofilm formation is largely dependent on the genes conferring the matrix production, the level of expression did not correlate with the complexities of biofilm structures. The variants of laboratory strain themselves differ significantly in their biofilm structures, which is due to the salient genomic differences in the genes governing the formation of biofilm matrix. Moreover, the presence of glucose or glycerol in the medium had huge effect on the colony structures. These observations demonstrate the need to consider the strain or sub-strain level differences while describing the factors influencing the biofilm formation.

Metal ions impact the colony structures and several processes in biofilm colonies.

The metal ions are the macro and microelements that influence various cellular mechanisms in bacteria. In the study following the influence of media components on biofilms, we studied the effect of Mn^{2+} on the rugose colony structures. Role of Mn^{2} in sporulation also affects the white chalky patterns on the colonies, making them architecturally distinct. Moreover, the study highlights the processes that are influenced by

the presence of Mn^{2+} in colony biofilms. ***Calcium ions affect the colony escape mechanisms.***

Cells at the periphery of the mature colony spread across in order to venture the new nutrient niches. This phenomenon requires the matrix and secreted components such as surfactin, and resembles the flagellar independent collective behavior called as sliding in bacteria. In a mature colony, this behavior can be described as an escape mechanism from nutrient depletion. It was observed that the presence of Ca^{2+} in the medium restrains this escaping by sequestering the secreted surfactin molecules. In the absence of surfactin these escaping mechanisms are not detected. Thus, this study suggests the influence of media components in maintaining the colony structure by restricting the escape and therefore, implies the possible activation of other survival strategies to counter starvation.

Efficient metabolic strategies emerge in biofilms.

Lastly, this work also features the study involving the tradeoff between maximization of growth rate versus yield in spatially structured communities such as biofilms. The selection and emergence of the yield strategists under spatial structured conditions was demonstrated in *B. subtilis* using an experimental evolution approach. The evolved stable yield strategists were competed with the rate strategists in structured and unstructured environments. While the unstructured environment competitively excluded the yield strategists, the structured environments seemed to favor their proliferation. The competition outcomes in biofilms imply the coexistence of both strategies. This emphasizes on the cooperative nature of spatial structures. The study also sketches the pathways and metabolic profile underlining the emergence of the yield strategists in *B. subtilis* population. Overall, this study aims to describe the interaction of metabolic strategies that influence biofilms.

In summary, this thesis outlines the key factors influencing bacterial multicellular behavior. using the combination of general microbiology, experimental evolution, microscopic and imaging techniques, It describes various biofilm setups such as the sessile colony structures, naturally formed root attachments, collective colony expansion and submerged surface adherence used in studying *B. subtilis* biofilms. Furthermore, the findings of this study largely contribute to the current understanding of the complexities and the topographies of bacterial biofilms.

Zusammenfassung

Die Lebensweise in bakteriellen Biofilmen ist einzigartig und komplexer als die planktonische Form. Wegen der hohen Anzahl an Biofilmen in natürlich vorkommenden Gemeinschaften konzentrieren sich aktuelle Studien auf verschiedene Methoden, um diese multizellulären Aggregate zu untersuchen. Dies reicht von im Labor untersuchten Biofilm-Formen wie Kolonie Biofilmen und Luft-Medium Mikrokosmen (sogenannte *Pellicles*) bis hin zu forschrittlichen mikroskopischen Methoden zur Beobachtung von Einzelzell-Interaktionen. Es gibt wenige Modell Mikroorganismen, deren Biofilm Bildung und Verhalten im Biofilm umfassend analysiert wurde. *Staphylococcus* und *Salmonella sp*. bilden infektiöse Biofilme im Menschen, während in Bakterien des Genus *Vibrio* die Bildung von marinen Biofilmen und ebenfalls Wirt-assoziierten Biofilmen untersucht wird. Weiterhin dominieren Bakterien der Genera *Bacillus* und *Pseudomonas* bakterielle Gemeinschaften im Boden. Die Ergebnisse dieser Biofilm Studien werden in verschiedenen ökologischen, medizinischen und industriellen Bereichen genutzt. Diese Dissertation konzentriert sich auf Biofilme von *Bacillus subtilis* mit Fokus auf die Umwelt betreffende und intrinsische metabolische Faktoren, welche das Verhalten der Zellen beeinflussen.

Komponenten des Mediums und Expressionslevel von Genen, die für die Biofilm Bildung verantwortlich sind, beeinflussen die Biofilm Morphologie in Kolonien und Pellicles.

Die erste Studie dieser Dissertation erfasst die Unterschiede zwischen domestizierten Laborstämmen und einem nicht domestizierten Stamm mit Bezug auf die Struktur ihrer Biofilme. Die Abfolge der Reaktionen, die die Expression der Biofilm Gene und Proteine beeinflussen, wies keine direkte Korrelation zu der Struktur des Biofilms auf. Jedoch war die Strukturierung der Biofilme mit geringeren Expressionsleveln ausgeprägter. Die Laborstämme selbst unterschieden sich signifikant in den komplexen Strukturen ihrer Biofilme, was durch Abweichungen in den Genen, die die Biofilm Bildung steuern, verursacht wird. Außerdem hatte die Präsenz von Glucose oder Glycerin im Medium einen starken Effect auf die Ausprägung der Strukturen des Kolonie Biofilms. Dies demonstriert die Notwendigkeit, Unterschiede zwischen den Stämmen bei der Analyse von Biofilmen zu berücksichtigen.

Metallionen haben Auswirkungen auf Strukturen und Prozesse in Kolonie Biofilmen.

Metallionen sind die Makro- und Mikroelemente, die verschiedene zelluläre Prozesse in Bakterien beeinflussen. In dieser Arbeit wurde der Effekt von Komponenten des Mediums, insbesondere Mn^{2+}, auf die komplexe Strukturierung des Biofilms untersucht. Durch den

Einfluss von Mn^{2+} auf die Sporulation werden auch die weißen Oberflächenmuster der Kolonie verändert, wodurch eine ausgeprägte Architektur entsteht. Darüber hinaus betont diese Arbeit das Profil des Transkriptoms der durch Mn^{2+} beeinflussten Prozesse in Kolonie Biofilmen.

Calciumionen beeinflussen Fluchtmechanismen aus der Kolonie.

Zellen in der Peripherie ausgereifter Kolonien verbreiten sich, um Zugang zu neuen Nährstoffen zu erhalten. Dies ähnelt der kollektiven, Flagellum-unabhängigen Bewegungsform *Sliding* und es werden Matrix- und sekretierte Komponenten wie Surfactin benötigt. In ausgereiften Kolonien kann dieses Verhalten als Fluchtmechanismus aufgrund von Nährstoffarmut beschrieben werden. Es wurde beobachtet, dass die Präsenz von Ca^{2+} im Medium diese Flucht verhindert, indem die sekretierten Surfactin Moleküle blockiert werden. In Abwesenheit von Surfactin tritt diese Flucht nicht auf. Demzufolge deutet diese Studie auf einen Einfluss der Komponenten des Mediums in der Aufrechterhaltung der Kolonie Struktur durch Verhinderung der Flucht hin. Dies impliziert eine mögliche Aktivierung von alternativen Überlebensstrategien bei Nährstoffmangel.

In Biofilmen entwickeln sich effiziente metabolische Strategien.

Zuletzt behandelt diese Arbeit den Ausgleich zwischen der Maximierung der Wachstumsrate und dem Ertrag in räumlich strukturierten Gemeinschaften wie Biofilmen. Die Selektion und das Auftreten von Ertragsstrategen unter räumlich strukturierten Bedingungen wurde durch experimentelle Evolution in *Bacillus subtilis* demonstriert. Die evolvierten und stabilen Ertragsstrategen wurden in Konkurrenzexperimenten in strukturierter und unstrukturierter Umgebung mit Wachstumsstrategen verglichen. Während die Ertragsstrategen in der unstrukturierten Umgebung im Nachteil waren, schien die strukturierte Umgebung ihre Proliferation zu selektieren. Die Ergebnisse der Konkurrenzexperimente lassen eine Koexistenz der beiden Strategien vermuten. Dies hebt die Kooperation unterstützende Natur von räumlichen Strukturen hervor. Diese Studie veranschaulicht außerdem die Signalwege und metabolischen Profile, welche dem Auftreten von Ertragsstrategen in *B. subtilis* Populationen zugrunde liegen. Insgesamt hat diese Arbeit zum Ziel, die Interaktionen von metabolischen Strategien zu beschreiben, die die Biofilm Bildung beeinflussen.

Diese Dissertation behandelt Schlüsselfaktoren, welche bakterielles multizelluläres Verhalten beeinflussen. Dafür wird eine Methoden Kombination aus allgemeiner Mikrobiologie, experimenteller Evolution, mikroskopischen und Bildgebungsverfahren verwendet. Es werden verschiedene Methoden zum Wachstum von *B. subtilis* Biofilm Formen beschrieben, wie sessile Kolonie Strukturen, natürlich vorkommende Anheftung an Wurzeln, kollektive Kolonie Expansion und submerse Anheftung an Oberflächen. Weiterhin tragen die Ergebnisse dieser Arbeit zum Verständnis der Komplexität und Topographie von bakteriellen Biofilmen bei.

Introduction

Introduction

[This chapter is partly published in or submitted to:

i. Mhatre E, Gallegos Monterrosa R, Kovács ÁT (2014) From environmental signals to regulators: modulation of biofilm development in Gram-positive bacteria*. (J. Basic Microbiol.)* 54(7): 616-632.

ii. Mhatre E, Kovács AT, Taking the road less travelled: emergence of rare strategies and metabolic interactions in spatially structured environments*. (To be submitted to NPJ Biofilms and Microbiomes)*]

Life on Earth is very challenging. Species adapt and evolve continuously in order to survive in the dynamic environment. Microorganisms offer excellent model systems to understand the adaptation and evolution of life in the living world. Due to their small genome sizes and rapid generation times, they become suitable to grow and study in laboratory settings. Moreover, their ability to grow or remain viable in extreme and nearly all environments makes them a fascinating tool to understand the survival strategies in eco-systems.

Earlier known as solitary beings, unicellular bacteria are now recognized to preferentially live as multicellular communities in their natural habitats. In these communities, cells secrete various molecules that form protective matrix, quorum signaling molecules, virulence factors, metabolic precursors and cooperative mechanisms[1]. The complex interactions that thus prevail make the communities spatially structured. Such bacterial communities are called as biofilms[2].

In recent years several studies have been published that aim to understand and describe the various signals and developmental pathways that drive the formation of bacterial biofilms. Mostly, different environmental signals and their threshold concentrations regulate and trigger biofilm formation leading to the activation of specific signaling cascades[3].

1. Features of bacterial biofilms

A great body of study has been dedicated to the biofilm mode of bacterial lifestyle[1,4-7]. Mainly due to their hazardous nature in medical and industrial settings, effective understanding of mechanisms that govern biofilm formation in bacteria and approaches that effectively help to disturb them are necessary[8,9]. Matrix-embedded bacterial cells are not only well protected against stress conditions, but the structure also effectively aids their survival in nutrient scarce conditions by activating complex pathways and

differentiation processes. The chronic infection of cystic fibrosis causing *Psuedomonas aeruginosa*, produces alginate based mucoid, exopolymeric substance around it that prevents its phagocytosis and makes it resistant to antibiotics[10]. Transcriptional regulator CodY in food contaminant, *Bacillus cereus* induces secretion of proteases and up regulates amino acid metabolism, which assists survival in starvation conditions, bacterial persistence and production of toxins in range of environments from human body, food sources to soil[11]. Due to their prominence in nature, it is important to understand the interactions that flourish in microbial biofilms.

1.1 Cooperation in multicellular communities

Bacterial secretions are often diffusible and available for the neighboring cells to utilize[12,13]. Due to the availability of the products in the environment, similar to the development of amino acid auxotrophies, sub population of cells trade-off their synthesis (theory described as the Black Queen Hypothesis)[14]. This facilitates numerous cooperative strategies and division of labor in biofilms[15]. Filamentous cyanobacteria differentiate from photosynthetic cells into diazotrophic heterocyst to overcome the dilemma that the N_2 fixing enzyme, nitrogenase is inactivated in the presence of O_2. The vegetative cells share the products of carbon metabolism and receive nitrogen products from heterocysts. Cells also communicate to exhibit the gliding motility in this blue green algae or swarming and aggregation in Myxobacteria displaying the multicellular lifestyles in microbes[15]. The advantages of such cooperative strategies are abundant- (1) swarming and sliding mechanisms in bacteria ease the access to the resources and niches, (2) being amidst the resistant population offers collective defenses against antimicrobial agents, (3) increases the population survival by cell differentiation into diverse phenotypes such as dormant cells or the metabolic specialists[16].

1.2 Quorum sensing and cellular signaling

Complex, density-dependent cell-to-cell signaling is involved where the signaling molecules, after reaching the so-called 'quorum', mediate the bacterial behavior in biofilms. These quorum signals are receptor specific, accumulated in high cell density and activate adaptive responses in the population[17]. Most quorum signaling molecules belong to the class of homoserine lactone derivatives, but they could also be other toxins and antimicrobial compounds that execute the signaling- group of quinolones that modulate Las and Rhl quorum sensing circuits in *P. aeruginosa,* extracellular death factors secreted by *E. coli* and *Bacillus* species that also initiate the interspecies cell death[18,19]. The production of luminescence in *Vibrio fischeri*, pyoverdine synthesis in *P. aeruginosa,* oligopeptides driving the competence in *Streptococcus pneumoniae* and *Bacillus subtilis* are some examples of quorum sensing mediated regulatory behaviors in bacteria[20-23].

Often there is a cost involved in production of these autoinducers and hence, non-producers or the defectors arise in the population, exploiting the benefits of freely shared goods and contributing nothing in return. These defectors have growth advantages, however, microbial biofilm communities have numerous mechanisms to keep the proliferation of non-producers in check[24-27]. Additionally, being a spatial structure, diffusion and genetic mixing is limited, thus, keeping the signaling molecules locally[28]. Besides, the pathways involved in production of shared products also play a role in production of antimicrobials keeping the sensitive competitors in control[29].

1.3 Bacterial life in spatially structured environment

In biofilms, cells have unique features than their planktonic stages. They are mostly attached to a surface and hence, due to spatial and nutritional restraints, undergo slow but efficient metabolism using available resources, like chitin in marine environments[30]. Planktonic stages mostly feature well-mixed or unstructured environments, allowing uniform resource distribution where microbial cells interact equally with each other resulting in steep, rugged fitness landscapes between the phenotypes[31]. In contrast, there are vast nutrient and signal gradients in structured environments and hence, at every spatial distances communities shape differently[32]. The resources are scarce and more privatized that enhance niche specialization, a process in which the species become well adapted to the conditions in the environment they thrive in and specialize in metabolism dependent on resource availability[33].

When resources are depleted, certain cells of the microbial community differentiate into scavengers and other phenotypes that can metabolize the waste products and metabolic intermediates secreted by the primary consumers. Spatially organized environments are therefore, models to study numerous microbial local interactions such as cooperation and competition as well as evolutionary processes such as adaptive radiation, a process in which the lineages diversify rapidly from the ancestral species when there is sudden change in environment[34,35]. In general, structured niches are considered to maintain the ecological balance by minimizing competition at population level and thus minimizing the steepness of their fitness landscapes among the diverse phenotypes[36]. The complexity of interactions in biofilm communities hinders our systematic understanding; therefore, the inspection of synthetic communities combined with mathematical models provides a simplified approach to reveal the importance of certain mechanisms in complex environments[37].

1.4 Metabolic strategies in spatially structured environments

Microbes evolve numerous strategies in order to adapt and maintain their growth in dynamic environments. Most of these mechanisms result in trade-offs between different

metabolic and structural functions, or in antagonistic pleiotrophy- when one gene confers two traits, one that is advantageous and other that leads to the fitness loss[38,39]. Growth strategies such as efficient and inefficient metabolism are the most essential tradeoffs that organisms undergo in their efforts for the optimal survival.

When the resources are abundant, cells in the population opt to utilize them rapidly, concurrently increasing their growth rate, just like copiotrophs (cells found in environments which are rich in nutrients)[40]. However, fast growth is accompanied with an inefficient metabolism as cells synthesize enzymes and activate pathways that are less costly, but maintain the prompt accession[13,41].

The Crabtree effect, where cells of *Saccharomyces cerevisiae* and some bacteria opt for fermentative metabolism, producing ethanol and acids rather than producing biomass through tri-carboxylic acid cycle is an important phenomena demonstrating the inefficient use[42]. Contrary, the efficient metabolism involves the use of resources optimally by producing maximum yield in terms of biomass and energy per substrate utilized. This involves preparing the cellular metabolism for energy efficient pathways at the cost of growth rate[43]. Thus, due to less fermentation waste products the population gets to scale up to a higher yield. Many studies have analogized these metabolic tradeoffs as r/k selection theory for macro ecology[40].

Most experimental conditions in the laboratory, including batch cultures and chemostats, favor microbes with maximized growth rate[44,45]. Therefore, mutants exhibiting efficient metabolism are mostly rare and easily outcompeted by the rate strategists (RS). However, even under laboratory conditions, there is a plethora of studies that examined experimental conditions favoring efficient metabolizers[46,47]. Using computational simulations on *S. cerevisiae* as a model system, Pfeiffer and colleagues (2001) demonstrated that high diffusion and resource influx select for fermenters (these convert the glycolytic metabolic end product- pyruvate to acids or alcohol, yielding less cellular energy in form of ATP) and outcompete the respirators (these are the efficient metabolizers channeling the pyruvate through the costly TCA cycle that involves complete conversion of carbon sources to biomass and CO_2)[48]. When the parameters like cell diffusion and resource influx decrease, just as in spatial structured environment; the outcome of the competition preferred respirators.

Roller and Schmidt (2015) suggested the importance of two additional factors that enable efficient metabolizers to emerge and maintain in structured environments[40]. First being, the resource availability, which is constrained and thus cells need to get maximum energy yield from the resources they utilize.

The other factor is the resource quality. Various organic compounds can substitute one another to suffice the cells' carbon and nitrogen requirements. For carbon metabolism alone, there are several pathways that utilize distinct carbon sources from sugars to

organic compounds resulting in different amounts of energy yield. However, the extent at which a C-resource is utilized efficiently depends directly on its heat of combustion.

Another rare metabolic feature that can be particularly observed in structured environments is the coexistence of generalists and specialists[49,50]. Generalists can grow on a large variety of substrates, while specialists are those that specialize to use a particular substrate. Their coexistence is possible in spatially structured environment due to complexity in substrate choices as well as selective pressure to minimize the competition. The following experiment with mixed culture of two genetically modified *E. coli* populations, one generalists, that can utilize lactose and maltose in the environment, and another specialists that can grow solely on maltose, demonstrates this coexistence[44]. Maltose here is a competitive substrate that can influence the paradigm of competition outcome. In continuous culture, when the environment becomes patchy in space, the generalist population undergoes a mutation making cells constitutive lactose utilizers, even at limiting concentrations of the sugar. Such a shift in the generalist population to utilize lactose resolves the competition in consuming maltose and enables the two groups to coexist.

Spatial segregation that limits competition among the lineages can be sufficient to enable the emergence of specialists or efficient metabolizers in the population[51-54]. In an attempt to select for rare growth phenotypes such as yield strategists, Bachmann and co-workers (2013) developed a unique emulsion-based droplet system that compartmentalizes *Lactococcus lactis* cells (Figure 1). Droplets mimicked the spatially structured system that abolished the competition by privatizing the resources within each emulsion droplet. While most common serial transfers of well-mixed cultures in microbial experimental evolution studies favor RS, increased cell division rates also increase the cellular damage and later have a direct effect on fitness costs[55,56]. This additionally promotes the increase of yield strategists (YS) in the droplet based selection regime.

In addition to experimental approaches, individual based modeling also predicted the emergence and abundance of yield strategists in the spatially structured environment of biofilms[54]. In the simulations of J.U. Kreft, when rate and yield strategist individuals are competed, rate strategists are favored initially, however, a steady increase of yield strategists' abundance was postulated in the population. The parameters that influence their emergence were the starting ratios, the extent of mixing (clusters versus mixed) and the maturation (i.e. duration) of the biofilm. While the spatial structure was suggested to select for rare growth strategies, the suggestion that these cell types are present in low densities and maintained across populations is a puzzling case of Prisoner's dilemma from the context of game theory[45,57]. Other mathematical models have further supported the existence of rare metabolic strategies in microbial populations and have gathered similar assumptions on the selection conditions that favor the proliferation of yield strategists[58-62].

Few key aspects of biofilms and the influence of environment on them are described in this study using the model organism, *B. subtilis.*

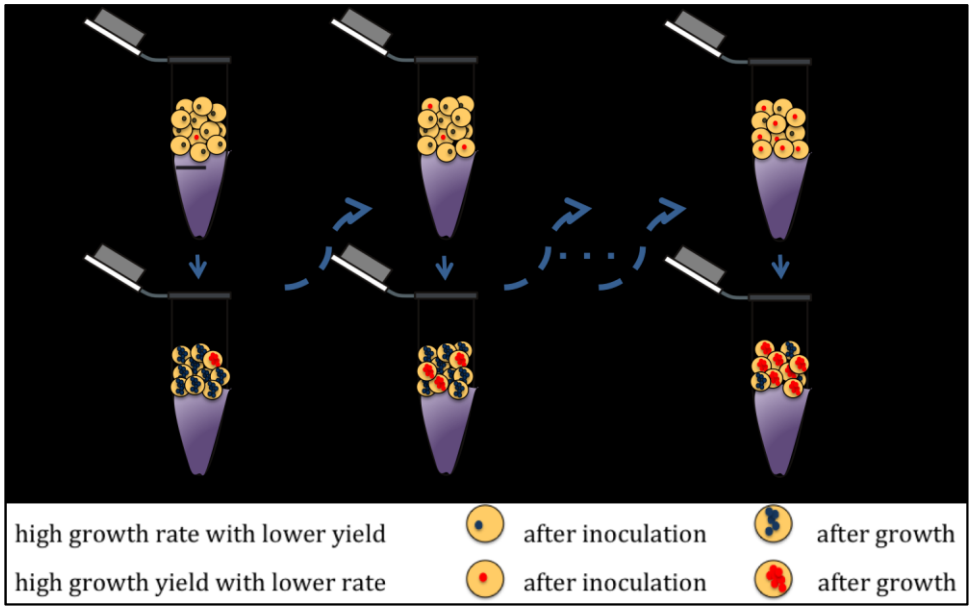

Figure 1. Schematic of droplet- based experimental evolution propagation. ***E***ach phenotype in an isogenic culture is confined in an emulsion droplet, minimizing the competition during growth and thus letting the subpopulation of YS to slowly increase in number. Figure redrawn from Bachmann *et al*, 2013[52].

2. Bacillus subtilis biofilms

B. subtilis is a Gram-positive bacteria well studied for its phenotypic heterogeneity, that enables the existence of various differentiated cell types and the subpopulation level of gene expressions[16].

B. subtilis, in the stationary phase, changes from peripatetic lifestyle to a sessile mode of growth. Like in other biotic systems, biofilm forming bacteria sense the environmental stimuli and modify its lifestyle to survive in a dynamic niche[63]. During development of *B. subtilis* biofilms, a subpopulation of isogenic community expresses certain genes related to biofilm formation. The *epsA–O*, a 15 gene-containing operon is important for the production of exopolysaccharide (EPS), while the *tasA* and *bslA* genes code for the protein components of biofilm: the fibrous scaffold playing role in attachment and the surface hydrophobic protein component, respectively, that all together protect the population from environmental stresses[64-69]. Biofilm formation capabilities of the versatile *B. subtilis* strains depend on both their genetic setup (loss of certain genes coding for the proteins during laboratory domestication) and the environmental make up (described further in this Thesis)[70,71].

2.1 Laboratory biofilm models

Under laboratory conditions, the biofilm models in *B. subtilis* include pellicle formation on the air–liquid surface, architecturally complex colonies on the agar surface, as well as submerged surface attached biofilms. Robust biofilm formation of *B. subtilis* is promoted on various defined minimal or complex media, containing components that elicit the transcription of genes that modulate matrix production and development. Common medium constituents include K^+, Mg^{2+}, Fe^{2+}, Mn^{2+} ions, carbon source in form of glucose and/or glycerol[72,73]. Though biofilm formation of *B. subtilis* is a natural process[74], numerous environmental factors, and extracellular signals are known to affect these complex changes in *B. subtilis*. Most of these environmental triggers allow the expression of genes important for matrix production through complex networking and signaling pathways. Several global transcription regulators have been described to be involved in the processes that lead to biofilm formation, including Spo0A, SinR, AbrB, SlrR, DegU, ComA, and Rok[75].

Although, extensively studied for its biofilm formation, the domesticated or laboratory adapted strains of *B. subtilis* show differences in the expression of genes and their biofilm forming abilities[63,76]. This is further highlighted in detail in the Thesis Chapter 1. In the study, few domesticated strains used in multiple laboratories are compared with the undomesticated *B. subtilis* NCIB 3610 for their biofilm formation on defined and complex media as well as in natural niches where bacilli colonize the roots.

3. Extrinsic factors playing role in biofilm formation of B. subtilis

The previous transcriptomic study reported that over 500 genes were differentially expressed at one or more time points as cells transitioned to a biofilm state[63]. The signal that appeared to affect gene expression during submerged biofilm formation is glucose depletion in the laboratory strains. Low concentration of glucose is required to promote submerged biofilm formation; a high amount of glucose inhibits biofilm formation via CcpA, the common catabolite repressor.

The threshold level of Spo0A~P required for biofilm formation is lower than for sporulation, and high level of Spo0A~P has rather inhibitory effects on the expression of biofilm genes. However, like for sporulation, the cytoplasmic and membrane-bound kinases-facilitated phosphorylation of Spo0A is required for biofilm formation. The diverse roles of the different *B. subtilis* kinases and the biofilm related triggering molecules are discussed below in details.

3.1 Role of Kin kinases in *B. subtilis* biofilm development

Phosphorylated Spo0A controls the transcription of many genes next to biofilm related genes, including sporulation, competence, and cannibalism toxin and immunity genes. The

level of phosphorylated Spo0A is controlled by the action of membrane bound histidine sensor kinases (KinA, B, C, D, and E). KinA is the most actively studied kinase due to its major role in sporulation. While the active kinase phosphorylates Spo0F response regulator, Spo0B phosphotransferase transfers the phosphoryl group from Spo0F to Spo0A. In absence of KinA and KinB kinases, KinC and KinD also phosphorylate Spo0A via Spo0F to the levels sufficient to activate biofilm genes but not sporulation[77]. Each kinase needs a different and specific concentration of the environmental cues to phosphorylate Spo0A and hence, induce matrix-forming genes (Table 1 and Figure 2). Recent studies showed that impaired respiration or oxidative phosphorylation stimulate wrinkling and matrix gene expression via KinA and KinB[78].

3.2 The paracrine-signaling network

While studying the association between *Streptomyces coelicolor* and *B. subtilis,* it was discovered that the production of surfactin by *B. subtilis* itself is required for the development of the aerial structures in the colony and that the mutant in surfactin production (*srfA*) is unable to form such aerial structures and forms thin, fragile pellicles[72,79]. Later studies on various compounds showed that surfactin, similar to many polyketides like nystatin, does not only reverse the phenotype in *srfA* mutant but also induces biofilm formation when supplemented in LB medium, a medium not regarded as optimum for biofilm study[80,81]. Nystatin and other structurally and functionally similar polyketides cause cation leakage by producing pores in the cell membrane. This leakage triggers biofilm formation signaling through the KinC kinase. Constructing altered *kinC* alleles lacking various domains in KinC, a PAS-PAC sensor domain was found to be important for KinC mediated induction of biofilm genes[80].

Along with nystatin, many other compounds like amphotericin, gramicidin, valinomycin and others found in soil that are mainly produced by soil dwelling bacteria trigger biofilm formation through a similar mechanism[80-82].

KinC localizes in the punctate microdomains together with the flotillin like proteins, FloT and FloA. Biofilm formation is reduced in the *floA* and *floT* mutants and this is also related to the delocalization of the FtsH protease[83]. As described above, induction of biofilm formation and sporulation requires given levels of Spo0A-P. FtsH influences the levels of Spo0A-P by degrading the proteins RapA, RapB, RapE and Spo0E that modulate the Spo0A-phosphorelay[83-85].

More evidence of how biofilm provides protection against toxic compounds is provided in a study where chlorine dioxide was found to trigger biofilm pellicle formation. ClO_2 is regarded as effective biocide agent but at sub lethal concentrations activates KinC by acting on membrane resulting in membrane potential changes[86].

3.3 Integrating environmental signals: from glycerol to plant polysaccharides

In natural environments, bacterial species are constantly evolving different mechanisms due to the interactions between different species and genera. When associated with *B. subtilis* stimulate distant species also biofilm formation[87]. During association of *B. subtilis* with *Arabidopsis thaliana* roots, bacteria require the production of EPS and other matrix components for the colonization of roots. The expression of biofilm genes under these conditions is triggered by contact with the roots. To investigate further what initiates biofilm formation during *A. thaliana* and *B. subtilis* interactions, plant extracts were purified. Plant cell wall polysaccharides such as xylan, pectin, and arabinogalactan trigger biofilm formation via KinC and KinD in cells grown on otherwise non-biofilm inducing medium[88]. Also, as galactose constitutes an essential part of EPS, many plant polysaccharides are used as a carbon source and its galactose residues are incorporated into matrix via GalE by converting UDP-glucose to UDP-galactose[89]. This study brings KinD into the spotlight as one of the kinases involved in mediating environmental signals for biofilm establishment, but the molecules and factors that directly activate transcription of biofilm genes are still not clearly understood.

Table 1. Overview of the molecules and the signaling cascade.

Molecules/ processes triggering biofilm formation	***Effect at the cellular level***	***Sensor kinase***
Impaired oxidative phosphorylation	Decrease in NAD^+ levels	KinA[78]
	Reduced electron transfer through cytochromes	KinB
Surfactin, nystatin, gramicidin	K^+ leakage	KinC[80, 90]
ClO_2	Altered membrane potential	KinC
Nisin	Increased population of matrix producers	Unknown[91]
Root exudates (tomato)	Maltose and other metabolites	KinD[92]
Glycerol	Glycerol uptake and metabolism	KinD[93]
Mn^{2+}	Cofactor in Spo0A phosphorylation via Spo0F	KinD[93]
Menaquinones	Respiration and growth	Unknown[94]
Osmosensitivity	Physiological forces governed by the biofilm matrix	KinD[95]

Structurally, KinD consists of two transmembrane helices, two cytoplasmic catalytic domains, and a periplasmic sensor domain. It differs from other Kin proteins of *B. subtilis*

by the presence of a CACHE domain, known as a calcium channel and chemotaxis receptor. This CACHE domain is responsible for rhizosphere associated biofilm induction on tomato plants[92,96]. The high amount of L-malic acid found in tomato root exudates indirectly activates KinD through CACHE or other unknown domains[92]. Electron density studies showed that this sensor domain preferably binds pyruvate and other carboxylic acids like propionate and butyrate[96]. Possibly, L-malate is converted to pyruvate and this molecule binds to the KinD sensor domain. Thus, KinD mediated activation of biofilm formation requires a complex response involving the CACHE domain that may recognize the small molecules secreted by plants or *B. subtilis* itself.

Similar to root exudates and plant polysaccharides, another carbon source, glycerol and its derivatives were also reported to activate biofilm genes of *B. subtilis* via KinD. The effect of glycerol on robust biofilm formation under otherwise non-inducing medium (i.e. Luria broth medium) depends on the addition of manganese (Mn^{2+}). The presence of glycerol and Mn^{2+} induce biofilm gene expression via KinD mediated phosphorylation of Spo0A-P[93]. Mn^{2+} seems to act as a cofactor creating a complex with Spo0F and possibly promoting the efficiency of phospho-transfer towards Spo0A.

Importantly, Mn^{2+} is an essential component of various biofilm media used for *B. subtilis*. Mn^{2+} has also other important effects in the bacterial cells, e.g. required for sporulation[97,98]. In one of the studies mentioned in this Thesis (Chapter 2), we studied the impact of Mn^{2+} on rugose colony structures *B. subtilis* and its presence modulating the various differentiation processes during biofilm development[99].

Osmotic pressure increase due to certain dextran polymers and PEG supplementation in the medium was reported to reduce the expression of matrix-related genes and pellicle robustness. The effects on biofilm development during the osmotic level shift is connected to the KinD sensor kinase, adding a physical cue in addition to the chemical signals[95].

The examples listed above show the diverse signals that determine the kinase activity of KinD resulting in increased level of Spo0A in the cell. In addition to this, KinD also acts as a checkpoint for delaying sporulation under biofilm conditions. KinD operates as a kinase keeping Spo0A-P level high enough to activate matrix production, but on the other hand, its phosphatase activity keeps the Spo0A-P level at an intermediate level to prevent the initiation of sporulation[100]. The presence of extracellular matrix components of the mature biofilm is required for KinD to switch the phosphatase mode to the kinase activity. Hence, matrix-embedded cells possess a high concentration of Spo0A-P and thus, are the ones that enter the sporulation first. This is the reason for the late onset of sporulation in the *eps* and *tasA* mutants of *B. subtilis*. In accordance with this, a *kinD* mutant sporulates early in biofilm[100].

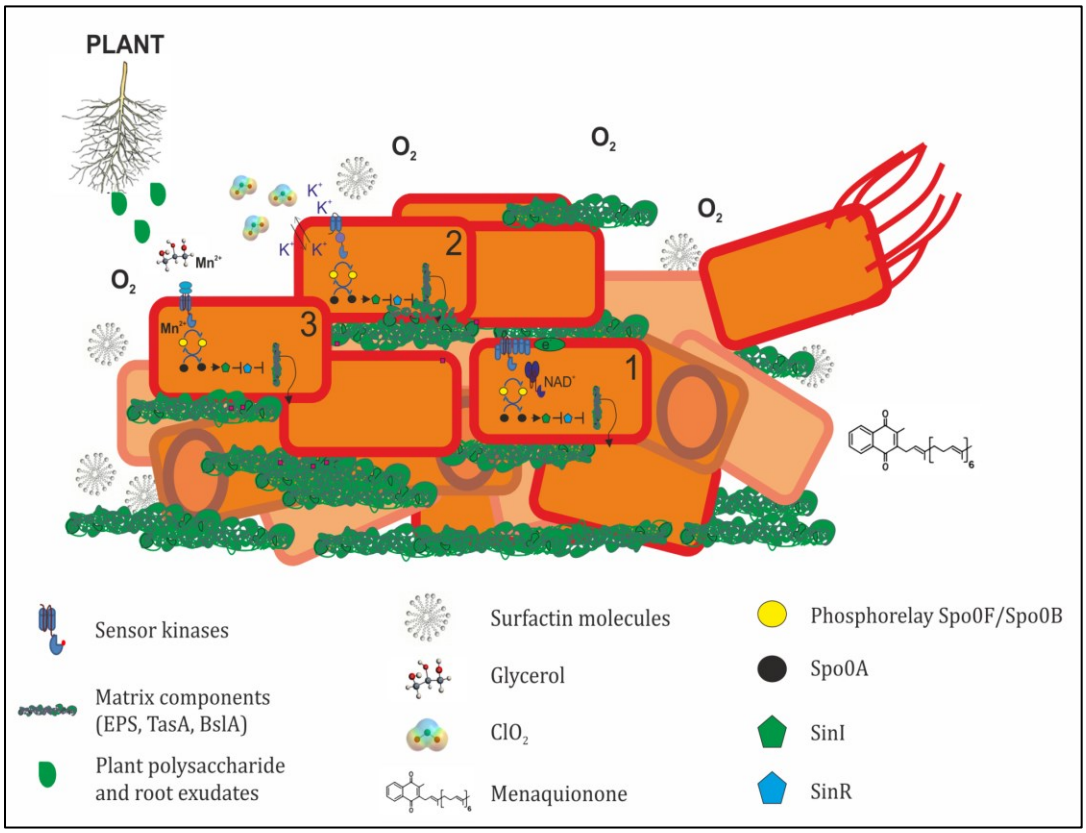

Figure 2. Signaling molecules that trigger biofilm formation of B. subtilis. Bacterial cells are depicted at the onset of biofilm formation. Molecules and signals are indicated below the figure. Arrows represent activation, while T shapes indicate repression. Numbers indicate the activation of KinA/KinB (1), KinC (2), or KinD (3) kinases by their respective signaling molecules at the cellular level. Figure adopted from Mhatre *et al*, 2014[101].

Recent studies with menaquinones have highlighted how these compounds aid in complex colony formation in *B. subtilis*[94]. The wild type strain, when grown on agar plates supplemented with diphenylamine (inhibitor of menaquinone biosynthesis), shows small colony with absence of irregular dendrites like structures, which are otherwise the character of a complex colony biofilm. A similar defect is observed in mutants with impaired menaquinone biosynthesis, which is reverted with externally supplemented menaquinone[94]. Previously, menaquinone was also shown to be important for sporulation[102]. However the direct sensing and triggering process of menaquinone on biofilm formation is unknown and it is undetermined whether one of the kinases plays a role in the activation pathway.

3.4 Environmental cues aiding maintenance of colony structure

Robust colony structures are one of the attributes of the biofilm forming bacteria. However, as the population undergoes nutrient limitation, various mechanisms are induced in order to survive in the starvation period. Sporulation and slowing of

metabolism are few such approaches[103]. Another mechanism exhibited by the peripheral cells of the colony is sliding. Sliding is a form of collective migration, independent of flagellar motility and usually aided by the secreted molecules. The kinases KinB and KinC play a role in inducing this mechanism in *B. subtilis*[104]. In this bacterium, surfactin forms the main component of lubricant along with EPS and BslA aiding the sliding of the cells in order to venture new nutrient sources[105,106]. Viscosity of the surface plays a huge role in the ability of the cells to slide. This explains the reason of using less concentrated agar to demonstrate sliding phenomenon in studies[107]. Recently, we identified another factor that targets the cells' ability to slide. Presence of Ca^{2+} was found to sequester the surfactin molecules thus, affecting the sliding and hence, maintaining the rugose structure of the biofilm forming colony. These observations are explained in details in Chapter 3 of this Thesis.

4. Intrinsic factors affecting biofilms

Bacterial metabolism and interactions in biofilm constitute the intrinsic factors that shape the community. Interactions like cooperation and competition are integral part of bacterial social community. This section highlights the cellular regulators, resulting interactions and metabolic strategies playing role in *B. subtilis* biofilms.

4.1 Global regulators affecting biofilm development of *B. subtilis.*

The main biofilm repressor, SinR, directly represses the operons expressing biofilm components, *epsA-O* and *tapA-sipW-tasA*. When the phosphorylated levels of Spo0A (Spo0A~P) reaches a given threshold level, it activates the transcription of *sinI* gene that codes an anti-repressor[108]. SinI then forms a complex with SinR and thus, permits the expression of matrix forming genes[109,110]. SlrR, a homologue of SinR plays another important role on the SinI-SinR switch during biofilm formation and motility[108,111]. SlrR also forms a complex with SinR and therefore, it titrates away SinR that would otherwise repress biofilm genes, although SlrR-SinR complex also represses the genes related to motility and cell lysis[112,113]. The SlrR-SinR interaction has an additional derepression effect on the *slrR* gene resulting in a positive feedback loop, observed as hystheresis or epigenetic switch that keeps the cells in the "high-SlrR" state for several cell divisions[113]. This results in the production of biofilm matrix for extended periods of time.

The activity of another global transcriptional regulator in *B. subtilis*, DegU is controlled by the sensor kinase DegS through phosphorylation[114]. The exact signal for DegS is unknown. In its unphosphorylated form, DegU activates the expression of *comK*, the main regulator of competence[115]. When the level of DegU~P slightly increases, the expression of motility genes is induced, followed by activation of biofilm formation at an intermediate DegU~P level and exoprotease production at a high level[73,116]. In laboratory strains, the role of

DegU~P in the production of PGA is related to the mucoid colony phenotype giving rise to the biofilm formation[63].

4.2 Cooperation and competition

It is not surprising that not all cells in *B. subtilis* biofilms contribute to the production of biofilm matrix. As mentioned previously, threshold of phosphorylated Spo0A contributes a great deal to this heterogeneity, priming cells to resist changes in the environment. The epigenetic switch of this bistable expression of genes maintains the phenotypic heterogeneity in *B. subtilis* biofilms. Reportedly, only 2% of cells in the population can express *sinI.* This creates *sinI*-OFF and *sinI*-ON bistable states, where only *sinI*-ON cells are able to repress the SinR and subsequently, allow the operons that encode components of biofilm matrix to express (Figure 3)[106]. Once expressed these matrix components are also shared amongst the non-producers. This was observed when the mutants in *eps* and *tasA* are unable to form complex biofilms individually, whereas, when complemented they give rise to the normal wild type like biofilms[64]*. B. subtilis* cells secrete signaling molecules like toxins, biosurfactants, degrading enzymes during growth and later in the stationary phase when the threshold of these secretions reach sufficient levels, specific receptors are activated. Post-translationally isoprenated, competence factor ComX, from ComQXPA quorum sensing system responsible for activation of more than 200 genes, is one such molecule that acts as a cue for the surfactin biosynthesis[117,118]. Other QS systems in *B. subtilis* reported are lantibiotics such as subtilisin and the autoinducer-2 production protein LuxS linked to the bacterial virulence and pathogenicity[119,120]. These signals are not only species specific but also specific for ecologically distinct phylogenetic groups (ecotypes) and pherotypes (same quorum sensing group) of a species[121]. This strongly suggests that the benefits associated with the responses are limited to the related groups of cells; ,, a mechanism to curb the exploiting cell types.

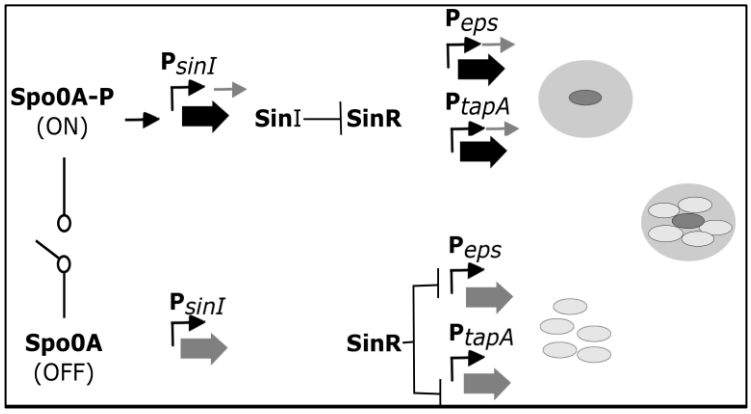

Figure 3. Bistable switch of sinI-ON and sinI-OFF state. Cells (grey) in *sinI*-ON state also express *eps* and *tapA* genes, thus, producing matrix around them (light grey circle). In biofilms, the matrix producers and non-producers coexist (adapted from Kearns, 2008)[122].

Recently, a kin discrimination mechanism was also described in *B. subtilis* swarming strains where the study claims that non-kins formed a distinct boundaries when the swarms met[123]. The frequencies of boundary lines were higher among the lower phylogenetically related strains, but the *Bacilli* swarms merged in the case of highly related ecotypes. Also, the related ecotypes existed closely in nature in contrast to the less related strains defining the social landscape of *B. subtilis* communities in natural habitats (Figure 4).

The subpopulation of cells producing the matrix components in the *B. subtilis* biofilm also exhibit antimicrobial activity towards the non-producers in an attempt to lessen the competition as well as to thrive on molecules released by lysed cells in nutrient limiting, biofilm conditions[80,124]. By producing toxins, these producers are also resistant to the antimicrobial peptides as they themselves also express immunity machinery required to repel the effects of these toxins[125].

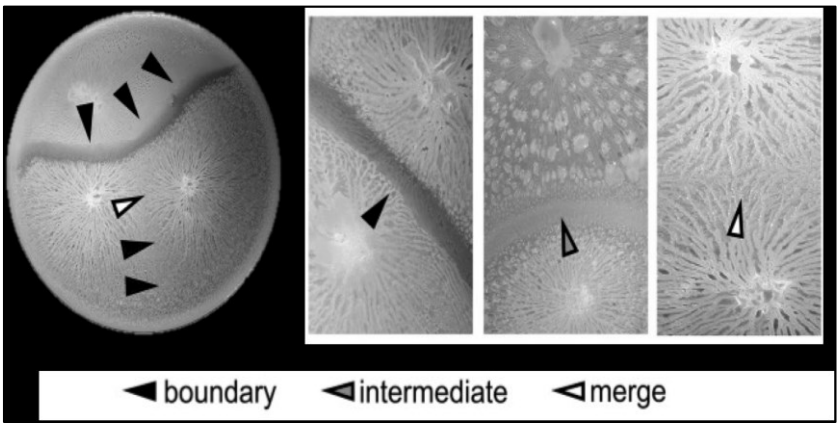

Figure 4. Frequency of boundary lines between B.subtilis swarms. (A) Merging and boundary forming swarms on a 9-cm-wide plate. (*B*) Close-up of boundary formation on the left, intermediate lines in the middle, and merging on the right (adopted from Stefanic *et al*, 2015)[123].

The production of toxins, especially Skf, also leads to an increased production of extracellular matrix and is observed through an improved colony wrinkling. Surfactin triggers the production of these cannibalism factors by activating the expression of *skfA-H* and *sdpABC* genes through KinC mediated activation of Spo0A~P[80]. The presence of the Skf and Sdp peptides and analogous molecules like nisin are also known to delay sporulation and thus, increase the ratio of matrix-producing cells in the biofilm population.

4.3 Metabolic strategies in *B. subtilis* biofilms

Metabolism in *B. subtilis* is vastly studied and many key features can be attributed to the metabolic strategies of cells in biofilm communities. Previously known as an obligate aerobe, reports have suggested that *B. subtilis* cells under certain conditions undergo substrate level phosphorylation giving rise to fermentation end products. Fermentative metabolism, as described previously as Crabtree effect in section 1.4, is considered as inefficient metabolism as compared to the oxidative phosphorylation, because of its lower energy yield and accumulation of acidic products that could be toxic to the viability of cells[126]. Nevertheless, under nutrient abundant conditions many organisms prefer inefficient metabolism due to following reasons: (1) most pathways involved in respiratory (efficient) metabolism require enzymes that either have the higher costs of production or have to be present in higher amounts (eg. Embden-Meyerhof-Parnas pathway versus Entner-Doudoroff pathway[43]); (2) although inefficient metabolism results in overflow metabolism, the growth rate is higher and hence, cells divide faster giving fitness advantages[127]; (3) under nutrient excess conditions, the diffusion is higher, thus, environment is unstructured conditioning the fitness landscape to favor higher growth rate[48].

B. subtilis, under excess of glucose, convert the glycolytic products such as pyruvate and acetyl- CoA to the by-products of metabolism such as lactate, acetate and acetoin.

These are then excreted into the extracellular environment. These are called as overflow pathways, where cells maintain redox balance and generate ATP without the dependence on the cytochrome system. When glucose is consumed, the by-products are then reused and metabolized further through the citric acid cycle or Tri-carboxylic acid cycle (TCA), which is efficient metabolism[128].

Is such efficient metabolism favored in nutrient and diffusion limiting conditions like biofilms? It was previously described that the operon required for the utilization of lactate also plays a role in influencing the architecturally complex biofilms in *B. subtilis*[129].

During competition between strains undergoing inefficient and efficient metabolism, environmental conditions will imply the fate of the competition. The inefficient metabolizers will have higher growth rate, however, due to fast depletion of resources and higher rate of accumulation of overflow substrates, will end up with lower yield (rate strategists-RS). The efficient metabolizers trade-off their growth rates with the growth yield (yield strategists-YS). During competition where environment is nutrient rich, RS will easily outcompete YS. However, in spatially structured niches, YS will emerge and both strategists will coexist. The experimental evidence of this phenomenon is described in Chapter 4 of this Thesis.

Metabolic trigger enzymes also play a role in shaping biofilm behavior strategies. For instance, enzyme acotinase that converts citrate to iso-citrate during TCA, also plays a role

in binding iron responsive elements (IRE) in mRNAs of certain genes stabilizing them. In absence of acotinase in *B. subtilis*, there is reduction in accumulation of *gerE* mRNA and hence, have defective sporulation. Sporulation is an important event under biofilm conditions and also plays a role in complex colony formation (discussed in Chapter 2 of this Thesis). Additionally absence of acotinase also increases the cellular citrate level. Citrate is an iron chelator and therefore, its accumulation results in iron limiting conditions[130]. Another role of trigger enzymes are those involved with ABC transporters that mediate the export of peptides. Certain secreted peptides act as antimicrobials and hence, while exportation they activate intra-membrane kinases that activate the defenses against secreted antimicrobials such as bacitracin.

The mechanistic properties that originate from the spatial structure of biofilms might also influence the metabolic interactions including co-dependences where the quest for nutrients and energy sources drives synergistic cooperative traits[131]. The presence of metabolic oscillations and alternate colony expansion of *Bacillus subtilis* biofilms under microfluidics setting is one such example[132]. Intrigued by the periodic halting of the expanding peripheral biofilm cells, Liu and colleagues (2015) observed that nitrogen limitation governs a metabolic co-dependence of peripheral cells on interior cells. When glutamate in the medium gets depleted in the interiors, the clusters no longer provide extracellular ammonia to the peripheral cells to support their expansion. This causes a halt, which in turn provides glutamate for the cells in the clusters to remain viable.

Such an arrangement of glutamate and ammonium transfer among the different part of the biofilm produce the periodic oscillations. When peripheral cells no longer depend on interior clusters for the source of ammonia, the oscillations are quenched and cells in the interior starve. Thus, these oscillations not only promote the viability of interior cells, but also maintain the resilience of the colony and facilitate to reach large size by outsourcing ammonia production conferring metabolic dependency.

This Thesis aims to demonstrate how certain extrinsic factors in form of media components (glucose/ glycerol- Chapter 1), and metal ions (Mn^{2+} and Ca^{2+}-Chapter 2 and 3) modulate the biofilm structure complexities, as well as to highlight the intrinsic factors in form of the efficient metabolic strategies that define the fitness of the population in *B. subtilis* biofilms. The empirical work stated in this Thesis is novel and contributes to the greater question- how organisms utilize and adapt to their environment optimally to survive better.

Aims and Outline of the Thesis

This dissertation includes the cumulative work that contributes to the biofilm formation in *B. subtilis*.
The four chapters include the projects carried out in the span of three and a half years.
The aim of the thesis is to study how the environment and metabolic strategies within the biofilm shape the robust and complex structure.
In order to precede I first studied the impact of certain medium components on the biofilm formation.

The objective of the Chapter 1 was to outline the properties of different laboratory strain variants of *B. subtilis* used around the globe in several laboratories. Though biofilm formation in this bacteria is studied extensively, previously it was describes that the laboratory strain, *B. subtilis* 168 is unable to form complex biofilm structures. In our variant of this strain we observed otherwise, when grown on complex rich medium. Hence we planned to observe the characteristics of this strain used in several laboratories. To our surprise, different laboratory strain variants of *B. subtilis* 168, show morphologically distinct biofilm formation. This chapter describes and studies these differences and emphasizes on the environmental conditions that play a major role and that is required to be considered while describing the biofilm related observations in bacteria.

The aim of the Chapter 2 was to describe the cellular processes that contribute to the complex colony structures and the impact of manganese on several of these processes. The transcriptomic study highlighted the up regulated and down regulated genes in presence and absence of Mn^{2+} in colony biofilm conditions. The idea here was to check which of these Mn^{2+} dependent processes aids in robust colony structure formation.

It was observed that the presence of calcium in medium restricts the peripheral cells from expanding in the mature biofilm colony. The aim of the Chapter 3 was to investigate this phenomenon and describe the influence of Ca^{2+} on the secreted molecules that play a role in colony expansion.

In the later part of my research I studied the influence and emergence of efficient metabolism leading to the higher yield, on the interactions in biofilm.

The aim was to evolve yield strategists in *B. subtilis* population and to study their fate in presence of rate strategists (higher growth mostly due to inefficient metabolism). The purpose was to contribute to the study on the tradeoff between yield and rate; and the influence of spatial structured environment in the competitive selection of either strategies. The experimental concept was based on and supported by numerous modeling and computational observations on growth rate and yield strategies.
The larger goal was to study the mechanism that contributes to the efficient growth in the heterogeneous population of *B. subtilis*.

The chapters describe the results and observations obtained in each of the studies. It states the methodologies used in studying various characteristics of *B. subtilis* biofilms.

CHAPTER 1

Chapter 1

Ramses Gallegos-Monterrosa, Eisha Mhatre, Ákos T. Kovács (2016)
Specific Bacillus subtilis 168 variants do form biofilms on nutrient rich medium
Accepted in Microbiology doi: 10.1099/mic.0.000371
(The content and the written parts are similar to the online manuscript; only typographical changes and style formatting have been applied.)

B*acillus subtilis* is an intensively studied Gram-positive bacterium that has become one of the models for biofilm development. *B. subtilis* 168 is a well-known domesticated strain that has been suggested to be deficient in robust biofilm formation. Moreover, the diversity of available *B. subtilis* laboratory strains and their derivatives has made it difficult to compare independent studies related to biofilm formation. Here, we have analyzed numerous 168 stocks from multiple laboratories for their ability to develop biofilms in different setups and media. We report a wide variation among the biofilm-forming capabilities of diverse stocks of *B. subtilis* 168, both in architecturally complex colonies and liquid-air interphase pellicles, as well as during plant root colonization. Some 168 variants are indeed unable to develop robust biofilm structures, while others do so as efficiently as the undomesticated NCIB 3610 strain. In all studied cases, the addition of glucose to the medium dramatically improves biofilm development of the laboratory strains. Furthermore, the expressions of biofilm matrix component operons, *epsA-O* and *tapA-sipW-tasA* were monitored during colony biofilm formation. We find lack of direct correlation between the expression of these genes and the complexity of wrinkles in colony biofilms. However, the presence of a single mutation in the EPS-related gene *epsC* does correlate with the ability of the tested stocks to form architecturally complex colonies, pellicles, and to colonize plant roots.

1. Introduction

Bacillus subtilis is a non-pathogenic model Gram-positive bacterium that has been extensively studied for over a century. Microbiologists have used *B. subtilis* to investigate a broad variety of biological questions, ranging from the intricacies of cell-metabolism to the community behavior and evolution[133,134]. As a consequence of the extended use of *B. subtilis*, multiple strains exist in laboratories and strain collections all over the globe. Some of these strains have been isolated from distinct environments and are used as wild-type reference strains, e.g.: NCIB 3610 (from here onwards, 3610) and PS216. Other commonly used strains have been described as "domesticated" due to their prolonged use under laboratory conditions, which have conferred them with characteristics that make them ideal research models, i.e. ease of genetic manipulation and efficient growth on commercially available media.

One of the key features of *B. subtilis* is its ability to form biofilms. Biofilms are complex multicellular communities that can develop in diverse environments and might have a great impact on multiple human activities, among others including an ominous progression of common infections or hampering biotechnological and industrial applications [135,136]. Formation of biofilms can be desirable under certain circumstances, *B. subtilis* biofilms, for example, have been implicated in crop protection, via preventing colonization of plant roots by pathogenic organisms[137].

B. subtilis has become one of the model organisms for biofilm research. The studies performed over the years have provided many insights regarding the processes involved in the development of these bacterial populations[101,138]. Strain 168 is the most well-known and widely used laboratory strain, it is an easily transformable tryptophan-auxotroph that was obtained via X-ray mutagenesis[139] and has been used in a multitude of academic and industrial studies. The intensive use of strain 168 has generated various derivative strains, several of which have been sequenced by a joint European-Japanese consortium and later re-sequenced using single strains[140-142].

The biofilms formed by *B. subtilis* have traditionally been studied as complex structured colonies on agar plates, or as pellicles formed at the liquid-air interface of static liquid cultures[75,143]. Branda and colleagues were the first to report the different biofilms developed by certain *B. subtilis* strains, noticing that domesticated laboratory strains derived from strain PY79 form deficient biofilms[72]. Since then, laboratory strains, including 168, have been largely considered as a non-biofilm former or poor biofilm former at best[144]. Different studies have investigated the genetic differences between this strain and wild-type 3610, reporting that these disparities are responsible for strain 168´s small, unstructured colonies and flat featureless pellicles[70,145]. Particularly, a deficiency in the

production of exopolysaccharide (EPS) has been highlighted as an important flaw of strain 168 related to biofilm formation[70,109].

In *B. subtilis*, EPS is produced by the proteins encoded in the *epsA-O* operon, and is a major component of the biofilm matrix[1,146]. Due to its relevance to the biofilm formation, different groups have investigated this polymer for its chemical nature. However, these studies have normally used different non-domesticated strains and media, therefore obtaining disparate results[89,147,148]. This phenomenon is a testament to the robustness of *B. subtilis*, a soil bacterium that has evolved the ability to survive on different nutrient sources, and therefore can use diverse compounds to produce the polymers that form the backbone of the biofilm matrix[149,150].

A problem that permeates *B. subtilis* research is the plethora of available strains and methods, making it difficult to compare experimental results. Here, we have compared the different biofilms developed by various laboratory stocks of strain 168 originating from various research groups around the globe. We have also analyzed the expression of the *eps* and *tapA-sipW-tasA* operons using a fluorescent reporter fusion. We report that the formation of complex colonies varies greatly among different 168 strains, some of them being able to form architecturally complex colonies similar to those developed by 3610 when grown on complex or supplemented media. In addition, we show that the expressions of P_{eps}-GFP and P_{tapA}-GFP fusions do not necessarily correlate with the formation of architecturally complex structures in these biofilms.

2. Results

2.1 Various stocks of *B. subtilis* 168 show diverse complex colony and pellicle morphologies

Different nutrients are known to have a profound effect on general metabolism and the production of signaling molecules that regulate biofilm formation in *B. subtilis*[101]. Previous publications suggest that the availability of complex nutrients might supplement the metabolic shortcomings of strain 168 and allow it to develop architecturally complex biofilms[99,151]. We were interested in testing various stocks of the 168 strain that are used by different laboratories. Importantly, these stocks might have diverged due to additional genetic differences possibly resulting in contrasting observations among the work groups related to biofilm formation.

We grew complex colonies of obtained 168 variants, the domesticated laboratory strain JH642 and the wild isolate 3610 on defined (i.e. MSgg) and complex (i.e. supplemented LB and 2xSG) media for 72 hours. LB, although rich in nutrients and commonly used by microbiologists, is not a biofilm-promoting medium. The colonies developed by *B. subtilis* on LB agar are small, flat and featureless, and pellicles do not develop on static liquid LB cultures (data not shown). We investigated the possibility that the addition of both manganese and carbon sources (glycerol or glucose) similar to those present in other

media could be sufficient to promote the development of complex *B. subtilis* biofilms on LB medium.

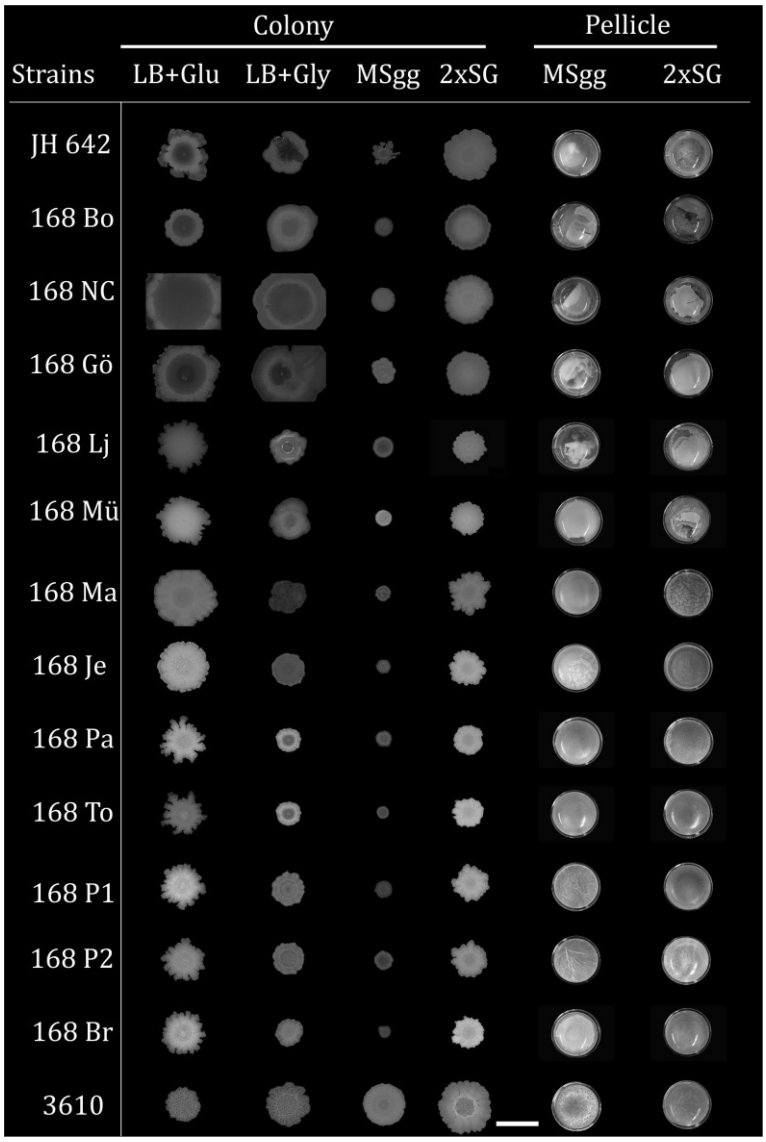

Figure 1. Comparison of complex colonies and pellicles of B. subtilis strain 3610 and 168 variants. Strains were grown on different media and imaged after 72 hours of incubation, arranged by increasing colony wrinkleality on 2xSG medium. The scale bar shown at the middle bottom represents 20 mm. Strain abbreviations are described in Table 1.

Using the chemically defined MSgg medium, we observed a marked difference between the colonies developed by all 168 variants and the undomesticated prototroph; namely, 3610 develops large (18-20 mm), opaque colonies with wrinkles, while all 168 variants develop smaller (5-8 mm) colonies with smooth bright surfaces in the periphery that show small or no wrinkles (Figure 1, Supporting Information for Chapter 1, hereafter S1 Figure1). The opacity in the wrinkles of a complex colony is suggested to be associated with increased

sporulation as the biofilm matures[152,153]. These phenotypes are in line with previous reports that define the domesticated 168 strain as a non-biofilm former when grown on MSgg medium[70,72]. However, the appearance of the biofilms changes drastically when grown on complex medium. On 2xSG, 3610 shows large colonies with increased architectural complexity, i.e. its colonies have larger and seemingly taller wrinkles with opaque white summits, while leaving a clear flat and smooth area in the center of the colony. On this media, the 168 variants form colonies almost as large as those developed by 3610 (15-20 mm), and their topography shows great diversity. 168 P2 and 168 Je, for example, form wrinkled opaque colonies that resemble those formed by 3610 on MSgg; while 168 Gö and 168 NC show a uniformly rugose bright surface. On the other hand, JH642 and 168 Bo colonies remain flat with a smooth surface, although they are also larger than those developed on MSgg (Figure 1, S1 Figure 1). The biofilm colonies grown on LB medium with additional manganese and carbon sources (glycerol and glucose) show an improvement in the development of wrinkles. 3610 shows an increased formation of wrinkles accompanied by a slightly smaller colony size (15-17 mm), while most 168 variants show large colonies that even surpass those of 3610, especially when the medium was supplemented with glucose. On LB-Glu medium, the 168 variants develop opaque colonies that seem indistinguishable from those of 3610 on MSgg, which suggest that and abundance of glucose might be sufficient to overcome the deficiencies observed while developing on MSgg. Strikingly, this is not the case for glycerol, which is the carbon source normally available in MSgg. The colonies developed on LB-Gly, although larger than those on MSgg, still show reduced complexity with brighter surfaces as shown before for stock 168 Je[99].

We tested the development of pellicle biofilms by all 168 variants and 3610 using common biofilm media 2xSG and MSgg after 72 hours (Figure 1, S1 Figure 1). MSgg promotes the formation of densely wrinkled pellicles by 3610, while most 168 variants form thin and flimsy pellicles (e.g. 168 Ma, Pa, To). The most fragile of these pellicles even collapse and sink to the bottom of the well (e.g. 168 Bo, Nc, Lj, Gö, JH642). Notable exceptions are the pellicles developed by 168 P1 and P2 strains, which develop thick wrinkled pellicles similar to those of 3610. Importantly, 2xSG medium promotes the appearance of dense floating biofilm in most 168 variants, except in those that form fragile or collapsed pellicles in MSgg (e.i. 168 Mü, Lj, Gö, NC, Bo and JH642) (Figure 1, S1 Figure 1). In sum, these experiments suggest that certain variants of *B. subtilis* 168 do develop complex structures on biofilm-promoting nutrient-rich medium.

2.2 Expression of the *epsA-O* and *tapA-sipW-tasA* operons does not correlates with the complexity of biofilm colony wrinkle formation

Biofilm formation by *B. subtilis* has been associated with the development of architecturally complex communities. In this regard, the most recognizable visual phenotype is the development of wrinkles or folds, both in colonies and pellicles[72,154]. As the production of EPS is closely associated with biofilm development in diverse species[1], we investigated if the relative expression of the *epsA-O* operon correlates with the appearance of architecturally complex communities. Specifically, we expected that the expression levels from a P_{eps}-GFP reporter fusion would be higher in those strains and under conditions, which efficiently develop opaque wrinkles, as compared to those that remain flat and featureless.

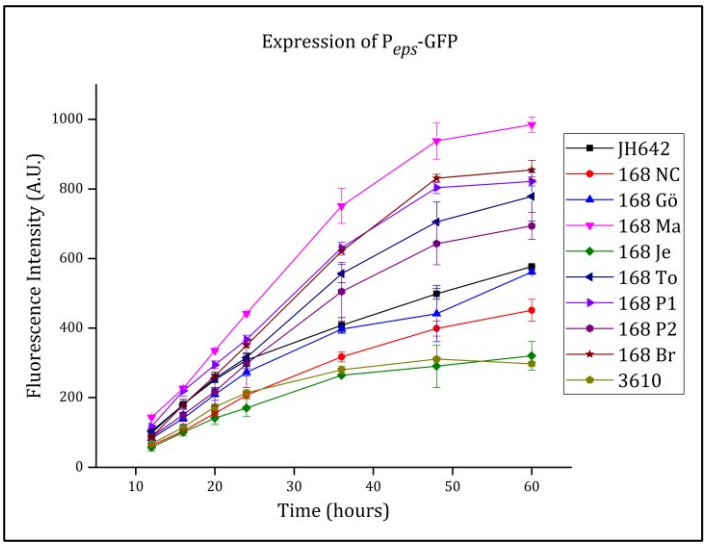

Figure 2. Fluorescence expression profiles of colonies of B. subtilis strain 3610 and 168 variants carrying a transcriptional P_{eps}-GFP fusion. Strains were grown on 2xSG medium and fluorescence determined at regular intervals as described in the materials and methods. Data points represent the average of 3 independent colonies. Error bars represent standard deviation. Strain abbreviations are described in Table 1.

To this end, we monitored the levels of green fluorescence during the development of complex colonies of 168 variants on 2xSG. We selected this media because the biofilm structures showed a wide range of complexity from the highly wrinkled 3610 reference strain towards the flat and featureless JH642. Surprisingly, we did not observe a correlation between the measured fluorescence levels and the appearance of complex structures in the colonies (Figure 2, S1 Figure 2). The expression levels of the reporter fusion increases in all 168 variants over time, especially after the onset of stationary phase when the colony size extension declines (around 24 hours). However, differences in fluorescence expression appear regardless to colony wrinkleality. 3610, for example, develops typically complex colonies while maintaining low fluorescence throughout colony development. An inverse correlation is not evident either; JH642 displays flat featureless colonies, but its fluorescence levels are inferior to those shown by 168 Ma and 168 Br. This result suggests that the expression of biofilm genes is not directly related to the development of wrinkles during complex colony biofilm formation.

To further test the involvement of other extracellular matrix components over the formation of wrinkles, we measured the expression levels of a P_{tapA}-GFP reporter fusion in the 168 variants. The *tapA-sipW-tasA* operon encodes the protein component of *B. subtilis* biofilms[64].

B. subtilis strains that lack both the *epsA-O* and *tapA-sipW-tasA* operons are unable to form biofilms[64,155,156]. We monitored the expression levels of a P_{tapA}-GFP reporter fusion during the development of complex colonies of 168 variants. As in the case of the *epsA-O* operon, 3610 developed a complex wrinkled colony while showing the lowest level of reporter fusion expression, while the 168 variants show all higher fluorescence levels without a clear correlation to wrinkle formation or colony opacity (Figure 3, S1 Figure 3).

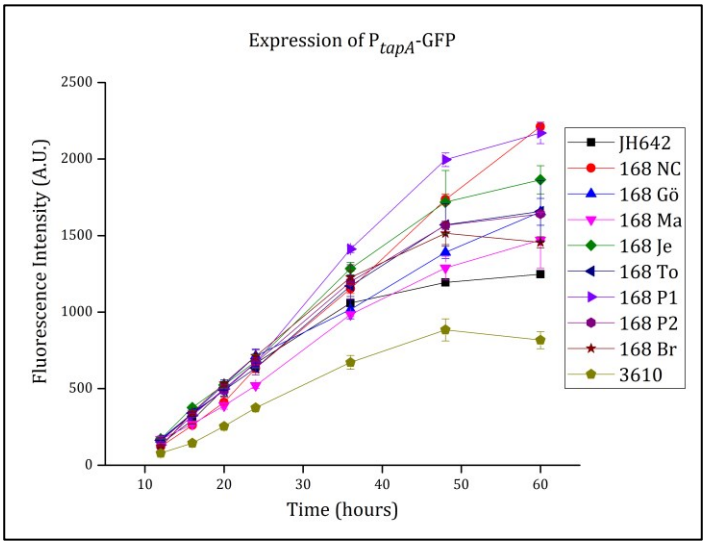

Figure 3. Fluorescence expression profiles of colonies of B. subtilis strain 3610 and 168 variants carrying a transcriptional P_{tapA}-GFP. Strains were grown on 2xSG medium and fluorescence determined at regular intervals as described in the materials and methods. Data points represent the average of 3 independent colonies. Error bars represent standard deviation. Strain abbreviations are described in Table 1.

Taken together, these results indicate that the relative expression of genes coding for the EPS and TasA protein matrix components does not directly correlate with the formation of wrinkles in complex colony biofilms of *B. subtilis*. Importantly, it is worth noting that in both reporter strains the expression of the corresponding reporter fusion was lowest in the undomesticated 3610 strain.

2.4 Differential biofilm formation on roots of *A. thaliana* by diverse 168 stocks

B. subtilis is a soil bacterium known for its ability to colonize plant roots via biofilm development[88,157]. We tested whether our previous observations on the colony and pellicle robustness hold true for a root colonization assay, which is a more natural biofilm development model than colonies on agar plates. We examined the colonization of *A. thaliana* roots after 24 hours of incubation with selected 168 stocks. The used stocks are representatives of the diverse colony morphologies previously observed, and were labeled with a $P_{hyperspank}$-GFP reporter fusion in order to detect the bacterial cells using

fluorescence microscopy analysis. We observed that the ability to colonize *A. thaliana* roots differs greatly among the tested 168 stocks. Importantly, there is a correlation between a stock´s ability to form architecturally complex colonies and root colonization by biofilm development. The undomesticated isolate, 3610 readily colonizes the roots in 24 hours by developing a large, multi-layered biofilm (Figure 4A). In contrast, stocks 168 Bo, Gö and Lj are barely present on the root surface, forming small, mono-layered attachments (Figure 4B, C and D). These stocks are all poor biofilm formers on agar plates. On the other hand, stocks 168 Je and P1 colonize the root surface in a similar fashion as 3610, by forming large biofilms with multiple cell layers (Figure 4E and F).

To quantitatively strengthen our observations, we estimated the attached bacteria per area of the root surface by measuring the fluorescent intensities originating from the bacterial cells. Using this approach, we corroborated that average fluorescence intensity per root area significantly higher in those roots colonized by strain 3610 or stocks 168 Je and P1, as compared to roots colonized by stocks 168 Bo, Gö and Lj (Figure 4G).

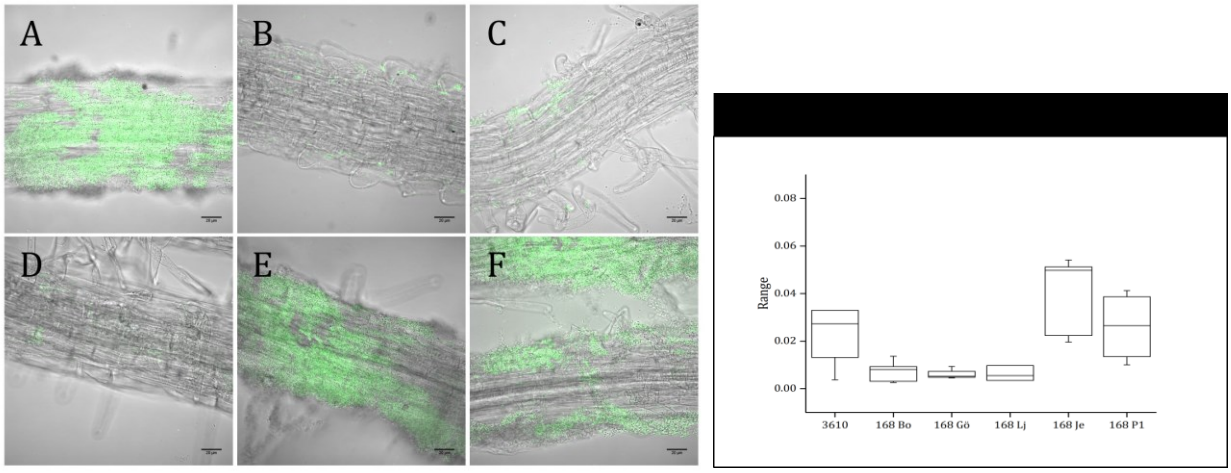

Figure 4. Colonization of A. thaliana roots by selected B. subtilis strains. Bacterial cells harboring a $P_{hyperspank}$-GFP fusion were visualized using fluorescence (false-colored green) attached to 10 to 12 day old seedlings of *A. thaliana*. Pictures are representative of at least 6 independent roots. The colonization of the plant root surface by *B. subtilis* strains 3610 (A), 168 Boston (B), 168 Göttingen (C), 168 Ljubljana (D), 168 Jena (E), 168 Pavia1 (F) were quantified as described in the materials and methods and the fluorescent area covered are presented using box plots (G) from at least 3 scanned areas of 3 independent roots. Strain abbreviations are described in Table 1.

These experiments directly correlate pellicle and colony wrinkleality of *B. subtilis* 168 with the ability to attach and develop biofilm on the plant root surface. Additionally, this also suggests that the biofilm-proficient variants of 168 could be exploited to study biofilms in the ecological settings.

2.4 *B. subtilis* 168 stocks with a point mutation in *epsC* are poor biofilm formers

Previously, it was reported that a single nucleotide mutation (C to T) at base pair 827 of the *epsC* gene of domesticated *B. subtilis* variants was partially responsible for deficiencies in biofilm development[70]. This mutation is responsible for a change from alanine codon 276 (GCG) to a valine codon (GTG), which possibly impairs EPS production. We sequenced a fragment of the *epsC* gene from all the studied 168 stocks in order to investigate if a consistent relationship exists between the presence of this mutation and deficiencies in biofilm development. We found that all 168 stocks that develop large and flat colonies on 2xSG agar show the C to T base substitution in *epsC* (Figure 5). Among these stocks are 168 Bo, Gö and Lj, which show feeble root colonization. Conversely, stocks, which develop architecturally complex colonies on rich media and show efficient root colonization possess the wild-type allele of *epsC* (Figure 5). The only exception for this trend is 168 Pa, which has the C to T mutation but develops architecturally complex colonies on rich media and robust pellicles. 168 Pa was obtained from a 168 parental strain transformed with genomic DNA to repair the tryptophan auxotrophy (Table 1), *epsC* might have been reverted to its wild-type allele during this process, while leaving other loci mutated compared to the 168 strains harboring complex wrinkles.

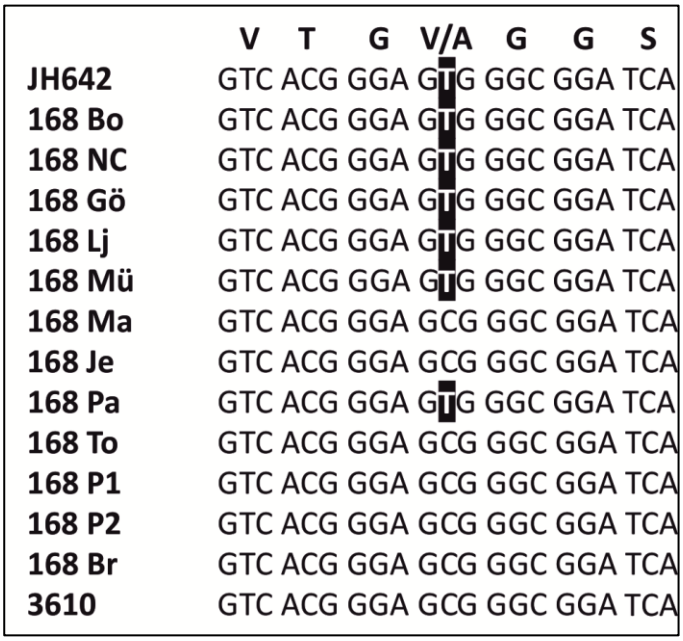

Figure 5. Allelic variation of the epsC gene in B. subtilis stocks. Alignment of resequenced *epsC* gene between base pairs 817-837 in all studied *B. subtilis* strains and variants; coded amino acids are indicated above the triplet sequences. The nucleotide at position 827 is shown with a black box for those sequences that present the mutated C to T allele. The sequences are arranged by the corresponding phenotype of increasing colony wrinkleality on 2xSG medium. Strain abbreviations are described in Table 1.

Additionally, we have sequenced the relevant fragments of *swrA*, *degQ* and *sfp* to further investigate previously reported gene defects that may be responsible for biofilm formation deficiencies[70]. Similar to previous observation[151], all studies 168 variants and the JH642 strain were found to contain the frame shift (*swrA*, *sfp*) or point (*degQ*) mutations as compared to the corresponding wild type alleles in 3610 (data not shown), thus likely

other loci are different among the different 168 stocks. These results confirm that minimal genetic differences in biofilm-related genes exist among diverse 168 stocks and can lead to drastic phenotypic differences.

3. Discussion

Despite *B. subtilis* being one of the most thoroughly studied bacteria, the process by which it develops its characteristic biofilms is still not completely understood. This may be due to the fact that previous studies focused mainly on the biotechnological potential and metabolic aspects of this organism[158-161], while its development, as a bacterial population has not enjoyed an intense research interest until more recently. Detailed investigations on *B. subtilis* interaction with other bacterial and fungal species have been only recently described [87,143,162-165]. The availability of diverse strains of *B. subtilis* has also hindered biofilm formation research, leading to contrasting observations about this phenomenon. In addition, other phenotypic features, including flagellum-dependent and -independent surface spreading, called swarming and sliding, respectively, are influenced by the strain and conditions applied[76,104,166]. Spurred by the reported differences among variants of *B. subtilis* 168 strain used in different research laboratories, we present here a thorough comparison of the biofilms developed by various stocks and compared to those of strain 3610. We note that complex rich media, especially if it contains abundant glucose as a carbon source (2xSG and LB-Glu), enables most 168 variants to form large structured colonies. This is strikingly different from the results obtained with MSgg, a chemically defined medium commonly used for biofilm development research, where all 168 variants are unable to develop architecturally complex colonies. Interestingly, carbon-enriched LB medium shows similar observations: the addition of glucose improves the biofilm development of most 168 variants, while glycerol is unable to do so. Additionally, we observe that the same 168 variants that form robust pellicles and complex colonies are able to efficiently colonize *A. thaliana* roots by developing biofilms over the root surface. Interestingly, the medium used in this assay (MSNg) utilizes glycerol as carbon source. The presence of plant exudates may be responsible for promoting efficient biofilm formation in this medium despite the lack of glucose[5,88]. Furthermore, all the 168 variants that consistently show poor biofilm formation have the same base-pair substitution in the *epsC* gene. This mutation has been previously suggested to be responsible for a decreased production of EPS and impaired biofilm formation in 168 variants[70].

The development of wrinkles in *B. subtilis* biofilms is perhaps the most recognizable characteristic of this bacterium. However, the process by which these structures are formed is complex. Localized cell death was shown to determine the location of wrinkle formation[167]. The channels formed below the wrinkles facilitate liquid flow towards the middle of the *B. subtilis* colony biofilms possibly facilitating nutrient and oxygen

transport[168]. Our experiments suggest no direct correlation between the magnitude of *epsA-O* and *tapA-sipW-tasA* expression and the formation of said wrinkles. Moreover, strain 3610 showed the lowest expression of the used reporter fusion, without any sign of expression peaks during early biofilm development, as would have perhaps been expected for an efficient biofilm former strain. It is possible that a feedback mechanism alters the expression of these reporter fusions, where efficient matrix production diminishes the expression of the tested promoters. Previously, it was reported that activation of sporulation in colony biofilms of 3610 is delayed in strains lacking EPS production[100]. In such case, the variants with a mutated *epsC* gene would have been expected to have the highest expression levels from P_{eps}-GFP, as they have an impaired production of EPS. However, these variants showed only medium expression levels of the reporter fusions, with some of the variants with wild-type alleles of *epsC* showing the highest expression levels of the reporter fusions.

To conclude, the development of biofilms by *B. subtilis* is acutely influenced by available nutrients, especially carbon source. Due to the variation present in strain 168, we recommend that researchers disclose the origin of the particular variant used in their studies. Although more research is necessary to solve the intricacies of these bacterial communities, researchers have to consider the metabolic needs of their laboratory strains before dismissing them as research models.

4.Methods

4.1 Strains and media

All the strains used in this study are listed in Table 1. These strains were pre-grown overnight in LB medium (Lysogeny broth, Carl Roth, Germany; 10g/L tryptone, 5 g/L yeast extract and 5 g/L NaCl) and later grown on LB supplemented with 0.1mM $MnCl_2$ and either 0.1% glucose (hereafter, LB-Glu) or 1% Glycerol (hereafter, LB-Gly), 2xSG medium (16 g/L nutrient broth (Difco), 2 g/L KCl, 0.5 g/L $MgSO_4 \cdot 7H_2O$, 1 mM $Ca(NO_3)_2$, 0.1 mM $MnCl_2 \cdot 4H_2O$, 1 µM $FeSO_4$ and 0.1% glucose) (Kobayashi, 2007) or defined MSgg medium (5 mM potassium phosphates buffer (pH 7), 100 mM MOPS, 2 mM $MgCl_2$, 700 µM $CaCl_2$, 100 µM $MnCl_2$, 50 µM $FeCl_3$, 1 µM $ZnCl_2$, 2 µM thiamine, 0.5% glycerol, 0.5% glutamate, 50 µM L-tryptophan and 50 µM L-phenylalanine) adapted from (Branda *et al.*, 2001). Murashige and Skoog (MS) medium was used for *A. thaliana* germination (MS basal salts mixture, Sigma-Aldrich, Germany; 2.2 g/L MS medium, pH 5.6-5.8), while MSNg medium was used for root surface colonization assays (5 mM potassium phosphates buffer (pH 7), 100 mM MOPS, 2 mM $MgCl_2$, 50 µM $MnCl_2$, 1 µM $ZnCl_2$, 2 µM thiamine, 0.2% NH_4Cl, 0.05% glycerol, 700 µM $CaCl_2$). Media were supplemented with Bacto agar 1.5 or 1% when solid plates were needed for bacterial colonies or plant seed germination, respectively. Unless otherwise stated, all liquid cultures were grown at 37 °C with 225 rpm shaking.

4.2 Strain construction

B. subtilis P_{eps}-GFP and P_{tapA}-GFP strains were obtained via natural competence transformation (Kunst & Rapoport, 1995) using genomic DNA from strains NRS2243 and NRS2394 respectively. Briefly, overnight cultures of the receiver strains were diluted to a 1:50 ratio with GCHE medium (1% glucose, 0.2% glutamate, 100 mM potassium phosphates buffer (pH 7), 3 mM trisodium citrate, 3 mM $MgSO_4$, 22 mg/L ferric ammonium citrate, 50 mg/L L-tryptophan and 0.1% casein hydrolysate), these cultures were incubated for 4 hours, after which 5-10 µg of genomic DNA were mixed with 500 µL of competent cells and further incubated for 2 hours before platting. $P_{hyperspank}$-GFP labeled strains were obtained via the same method using plasmid phyGFP that integrates into the *amyE* locus of *B. subtilis*[169]. Transformants were selected on LB plates with 5 µg/ml kanamycin or 5 µg/ml chloramphenicol. Successful transformation was validated using the fluorescence reporter activity of the strains or amylase-negative phenotype on 1% starch agar plates[170]. DK1042 was used instead of NCIB 3610 to obtain fluorescently labeled strains due to its improved transformability[171].

4.3 Biofilm development as pellicles and architecturally complex colonies

The studied strains were pre-grown in 3 ml LB medium overnight. 1:50 dilutions of these cultures in 2xSG and MSgg media were used to inoculate 24 well plates for pellicle formation. For biofilm colony structures, the four types of media (LB-Glu, LB- Gly, 2xSG and MSgg) were supplemented with 1.5% agar, tempered to 55 °C, and 25 ml of the medium were poured into a 90 mm diameter petri dish. Once solid, plates were dried completely open in a laminar airflow bench for exactly 15 minutes. The plates were closed and 2 µl drop of each strain was inoculated on the plate. To avoid growth inhibition and constrain caused by two different *B. subtilis* strains, only three strains were inoculated per plate and each had the reference 168 Je strain to compare the morphology. The plates for the pellicles and colonies were incubated at 30 °C for 72 hours.

4.4 Biofilm development on root surfaces

Seeds of *Arabidopsis thaliana* ecotype Col-0 were surface sterilized by incubating them in 1 ml of 2% NaClO solution for 20 minutes on an orbital mixer. The seeds were washed 5 times with 1 ml of sterile distilled water and placed on MS medium supplemented with 1% agar[172]. The seeds were planted with a separation of 15 mm to avoid entanglement of the roots. The MS plates were parafilm-sealed and incubated at 4 °C for 72 hours, afterwards they were placed at room temperature in a windowsill for 10-12 days to allow the seeds to germinate and develop roots of approximately 1 cm in length. Overnight cultures of the test strains were adjusted to OD_{600} of 0.2 and then further diluted 10 fold using MSNg medium. The seedlings were then placed in 300ul of these cultures in a 48 well micro plate.

The roots of the seedlings were completely submerged in the bacterial dilutions. The micro plate was incubated at 28 °C with 90 rpm shaking for 24 hours. After the incubation period, the seedling roots were gently washed 3 times with sterile MSNg medium, placed on microscopy slides, covered with coverslips and examined without further treatment.

4.5 Microscopy and image analysis

All bright-field and green-fluorescence images of colonies and pellicles were obtained with an Axio Zoom V16 stereomicroscope (Carl Zeiss, Jena, Germany) equipped with a Zeiss CL 9000 LED light source, HE eGFP filter set (excitation at 470/40 nm and emission at 525/50 nm) and an AxioCam MRm monochrome camera (Carl Zeiss). For colony and pellicle morphology comparison, pictures were obtained after 72 hours of incubation at 5 and 20x magnifications. For P_{eps}-GFP and P_{tapA}-GFP reporter fusion expression comparisons, images were taken at different time points using a 3.5x magnification and exposure times of 2500 ms for green fluorescence and 10 ms for bright field.

The expression of green fluorescence of colonies was analyzed using ImageJ (National Institute of Health, Bethesda, MD, USA). Briefly, images were batch-processed to subtract a background value, this value was calculated using a circular region of interest (ROI) of 1 mm radius and measuring the average fluorescence intensity in 36 non-colony areas selected from random pictures in all time points using only the green channel information. Afterwards, the colony area of each image was selected using the bright field channel and the tracing tool with legacy mode and a tolerance of 100. Using the selected ROI, the corresponding colony areas were marked on the green-fluorescence images and their average fluorescence intensity was measured.

All bright-field and green-fluorescence images of *A. thaliana* roots were obtained with an AxioObserver 780 Laser Scanning Confocal Microscope (Carl Zeiss, Jena, Germany) equipped with a Plan-Apochromat 63x/1.4 Oil DIC M27 objective, an Argon laser for stimulation of green fluorescence (excitation at 488 nm and emission at 540/40 nm), a halogen HAL-100 lamp for transmitted light microscopy and a AxioCam MRc color camera (Carl Zeiss, Jena, Germany). The images were obtained as a Z-stack of 10 slices covering 3.8 µm in the Z-axis. The images were later merged with ImageJ using an average intensity Z-projection. The average fluorescence intensity on the roots was measured by selecting the root area as a ROI in the bright field channel, and then measuring the fluorescence intensity in the corresponding area of the green channel- Z-projections only.

4.6 Sequencing of *epsC*, *swrA*, *degQ* and *sfp* alleles

A 788 bp fragment of *epsC* was PCR amplified from genomic DNA of the tested *B. subtilis* stocks using primers oTB110 (5'-CGAACTGCCGGACAAATC-3') and oTB111 (5'-

ACGGGCTCTCCCATATC-3'). The other primers used are described in Table 2. The fragments were sequenced using oTB110 (GATC Biotech, Constance, Germany).

Acknowledgments

We thank Romain Briandet (INRA Jouy-en-Josas, France), Cinzia Calvio (University of Pavia, Italy), Roberto Grau (University of Rosario, Argentina), Elisabeth Härtig (Technische Universität Braunschweig, Germany), Ines Mandić-Mulec (University of Ljubljana, Slovenia), Thorsten Mascher (Technische Universität Dresden, Germany), Mitsuo Ogura (Tokai University, Japan), Jörg Stülke (Georg-August-Universität Göttingen, Germany), Diego Romero (University of Málaga, Spain), Jan-Willem Veening (University of Groningen, The Netherlands) for kindly providing the various 168 strains and Nicola Stanley-Wall (University of Dundee, UK) for strains NRS2243 and NRS2394.

The laboratory of Á.T.K. was supported by a Marie Skłodowska Curie career integration grant (PheHetBacBiofilm), and grants KO4741/2-1 and KO4741/3-1 from the Deutsche Forschungsgemeinschaft (DFG). R.G.-M. and E.M. were supported by Consejo Nacional de Ciencia y Tecnología-German Academic Exchange Service (CONACyT-DAAD) and Jena School for Microbial Communications (JSMC) fellowships, respectively. The LSCM780 microscope was financed by a grant from Thüringer Ministerium für Bildung, Wissenschaft und Kultur (project B11024-715).

Supporting Information for this Chapter is on page no: 124.

Table 1. Strains used in this study.

Strain	***Characteristics***	***Abbreviation***	***Reference***
NCIB 3610	Prototroph, wild-type	3610	Bacillus Genetic Stock Center (BGSC)
DK1042	3610 *comI*^{Q12I}		[171]
NRS2243	3610 *sacA*::P$_{epsA}$-*gfp* (*neo*), *hag*::*cat*		[114]
NRS2394	3610 *sacA*::P$_{tapA}$-*gfp* (*neo*)		[114]
JH642	*ΔtrpC2 ΔpheA1 citS642*, derived from Marburg strain		Lab Stock (Grau, R., originally from Hoch, J.A.)
168 (Boston)	*ΔtrpC2*, derived from 168	168 Bo	Lab Stock (Romero, D., originally from Kolter, R.)
168 (Braunschweig)	*ΔtrpC2*, derived from 168	168 Br	Lab Stock (Härtig, E.)
168 (Göttingen)	*ΔtrpC2*, derived from 168	168 Gö	Lab Stock (Stülke, J.)
168 (Jena)	*ΔtrpC2*, derived from 168 1A700	168 Je	Lab Stock (Terrestrial Biofilms Group, originally from University of Groningen and BGSC)

168 (Ljubljana)	*ΔtrpC2*, derived from 168 1A1	168 Lj	Lab Stock (Mandić-Mulec, I., originally from BGSC)
168 (Malaga)	*ΔtrpC2*, derived from 168	168 Ma	Lab Stock (Romero, D.)
168 (Münich)	*ΔtrpC2*, derived from 168	168 Mü	Lab Stock (Thorsten, M., originally from Stülke, J.)
168 (New Castle)	*ΔtrpC2*, derived from 168 1A1	168 NC	Lab Stock (Veening, J.-W. and Errington, J., originally from BGSC)
168 (Paris)	trp+, tryptophan-prototrophic derivative of 168 (reconstituted *trpC* gene)	168 Pa	Lab Stock (Briandet, R., BaSysBio reference strain, BSB1) (Nicolas *et al.*, 2012)
168 (Pavia 1)	*ΔtrpC2*, derived from 168	168 P1	Lab Stock (Calvio, C., originally from Anagnostopoulos)
168 (Pavia 2)	*ΔtrpC2*, derived from 168	168 P2	Lab Stock (Calvio, C., originally from Burkholder and Giles)
168 (Tokai)	*ΔtrpC2*, derived from 168	168 To	Lab Stock (Ogura, M., originally from the EU sequencing consortium)
TB356	168 NC *sacA*::P_{epsA}-*gfp* (*neo*)		This study
TB357	168 Gö *sacA*::P_{epsA}-*gfp* (*neo*)		This study
TB358	168 To *sacA*::P_{epsA}-*gfp* (*neo*)		This study
TB359	168 Br *sacA*::P_{epsA}-*gfp* (*neo*)		This study
TB360	168 P1 *sacA*::P_{epsA}-*gfp* (*neo*)		This study
TB361	168 P2 *sacA*::P_{epsA}-*gfp* (*neo*)		This study
TB362	JH642 *sacA*::P_{epsA}-*gfp* (*neo*)		This study
TB363	DK1042 *sacA*::P_{epsA}-*gfp* (*neo*)		This study
TB365	168 Je *sacA*::P_{epsA}-*gfp* (*neo*)		This study
TB392	168 Bo *sacA*::P_{epsA}-*gfp* (*neo*)		This study
TB394	168 Ma *sacA*::P_{epsA}-*gfp* (*neo*)		This study
TB366	168 NC *sacA*::P_{tapA}-*gfp* (*neo*)		This study
TB367	168 Gö *sacA*::P_{tapA}-*gfp* (*neo*)		This study
TB368	168 To *sacA*::P_{tapA}-*gfp* (*neo*)		This study
TB369	168 Br *sacA*::P_{tapA}-*gfp* (*neo*)		This study
TB370	168 P1 *sacA*::P_{tapA}-*gfp* (*neo*)		This study
TB371	168 P2 *sacA*::P_{tapA}-*gfp* (*neo*)		This study
TB372	JH642 *sacA*::P_{tapA}-*gfp* (*neo*)		This study
TB373	DK1042 *sacA*::P_{tapA}-*gfp* (*neo*)		This study
TB375	168 Je *sacA*::P_{tapA}-*gfp* (*neo*)		This study
TB393	168 Bo *sacA*::P_{tapA}-*gfp* (*neo*)		This study
TB395	168 Ma *sacA*::P_{tapA}-*gfp* (*neo*)		This study
TB34	DK1042 *amyE*::$P_{hyperspank}$-*gfp* (*cat*)		[173]
TB49	168 Je *amyE*::$P_{hyperspank}$-*gfp* (*cat*)		[169]
TB707	168 Bo *amyE*::$P_{hyperspank}$-*gfp* (*cat*)		This study

TB709	168 P1 *amyE*::$P_{hyperspank}$-*gfp* (*cat*)		This study
TB722	168 Gö *amyE*::$P_{hyperspank}$-*gfp* (*cat*)		This study
TB723	168 Lj *amyE*::$P_{hyperspank}$-*gfp* (*cat*)		This study

(Lab= Laboratory)

Table 2. Primers used in this study.

Primer	***Sequence (5'□3')***	***Target Locus***
oTB110	CGAACTGCCGGACAAATC	*epsC*
oTB111	ACGGGCTCTCCCATATC	*epsC*
oTB130	GGTTATGGCTTTTCAGGATCAAAAC	*swrA*
oTB131	TCTATCAAATATTAAATGGCTTGGATAT	*swrA*
oTB132	CTGTCGTTTCTTTAATATC	*degQ*
oTB133	ACCAGGGATAACGATATCTC	*degQ*
oTB134	GGTGTCAAGCTGTTGATGAG	*sfp*
oTB135	AAGCATCTCCGCCTGTACAC	*sfp*

CHAPTER 2

Chapter 2

Eisha Mhatre, Agnieszka Troszok, Ramses Gallegos-Monterrosa , Stefanie Lindstaedt, Theresa Hölscher , Oscar P. Kuipers, Ákos T. Kovács (2016)
The impact of manganese on biofilm development of Bacillus subtilis
Accepted in Microbiology (1468-1478, doi: 10.1099/mic.0.000320)
(The content and the written parts are similar to the online manuscript; only typographical changes and style formatting have been applied.)

Bacterial biofilms are dynamic and structurally complex communities, involving cell-to-cell interactions. In recent years, various environmental signals were identified that induce the complex biofilm development of Gram-positive bacterium *Bacillus subtilis* have been identified. These signaling molecules are often the media components or molecules produced by the cells themselves, as well as those of other interacting species. The responses can also be due to depletion of certain molecules in the vicinity of the cells. Extracellular manganese (Mn^{2+}) is essential for proper biofilm development of *B. subtilis*. Mn^{2+} is also a component of practically all laboratory biofilm-promoting media used for *B. subtilis*. Comparison of complex colony biofilms in the presence or absence of supplemented Mn^{2+} using microarray analyses revealed that genes involved in biofilm formation are indeed down regulated in the absence of Mn^{2+}. Additionally, Mn^{2+} also affects the transcription of several other genes involved in distinct differentiation pathways of various cellular processes. The effects of Mn^{2+} on other biofilm related traits like motility, antimicrobial production, stress and sporulation were followed using fluorescent reporter strains. This global transcriptome and morphology studies highlight the importance of Mn^{2+} during biofilm development and aids to better understand the phenotype of colony biofilms in *B. subtilis.*

1. Introduction

Environmental cues and the spatial distributions of nutrients govern various microbial interactions, i.e. quorum sensing, sporulation and formation of fruiting bodies[174-177]. The surface attachment and formation of sessile bacterial communities, yielding the so-called biofilms, are also induced by certain concentrations of nutrients and self-produced signaling molecules. Biofilm formation in *Bacillus subtilis* has been extensively studied and various molecules such as self-secreted surfactin, plant polysaccharides, chlorine dioxides, and combination of glycerol and manganese have been reported to induce a cascade of reactions leading to the production of biofilm matrix components[75,86,88,93,101,178]. These signal molecules act on distinct histidine sensor kinases and activate Spo0A, which is also required for sporulation through the phosphorelay pathway[179]. Increase in the level of phosphorylated Spo0A (Spo0A~P) results in de-repression of *epsA-O* and *tapA-sipW-tasA* operons that are involved in the synthesis of exopolysaccharide (EPS) and protein (TasA) matrix components, respectively. EPS and TasA promote the attachment of cells to the surfaces or to each other and give rise to complex biofilm structures that help the cells to form pellicles at the air-liquid interface, architecturally complex colonies or submerged aggregates[64,72]. A surface localized amphiphilic protein, BslA that aids the biofilm surface repellency, protects the matured biofilm[66-68].

Certain levels of Spo0A~P determine the fate of the cell's commitment to biofilm formation or sporulation, and this is coordinated by a phosphorelay mechanism activated by specific membrane-bound kinases, KinA to KinE[178]. While the kinases KinA and KinB are mainly important for efficient sporulation, which requires high levels of Spo0A~P[77,180], KinC and KinD play a role in induction of biofilm development with low levels of Spo0A~P[75,91]. During the late log phase, cells face many challenges such as depletion of nutrients, oxygen stress, production of toxins and waste molecules, and the presence of surfactin-like molecules that cause membrane leakage[101]. These molecules act as environmental cues leading to the activation of kinases that in turn facilitate the transfer of phosphate group via Spo0F and Spo0B to Spo0A. Several other global transcriptional regulators, like AbrB, DegS/DegU, SlrR, SinI/SinR contribute to the complex signaling pathway and interconnected processes aiding the biofilm development of *B. subtilis*[75,178,181]. Various biofilm-related developmental processes were identified in *B. subtilis* biofilms involving rugose colony structures[93], reduction of cell motility[109], production of antimicrobial peptides like sporulation killing factor (Skf) and sporulation delay protein (Sdp)[91], ESP and TasA secretion or ϒ-poly-DL-glutamic acid production[63].

In this study, we report the impact of manganese (Mn^{2+}) on colony biofilm development and related cellular processes in *B. subtilis* laboratory strain 168 (hereafter WT168). Manganese ions have diverse functions in living cells: Mn^{2+} containing metalloenzymes are

required for oxidative photosynthesis and various metabolic pathways including the 3-phosphoglycerate
mutase, a glycolytic enzyme[182]. Mn^{2+} plays a crucial part in several developmental pathways in bacteria[183]. Particularly, those belonging to the genus *Bacillus* where reportedly it acts on diverse cell division proteins, including DnaA[98]. Moreover, Mn^{2+} is required for the initiation of sporulation by acting as obligate cofactor for the enzyme phosphoglycerate phosphomutase[184]. Due to the importance of Mn^{2+} in growth and maintenance of cytoplasmic processes in *Bacilli*, its transport and homeostasis have been actively studied[183]. Suboptimal concentrations of Mn^{2+} result in decreased single or mixed species biofilm formation of *Lactobacillus plantarium*[185]. Interestingly, recent study has highlighted the requirement of Mn^{2+} as a cofactor in glycerol mediated robust colony biofilm initiation of *B. subtilis* NCIB 3610 under non-biofilm inducing conditions[93].
Our transcriptional analysis of colony biofilms grown in the presence or absence of supplemented Mn^{2+} showed that several intertwined processes were down regulated when Mn^{2+} was not supplemented to the medium. The colony structures lacked the white rugose patterns that we describe as chalky patterns; which otherwise are seen in the presence of Mn^{2+}. Testing selected processes that were down regulated in colonies without the addition of Mn^{2+} to the medium, we identified *gerR* as important gene for the formation of the chalky patterns in colonies.

2. Results

2.1 Mn^{2+} influences robust pellicle formation and rugose colony structure

To examine the importance of Mn^{2+} on the biofilm-proficient laboratory strain WT168, pellicle and colony structures were studied with or without addition of Mn^{2+} in the media. 2xSG medium was utilized, as this medium efficiently promotes the formation of complex biofilm structures of *B. subtilis* WT168 compared to the previously used MSgg minimal medium for wild isolates of *B. subtilis* [186]. No pellicle formation was observed in the absence of added Mn^{2+} in the 2xSG medium (Figure 1A). Intrigued by this observation, we also tested undomesticated strain NCIB 3610 in MSgg medium in the absence of $MnCl_2$. The pellicle so formed was weak and fragile as compared to the normal pellicle in presence of manganese (Figure 1A). The inability of *B. subtilis* cells to form robust pellicles in the absence of Mn^{2+} suggests that it is essential for the proper induction of this developmental pathway. Furthermore, omitting any other ion component of the 2xSG medium, other than Mn^{2+}, had less or no effect on pellicle formation (data not shown).
Consequently, the colony biofilms showed distinguishable patterns on agar plates with and without added Mn^{2+}. Colony biofilms are rugose with vein-like structures projecting from the agar surface and bundles of cells chained together in a parallel pattern[72,143]. A close examination of colony biofilms in WT168 reveals concentric white chalky patterns that

become less and less evident at the edges of the colony. These chalky patterns were absent in

colonies grown on 2xSG medium without addition of Mn^{2+} making the colonies appear pale (Figure 1B), but not as shiny as strains lacking EPS production (e.g. *epsG* mutant descrined in[151]). Similar observations were made when colonies were grown on LB agar supplemented with either glucose or glycerol in the absence and presence of added Mn^{2+} (Figure 1C). In absence of added Mn^{2+} in the MSgg medium, even NCIB 3610 showed pale colonies lacking the white chalky patterns (Supporting Information for Chapter 2, hereafter, S2 Figure 1).

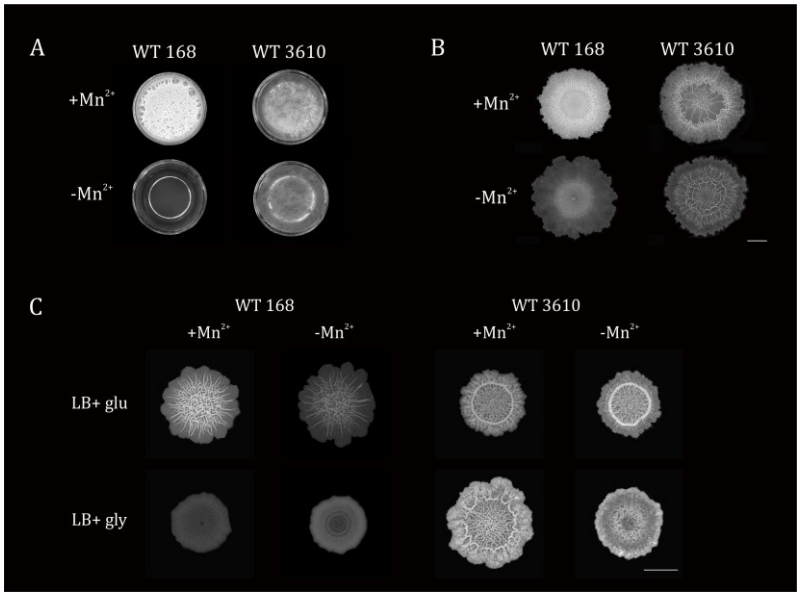

Figure 1. Effect of Mn^{2+} on B. subtilis biofilms. Air-medium pellicle (A) and complex colony structures (B and C) of laboratory (WT 168) and undomesticated (NCIB 3610) *B. subtilis* are shown in various media with or without supplemented Mn^{2+}. The colony structures were assayed in Mn^{2+} proficient or deficient conditions on 2xSG (B) or LB medium with glucose (0.1%) or glycerol (1%) (C). The scale bars at the lower right corner in panel B and C represent 5mm.

2.2 Transcriptional profiling of biofilm colonies grown with different Mn^{2+} concentrations

We were interested to check whether other processes within colony biofilms are also altered due to the the lack of Mn^{2+}; in other words, if Mn^{2+} has a global and important effect in biofilm development.

In order to pursue this query, colony biofilms were harvested from 2xSG medium agar plates with and without supplemented Mn^{2+}. Whole genome DNA-microarray experiments were performed on these colonies that revealed the significant up- and down-regulation of transcription of 133 and 305 genes, respectively (S2 Table 1), by at least fourfold (Bayesian p value $<10^{-4}$). The list of differentially transcribed genes was extensive, involving about 10% of the genes on the genome of *B. subtilis*, and included various basic metabolic processes as well. Therefore, Mn^{2+} may play a pleiotropic role in the colony biofilm development of *B. subtilis*. As expected, genes related to Mn^{2+} transport (*mntA*, *mntB*, *mntC* and *mntH*) were up-regulated in the absence of supplemented Mn^{2+} in the

medium (S2 Table 1). Microarray results clearly showed that the genes related to the biofilm formation (e.g. *epsA-O* and *tapA-sipW-tasA* operons) and sporulation (including various *spo*, *cot*, *sps*, *ssp*, *ger* genes) are down regulated when Mn^{2+} is not supplied in the medium (S2 Table 1).

Interestingly, at the same instant when biofilm formation is reduced, genes related to flagellar motility were transcribed at a higher level in colony biofilms grown on Mn^{2+} depleted medium.

Transcriptions of various other genes related to antimicrobial peptide production (e.g. *sboA*, *skfA-E*, and *sdpA-D*), sporulation (*spoIIA, gerR*), iron uptake in cells (*ymfD)*, sulfate reduction (*yitB)*, and few genes of unknown functions (*ywoF*) were downregulated when Mn^{2+} was not supplied in the 2xSG medium.

2. 3 Role of Mn^{2+} in sporulation results in the presence of chalky patterns

Previous studies on sporulation in planktonic cultures have demonstrated that Mn^{2+} plays a role in activating the key enzymes needed for spore formation in *B. subtilis.* These studies report that Mn^{2+} affects the initiation of sporulation and is a critical component of the media used for these studies already during the early growth phases before the spores appear; as the subsequent addition of Mn^{2+} salts did not facilitate spore formation[97]. Later studies linked Mn^{2+} to phosphoglycerate phosphomutase, an enzyme needed for the sporulation in the basic sporulation media[184]. To confirm whether the chalky pattern of complex colonies is caused by the presence of spores and not just cell debris[187], we observed the colony biofilms of a *sigF* mutant that had a sporulation defect. The complex colony of the *sigF* mutant lacks the chalky pattern even in the conditions where Mn^{2+} is present, similar to WT168 grown in absence of Mn^{2+} (Figure 2A). Thus, the sporulation pattern in colonies is affected by the absence of Mn^{2+}, and spores are important in regards to the appearance of the chalky structures.

Transcriptome analysis done on colonies harvested from the medium with and without supplemented Mn^{2+} revealed that sporulation process and the genes related to the formation of spore coat proteins (*gerPB*, *gerPD* and *gerPE*) are down regulated in absence of Mn^{2+}. In our screening for mutants with altered biofilm development (see the description of screening in the subsequent texts) that phenotypically lack the chalky patterns, the *gerR* mutant was observed to show the reduction in the chalky patterns even in the presence of Mn^{2+}. In lack of Mn^{2+}, the colony structure further reduced (Figure 2A). The structures were restored partially after re-introducing the *gerR* gene into the *amyE* locus of the *gerR* mutant strain. Sporulation efficiency in complex colonies was also quantified by enumerating germinated spores after the heat treatment. We observed that the spore count was reduced in the absence of Mn^{2+} in the growth medium in both WT168 and *gerR* (Figure 2B). The *sigF* mutant colonies were checked as control as this mutant is

reported to be defective in spore formation[188].

It was previously shown that although GerR does not appear to play a direct role in the expression of genes, many σ^E- and SpoIIID- controlled genes are down regulated in its absence[189]. GerR also plays a role in spore coat development[190] and hence, the alterations in spore properties might explain the absence of the white rugose structures and the pale colony appearance. However, the colony morphology of a *cotC* mutant exhibiting a defect in the outer spore coat protein shows no phenotypic differences in colony structure (S2 Figure 2)

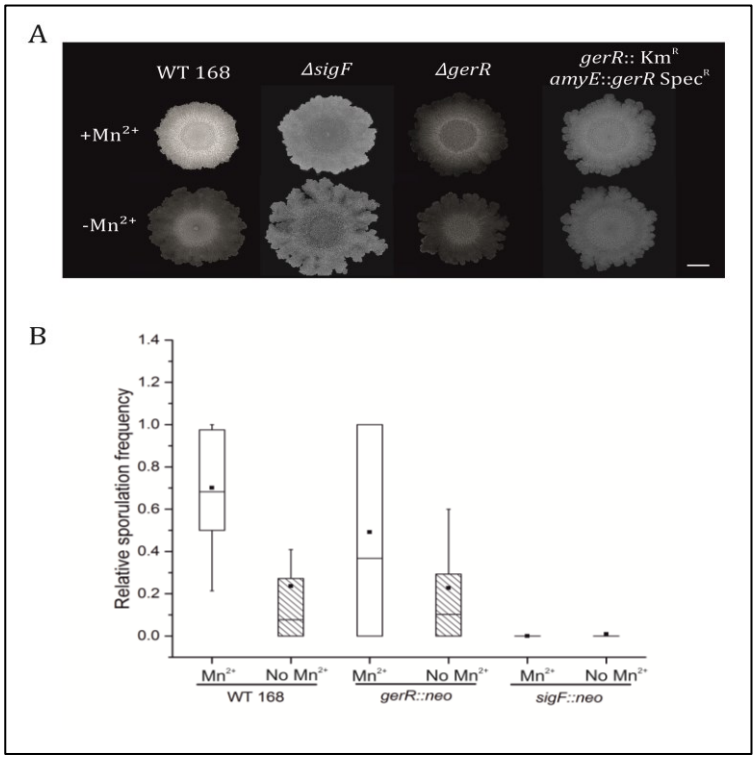

Figure 2. Mutation in gerR affects rugose patterns in B. subtilis colonies. (A) Colony structures in *sigF* and *gerR* mutants were tested in presence and absence of supplemented Mn^{2+}. The scale bar at the lower right corner represents 5mm. (B) The relative spore count is shown in WT168, *gerR* and *sigF* colony biofilms in the presence or absence of Mn^{2+} supplemented.

2.4 <u>Mn^{2+} affects the surface coverage in submerged biofilm</u>

To determine whether the presence of Mn^{2+} is also essential for the formation of submerged biofilms, WT168 cells were inoculated on an optical microtiter-plate using medium described previously for submerged biofilm formation in *B. subtilis* [191]. The bottom surface area of the wells containing Mn^{2+}-supplemented medium was entirely or mostly covered with biofilms while in the wells with Mn^{2+}-limited medium, the surface coverage by cells was reduced (Figure 3). This suggests that Mn^{2+} is required for the cell attachment and/or biofilm development on the submerged surface of the medium.

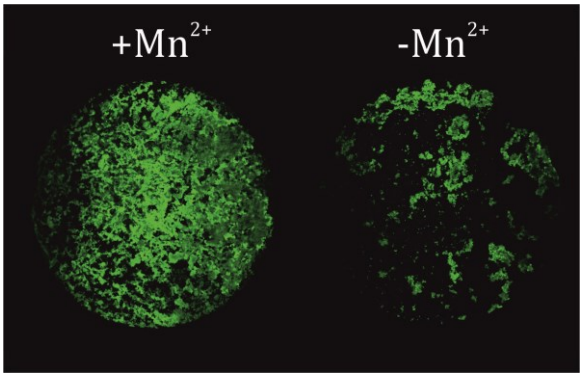

Figure 3. Effect of Mn^{2+} on submerged biofilms. Submerged biofilms were grown for 24 hours at 30^0C and the images were taken using Zeiss CLSM tile scan at 10X magnification. Representative wells are shown for both conditions.

2.5 The presence or absence of Mn^{2+} affects processes including motility, biofilm matrix production, sporulation, and antimicrobial peptide production

To validate the microarray experiments performed on biofilms grown at different Mn^{2+} levels, promoter fusion constructs were used to follow the expression of genes related to motility ($P_{hag\text{-}gfp}$)[192], biofilm matrix protein production ($P_{tapA\text{-}yfp}$)[193], sporulation ($P_{spoIIE\text{-}gfp}$)[194] and antimicrobial peptide production ($P_{sboA\text{-}gfp}$). The expression of these genes was followed in microtiter plates for 20 hours using 2xSG medium with and without the addition of Mn^{2+} (Figure 4). Under these well-mixed growth conditions, expression of the *hag* gene was similar at the start of the growth, but showed a diminished expression in Mn^{2+} supplemented medium during the stationary phase of growth. The $P_{tapA\text{-}yfp}$ and $P_{spoIIE\text{-}gfp}$ constructs showed gradual but linear increase in expression in the cells grown in the presence of Mn^{2+} and were at their peak during the stationary phase. The expression profile of the *sboA* gene, involved in production of the cyclic bacteriocin subtilosin [195], showed a linear increase, with a peak at 12^{th} hour of the growth followed by reduction in stationary phase. These experiments clearly showed the Mn^{2+}-dependent expression of selected genes not only in colony biofilms, but also in planktonic cells grown in well agitated, but otherwise biofilm inducing medium. It was also examined if Mn^2 affects the growth of WT168 in liquid or solid 2xSG medium. The fact that the colony sizes in the presence and absence of Mn^2 were comparable suggests no severe growth defect. The growth rates of WT168 under planktonic conditions with or without Mn^{2+} addition were similar except that the final yield in absence of supplemented Mn^{2+} was slightly lower (S2 Figure 2).

2.6 Mn^{2+} affects colony biofilm development in *B. subtilis* WT168 independently of KinC and KinD histidine kinases

The effects of signaling molecules that induce biofilm formation and sporulation in *B. subtilis* are often facilitated via membrane bound histidine kinases that increase the level of

phosphorylated Spo0A through a phosphorelay [75,101]. The presence of molecules such as surfactin, nystatin and their derivatives was suggested to induce pore formation in the cell membrane leading to potassium leakage, which activates the signaling domain of KinC[80,81,196]; however, the impact of surfactin on KinC- mediated activation is debated and might be condition or strain specific. In addition, the plant polysaccharides and secreted sugars activate KinD[88,92]. Mn^{2+} was suggested to act as a cofactor mediating phosphate transfer in response to the presence of glycerol under biofilm non-promoting conditions[93]. Therefore, the effect of inactivating *kinC* or *kinD* genes was assayed on colony biofilm development with and without Mn^{2+} addition. While mutations in either or both of *kinC* and *kinD* resulted in altered colony architecture, the biofilm colonies on 2xSG medium with or without addition of Mn^{2+} still differed suggesting that Mn^{2+} influences colony development at least partially independent of the KinC and KinD kinases (Figure 5).

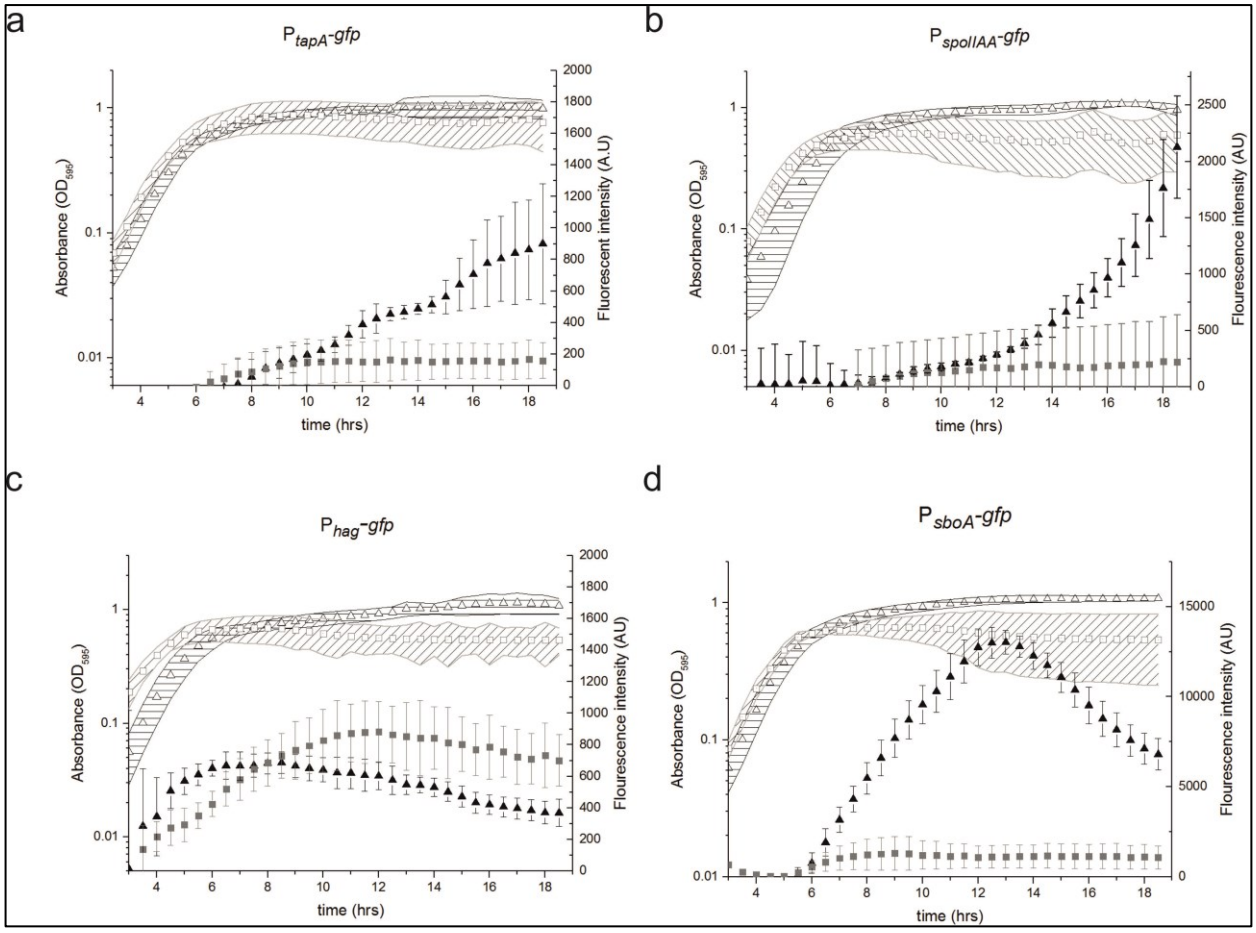

Figure 4. Expression levels of genes playing role during onset of biofilm formation.

Expression levels of *tapA* (a), *spoIIAA* (b), *hagA* (c) and *sboA* (d) genes were measured in TECAN during agitated growth with (filled triangles) and without (filled squares) supplementation of Mn^{2+} in the 2xSG

medium. The optical densities of the cultures are shown with (open triangles) or without (open squares) supplementation of Mn^{2+} in the medium.

2.7 Testing the impact of selected Mn^{2+}-influenced processes on colony biofilm development

The microarray analysis showed that the transcription of several genes was reduced in the medium depleted for Mn^{2+}, including that of the genes related to biofilm formation. Could any of these genes be involved in rugose colony formation? To identify additional genes that are required for the development of architecturally complex colonies, we have selected the so-called '*y*' genes that were annotated as the genes of unknown functions when the genome sequence was published[141]. The library of insertion mutants (Bacillus functional analysis, BFA) was used that was created previously in various European laboratories and contains around 1200 mutants of the ~2600 '*y*' genes[197]. The genes that had an altered expression in this transcriptome study with respect to supplemented Mn^{2+} levels were selected and mutants were tested for colony formation on 2xSG. From this screen, several BFA mutants were identified with potentially altered colony biofilm structure. As these BFA strains were created in various laboratories in Europe, genomic DNA was extracted and transformed into WT168 to circumvent the effects that might have originated from the usage of genetically distinct parental strains. Since most BFA mutants used for screening were constructed by single recombinant event, selected down regulated genes (*yitB*, *ywoF*, *gerR*) were chosen to create double recombinant knockouts and to check the colony morphology. As presented earlier, the *gerR* mutant had altered colony morphology. However, the other mutants (*yitB* and *ywoF*) showed no altered colony morphology under colony biofilm conditions (S2 figure 2).

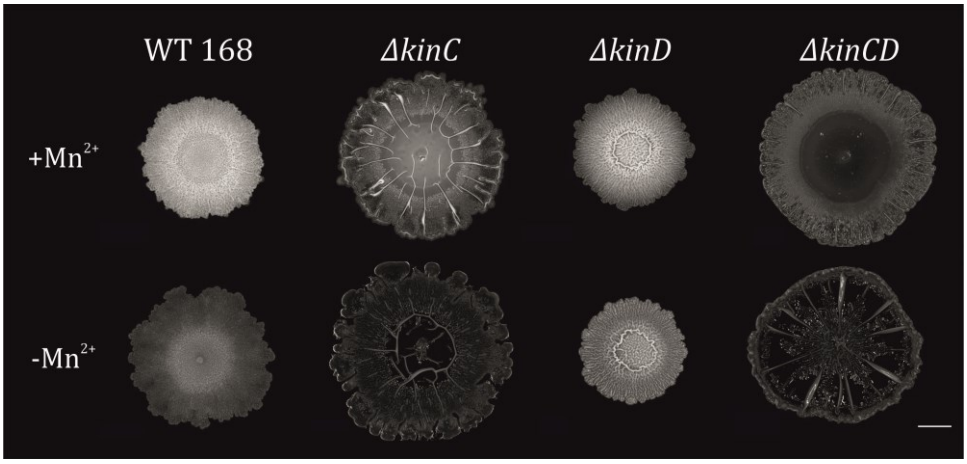

Figure 5. Mn^{2+} effect on colony structures is independent of the membrane bound histidine kinases, KinC and KinD. The colony structures of WT168, *kinC*, *kinD* single and double mutants are shown with

and without supplemented Mn^{2+} in the 2xSG medium. The scale bar at the lower right corner represents 5mm.

3. Discussion

In this study, the role of an essential and abundantly occurring element Mn^{2+} is examined during biofilm formation and during the processes that are orchestrating *B. subtilis* biofilms. Most media used in studying biofilm formation in *B. subtilis* include Mn^{2+} salts as one of their minor, but important components[188]. Recently, glycerol in combination with Mn^{2+} under biofilm non-promoting conditions, i.e. LB medium, was described to stimulate the formation of structured colony biofilms in *B. subtilis* NCIB 3610. WT168 grows better in presence of glucose than glycerol and we see that Mn^{2+} itself has major impact on its characteristic white rugose structures that we describe as chalky patterns. Moreover, omitting Mn^{2+} salts in a rich medium such as 2xSG stalls the pellicle formation.

It is clear that Mn^{2+} dependent processes cause the chalky structures and also aid in pellicle formation. We proceeded to perform DNA microarray studies on colonies grown in the presence and absence of supplemented Mn^{2+} to identify the up- and down-regulated processes in WT168 during biofilm development.

The list of down regulated processes includes biofilm formation (*epsA-O, tapA-sipW- tasA* operons), sporulation genes and regulators (*spo, sps, spp, cot, ger* genes), amino acids and sugar transporters (*yveA, yocN*), surfactin production, cannibalism and antimicrobial peptide production (*sboA, sdpA, skf*). Importantly, the transcriptions of several differentially expressed genes, including the sporulation related genes, biofilm development genes and the *skf* and *sdp* operons are also regulated by different levels of phosphorylated Spo0A[198]. This suggests that Spo0A~P levels might be altered in the absence of Mn^{2+}. Notably, a few processes were also up regulated, such as ion transporters especially Mn^{2+} (*mntABC, mntH*), Zn^{2+} (*zosA*) and Fe-S clusters (*sufC*), motility (*hag*), cell shape and elongation (*rodA*) and the regulators of stress and phosphorelay pathways (*yaaT*). The screening of BFA single recombinant mutant library to identify novel biofilm related genes, showed an overlap with the differently regulated genes. However, clean deletions of some of these candidate genes (constructing recombinant deletions), except for *gerR*, provided no altered biofilm phenotypes suggesting that the identified biofilm mutants during the screening were false negatives possible because of the constructive method of BFA mutants or due to the use of different 168 derivatives for the library construction.

Previous studies have highlighted the crucial role of Mn^{2+} during the initiation and germination of spores in many bacteria belonging to the genus, Bacillus[184]. We propose that the alteration in sporulation properties of the colony biofilms explain the absence of

the chalky white patterns observed in mature colony biofilms of *B. subtilis* in the absence of Mn^{2+}. The sporulation mutant *sigF* and late sporulation regulator *gerR* show either absence of or reduced chalky structures respectively, in 2xSG medium; whereas complementing *gerR* restored the patterns partially. Using a different strain (NCIB 3610) and a different medium (MSgg), Branda and colleagues (2001) showed that the absence of spores did not affect the formation of aerial structures, and the colonies formed by a *sigF* mutant were similarly rugose to the wild-type strain[72]. This controversy might be due to the differences between the strains or media used.

GerR regulates the expression of late sporulation genes, mainly the sigma factors and the spore-coat proteins[189,199]. In its absence, cells are still able to form spores and this sporulation efficiency is further reduced in absence of Mn^{2+}. Thus, our results clearly suggest that both early and late sporulation related processes are essential for the chalky patterns. These results efficiently combine the colony biofilm characteristics with respect to the sporulation patterns. During biofilm development of *B. subtilis*, many different cell-types coexist and the population is phenotypically diverse. Similarly, sporulation is also a heterogeneous process as only a sub-population of cells activates the genes related to this process. This might explain why the chalky patterns are not present uniformly in the colony and are mostly evident in a periphery around the center of the colony.

We additionally screened mutants of genes that down regulated in our microarray experiment, however, no other Mn^{2+} dependent process changes the colony morphology distinctively from the wild type. Monitoring the gene expression of certain biofilm related processes, e.g. matrix production, cannibalism via the Skf/Sdp protein, and sporulation, confirmed that Mn^{2+} plays a role in their expression as well as regulatory makeup. Divalent anions are known to play a role in regulatory and metabolic networks, however the effect of Mn^{2+} is more pronounced under biofilm inducing conditions in *B. subtilis.* The straightforward mechanism for Mn^{2+} mediated induction of biofilm processes is yet not clear. It can be said that Mn^{2+} plays diverse functions that are entangled between the growth and other biofilm related processes.

In this study, we defined the colony characters on the basis of concentric chalky patterns that are observed in WT168 when grown on 2xSG medium in presence of Mn^{2+}. This study highlights the importance of Mn^{2+} during biofilm development and provides information to help the identification of genes with Mn^{2+} dependent expression that could be related to biofilm formation.

4. Methods

4.1 Strains and growth media

B. subtilis strains used and generated in this study are listed in Table 1. The overnight cultures were grown in LB medium (Lysogeny broth, Carl Roth, Germany; 1% tryptone,

0.5% yeast extract, 0.5% NaCl). For architecturally complex colonies, 2x Schaeffer's sporulation medium containing 0.1% glucose (2xSG) and 1.5% agar was used containing 0.1mM of $MnCl_2$, unless omitted[154,186]. The colony biofilms were also assayed on LB medium containing 0.1mM $MnCl_2$ and 0.1% glucose or 1% glycerol with 1.5% agar and MSgg medium as described earlier[72]. For submerged biofilms, biofilm growth medium (BGM) consisting of LB supplemented with 0.15 M $(NH_4)_2SO_4$, 100 mM $K_xH_yPO_4$ (pH 7), 34 mM Na-citrate, 1 mM $MgSO_4$, 0.1% glucose and 0.1mM $MnCl_2$ was used as described previously[191]. *Escherichia coli* strain (MC1061) used for molecular cloning was grown at 37℃ in LB medium. Antibiotics were included wherever appropriate at the following concentrations: 7.5 µg/ml of tetracycline, 5 µg/ml of kanamycin, 100 µg/ml of spectinomycin, 5 µg/ml of chloramphenicol, 100 µg/ml of ampicillin, and 12.5 µg/ml of lincomycin together with 1 µg/ml of erythromycin (for Mls resistance).

4.2 Colony Biofilm and imaging

Overnight grown *B. subtilis* cultures were inoculated at 1% concentration in 2xSG medium in 24 well plates for pellicle biofilms or 2 µl was spotted on 2xSG, MSgg or LB medium (with $MnCl_2$ and glucose or glycerol) agar plates for observing complex colonies, and incubated at 30°C for 3 days. Both pellicle and colony biofilms were observed after 3 days and images were taken using an AxioZoom V16 microscope equipped with an AxioCam MRm monochrome camera (Carl Zeiss Microscopy GmbH, Jena, Germany).

4.3 Strain constructions

The mutants and the reporter gene constructs used in this study were introduced into parental *B. subtilis* strain 168 (WT168) by transforming genomic DNA extracted from various strains listed in the Table 1 using 2-step transformation protocol[200]. To construct the P*sboA-gfp* fusion, the *sboA* promoter region was PCR amplified using primers oEM3 and oEM4 (Table 2), digested with *Eco*RI and *Nhe*I enzymes, ligated into the corresponding sites of pGFP-rrnB[201], and transformed into *E. coli*. The resulting plasmid, pTB65 was then transferred into *B. subtilis* WT168 and double recombination into the *amyE* locus was verified. For the construction of mutants, Δ*yitB* and Δ*ywoF*, the upstream and the downstream regions of the genes were PCR amplified (see Table 2 for primers sequences) and sequentially cloned into the *Kpn*I-*Sal*I and *Bam*HI-*Xba*I sites of pTB120[202]. The resulting plasmids pTB591 and pTB592 were then transferred into *B. subtilis* and deletions were verified by PCR. The sequences of all newly generated plasmids were verified by DNA sequencing at GATC Biotech (Cologne, Germany). Transformants obtained using genomic DNA of mutant strains with antibiotic cassettes were verified using PCR with primers indicated in Table 2.

4.4 Transcriptome analysis

Colonies were harvested after 3 days of growth on 2xSG medium with or in the absence of Mn^{2+} supplementation. RNA extraction was performed with the Macaloid/Roche protocol[186] with two additional steps of phenol-chloroform washing. RNA concentration and purity were assessed using a NanoDrop ND-1000 Spectrophotometer (Thermo Fisher Scientific). RNA samples were reverse transcribed into cDNA using the Superscript III reverse transcriptase kit (Invitrogen, Carlsbad, USA) and labeled with Cy3 or Cy5 monoreactive dye (GE Healthcare, Amersham, The Netherlands). Labeled and purified cDNA samples (Nucleospin Extract II, Biokè, Leiden, The Netherlands) were hybridized in Ambion Slidehyb #1 buffer (Ambion Europe Ltd) at 48°C for 16 h. The DNA-microarrays were constructed as described previously[203]. Briefly, specific oligonucleotides for all 4.107 open reading frames of WT168 were spotted in duplicate onto aldehyde-coated slides (Cell Associates) and further handled using standard protocols for aldehyde slides. Slide spotting, slide treatment after spotting and slide quality control were done as before[204]. After hybridization, slides were washed for 5 min in 2x SSC with 0.5% SDS, 2 times 5 min in 1x SSC with 0.25% SDS, 5 min in 1x SSC 0.1% SDS, dried by centrifugation (2 min, 2.000 rpm) and scanned in GenePix 4200AL (Axon Instruments, CA, USA). Fluorescent signals were quantified using ArrayPro 4.5 (Media Cybernetics Inc., Silver Spring, MD, USA) and further processed and normalized with MicroPrep[203]. CyberT[205] was used to perform statistical analysis. Genes with a Bayes P-value of $\leq 1.0 \times 10^{-4}$ were considered significantly affected. Microarray data have been deposited in the Gene Expression Omnibus database (Accession No. GSE61232).

4.5 Fluorescence measurement

B. subtilis strains harboring given promoter fusion constructs were grown overnight in LB medium and inoculated at 1% concentration in 2xSG medium with or without supplementation of Mn^{2+} into 96-well plates and incubated at 30°C under continuous shaking using a microplate reader (Infinite 200 PRO, Switzerland). i-Control software was used to monitor the fluorescence (gain used: 40) with GFP [excitation at 485 nm (20-nm width) and emission at 535 nm (10-nm width)] or YFP filter sets [excitation at 495 nm (10-nm width) and emission at 540 nm (25-nm width)] every 15 minutes for 20 hours. Emission from medium only control wells was subtracted from the data and normalized to the optical density of the culture measured at 595 nm. The graphs were plotted using OriginLab 2015 software.

4.6 Submerged biofilm assay

The fluorescent-labeled cultures of WT168 (TB48)[169] were pre-grown in LB medium and transferred to BGM medium to obtain overnight cultures at 37°C under well-shaken

conditions. Next, 2 µl of overnight culture was added to 200 µl of BGM medium with and without added Mn^{2+} in Falcon 96 well black flat bottom TC-treated Microplate (Corning Life Science, USA) and incubated at 30°C under static conditions. After 6 hours, the samples were mixed thoroughly and the medium was changed every 12 hours. After 24 hours, the biofilms were observed using a Zeiss LSM780 confocal laser-scanning microscope fitted with a 488-nm laser and an EC Plan-Neofluar 10× differential interference contrast M27 objective (Carl Zeiss Microscopy GmbH, Jena, Germany). Tile scan of the entire well was taken and the images were captured with Zen Black software (Carl Zeiss Microscopy GmbH, Jena, Germany).

4.7 Sporulation assay

The 3-day-old grown complex colonies of WT168, Δ*gerR* and Δ*sigF* from 2xSG agar plates with and without $MnCl_2$ were harvested and suspended in 1 ml of 2xSG medium. The colony clumps were sonicated (2x 12 pulses of 1s with 30% amplitude; Ultrasonic Processor VCX-130, Zinsser Analytics, Frankfurt am Main, Germany). Cells were then diluted and plated on LB agar medium to determine the viable colony count. Samples were then incubated at 80°C for 20 mins and plated on LB agar medium to record the spore count. Sporulation efficiency was calculated by dividing the spore number by the viable cell number[206]. The experiment was performed twice on independent occasions with 4 replicates each time.

Table 1 Strains and plasmid used.

Strain	***Genotype****	***Reference or source***
B. subtilis		
168 1A700	*trpC2*	Laboratory collection [207]
NCIB 3610	undomesticated wild type	[72]
GC260	PY79 *ΔgerR*::Km^R	[199]
TB61	168 *ΔgerR*::Km^R	This study
DL227	NCIB 3610 *ΔkinC*::Mls^R	[80]
DL153	NCIB 3610 *ΔkinD*::Tet^R	
TB148	168 *ΔkinC*::Mls^R	This study
TB149	168 *ΔkinC*::Mls^R *ΔkinC*::Tet^R	This study
TB126	168 *ΔkinD*::Tet^R	This study
TB417	168 *ΔgerR*:: Km^R, *amyE*::*gerR* $Spec^R$	This study
TB65	168 *amyE::P_{sboA}-gfp* Cm^R	This study
	168 *P_{hag}-gfp* Cm^R	[192]
	168 *$P_{spoIIAA}$-gfp* Cm^R	[194]
	168 *ΔsigF*::Km^R	Ref
DL821	NCIB 3610 *lacA::P_{tapA}-yfp* Mls^R	[193]

TB64	168 *lacA::P$_{tapA}$-yfp* Mls^R	This study
TB49	168 *amyE::*Phyperspank- *gfp* Cm^R	[169]
RL52	*ΔcotC::* Km^R *trpC2*	[208]
TB416	168 *ΔcotC::* Km^R	This study
TB553	168 *ΔyitB::* Km^R	This study
TB554	168 *ΔywoF::* Km^R	This study
E. coli		
MC1061	F$^-$ Δ(*ara-leu*)769 [*araD*139]$_{B/r}$ Δ(*codB-lacI*)3 *galK*16 *galE*15 λ$^-$ e14$^-$ *mcrA*0 *relA*1 *rpsL*150(Str^R) *spoT*1 *mcrB*1 *hsdR*2(r$^-$m$^+$)	[209]
Plasmids	***Genotype***	***Reference***
pGFP-rrnB	*amyE*, P$_{rrnB}$-*gfp*+ , Cm^R, Spec^R, Amp^R	[201]
pTB65	P$_{sboA}$ cloned into pGFP-rrnB, Amp^R, Cm^R	This study
pWK-Sp	*amyE*, Amp^R, Spec^R derived from pDG1727	[210]
pTB417	*gerR* cloned into pWK-Sp, Amp^R, Spec^R	This study
pTB120	Nm^R cassette cloned into pBluescript SK +	[202]
pTB591	Nm^R cassette with upstream and downstream regions of *B. subtilis yitB*	This study
pTB592	Nm^R cassette with upstream and downstream regions of *B. subtilis ywoF*	This study

Table 2 Oligonucleotides used

Oligo name	***Sequence***	***Target locus or marker***
oEM3	5'-GTGGTGCGGAATTCGATGAC-3'	*sboA* promoter
oEM4	5'-CGAGGCTAGCGACAGCTTTTTTCATAATTG-3'	*sboA* promoter
oEM25	5'-TGGACAGTTGCGGATGTACTTCAG-3'	*km* marker check
oEM28	5'-TTCAGCCACTGCATTTCC-3'	*spec* marker check
oEM33	5'-TCCGCTGTCAACGATACTTC-3'	*gerR* check primer
oEM34	5'-TGAAGCTGATGCTGCTTCAC-3'	*gerR* check primer
oEM35	5'-GATTGGCCGCTTACACATGG-3'	*neo* marker check
oEM44	5`- ATGGATCCTGCGGATCATACAACGG -3`	*gerR* complementation
oEM45	5`- ATTCTAGAGATGACACCGGGAGAGTCTGC -3`	*gerR* complementation
oEM6	5`- GCAGGTCGACAACGAAAGCGAGGATGACAG -3`	*ywoF* upstream
oEM46	5'- ATGGTACCGCGTTCGGAGAGCCGATTTG -3'	*ywoF* upstream
oEM47	5'- ATGGATCCTGATTCACCTGCGCGGCCTG -3'	*ywoF* downstream
oEM48	5'- ATGCGGCCGCCAGCCTTTGCGCTGTTTATG -3'	*ywoF* downstream
oEM13	5`- CGAGGTCGACAACACATCGAGCTCATC -3`	*yitB* upstream
oEM49	5`- ATGGTACCCGCAGCCGTTACCACATTTG -3`	*yitB* upstream
oEM50	5`- ATGGATCCGATGAGAGGGCTGGAAGATG -3`	*yitB* downstream
oEM51	5`- GCTCTAGATCTCCGACAAGTGGGTGAAG -3`	*yitB* downstream
oEM5	5'- TGATATTGCTGGAGGATTGG -3'	*ywoF* check primer

oEM8	5`- ATTGCCGCTGATATTATTCC -3`	*ywoF* check primer
oEM21	5`- TTTGGGCGTCGTATGTTCC -3`	*yitB* check primer
oEM22	5`- CGGCTATCGCATCTTTG -3`	*yitB* check primer

[* Km^R - kanamycin resistance, Cm^R - chloramphenicol resistance, Tet^R - tetracycline resistance, $Spec^R$ - spectinomycin resistance, Amp^R - ampicillin resistance, Mls^R – macrolide resistance (erythromycin+lincomycin)]

Acknowledgments

We thank Ezio Ricca (Federico II University), and Daniel Lopez (University of Würzburg) for kindly providing strains. The laboratory of Á.T.K. was supported by a Marie Skłodowska Curie career integration grant (PheHetBacBiofilm), grants KO4741/2-1 and KO4741/3-1 from the Deutsche Forschungsgemeinschaft (DFG). E.M., T.H., and R.G.-M. were supported by Jena School for Microbial Communications (JSMC), International Max Planck Research School, Consejo Nacional de Ciencia y Tecnología-German Academic Exchange Service (CONACyT-DAAD) fellowships, respectively. A.T. was supported by an Erasmus scholarship in Groningen.

Supporting Information for this Chapter is on page no: 126.

CHAPTER 3

Chapter 3

Eisha Mhatre, Anandaroopan Sundaram, Theresa Hölscher, Mike Mühlstädt, Jörg Bossert, Ákos T. Kovács (2016)

Presence of calcium maintains rugose biofilm structure of Bacillus subtilis

Under Review in: Journal of Bacteriology (JB00747-16)

(The content and the written parts are similar to the submitted manuscript; only typographical changes and style formatting have been applied.)

Robust colony formation by *Bacillus subtilis* is recognized as one of the sessile, multicellular lifestyles of this bacterium. Numerous pathways and genes are responsible for the architecturally complex colony structure development. Cells in the biofilm colony secrete extracellular polysaccharides (EPS) and protein components (TasA and the hydrophobin BslA) that hold them together and provide a protective hydrophobic shield. Cells also secrete surfactin with antimicrobial as well as surface tension reducing properties that aid cells to colonize the solid surface. Depending on the environmental conditions, these secreted components of the colony biofilm can also promote this flagellum-independent surface spreading of *B. subtilis*, called sliding.

In this study, we emphasize the influence of Ca^{2+} in the environment on robust colony structures of *B. subtilis*. Interestingly, the availability of Ca^{2+} has no major impact on induction of complex colony formation. However, in the absence of this divalent ion peripheral cells of the colony expand radially at later stages of development causing colony size to increase. We demonstrate that the secreted extracellular compounds, EPS, BslA, and surfactin facilitate colony expansion after biofilm maturation. We propose that Ca^{2+} hinders biofilm colony expansion by modifying the amphiphilic properties of surfactin.

1. The originality and significance

Microorganisms produce complex surface attached biofilms to occupy a certain niche and protect themselves from stressful environmental conditions, however, when nutrients are scare, cells disperse from this shelter. Colonies of *Bacillus subtilis* seem to follow a similar strategy after maturation of the biofilm. This study highlights that in the absence of Ca^{2+}, cells escape outwards from the mature biofilm colony using components of the biofilm matrix and surfactin that is reminiscent of sliding. Surplus Ca^{2+} alters the surfactin generated surface tension reduction therefore possibly inhibiting the colony escape. Environmental factors, including various ions seem to act as important triggers not only in influencing biofilm development, but also during dispersal.

2. Introduction

Bacteria tend to form sessile, multicellular communities under environmental settings, known as biofilms. In these communities, cells embed themselves in secreted compounds that facilitate adherence to surfaces as well as to neighboring cells. The structures of architecturally complex colonies have been correlated to the general ability of bacteria to develop biofilms[72,211]. When establishing a biofilm, cells of the Gram-positive soil dwelling microbe, *Bacillus subtilis* secrete extracellular polysaccharides (EPS), a matrix protein component (TasA), and a hydrophobin protein that assembles on the surface (BslA)[64,66,67,75]. In addition, antimicrobial compounds, including surfactin, are secreted that increase the competitiveness of *B. subtilis* against other microbes[212]. The biofilm matrix components carry out numerous functions in addition to the attachment and the colony structure complexity, such as protection from environmental attacks[68], colony spreading[213], or sliding[104,106]. Importantly, colonies lacking EPS and TasA production have reduced morphologies and appear smooth[64]. Cells devoid of BslA lose their hydrophobicity and are prone to water-soluble antimicrobials[66,67]. These above described components, EPS, BslA and surfactin seem to collectively aid flagellum-independent surface spreading, a collective behavior observed in bacteria[104-106].

The expression and synthesis of these secreted products that facilitate biofilm formation and surface spreading are tightly regulated at the level of transcription and affected by the membrane bound histidine kinases and subsequent cytoplasmic response regulators[75,101,181]. The cytoplasmic and membrane bound histidine kinases (KinA, KinB, KinC, and KinD), in response to dynamic and challenging environmental cues, initiate the phosphorylation of Spo0A (Spo0A~P), the main regulator of various stationary stage processes, via a phosphorelay pathway. The gradual increase in Spo0A~P level influence the cells' commitment towards certain differentiation processes. KinA and KinB activation results in a large pool of Spo0A~P, sufficient for the cells to undergo sporulation[77,180]. Moreover, KinC and KinD were described to respond to a plethora of signals to maintain a

low amount of Spo0A~P that is sufficient to activate the expression of genes responsible for biofilm matrix production[75,101]. Recently, it was demonstrated that KinB and KinC collectively induce *B. subtilis* sliding in a spatiotemporal manner[104]. Apart from being a collective behavior strategy, sliding is also studied in the context of cooperative strategies in bacteria. Heterogeneity in expression of genes required for the secreted components that aid sliding creates a division of labor between surfactin- and matrix-producing cells at the expanding front of the colony[106].

Examination of the factors and processes that influence colony growth and spreading properties in bacteria facilitate our understanding of bacterial population level behaviors. Here, we report that the presence of Ca^{2+} ions in the environment restricts colony expansion following colony biofilm development. The mature colony formation of *B. subtilis* under laboratory conditions requires 3-4 days after which the colonies are rugose, structurally complex and display white chalky patterns attributed to sporulation[72,99]. After maturation of *B. subtilis* biofilms, cells in the middle grow slowly, are encapsulated and well protected, while the peripheral cells continue to grow in the direction of new nutrient sources[132]. Our experiments show that when the growth medium was lacking Ca^{2+} salts, biofilm colonies continue to expand in a way that resembles sliding. Considering that most media used to study biofilm colony structures contain Ca^{2+} salts, this phenomenon is seldom observed. Further, we propose that an interaction between Ca^{2+} and surfactin might be responsible for preventing the colony expansion in the presence of Ca^{2+} in the medium.

3. Results

3.1 Presence of Ca^{2+} prevents cells to spread out from matured biofilm colonies

When previously examining the impact on Mn^{2+} on colony biofilm development of *B. subtilis*[99], we also tested whether the lack of other components in the medium 2×SG has an effect on the colony biofilm development of various *B. subtilis* strains. Interestingly, we observed that the colonies of *B. subtilis* DK1042 (the naturally competent derivative of the undomesticated NCIB 3610) grown on 2×SG plates without the supplemented $Ca(NO_3)_2$ grew normally until day 3, after which the peripheral cells began to spread and the colony size kept on increasing (Figure 1A). To distinguish from simple colony growth, we term this phenomenon as “colony escape” that denotes the radial expansion of cells after biofilm colony maturation. The 2×SG medium contains $Ca(NO_3)_2$ as one of its components. Hence, under normal conditions where all the medium components were supplemented, the colonies were rugose with concentric white chalky patterns around (Figure 1A and [99]). In contrast, when the medium lacked $Ca(NO_3)_2$, the cells at the colony periphery started to expand on the agar surface after 3-4 days of incubation. To test whether omitting Ca^{2+} or NO_3^- triggers the colony escape at this later time point of colony development, other salts

were tested in 2×SG medium. Neither NO_3^- nor other divalent cations restricted colony escape similar to Ca^{2+} (Supporting Information for Chapter 3, hereafter S3 Figure 1).

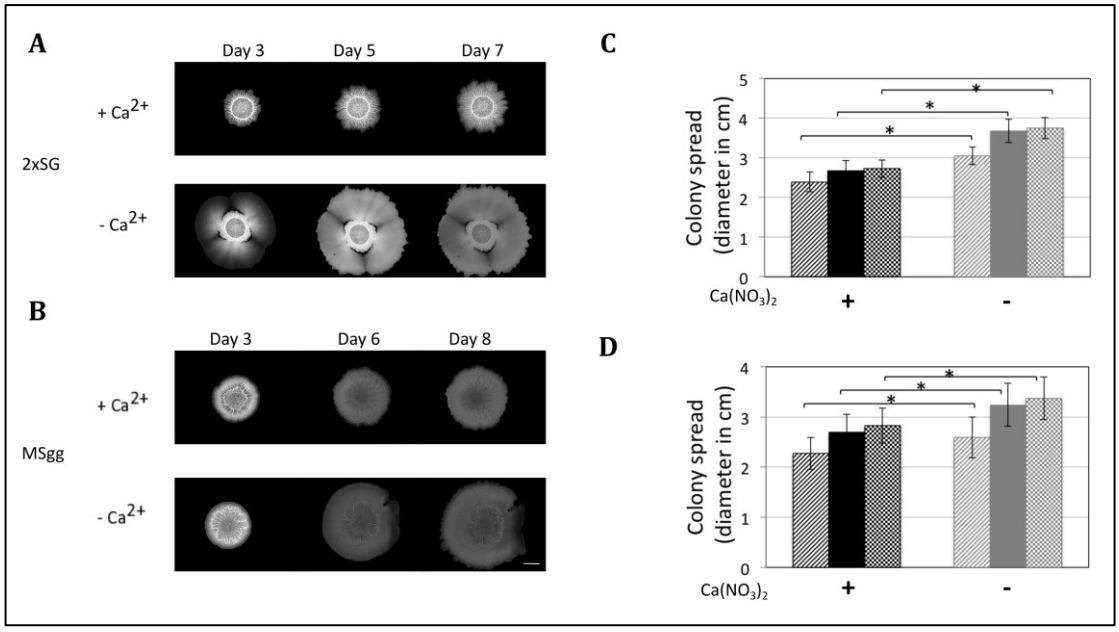

Figure 1. Presence of Ca^{2+} restricts colony escape. Colonies of *B. subtilis* are shown in the presence and absence of Ca^{2+} on 2×SG (A) and MSgg (B) media at different days after inoculation. The scale bar at the lower right corner denotes 5mm. The colony expansion diameters are presented on 2×SG (C) and MSgg (D) media after 3 or 4 (striped), 5 or 6 (filled), and 7 or 8 (checked) days, respectively, after inoculation in the presence (black bars) or absence (grey bars) Ca^2. The error bars indicate 95% confidence intervals. * denotes significant differences ($p<0.05$) analyzed with paired t-test.

In addition, omitting Ca^{2+} in the biofilm inducing minimal medium, MSgg had similar impact on the colony spreading (Fig 1B). Quantitative measurement of the colony size on 2×SG and MSgg medium revealed that in the absence of Ca^{2+}, biofilm colonies spread more and are significantly bigger in size than in the presence of Ca^{2+} (Figure 1C and D). Excluding Ca^{2+} had no major impact on pellicle development on 2×SG medium (S3 Figure 2).

3.2 Ca^{2+} restricts flagellum-independent expansion of biofilm colonies

The colony escape in the absence of Ca^{2+} was also influenced by nutrient depletion, since cells showed no outgrowth when Ca^{2+} was omitted from 4×SG medium that consisted of twice as much nutrients as 2×SG, while colony escape was observed when nutrient were reduced (S3 Figure 2). Dispersal has been described as the ultimate stage of the biofilm lifecycle following nutrient depletion and overcrowding of the sessile population[2]. Colony escape might be an alternative mechanism to those observed during dispersal. Fleeing

from the biofilm is generally facilitated by single cell motility or via small cluster of cells breaking off.

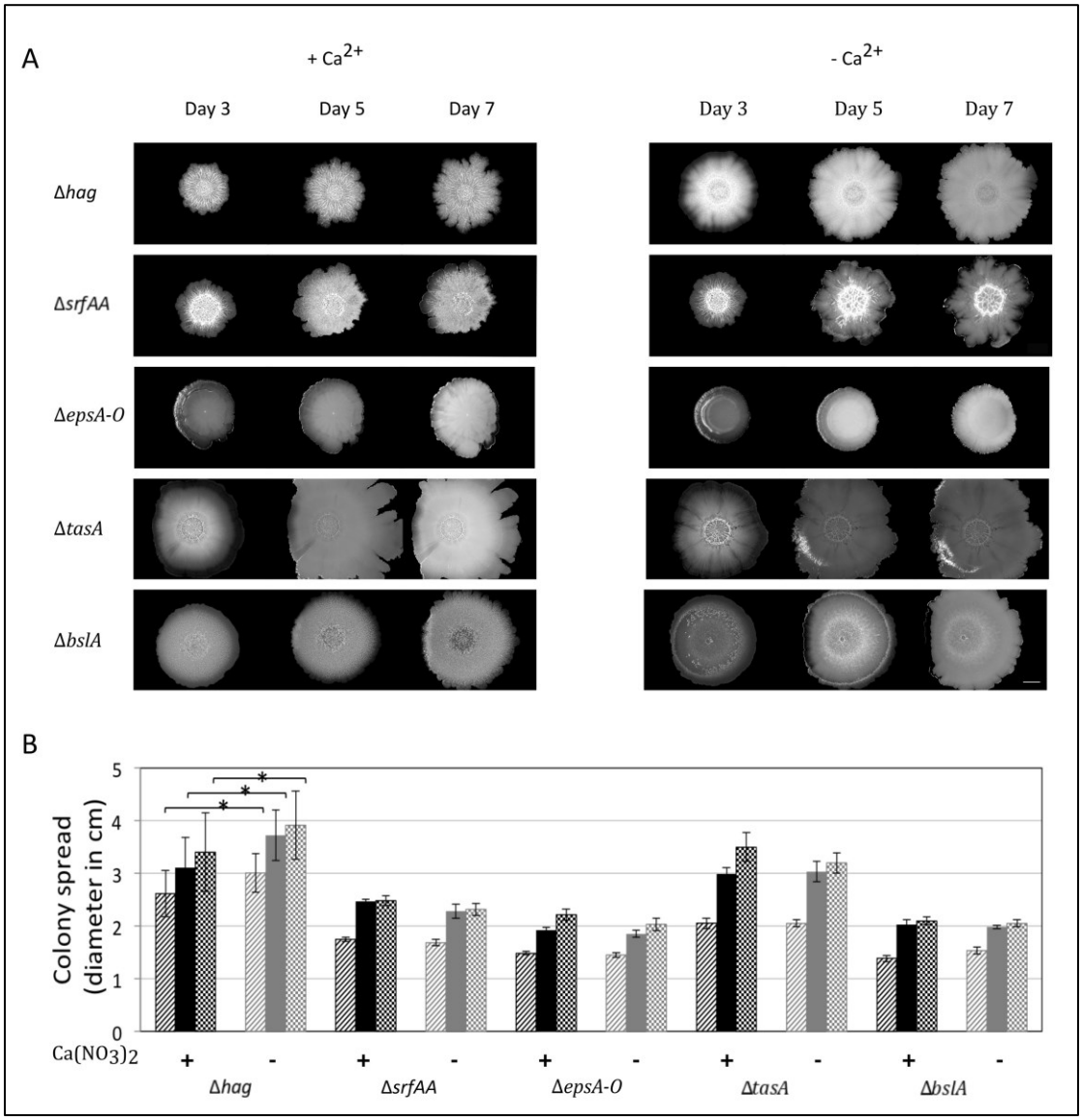

Figure 2. Colony expansion of various mutants of B. subtilis. (A) The colony images of Δ*hag*, Δ*srfAA*, Δ*epsA-O*, Δ*bslA*, and Δ*tasA* strains are shown after 3, 5, and 7 days after inoculation on 2×SG medium in presence or absence of Ca^{2+}. The scale bar indicates 5mm. (B) The colony expansion diameters of the mutants presented in panel A are shown after 3 (striped), 5 (filled), and 7 (checked) days. Black bars present data in presence of Ca^{2+}, while grey bars indicate in absence of Ca^{2}. The error bars indicate 95% confidence intervals. Data was analyzed with paired t-test for significantly different samples (*= $p<0.05$).

As the presence of Ca^{2+} ions restricted the dispersal of complex biofilm colonies, we questioned whether flagellum-dependent motility is necessary for the observed surface spreading. Colony escape of *B. subtilis* strains, lacking the *hag* gene encoding the flagellin protein was assayed in presence and absence of Ca^{2+}. The Δ*hag* strain behaved similar to

the *B. subtilis* wild type (WT) as lack of Ca^{2+} supplementation in the medium increased spreading
(Figure 2). Interestingly, the spreading of Δ*hag* was more uniform compared to the WT where expansion was observable from small sectors of the matured biofilm colonies (Figure 1).

3.3 Components required for sliding facilitate colony escape on medium without Ca^{2+} supplementation

Surface spreading of *B. subtilis* has been generally examined using semi-solid medium containing 0.5-0.7% agar. Under these conditions, *B. subtilis* can colonize the agar medium surface using flagellum-dependent swarming or flagellum-independent sliding[104,106,214]. As flagellum-dependent motility was not required for colony escape, we hypothesized that the observed spreading is similar to sliding that necessitates the collective secretion of EPS, TasA, BslA and surfactin. Deletion any of the genes essential for production of these components prevents colony escape on 2×SG medium without Ca^{2+} supplementation (Figure 2A and B). Therefore, the sliding machinery facilitates the colony escape after biofilm maturation. A similar trend was observed when the colony sizes of the mutant strains were recorded on MSgg medium in the presence or absence of Ca^{2+} (S3 Figure 3A). To examine if swarming or sliding are influenced by excess Ca^{2+} in the medium, surface colonization of wild-type and Δ*hag* strains of *B. subtilis*, exhibiting swarming and sliding, respectively, were assayed on both LB and 2×SG media containing 0.7% agar and $Ca(NO_3)_2$. The swarming and sliding of *B. subtilis* was reduced when 100 mM Ca^{2+} was supplemented in the different media suggesting that Ca^{2+} targets a component that is required for both swarming and sliding (S3 Figure 4A and B). Importantly, the increased $Ca(NO_3)_2$ concentration had no or minor impact on the growth rate of *B. subtilis* cultivated in liquid 2×SG medium although addition of 100 mM $Ca(NO_3)_2$ slightly delayed the growth at the start and decreased the final yield (S3 Figure 4).
A recent study demonstrated that calcium mineralization in *B. subtilis* colonies impacts biofilm rigidity and scaffolding. This study demonstrated the importance of *lcfA* in bio-mineralization in colonies[215,216]. Incidentally, LcfA is also involved in fatty acid degradation during surfactin production[217]. Nevertheless, mutation in *lcfA* gene did not prevent colony escape in absence of Ca^{2+} (S3 Figure 3B).

3.4 Colony escape on Ca^{2+} limited medium depends on KinB and KinC, the major sliding-inducing sensor kinases

Since KinB and KinC were reported to activate sliding in *B. subtilis* [104], mutants lacking individual genes coding for the Kin histidine kinases were tested for the colony escape

abilities in the absence of Ca^{2+}. None of the single mutants was reduced for colony escape spreading in Ca^{2+}-depleted medium (Figure 3 and S3 Figure 3B).

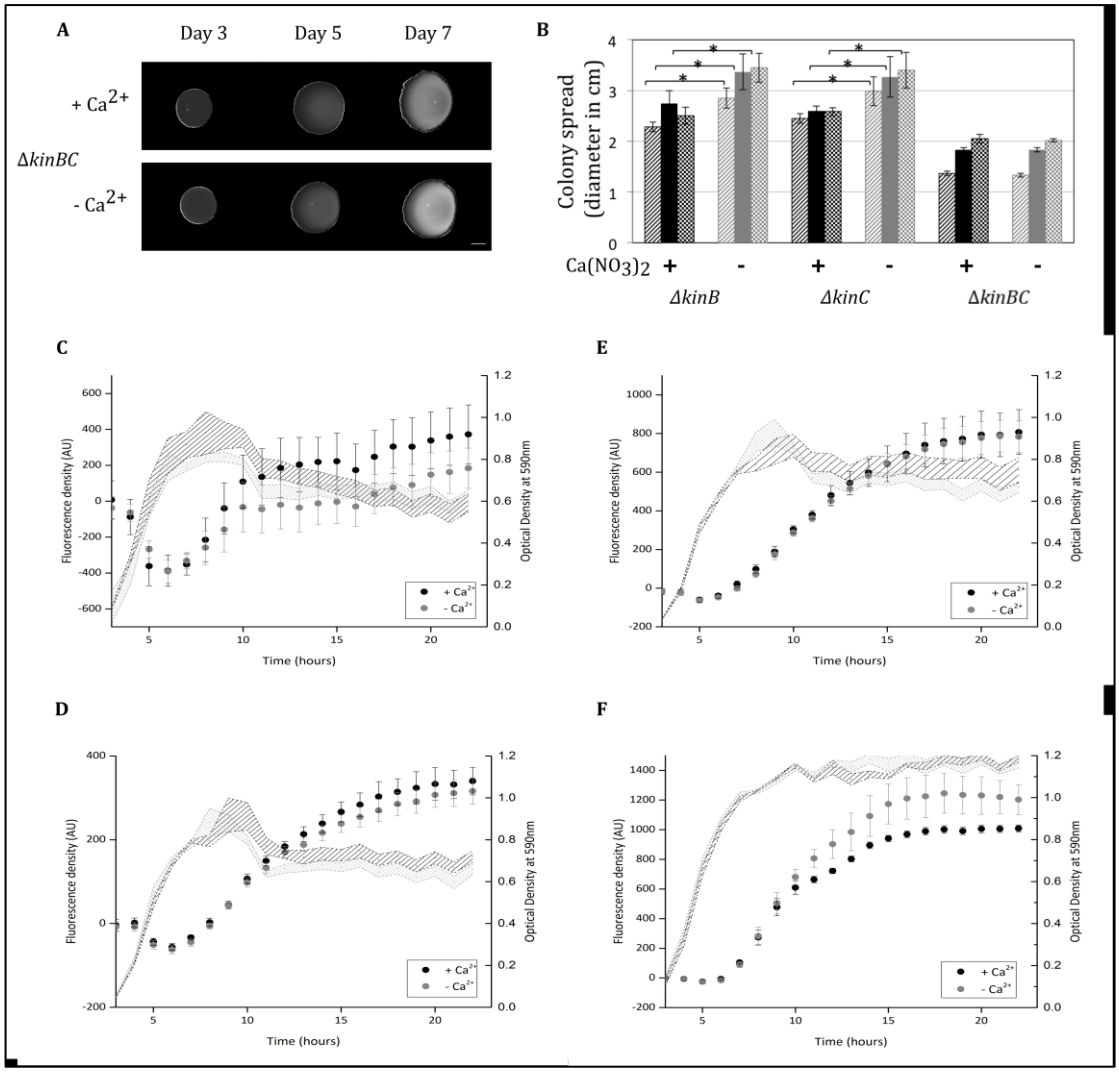

Figure 3. Colony expansion of histidine kinase mutant and expression of selected genes in the presence or absence of Ca^{2+}. (A) Colony expansion of the Δ*kinB*Δ*kinC* double mutant after 3, 5, and 7 days. Scale bar indicates 5mm. (B) The colony expansion diameters of the Δ*kinB*, Δ*kinC* single, and Δ*kinB*Δ*kinC* double mutant are shown after 3 (striped), 5 (filled), and 7 (checked) days. Black bars present data in presence of Ca^{2+}, while grey bars indicate in absence of Ca^{2+}. The error bars indicate 95% confidence interval. * denotes significant differences ($p<0.05$) analyzed with paired t-test. Relative fluorescence and growth profile (optical density) of *B. subtilis* strains in presence (denoted in black) or the absence (denoted in grey) of Ca^{2+} harboring the (C) P_{srfAA}-*yfp*, (D) P_{epsA}-*gfp*, (E) P_{tapA}-*gfp*, or (F) P_{bslA}-*gfp*, constructs.

While both KinB and KinC are important for full activation of sliding in *B. subtilis*, only deletion of both kinases results in sliding-deficient phenotype[104]. Consistently, *B. subtilis* harboring both *kinB* and *kinC* deletions lacked the ability to spread in absence of Ca^{2+}

(Figure 3). As the DegS-DegU two component system was previously described to indirectly activate *bslA* transcription[207,218,219], we tested a strain with a deletion of the *degU* gene for colony escape. However, the *degU* mutant colony escape spreading was increased in the absence of Ca^{2+} supplementation (S3 Figure 3B).

3.5 Ca^{2+} does not impact the expression of the eps, tasA and srfA genes

The colony escape in the absence of Ca^{2+} could be related to changes in the expression levels of the *srfAA*, *epsA-O*, *tasA*, or *bslA* genes. Therefore, the impact of Ca^{2+} supplementation in the 2×SG liquid medium was tested on strain harboring P*srfAA-yfp*, P*epsA-gfp*, P*tapA-gfp* or P*bslA-gfp* fusions. Following the reporter activity over time revealed that the gene expressions of *epsA-O*, and *tapA-sipW-tasA*, and *srfAA-AC* were unaffected, while *bslA* was barely increased in liquid culture grown in the presence of Ca^{2+} supplementation (Figure 3C, D, E and F). Importantly, the possibility cannot be excluded that gene expression in matured colony biofilm is increased locally in the absence of Ca^{2+}, influencing the expression of genes responsible for colony escape.

3.6 Ca^{2+} disturbs the amphiphilic properties of surfactin molecules

Next, we addressed the question how the presence of Ca^{2+} could disturb colony escape independent of affecting gene expression of genes related to sliding. Previous studies demonstrated that divalent cations, including Ca^{2+} form complexes with surfactin secreted by *B. subtilis*[220]. Thus, if the Ca^{2+} supplemented in the medium forms a complex with surfactin and alters its amphiphilic property (i.e. surface tension reduction), surfactin facilitated sliding properties might change. To demonstrate that Ca^{2+} can directly influence surfactin properties, surface tensions of spent media (overnight grown culture supernatants) from different strains were recorded in the presence of increasing amounts of Ca^{2+} using the Wilhelmy plate method[8]. When culture supernatant contained surfactin (e.g. WT and *epsA-O* strain), the surface tension was lower compared to the medium control and the supernatant of Δ*srfAA* strain (Figure 4A).

The absence or presence of 1mM of Ca^{2+} had no significant impact on the surface tension of the 2×SG medium. However, when the Ca^{2+} concentration was gradually increased to 100-500mM, the surface tension values of the medium elevated (Figure 4B). The amount of surplus Ca^{2+} was possibly high enough to form complexes with most of the surfactin molecules in the medium abolishing its surface tension reducing properties. When Ca^{2+} was added to the medium control or the Δ*srfAA* supernatant, the surface tension was unchanging and similar to the WT supernatant with high amount of Ca^{2+}.

4. Discussion

The quantity of ions in the environment influences various cellular pathways in *B. subtilis* including biofilm development[81,93,99,219,221]. In our study, we highlighted the role of Ca^{2+} in maintaining the integrity and robust structure of biofilm colonies. In generally used laboratory media that promote colony biofilm development of *B. subtilis*, cells attach to the agar surface and produce complex robust structures within 3-4 days. The biofilm matrix components such as EPS, TasA, and BslA play an essential role in colony wrinkleality as well as influence the indentation on the agar surface[222,223].

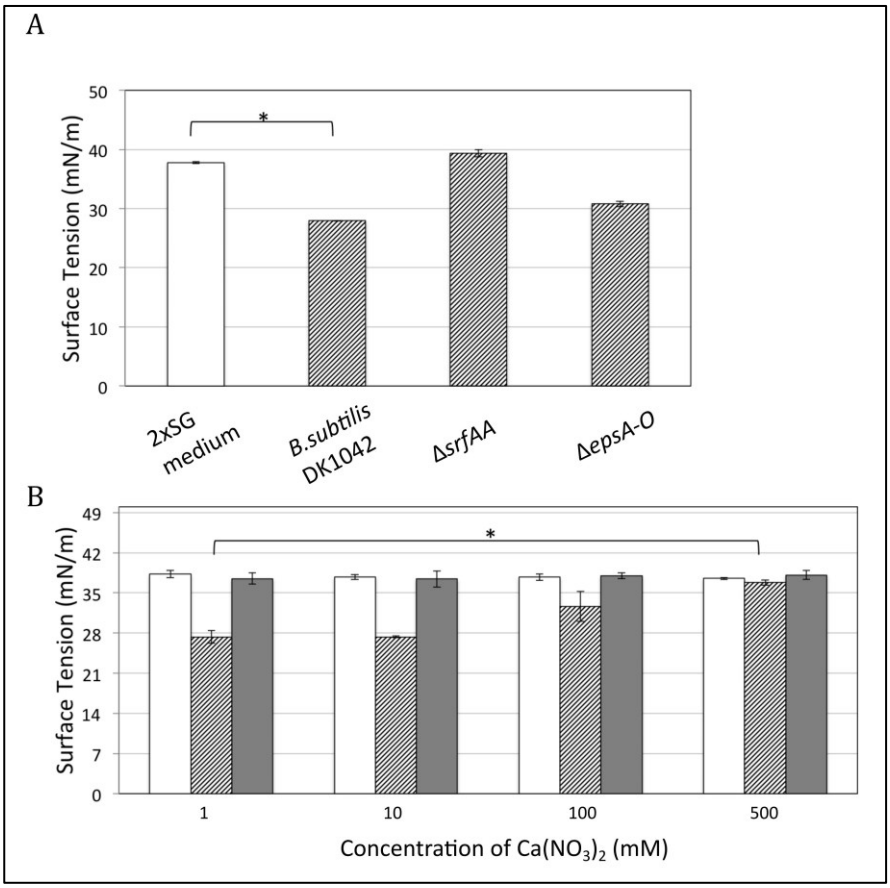

***Figure 4*. Surface tension measurement of the 2×SG medium and the supernatants of various *B. subtilis* mutants in the presence of different Ca^{2+} levels**. (A) Surface tension of the 2×SG medium (white bar), wild type, Δ*srfAA*, and Δ*epsA-O* mutant supernatants (black striped bars). (B) Surface tension of the 2×SG medium (white bars), the supernatants of WT (striped bars), and of Δ*srfAA* (filled bars) strains in the presence of different Ca^{2+} concentrations. The error bars indicate 95% confidence intervals. Data was analyzed with paired t-test for significantly different samples (*= $p<0.05$).

Interestingly, in the absence of Ca^{2+}, peripheral cells in the complex colonies expand radially after 4 days, likely due to nutrient depletion. In presence of Ca^{2+}, however, the structure is maintained and colony size barely increases. Here, we demonstrated that

extracellular polymeric substances and surfactants that are essential for expansion by sliding play an important role in the colony escape. Mutants that do not produce either surfactin, EPS, the hydrophobin BslA, or the protein component TasA failed to expand from the matured biofilm colonies in medium with reduced Ca^{2+} level, while the presence or the absence of Ca^{2+} had no major influence on the structural properties of the developing biofilm colonies.

Divalent cations, including Ca^{2+} are known to influence electrostatic interactions and bacterial attachment processes[224,225]. Ca^{2+} is also required for poly-γ-glutamate acid production in *B. subtilis* natto[226]. The influence of Ca^{2+} on surfactin has been extensively studied in X-ray diffraction experiments to demonstrate how the surfactin properties are altered during complex formation[220,227]. Moreover, Ca^{2+} also captures and localizes the ionized surfactin molecules in the phospholipid bilayers of the cell membrane. During colony development of *B. subtilis*, Ca^{2+}-carbonate present in the agar medium plays an important role during bio-mineralization, establishing scaffold formation and nutrient channeling in the biofilms[215]. The ability of Ca^{2+} to establish complexes with surfactin molecules might explain the lack of colony escape on an agar medium supplemented with Ca^{2+}. Surface tension measurements with bacterial supernatant demonstrated that high surplus of Ca^{2+} can preclude surfactin dependent reduction of the surface tension. Notably, the amount of Ca^{2+} required for the *in vitro* inhibition of the surfactin activity is two magnitudes higher than used in the colony experiments. This conflicting observation could be possibly resolved by the possibility that the presence of Ca^{2+} might impact the freshly secreted surfactin at the biofilm colony edge, while Ca^{2+}-surfactin complex formation in fluids with high diffusion is less stable. Colony escape observed in our experiments on highly viscous medium, i.e. with 1.5% agar, might be more sensitive to alteration in surfactin properties. Moreover, elevated Ca^{2+} levels in various media were able to diminish swarming and sliding of *B. subtilis*. As both swarming and sliding necessitates the reduction of surface tension by surfactin, these experiments further prove that interaction of Ca^{2+} and surfactin has great impact on surface spreading on agar medium.

This study adds to our understanding of rugose colony structure development in *B. subtilis* and the factors involved in maintaining these structures. The presence of Ca^{2+} in the medium not only prevents the escape of the cells from the colonies but also restricts them in nutritionally depleted environment thus probably indirectly promoting late stationary processes such as sporulation. The cells in the colonies were previously described to form white rugose structures due to sporulation. Thus Ca^{2+} has a substantial impact on the fate of colonies and the differentiation properties of these complex biofilm populations.

5. Methods

5.1 Bacterial strains, plasmids and media

B. subtilis DK1042 (naturally competent derivative of the undomesticated NCIB 3610) and its derived mutants were used in this study (Table 1). The strains were inoculated from glycerol cryo-stocks in LB medium (Lysogeny broth, 1 % tryptone, 0.5 % yeast extract, 0.5 % NaCl) overnight before spotting them on the agar plates for complex colony formation. The media used for colony studies are 2×SG[154] and MSgg[72] with 1.5 or 0.7% agar concentration. For generation of strains, genomic or plasmid DNA was transformed into DK1042 using natural competence[171] and the cells were selected on the LB agar with respective antibiotic concentrations. The antibiotic concentrations used were same as stated previously[99]. For construction of the P_{bslA}-*gfp* reporter plasmid (pTB670), the *bslA* promoter region was PCR amplified using primers oTH23 (5'-ACTGAATTCGGGAGCGGGAGGTTCAAGTG-3') and oTH24 (5'-GCAGCTAGCGCGTTTCATAACAAAATTCC-3') from *B. subtilis* 3610 genomic DNA, restricted with *Eco*RI and *Nhe*I, cloned into the corresponding sites of p*rrnB*-GFP plasmid[201] and transformed into *Escherichia coli* MC1061. To construct plasmid pTB497 harboring a constitutively expressed *gfp* gene, the $P_{hyperspank}$-*gfp* fragment was PCR amplified with primers oTH1 (5'-GCATCTAGAGTTGCTCGCGGGTAAATGTG-3') and oTH2 (5'-CGAGAATTCATCCAGAAGCCTTGCATATC-3') from plasmid phy-GFP[169], digested with *Xba*I and *Eco*RI, ligated into plasmid pWK-Sp[228], and transformed into *E. coli* MC1061. Resulting plasmids were verified by sequencing.

5.2 Colony biofilm formation

For colony spotting, 2×SG or MSgg medium with 1.5% agar were poured and allowed to solidify with closed petri dish lid. Both media were prepared with or without the supplementation of 1mM $Ca(NO_3)_2$. Once solidified, the plates were opened completely under sterile laminar airflow conditions and dried for 20 minutes. Once dried, 2µl of the overnight grown cultures were spotted on the plate (not more than 2 colonies per plate) and the lids were closed once the spotted culture dried. The plates were incubated at 30°C for seven to eight days.

5.3 Swarming and sliding

Swarming and sliding was assayed on LB or 2×SG medium solidified with 0.7% agar. The exact preparation of media and plates were previously described[10]. Plates were incubated at 37°C and swarming diameter was recorded every hour between 3 and 7 hours after inoculation, while sliding was documented after 24 and 48 hours.

5.4 Imaging and colony size measurements

The colonies grown on the 1.5% agar plates were imaged depending on the medium using an AxioZoom V16 microscope equipped with an AxioCam MRm monochrome camera (Carl Zeiss Microscopy GmbH, Jena, Germany). The colony diameters were also measured to quantitate the colony spread in presence and absence of the supplemented Ca^{2+}. Images were calibrated using Image J version 2.0.0-rc-15. Sliding and swarming disks were recorded using a Nikon D3300 camera equipped with a Nikon AF-S DX Nikkor 18 - 55 mm objective.

5.5 Growth and fluorescent reporter assays

Overnight cultures of *B. subtilis* strains were diluted 100-fold in 2×SG medium supplemented with different amount of $Ca(NO_3)_2$, 200 µl aliquots of the culture were placed in the wells of a 96-well plate and incubated under shaken conditions at 30°C. Growth and fluorescence intensity were recorded every 15 minutes using an infinite F200PRO plate reader (TECAN Group Ltd, Männedorf, Switzerland).

5.6 Surface tension measurements

Wild-type or mutant strains were grown overnight in 20 ml 2×SG medium in 50 ml bottles at 37°C under well agitated conditions. The cells were removed by centrifugation and the culture supernatant was used. The surface tension was measured according to the Wilhelmy plate method using a tensiometer (DCAT 21, DataPhysics) interfaced to a computer using the SCAT-33 software. Briefly, 5-10 ml of the supernatants were added to the vessel and the Wilhelmy plate (platinum-iridium plate) was then slowly allowed to dip in it at room temperature. 10 measurements were recorded for each sample and the experiment was repeated for three biological samples and performed independently twice. The Wilhelmy plate was rinsed with deionized water and subsequently flamed red-hot before each measurement. The measurements on the various samples were also performed with increasing concentrations of $Ca(NO_3)_2$ to observe the alteration in surface tension.

Table 1

Strain	***Genotype***	***Reference, source or construction***
DK1042	3610 *comI*^{Q12I}	[171]
TB500	3610 *comI*^{Q12I} *amyE*::$P_{hysperpank}$-*gfp*(*spec*^{R})	pTB497 → DK1042
TB602	3610 *comI*^{Q12I} Δ*tasA::spec*^{R}	TB163 [104] → DK1042
TB277	3610 *comI*^{Q12I} Δ*srfAA::Cm*	RG551 [104] → DK1042
TB530	3610 *comI*^{Q12I} Δ*hag::neo*	TB24 [104] → TB500

TB524	3610 *comI*^{Q12I} Δ*epsA-O::tet*^{R}	DL1032 [193] → TB500
TB526	3610 *comI*^{Q12I} Δ*bslA::cm*^{R}	NRS 2097 [219] → TB500
TB398	3610 *comI*^{Q12I} Δ*kinA::mls*^{R}	JH12638 [104] → DK1042
TB399	3610 *comI*^{Q12I} Δ*kinB::tet*^{R}	JH19980 [104] → DK1042
TB400	3610 *comI*^{Q12I} Δ*kinC::spec*^{R}	BAL393 [104] → DK1042
TB401	3610 *comI*^{Q12I} Δ*kinD::cm*^{R}	BAL691 [104] → DK1042
TB402	3610 *comI*^{Q12I} Δ*kinE::cm*^{R}	BAL692 [104] → DK1042
TB672	3610 *comI*^{Q12I} Δ*kinB::tet*^{R} Δ*kinC::spec*^{R}	TB400 → TB399
TB656	3610 *comI*^{Q12I} Δ*kinC::spec*^{R} Δ*kinD::cm*^{R}	TB400 → TB401
TB671	3610 *comI*^{Q12I} Δ*degU::neo*^{R}	Δ*degU* [207]→ DK1042
TB51	3610 *comI*^{Q12I} Δ*lcfA::mls*^{R}	MW2 [217] → DK1042
TB363	3610 *comI*^{Q12I} *sacA*::P$_{epsA}$-*gfp*(*neo*^{R})	[105]
TB373	3610 *comI*^{Q12I} *sacA*::P$_{tapA}$-*gfp*(*neo*^{R})	[105]
TB685	3610 *comI*^{Q12I} *amyE*::P$_{bslA}$-*gfp*(*cm*^{R})	pTB670 → DK1042
TB740	3610 *comI*^{Q12I} P$_{srfAA}$-*gfp*(*spec*^{R})	BD4720 [229]→ DK1042

Acknowledgments

The laboratory of Á.T.K. was supported by a Marie Skłodowska Curie career integration grant (PheHetBacBiofilm), and grants KO4741/2-1 and KO4741/3-1 from the Deutsche Forschungsgemeinschaft (DFG). E.M. and T.H. were supported by Jena School for Microbial Communications (JSMC) and International Max Planck Research School (IMPRS) fellowships, respectively.

Supporting Information for this Chapter is on page no: 138

CHAPTER 4

Chapter 4

Eisha Mhatre, Benjamin Bartels, Gergely Maróti, Balázs Bálint, Ákos T. Kovács (2016)

Spatially structured environment facilitates the emergence of yield strategists

To be submitted to Nature/Nature Communications

(The format and the style is similar to the current manuscript draft)

Every organism from unicellular bacteria to higher eukaryotes aim to maximize their growth and survival; and in doing so employ numerous strategies to maximize their fitness. Most experimental evolution studies on bacteria have demonstrated that there is a high selection pressure on growth rate. This observation can also explain why bacteria often use energy spilling pathways to maximize their growth rate when resource availability is high, leading to overflow metabolism, in contrast to using an energy efficient approach. The trade-off between using an energetically efficient metabolism to maximize yield (yield strategy) over maximizing the growth rate (rate strategy) has been a long-standing question in microbial population biology. A decade ago, a computational study based on iDynomics model described how spatially structured environment like biofilms select for lineages showing efficient use of resources at the cost of their growth rates. We tested these predictions experimentally with a robust biofilm former and a well-studied model system, *Bacillus subtilis* to show that during interactions between yield strategists and rate strategists in biofilms, the competitive advantage of the yield strategist depends on the spatially structured environment.

1. Introduction

Metabolic tradeoffs have an extensive impact on microbial population dynamics in fluctuating environments[42,230]. Existence of diverse metabolic strategies often gives rise to a bet-hedging sub-population of cells, and implement altruistic and cooperative interactions[44,46,54,231]. Under adverse conditions, like antibiotic stress or severe starvation, certain individuals of a bacterial population compromise their active metabolism to enter persistence state or invest in costly pathways, such as sporulation[232,233]. The price of altering the metabolism is rewarded by a protective state, for aiding the bacterial survival.

The metabolic trade-offs also exist in relatively homogenous environments, thus making them complex to understand[53,61,234,235]. Their occurrence in natural and laboratory microbial communities is puzzling due to the potential disparity of costs and benefits for the whole group. One such phenomenon is the tradeoff between growth yield (YS- yield strategists) and rate strategies (RS)[47,236-238]. In a traditional point of view, it was postulated that maintaining higher growth rate implies increased ribosomal content, protein synthesis, more cell divisions, and therefore, increased progeny and yield[239]. However, after recognizing efficient and inefficient metabolic strategies, it is now understood that achieving higher yield often results in a trade-off against the growth rate[42,238]. Under nutrient abundant conditions, a population is mostly benefitted from maximizing the growth rate and utilizing easily metabolized food sources. For example, in the presence of elevated glucose level, the glucose uptake rate is higher than during limiting conditions[240]. The inefficient metabolism leads to the overflow of various metabolic intermediates and accumulation of toxic fermentative end products, such as acids[128]. Under these conditions, cells encounter difficulties to maintain the constant growth rate above a certain cell density; followed by the exhaustion of resources that constraint cells to enter the stationary phase[42].

Contrary, cells committed to YS use the resources efficiently, analogous to the k-strategy phenomenon[241]. Optimal energy gain is retrieved for each mole of substrate, even though additional costly pathways are triggered in order to utilize the overflowing metabolic intermediates[43,128]. While this often diminishes growth rate, the population growth is maintained during the onset of nutrient depletion eventuating a higher yield. Theoretical predictions further imply that changing environments alter the abundance of yield versus rate strategists in a population[58-60,62]. Abundant resources and higher diffusion rates favor rate strategists (i.e. fermenters of a yeast population), while a shift to limiting nutrients with lower diffusion rates favor the emergence of YS (i.e. respirators) [40,48].

Phenotypic heterogeneity has been also observed in microbial populations where production of metabolically costly components contributes to the overall fitness of the

population, exhibiting a simple division of labor, e.g. biofilm formation or surface colonization[106,108].

Occasionally, division of labor in metabolism among diverse species eventuates cross-feeding interaction among metabolically deficient lineages[14,242,243]. Importantly, all these ecological interactions are greatly affected by the spatial structure. While a well-mixed milieu allows exploitative descendants to emerge, structured environment and concomitant assortment facilitate cooperative lineages[25,27,244]. Mathematical simulations involving individual based modeling suggest that the spatial structure existing in biofilms allow the coexistence of diverse metabolic strategies[245,246]. One such individual based model has suggested that spatial constraints promote the emergence of cells undergoing metabolism that favor maximizing growth yield in the biofilms[54]. This presented model predicts the positive selection of rate strategists under well-mixed conditions, while among the cells grown on a substratum, - appear at a later stage of development, in spite of initial disadvantage. However, this prediction has never been experimentally verified due to the lack of isogenic strains that follow different metabolic strategies. In order to experimentally test this theoretical prediction, a yield strategist bacterial strain was generated in a laboratory evolution experiment and its abundance was tested in the presence of a rate strategist under unstructured planktonic and structured biofilm conditions.

2. Results and Discussion

Evolving rare phenotypes like YS, within a laboratory microbial population is a challenge; as the clones with higher growth rate always have an advantage. To avoid this limitation, competition among the evolving bacterial progenies was reduced using a recently described selection regime that involves compartmentalization of individual bacterial cells within the emulsion droplets[52]. Single cells encased in each droplet lack competition with other clone mates, metabolize the available local nutrients, proliferate, and form aggregates. After 48 hours, the droplets were dispersed and a new growth cycle was initiated with appropriate dilution. Assaying the growth properties of selected individuals regularly, a yield strategist of *B. subtilis* with a growth delay, but higher yield was isolated after 40 rounds of propagation (strain YS1). From the same transfer, a control strain with no alteration in growth curve was also obtained (strain RS1).

The growth of the isolated yield strategist strain, YS1 on rich medium displayed higher optical density at the end of stationary phase, the culture biomass was elevated, and the total cell count increased compared to the ancestor, JH642 and the control evolved isolate, RS1 (Figure 1 and Supporting Information for chapter 4, hereafter S4 Figure 1 and 2A). Similarly, the growth of YS1 remained delayed with an elevated yield when cultured in chemically defined CSE medium, irrespective of the main carbon source supplied, i.e. in the

presence of glucose, malate, fructose or glycerol (S4 Figure 1). Importantly, the growth rate under these conditions was unaffected, but the strains displayed a consistent delay at the start of the growth.

Further, the improved growth yield possibly originated from the elongated exponential phase of YS1 reminiscent of an efficient metabolic strategy bacterial metabolic strategy[128]. Interestingly, when CSE medium was lacking both succinate and glutamate, the growth delay in YS1 was still observed, whereas the improved yield of YS1 was compromised suggesting that post glycolysis metabolism and/or nitrogen metabolism might be responsible for the increased growth yield in the isolated *B. subtilis* evolved strain.

Fascinatingly, the transition point in the growth curve, measured using the optical density, coincides with the change in the rate of glucose consumed. Although glucose in the medium is fully consumed at the end of the growth cycle, its initial utilization rate differs in JH642 and YS1. At a point where YS1 and JH642 reach the same OD is also the point where the concentration of glucose utilized sync (S4 Figure 2B). This is also observed in the case of protein content, where at 18^{th} hour the total protein content in JH642 and YS1 is comparable. After this point, the total protein of JH642 decreases, probably due to growth exhaustion and cell death; while that of YS1 increases further (S4 Figure 2C). The total protein content of the culture is the direct measure of the cell density.

Since there is an initial growth delay and the growth rate (slope of the exponential growth) are significantly comparable between the JH642 and YS1, how do the YS1 manage to reach to the same point as the JH642? The investigate this query, the cell length and area of the two cultures were compared. Indeed, the cell area in YS is slightly but significantly greater than that of the ancestor (S4 Figure 2D).

Having a yield strategist bacterial strain (YS1) available next to the control rate strategists, i.e. its ancestor (JH642) and an isolate with unaltered growth properties (RS1) from the same regime as the YS1, we set up to confirm the long standing theoretical predictions about the impact of spatial structure on the dynamics of yield versus the rate strategists. In spatially unstructured environment, the nutrients are constantly mixed in the medium and therefore cells with high growth rate are selected for. Indeed, the YS1 strain was outnumbered by JH642 when initiated at equal ratio and co-cultivated for 24 or 48 hours in a well-shaken broth (Figure 2A left). On the contrary, the RS1 strain that exhibited comparable growth properties to the ancestor in monocultures, coexisted with JH642 under these conditions (Figure 2A right). Thus indeed, once a strain is delayed in growth at the initiation of the population, it remains outnumbered in unstructured environment in spite of the capacity to reach subsequent enhanced yield when grown in monocultures.

Unlike well-mixed environment, nutrients in an emulsion droplet that was employed as a selection regime are compartmentalized and confined within a definite space.

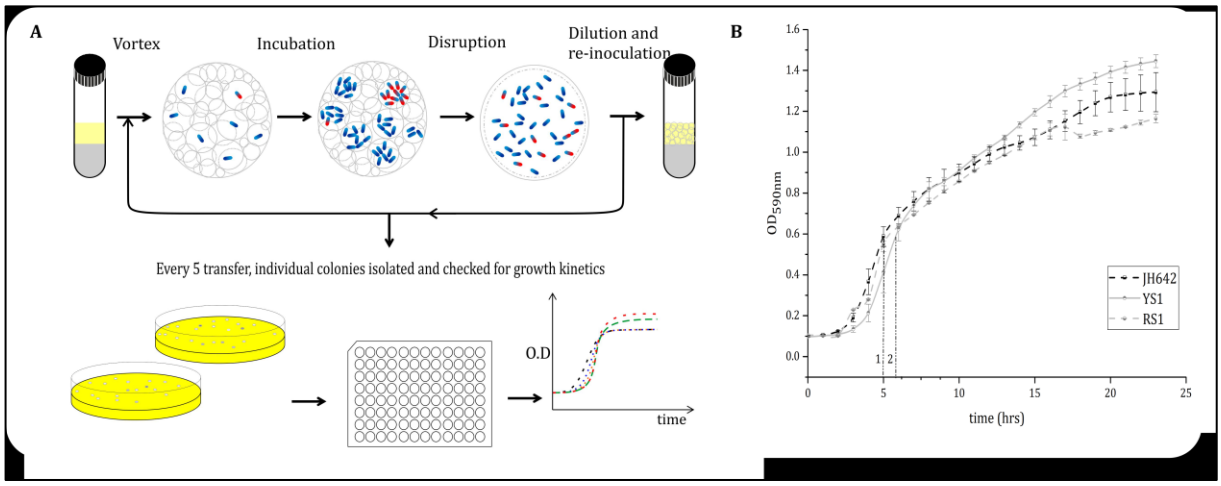

Figure 1 | Emulsion droplet based laboratory evolution was used to select yield strategist B. subtilis (YS). (A) Schematic representation of experimental procedure presents the selection regime and the isolation of yield strategy phenotypes from the population. Appropriately diluted bacterial culture (0.0025 at OD_{600}) was mixed 1:2 with sterile pico-surf in a 5 ml vial and the droplets (grey circles) surrounding bacterial cells (blue and red phenotypes) formed by uniform vortexing. After incubation under static conditions at 30°C for two days, perfluorooctanol was added to disrupt the droplets. One fraction of the population was used to create a new droplet suspension while the rest is frozen. At every five transfers, selected colonies were screened for isolates with YS growth phenotype. (B) Growth properties were assayed in LB medium showing the ancestor JH642 (black dashed; 1- 0.6 at OD_{595} ~5 hours after inoculation), the YS1 strain that has an hour delay, but increased final yield (grey line; 2- 0.6 at OD_{595} ~6 hours after inoculation) and the RS1 (a rate strategist isolated from the same population as YS1; grey dashed).

Initially mixed strains were introduced into emulsion droplet similar to the selection experiment, creating the isolated microcosms for single cells. Emulsions were disrupted after 48 hours, colony count was determined and the selection coefficient was calculated. As the spatial structure created by the emulsion droplets permitted clonal cells to utilize the available nutrient at their own pace, contributed to the selection of YS1 under these conditions (Figure 2B).

In addition, the relative frequency of RS1 was not enhanced significantly when competed with JH642 (Figure 2B), though a minor increase was observed, as expected for a strain that was cultured for ~400 generations under these conditions. These experiments thus substantiated the robustness of YS1 under spatially structured environment as compared with a well-mixed niche.

Mathematical simulation speculated that abundance of bacterial cells committed to yield strategy metabolism is dynamic and such lineages emerge within a biofilm population at a later stage after an initial disadvantage[54]. As previous simulations concentrated on cells with reduced growth rate instead of delayed growth observed with our isolate YS1, modified mathematical simulations are being employed to predict the outcome of

competition between a rate strategist and a yield strategist with delayed initiation of growth (collaboration with the group of Prof. Dr. Stefan Klumpp, George August University of Gottingen, Germany).

Bacterial cells in biofilms are attached to a surface or one another and propagate in close vicinity side by side. The spatially restricted environment, like biofilms, restrains the nutrient flux and increases the need to utilize the available resources efficiently. Therefore, the dynamics of competing rate and yield strategist *B. subtilis* strains were inspected in surface attached submerge biofilms and monitored their abundance at different time points.

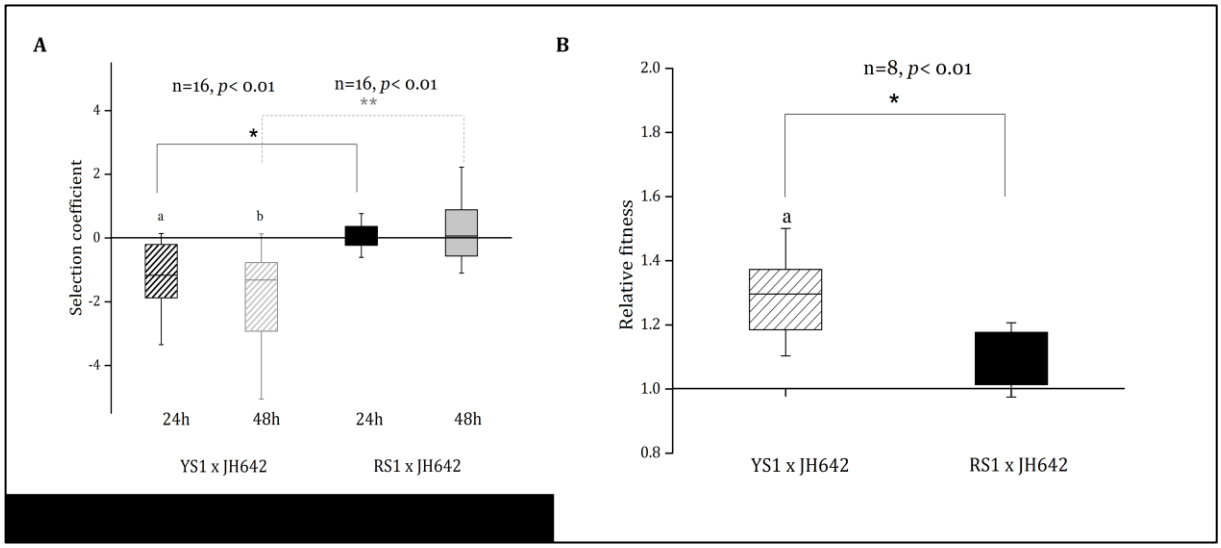

Figure 2 | Competition between YS and RS lineages in well-mixed and spatially structured environments. Two competing strains were mixed 1:1 and their selection coefficient was determined in comparison to JH642 ancestor. (A) Data using planktonic cultures showed that the YS1 got selected against at 24 (a= s= 0.005, p< 0.01, one sample t-test), as well as after 48 hours of incubation (b= s= 0, p< 0.01, one sample t-test). * (s= 0.005, p< 0.01, paired t-test) and ** (grey) (s= 0, p< 0.01, paired t-test) indicates significant differences between YS and RS in the competition experiments. (B) Spatially structured environment of emulsion droplets generated a selective advantage for YS1 (s= 0.002, p< 0.01, one sample t-test) that was significantly different from RS, indicated with * (s= 1.00E-03, p< 0.01, paired t-test). In all cases, the error bars indicate the 95% confidence interval.

First, YS1 was competed against JH642. Initially, the strains attached equally to the substratum (S4 Figure 3A). Also, the individual biofilms in both the strains gave rise to the comparable biomass (S4 Figure 3B) Interestingly, the relative biomass of JH642 was superior to YS1 in the biofilm after 24h (Figure 3 and S4 Figure 3C). In contrast, longer incubation allowed YS1 to emerge from the small focal islands and establish a comparable biomass level to JH642. Such an alternating abundance variation was not observed with the RS1 when competed with the ancestor (Figure 3 and S4 Figure 3C). Thus, similar to the

emulsion droplets, the spatial restriction in biofilms allow local privatization of resources and hence YS1 rise in the population despite the initial detriment.

The possibility of sporulation or YS mediated dispersion of JH642 was ruled out by determining the sporulation frequencies and cell counts of JH642 in presence of spent supernatant of YS (S4 Figure 3D and E). Sporulation in surface attached submerged biofilms in very low stating that it is not the reason facilitating the emergence of the YS later in the biofilms. Additionally, the medium being replenished periodically also does not trigger starvation mechanism in the population, hence the decreasing spore outcomes. The transitions in the emergence of YS1 in the population may be due to the constant dispersal rate in the biofilm. However, the presence of YS1 or its secreted diffusible molecules have no effect on the dispersal rate allowing its increased distribution.

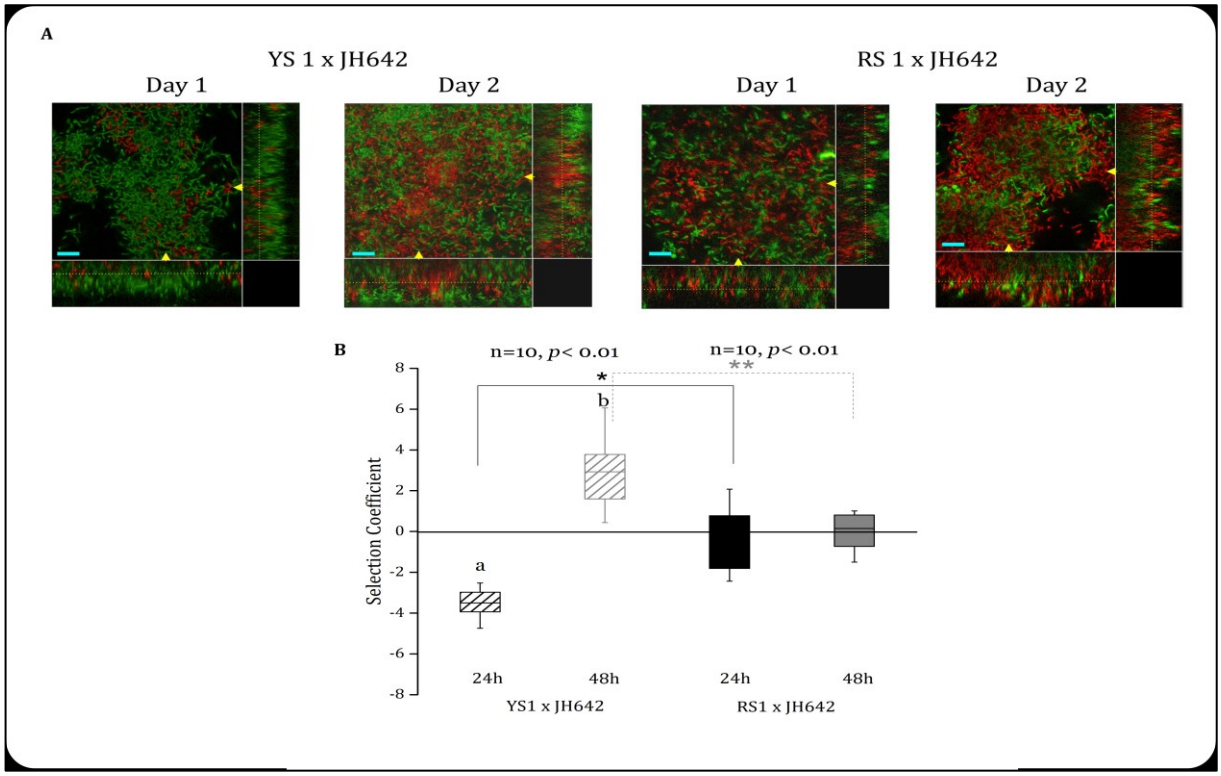

Figure 3* | *Competition experiment using YS and RS strains in submerged biofilms. (A) The orthogonal views of biofilm structure after 1 or 2 days of incubation is presented that highlights the emergence of YS1 after 2 days. The yellow arrows indicate the lateral and transverse cut positions that are shown on the horizontal and vertical panels. The dotted lines on the side panels show the z-position that is showed in the main panel. The scale bars indicate 30 μm. (B) Using random positions of replicate biofilms, the biomass was estimated using Comstat and extracted data was used to calculate the selection coefficient of YS1 and RS1 compared to the ancestor JH642. The significant differences from value 0 were calculated for 24 (a, s= 0, p<0.01, one sample t-test) and 48 hour samples (b, s= 0, p<0.01, one sample t-test) and between YS1 and RS1 competitions (*, s= 0, p<0.01, paired t-test). The error bars indicate 95% confidence interval.

Inquisitive about what mutations direct the evolution of YS phenotype, the genomic DNA from few YS isolated from 4 different transfers were re-sequenced. The sequencing revealed few single and multi- nucleotide variations (SNV and MNV) in genes expressing anti- sigma factors (*rsgI* and *yhdL*), sugar transporting system (*ptsG*) and amino acid metabolism (*leuB*) (S4 Figure 4). Additionally, few deletions were found in *ybgE* gene and non-ribosomal peptide synthesis related gene, *ppsA*. Although further experiments are needed to verify the mutations conferring YS phenotypes, the possibility of altered PtsG and eventually shifting the glucose uptake rate is one plausible cause of the initial delay[159]. Additionally, *ilvE* homologue *ybgE* (aminotransferase), involved in catalytic activity of the branched chain amino acids, play role in balancing the distribution of pyruvate and 2-oxoglutarate that are involved various metabolic processes. These processes channel the metabolic flux contributing to the efficient growth[128,247]. Further studies involving metabolic profiling of these evolved YS are being performed and should provide deeper insight of this phenomenon in *B. subtilis.*

Previous laboratory experimental regimes using well mixed cultures of bacteria, including the long-term evolution experiment of *Escherichia coli*, revealed that unstructured environments mostly facilitate progenies adapting to the certain niche complemented with high growth rate[237]. The spatially structured droplet regime on other hand, facilitated the evolution of rare growth strategy mutants in *Lactococcus lactis*[52]. The YS strains thus evolved showed lower growth rate but higher growth yield including the increase in the cell size.

Studies have defined yield strategy as the altruistic strategy as it involves costs and compromised growth rates or delays[54]. Also presence of YS in nutrient abundant environment is benefiting the rate strategists. However, at the level of subpopulation, yield strategy can be a cooperating strategy. It does not add to cell-cell competition. On other hand it puts in costs to efficiently utilize the resources minimizing the overflow metabolism[248].

The importance of spatially organized environments in facilitating cooperative growth has been highlighted in various experimental set-ups[249]. Long-term experimental evolution of *Burkholderia cenocepacia* biofilms also resulted in the formation of community synergy that encompass a rare phenotype, wrinkly spreader that although being improved in biofilm attachment, has a trade off during slower growth[250]. Furthermore, the spatial structure of biofilms has crucial impact on the evolution of complex ecological interactions that ultimately influence the growth properties of the community members[251].

Thus this study makes few unique contributions in understanding growth strategies in different environments. The previous computational simulations are tested experimentally and some new results have surfaced in understanding the fate of competition in spatially

structured environments. It is interesting to see that the YS are delayed initially, yet the environment facilitates its selection and they later coexist with the rate strategists. These experimental outcomes are distinctive to the spatially structured environments that feature niche specialization and resulting niche differentiation in the environment[252,253]. Particularly, this study outlines the outcomes of various metabolic interactions that harbor in multicellular communities like biofilms.

3. Methods

No statistical methods were used to predetermine sample size. The experiments were not randomized. The investigators were not blinded to allocation during experiments and outcome assessment.

3.1 Strains and cultivating media

The laboratory strain *Bacillus subtilis* JH642 was used in this study that was previously shown to form submerged surface attached biofilms[191]. The ancestor and evolved isolates (S4 Table 1) were labeled with green ($P_{hyperspank}$-GFP; Cm^R) and red ($P_{hyperspank}$-mKATE, Cm^R) fluorescent markers for microscopic imaging[244]. No significant alteration in the growth properties was observed after introduction of fluorescent markers. For the colony forming unit based competition experiments, GFP labeled strains were used, where Cm^R cassette was replaced by Nm^R marker in one of the strain using the pCm:Nm antibiotic marker exchange vector[254]. Exchange of antibiotic marker had no detectable effect on the growth properties of the strains.

For pre-cultivation of the strains, LB (Lysogeny broth, Carl Roth, Germany; 10 g l^{-1} tryptone, 5 g l^{-1} yeast extract and 5 g l^{-1} NaCl) liquid or 1.5% agar-solidified medium was used. Biofilm promoting BGM medium was used for the emulsion droplet-based laboratory evolution and the biofilm competition experiments[99]. For the growth profiling, CSE minimal-medium[255] was used supplemented with 50 µg ml^{-1} phenylalanine and appropriate carbon sources, glucose, fructose, malate, or glycerol at 0.5% concentration. Ampicillin (100 µg ml^{-1}), chloramphenicol (5 µg ml^{-1}), kanamycin (5 µg ml^{-1}) was used for liquid cultures and agar plates. Unless otherwise stated, all chemicals and reagents were obtained from Carl-Roth or VWR (Germany).

3.2 Droplet based experimental evolution regime

Preparation of the emulsion droplets was based on previous protocol[52]. A single colony of *B. subtilis* JH642 was selected and inoculated in LB medium and grown for 16 hours before diluting in BGM medium with an OD_{600} of 0.0025. 300 µl of diluted cell culture was added to 700 µl of filter sterilized 0.5% Pico-Surf 1 solution (Dolomite Microfluidics, Royston, United Kingdom) dissolved in Novec 7500 (IoLiTec GmbH, Heilbronn, Germany) in a 5 mL reaction vial. The tube was rigorously stirred on a Vortex Genie 2 mixer (Scientific

Industries Inc, USA) at 2500 rpm for 3.5 min. This ensured the droplet formation (42±3.6μm diameter) that was verified using a Dino-Lite digital microscope (Dino-Lite Europe, Naarden, The Netherlands). Once a stable emulsion was formed, 550 μl of the bottom oil phase was carefully removed and stored for the later re-use. The emulsion tubes were incubated under static conditions at 30 °C for 48 hours. During this period, cells in the droplets multiplied and formed aggregations. The emulsion was disrupted by adding 150 μl of filter sterilized 1H,1H,2H,2H-perfluoro-1-octanol. The tubes were then gently tapped until a floating aqueous phase was visible. This phase was carefully transferred to a new tube and OD_{600} was measured, re-diluted to OD_{600} of 0.0025 and re-inoculated in a new surfactant mixture to create a new droplet system. The remaining disrupted, but undiluted culture was stored as frozen stocks. Every 5 transfers, the population were spread on agar plates to randomly select individual colonies. These colonies were monitored for their growth kinetics in a 96 well plate using Infinite F200PRO plate reader (TECAN Group Ltd, Männedorf, Switzerland). Certain candidates with slight alterations in growth rate and yield were clean-streaked and stored as individual cultures.
The droplet based experimental evolution transfer was continued until 50 transfers (~400 generations). After 40 transfers, evolved clones with delayed initial growth, but higher final yield, were obtained. One such strain showing reproducible growth delay but, higher yield (YS1) was preserved and used for the competition experiments. From the same population, a colony showing growth kinetics similar to the ancestor was also selected and used as evolved RS for the competition experiments; designated as RS1.

3.3 Growth characteristics of strains in the presence of different carbon sources

The frozen glycerol stocks of strains JH642, YS1, RS1 were streaked on LB agar plates and few single colonies of each strain were inoculated in 2 ml LB medium on the following day. After 4 hours of pre-growth, cells were pelleted and re-suspended in CSE medium. OD_{600} was measured and adjusted to 0.005 in 200 μl or 30 ml medium for plate reader or batch cultures, respectively. Each 200 μl diluted culture was added to a 96 well-plate to measure the growth kinetics at 30 °C using an Infinite F200PRO plate reader (TECAN Group Ltd, Männedorf, Switzerland) under shaken conditions (200 rpm). The 30 ml cultures were inoculated in 100 ml glass bottles and incubated in shaken conditions at 30 °C (200 rpm). The growth kinetics was measured for 30 hours. Every culture had at least 3 biological replicates per experiment. For different sugar sources, the glucose in the original CSE medium was replaced with malate, fructose, or glycerol at the same concentration. The experiments were also performed by (i) omitting the sugar source (i.e. no glucose) or (ii) excluding both sodium-succinate and potassium glutamate from the CSE medium, but adding glucose.

3.4 Cell morphology and area measurements

The cultures of JH642 and YS1 were grown in biofilm growth medium, LB medium, or CSE-glucose medium as described above. The cells were grown at 30 °C, shaken conditions until mid-log phase (about 6 hours). 1% agarose was added uniformly on the microscopy slides and after 10 mins of drying, a drop of cells was added in the middle of the slide. A glass coverslip was placed on the drop and the cells were visualized using Zeiss Axioplan2 fluorescent-phase contrast microscope (Carl Zeiss, Jena, Germany). Oufti software was used to detect cells in the images and area measurements were performed[256].

3.5 Competition experiments to determine the selection coefficient

For the competitions in well-mixed environment, overnight grown colonies of *B. subtilis* TB237, TB719, YS1.1, YS1.2, RS1.1 and RS1.2 were inoculated in 2ml LB medium and incubated at 30 °C shaken conditions for 4 h, after which the cultures were adjusted to OD_{600} of 0.005 in LB medium. For the competition experiments, ancestor strain harboring Cm^R marker was mixed in equal amount with evolved YS1 or RS1 strains that were carrying Km^R marker. Similar experiments were performed with the antibiotic resistance swapped among the strains. Identical strains with different antibiotic markers were also competed as controls. These mixtures were incubated at 30°C under shaken conditions and colony forming units were determined at 0, 24, and 48 h by selecting on the respective antibiotic markers. The colony numbers were used to calculate the selective coefficient [$S = \ln(R_t/R_0)$]; where R_0 is the CFU ratio of the competing strains at 0 h, while R_t is the CFU ratio of the competing strains at 24 or 48 h.

For competition experiments in emulsion droplets, the same combination of cultures was used as for the well-mixed environment, but after the pre-cultivation of the strains, the OD_{600} of each culture was adjusted to 0.0025 in BGM medium. After equal mix of the strains, 300 µl of the co-culture was added to 700 µl of filter sterilized 0.5% Pico-Surf 1 solution dissolved in Novec 7500 and vortexed for droplet formation as described above. The samples were incubated at 30°C under static conditions. To determine the colony forming units in the emulsion droplets, 150 µl of 1H,1H,2H,2H-perfluoro-1-octanol was added after 48 h and the floating aqueous phase was used for the CFU determination. Appropriate dilutions were spread on LB agar plates containing appropriate antibiotics. The selective coefficients of YS1 and RS1 were calculated compared to the ancestor as above.

For submerged biofilm competitions, cultures of the red- and green-fluorescent labeled evolved and ancestor strains, respectively, were adjusted to OD_{600} of 0.5, mixed at equal amounts, and 200 µl of mixtures were added to the wells of a 96-well tissue culture treated plate with optically-clear bottom (Corning, New York, USA). Experiments were repeated with swapped fluorescent markers in the strains. The plate was incubated at 30°C static

conditions. After 2 hours, the supernatant culture was removed and replaced with new BGM medium to select only for the attached cells during the biofilm competition experiments. Every 12 h, the medium fraction was replaced with new BGM medium to remove planktonic cells and to avoid the formation of floating microcosm. The attached cells and biofilm were imaged at 2, 24 and 48 h using an Axio Observer 780 Laser Scanning Confocal Microscope (Carl Zeiss Microscopy GmbH, Jena, Germany) equipped with a Plan-Apochromat 63x/1.4 Oil DIC M27 objective, appropriate lasers for green- (488 nm) and red- fluorescence (568 nm) excitation. The biomass of the competing strains in each image stack was calculated using COMSTAT[257] and the biomass values at 2, 24 and 48 h were used to calculate the selective coefficient of the evolved strains compared to the ancestor as described above. To determine the CFU at each time points, similar experiments were performed with submerged biofilms, except green fluorescent strains were replaced with dissimilar antibiotic markers to facilitate CFU determination of the competing strains.

3.6 Genome sequencing

The genomic DNAs of the ancestor JH642 and YS isolated from different transfers were extracted using the Eurx GeneMATRIX Basic DNA purification kit (Gdansk, Polland). The samples were measured for the DNA concentration using a NanoDrop and the samples with the concentrations between 30-100ng/µl were sent for Sanger sequencing (collaboration with Gergely Maróti, Institute of Biochemistry, Biological Research Centre, Hungarian Academy of Sciences, Szeged, Hungary and Balázs Bálint, Seqomics Biotechnology Ltd., Mórahalom, Hungary)

Acknowledgements We thank C. Kost, J.U. Kreft for valuable discussions and H. Bachmann for suggestions on the droplet emulsion system. Research support was provided to Á.T.K. by a Marie Skłodowska Curie Career Integration Grant (PheHetBacBiofilm) and to E.M. by a Jena School for Microbial Communications fellowship.

Authors contributions Á.T.K. conceived the project; E.M. and Á.T.K. designed the experiments; B.B. developed the emulsion based selection method; E.M. isolated the evolved bacterial strains, performed the fitness and growth assays, and executed the microscopy experiments; E.M. and Á.T.K. interpreted results and wrote the paper

Author Information The authors declare no competing financial interest. Correspondence and requests for materials should be addressed to Á.T.K. (akos-tibor.kovacs@uni-jena.de)

Supporting Information for this Chapter is on page no: 142.

General Discussion

General Discussion

[The part of this Discussion will be submitted to:

Mhatre E, Kovács ÁT, Taking the road less travelled: emergence of rare strategies and metabolic interactions in spatially structured environments*. (in preparation to NPJ Biofilms and Microbiomes)*]

Bacterial biofilms consist of genetically and phenotypically diverse microbial assemblies. The spatial and temporal heterogeneity, benefit the overall population to maintain different phenotypes in the anticipation of the environmental change. For instance, the *recA*- dependent genetic diversification in *P. aeruginosa* biofilms is considered as the self-generated insurance to safe guard the community and withstand fluctuating environmental conditions[258]. The bistability of certain transcription regulators contribute to the differential expression of genes that results in the ON and OFF states of the subpopulation[6]. In *Salmonella typhimurium*, *fliC*-ON and *fliC*-OFF cells are both present in the population; the former group of cells have active flagella and thus, migrate to the nutrient rich sources while the later escapes the host inflammatory response by resistance mechanisms[7].

The other factors that contribute to the cellular heterogeneity are mutational events and genetic drift. The mutational driven changes are the result of the evolutionary adaptations. During the selection on limiting nutrient condition, the mutations cause the structural re-arrangement or rewiring of functions[259]. Prominent example being, the ability of *E. coli* to utilize citrate under aerobic condition due to the structural rearrangement in the promoter region of *citT* gene leading to the expression of citrate transporter[260]. Heterogeneity of mutational outcomes can be attributed to alternative adaptive possibilities[261]. The wrinkly spreader morphs that frequently arise in *P. fluorecens* biofilms were recently described to result from 13 alternate mutational pathways[262]. Of course the frequency of selection of some pathways is higher than others.

Genetic drift on other hand occurs drastically in a small subset of population due to the shift in allelic frequencies over time. The occurrence of genetic drift in a spatial structure of *E. coli* colony resulted in the genetic isolation of donor and recipient cells suppressing the conjugation event[263]. Small regulatory RNAs (sRNAs) play a role in fine-tuning the mRNA or the protein levels in the cell. The study by Mars and co workers highlight the role of *B. subtilis* sRNA RNAC/S1022 in contributing to the heterogeneity of exponential growth

rates[264]. This sRNA modulates the cellular levels of AbrB, a transcriptional regulator that represses the gene expression of matrix producing operons during the growth phase. The transcriptional interaction of sRNA-*abrB* increases the cell-to-cell variation in the levels of AbrB resulting in heterogeneity in growth rates during the exponential growth phase.

1. Laboratory strains of B. subtilis differ in their biofilm formation abilities

The goal of my doctoral research was to contribute to the increase of our present understanding of the factors influencing the *B. subtilis* biofilm development.

B. subtilis cells express high level of heterogeneity even under the most homogenous environmental conditions. Thus, a vast variety of strains and morphs of *B. subtilis* are presently identified and extensively studied. The legacy of the *B. subtilis* strains, starting from its first documented isolation in Marburg, Germany to its current genomic hybrid derivative- SMY (subtilis Marburg Yale) is wonderfully explained by Zeiger and collegues (2008) (Figure 1)[142].

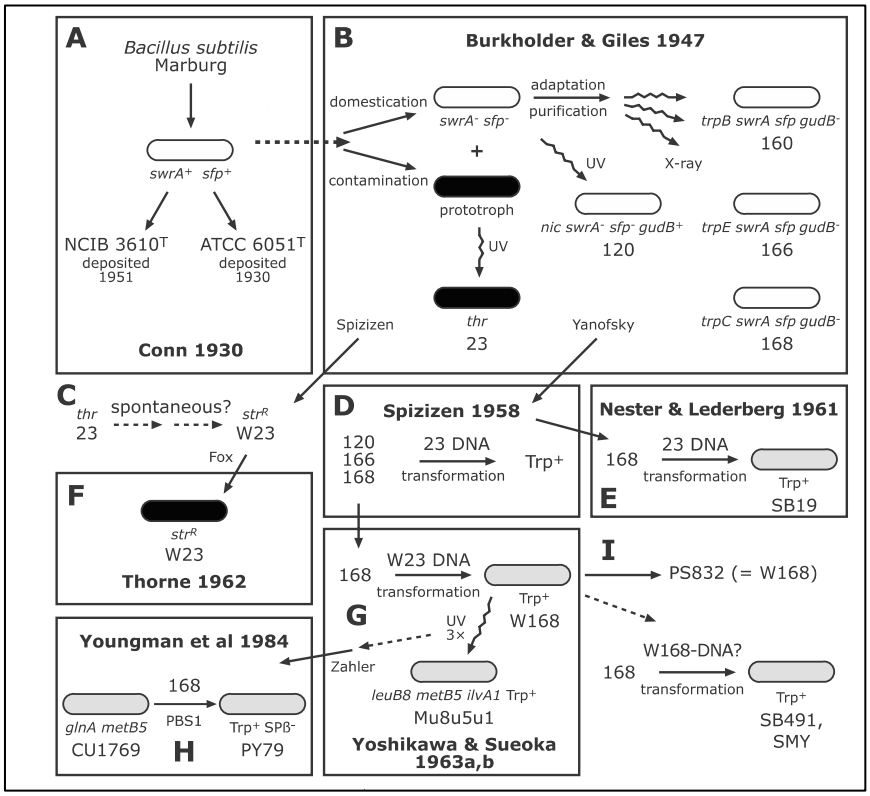

Figure 1. Description of B. subtilis (Trp+) legacy strains. (A) The Marburg strain which is the common ancestor of the genetically similar strains to 168 (white cells). (B) The straight arrows indicate the isolation events due to transformation, transduction, domestication, contamination events. The zig-zag arrows denote the mutagenesis through radiation. (C and F) The W23 isolate similar to its parent S23 is 94% identical to the Marburg strain and reported to be isolated due to contamination event (black cells). The boxes indicate the isolation events. (E, G, H and I) the strains PY79 and SMY are the genomic hybrids between 168 and W23 strains (grey cells). The dashed lines denote the undocumented events. Figure is adopted from Ziegler *et al*, 2008 and also based on the results from others[139,142,265-269]. The

genotypic differences in the course of the evolutionary changes, give rise to different ecotypes within the same species[270]. An ecotypes, in bacterial terms, is the population of cells occupying the same ecological niche[271]. Since bacteria evolve continuously, it is possible that distinct ecotypes of a particular strain already exist specific to the cultivating conditions in particular laboratories. To classify them as ecotypes or stock variants is yet another question and requires further examination. However, the frame shift or the point mutations in genes and regulators of biofilm processes contribute and correlate to the variation in the biofilm properties of these *B. subtilis* laboratory isolates[272]. The study described in Chapter 1 and now a peer-reviewed manuscript describes these alterations in colony and pellicle morphologies in various selected laboratory, domesticated strains compared to the wild isolate, *B. subtilis* NCIB 3610 on different media[272]. In *B. subtilis*, the laboratory strain 168 differs from the wild isolate; NCIB 3610 in its ability to produce surfactin and thus surfactin mediated sliding[105]. Few 168 isolates were also previously reported to have impaired biofilm formation[273]. Our results do highlight these previously stated impaired biofilm structures in some laboratory 168 variants. Interestingly, it also puts forward the fact that other 168 isolate variants do form wrinkled colony and pellicle structures comparable to the wild-isolate. The other laboratory strain, *B. subtilis* JH642 showed absence of complex colony biofilm structures, but is studied for its role in submerged surface attached biofilms[191]. The other important fact to be noted here is that the previous studies that demonstrated the defect in biofilm formation of laboratory strains used glycerol based defined medium. *B. subtilis* 168 grows poorly in presence of glycerol and thus the results in forming poor biofilms in the biofilm inducing medium MSgg that contains glycerol. However, when glycerol is replaced with glucose the growth defect is corrected and cells form rugose colony structures. This notably highlights that though the variation in biofilms is the matter of inherent complexity of bacterial strains, environmental factors play a huge role in shaping their behavior. Thus distinct media components are often used to demonstrate biofilm characteristics in laboratory experiments.

2. Environmental cues impact biofilm formation and development

Environment shapes myriad bacterial mechanisms. Most soil dwelling bacteria thrive on plant polysaccharides and root exudates as signaling molecules[274]. One of these signals induce the secretion of Nod factors by the *Rhizobium* that in-turn stimulate the root nodule formation in leguminous plants for the bacterium to fix nitrogen[275]. The virulence mechanisms and toxin production in pathogens is also induced as reaction to the host's immune responses[276]. Many developmental pathways such as competence and sporulation in *B. subtilis* are similarly the effects of subtle changes in environment[178].

The complex biofilm formation in bacteria also depends on the environmental characteristics. Host's plasma components and mucosal secretions induce complex

aggregates of *Streptococcus mutans* to adhere to the epithelial cells[277]. Sub-inhibitory concentrations of antimicrobials stimulate the biofilm formation in *P. aeruginosa*[278,279]. The physical properties such as the hydrodynamic shear force in reactors also influence the compact, stable and dense biofilm formation in activated sludge used in waste water treatments[280].

Many studies have reviewed the extrinsic factors inducing biofilm formation in *B. subtilis*[75,101,138,143]. The Chapters 2 and 3 of this thesis highlight the role of cations and their threshold concentrations during biofilm development in *B. subtilis*.

Both, Mn^{2+} and Ca^{2+} are important micro elements in bacterial nutrient requirements[281]. Mn^{2+} acts as a coenzyme in several metabolic reactions and has a huge impact on sporulation process while, in biofilms it contributes to the pellicle development and formation of white rugose patterns that are the features of the *B. subtilis* complex colony. Though its clear role in induction of these complex structures is not yet known, its absence makes the colony patterns look pale. This is observed in the laboratory strain grown on complex medium containing glucose as well as in the undomesticated strain NCIB 3610 grown on glycerol containing medium[93,99]. Our study also focuses on various processes that are transcriptionally activated in presence of Mn^{2+} in the colony biofilms. This study unravels the complex, Mn^{2+} dependent, late-log phase pathways that accompany the biofilm formation in bacteria.

The initial attachment of the cells marks the first step in formation of biofilms. The growth and development of cells in biofilms is also governed by the surrounding factors.

Cells in a biofilm secrete extra polymeric substances, EPS that include complex polysaccharides, nucleic acids, proteins and lipids. These substances form matrix around the cells, aid in the adhesion and scaffolding of the cells together, and maintain the rigidity of the biofilm. The sticky nature of the matrix also retains various QS signals, extracellular enzymes and metabolic products in the vicinity[282]. Many bacteria also use host or environment derived adhesion molecules to gain advantages such as antimicrobial resistance in biofilms[283,284]. Among other environmental factors influencing the development of biofilms, change in pH and temperature greatly alter the resulting EPS composition[285,286].

3. Environmental factors restrict colony escape

The bacterial cells in the biofilm escape or disperse from the sessile communities when the environment becomes unfavorable. These unfavorable conditions could be anything from antimicrobial attack, temperature or pH stress, desiccation to the starvation[287]. The other form of escape seen mostly in biofilms on solid surfaces, like agar or plant roots, is collective migration of cells called as swarming and sliding. Many bacteria exhibit swarming and sliding behaviors as chemotaxis mediated processes or in order to venture new nutrient sources[106,202].

Swarming motility is spreading of cell collectives with the active use of flagella. Many bacteria exhibit this phenomenon not only under laboratory conditions but also in the multicellular communities found in the natural settings. To state few examples, the swarms of *Paenibacillus votex* transport *Aspergillus fumigatus* conidia over long distances, gentamycin sensitive *P. aeruginosa* co-swarm or transport the non swarming, gentamycin resistant, cooperating partner *B. cepacia* to colonize gentamycin harboring areas, *B. subtilis* swarms on root surfaces form boundaries and inhibit the merging with non-related ecotypes[123,288,289].

On contrary, the sliding mechanisms in bacteria are flagella-independent processes and rely on secreted molecules having bio-surfactant and elastic properties. Mutants defective in motility or non-motile bacteria, like cocci, also exhibit this mechanism. *S. aureus* uses self secreted slimy matrix to spread passively on surfaces[290]. The mutants lacking flagella in *B. subtilis* secrete surfactin, EPS and hydrophobin proteins to spread along the agar surfaces.

The ability of biofilms to retain water is another physical force that shapes the biofilm structure[291]. The surface tension generated by the water molecules restricts the cellular movement and increases the cell density. The resulting QS mediated response activates the surfactin production. Surfactin molecules decrease the surface tension making water to flow in thin layer on the agar surface, hence, allowing bacteria to migrate on the surface rapidly.

The Chapter 3 of this cumulative Thesis demonstrates the role of Ca^{2+} in restricting the surfactin mediated surface spread in *B. subtilis*. The high concentrations of Ca^{2+} ions themselves do not affect growth or biofilm related gene expression in *B. subtilis*. However, the increased presence of Ca^{2+} forms a physical complex with the surfactin molecules on the edge of biofilm. Thus, in the presence of high Ca^{2+}, the cells lack the threshold levels of surfactin needed in order to spread on the surface after nutrient deprivation in the matured biofilm colony (Figure 2). This was also demonstrated in liquid medium, where the increasing amounts of Ca^{2+} resulted in proportionally increasing the surface tension by sequestering the surfactin molecules in the spent medium. This study highlights the fact that the nutrient starvation activates the colony escape in biofilms and the secreted molecules such as surfactin, EPS, protein components such as BslA and TasA, aid this surface spreading process. The mutants lacking either of these components failed to spread. This observation further opens the questions on what nutrient stress responses are activated in presence of Ca^{2+} where the spreading is restricted.

In *B. subtilis* complex pathways, the loss of flagella mediated motility is coupled to the production of EPS[292]. The role of EPS in passive colony expansion is highlighted in the study involving theoretical model, which states that the secretion of EPS generates osmotic pressure. This prompts the peripheral cells to divide and push the neighboring cells outward[213]. This further explains why the mutant in EPS production lacks the ability to spread on the surface.

4. Spatially structured environments allow emergence of rare strategies.

Maintaining metabolic enzymes consumes lot of cellular components like energy (ATP), RNA polymerases and sigma factors. Hence, an individual cell rarely metabolizes large range of substrates simultaneously. Most cells develop machinery to metabolize subset of substrates leading to metabolic specialization[293]. In a well-mixed, nutrient rich environment most cells prefer specialization towards easily utilizable substrate, which is mostly glucose. However, in biofilms the substrates are generally at limiting concentrations and hence cells exhibit metabolic heterogeneity. This metabolically heterogeneous population also cater to the needs of other neighboring cells and in return benefit from outsourcing the metabolic functions thus, avoiding the biochemical conflicts[37]. Lactose utilizing *E. coli* in spatially structured environments metabolically cooperates with *S. typhi* providing it with the cellular waste products like acetate and in return receiving amino acid it needs. This arrangement discontinued when the spatial structure was removed[35]. Thus, spatial structures select for rare strategies, resulting in cooperation, existing prominently due to the resource and diffusion constrain.

Spatial structures also promote efficient metabolism and favor yield strategists, YS. This has been demonstrated before using the mathematical simulations[48,54]. Bachmann and colleagues also developed a droplet-based compartmentalization set-up mimicking spatial structure to effectively select for yield strategists from a population largely exhibiting RS phenotype. This selection regime was applied to the *B. subtilis* population in order to select for stable YS phenotypes in the population and is described in Chapter 4 of this thesis. The droplets insulate the cells from the fast-growing competitive neighbors thus favoring the emergence of slow growing but importantly high yield phenotypes.

After evolving stable yield strategists, competition experiments were carried between evolved RS and YS in structured and unstructured environments. This was importantly done to check if the experimental outcomes coincide with the simulations. As predicted, rapid growth rate is favored in well-mixed conditions. Thus, YS have fitness disadvantage resulting in their competitive exclusion. In droplets that imitate the structured environment, YS have fitness advantages over RS.

However, competition outcomes in biofilms are the highlight of this study. While previous predictions stated that spatially structured environments favor YS phenotypes due to spatial nutrient and diffusion constrains, some studies also referred to the competitive coexistence in such environments[294,295].

The fate of competition in biofilms was as follows. The fast growing RS cells dominated the one-day-old mixed biofilms. However, on the 2nd day the slow growing YS caught up and emerged in the population highlighting the coexistence of the two strategies in biofilms.

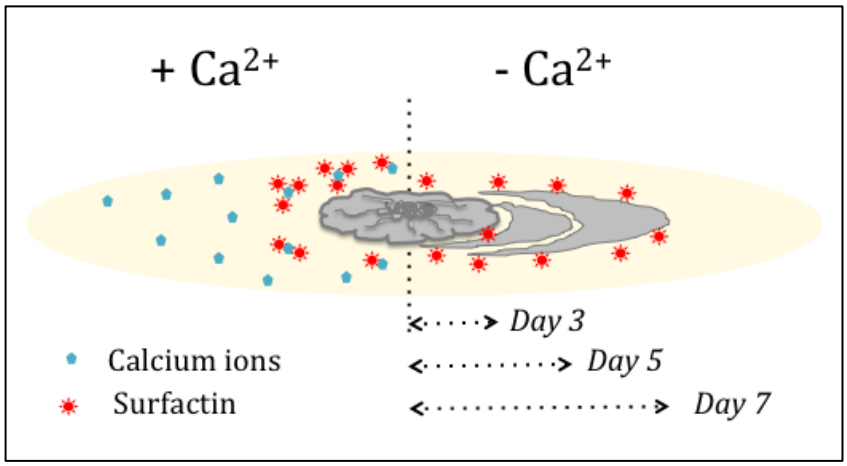

Figure 2. Graphical model of Ca^{2+}- surfactin complex formation The surfactin complex formation in presence of Ca^{2+} (right), while in absence of Ca^{2+} surfactin mediates the colony spread (right).

Such coexistence of the two strategies imply that there is selection of the flattest in these biofilms where the most fit phenotype always surrounds the non-fit near mutational neighbor in the presence of low fitness peaks that are mutationally robust[36]. Another reason for the competing phenotypes to coexist is the niche differentiation. This occurs when the competing strains differentiate their niches by metabolic specialization or by occupying separate parts in the environment[230,296]. Numerous other competitive outcomes in spatially structured environments have resulted in the rare coexistence of competing phenotypes, stating that such environments promote cooperative strategies[44,49,297,298].

The emergence of RS in the population is an example of individual level selection, where as emergence of YS is the example of population level selection as their fitness contributes to the overall population fitness. This makes YS hallmark of cooperative population[13,42].

Cooperative traits also enhance the rare phenotypes to thrive in spatial structured environments. For example, the culture-impaired natural isolate of cystic fibrosis infections causing *P. aeruginosa* grows abundantly in biofilms but in planktonic state, mutant variants produce antimicrobials that caused killing[299].

Existence of toxic pollutant pentachlorophenol degrading *Sphingobilum chlorophenolicum* in the contaminated environment is only possible in spatial structure where it is surrounded by *Ralstonia metallidurans* that reduces toxic Hg^{2+} in the vicinity[300,301].

Many soil bacteria develop as colony more efficiently in the presence of other microbial species within the community[302]. Other cooperative traits like the utilization of starch as sole carbon source are promoted by spatial environments that allow growth in patches of cooperating individuals [249]. The chance to utilize the amylase degraded products caused the cells to aggregate as well as to keep the resources local. Spatial segregation thus facilitates the production of genetically related cell groups favoring localized cooperation[303].

5. Factors responsible for yield strategy phenotype

Bacterial growth rate and yield are fundamentals of their lifestyle. Is there a relationship between the two? The examples discussed above and the experimental observations discussed in Chapter 4 of this thesis clearly emphasizes that there is a tradeoff between the maximization of growth rate and maximization of yield. However, in efforts to incorporate microbial growth kinetics to the large-scale ecosystem studies, reports have shown varied proportionality between observed biomass yield and growth rate (Figure 3).

In oligotrophic aquatic environments and under chemostat conditions with low dilution rates, it favors the population to maintain both growth rate and yield at a low level. In such cases the relationship is positively linear[238]. The social myxobacterium, *Sorangium cellulosum,* when grown on glucose as carbon source and asparagine as nitrogen source, employs EMP and Pentose phosphate pathway as major catabolic pathways enabling higher energy gain in form of ATP. However, it gives low yield of biomass as 90% of the cellular energy is required for the maintenance investment in lipid and secondary signaling molecules[304]. Thus showcasing lower rate as well as yield.

The substrate utilized by the cell is used for two purposes during microbial growth- (1) to produce new cells and contribute to the biomass, and (2) to maintain the cells.

The slower the growth rate, more is the energy requirement for cell maintenance and less is the biomass yield[239]. However, cells with the higher initial growth rates, RS, tend to increase the maintenance energies at faster rate due to shifts in metabolic pathways and energy spilling reactions slowing down the rate. Thus, they incur lower yield. Whereas efficient metabolism with higher energy output, maintains a constant lower growth rate thus leading to the higher yield. This imparts a negative relationship between growth rate and yield.

The anaerobic bacterium *Halophaga foetida* metabolizes the methyl groups of aromatic compounds either to high energy conserving product, acetate or to dimethyl sulphide[305]. In situation of substrate excess, methyl groups are transferred to sulphide. This results in increased growth rate but lower growth yield. Under substrate limiting condition, the considerable methyl groups are converted to acetate giving rise to Gibbs free energy. The physiological nature of this interaction where the bacterium adjusts its metabolism according to the growth conditions maintains the tradeoff that can be described with a negative sigmoid curve.

The relationship is negative linear when the organism can maintain only either of the two strategies. When soil respiration rate that depends on microbial population, is seasonally studied, it reveals that the microbial species that dominate during summer and winter conditions differ significantly[306]. In winter when the soil is under snow, selection drives the maintenance of microbial species with higher growth rate but lower yield. The maintenance energy for the cold conditions causes growth inhibitors to retain the

population at lower yiemaking these unculturable. However, the exposed soil favored metabolizers with higher biomass specific respiration rates.

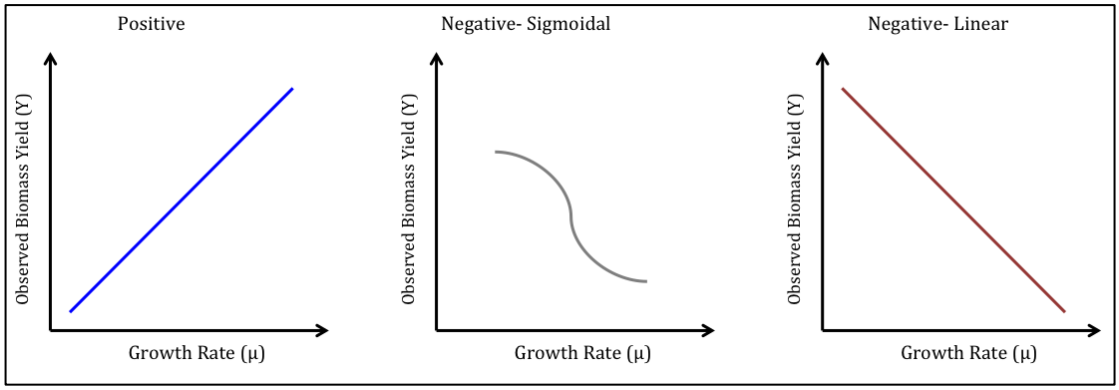

Figure 3. Relationship between observed biomass yield and growth rate. The relationship is positive at the start in environment where maintenance energy is high at low nutrient and low diffusion conditions. The relationship is negative sigmoid in spatially structured environment with varying resources while is negative linear in rich growth media. Figure adapted from Lipson, 2015[238].

The selection of the optimum growth strategy, RS or YS varies under certain conditions. From thermodynamic point of view, 100% efficient growth involves energy of the reactants to equal to the energy of products, and the conversion of energy in form of ATP to heat[48,307]. With rapid growth rate, the anabolism and catabolism is unbalanced. Thus, the energy is utilized for the energy spilling reactions, production of excess metabolites resulting in overflow metabolism and high rates of protein synthesis[307].

Fast growth also implies inefficient metabolism and likewise, slow growth implies efficient metabolic pathway. The evolved YS, showed delayed intial growth but higher yield, protein content, significant increase in cell size compared to the ancestor and the RS strain.

When the evolved YS, described in Chapter 4, were grown on minimal medium with varying types of sugars; the YS phenotypes showed higher yield under all conditions. This states that in most carbon catabolizing pathways these undergo efficient metabolism.

Further, the nitrogen source, glutamate and one of the TCA cycle intermediate succinate were found to have great effect on the growth yield advantage. When the medium is devoid of these two sources simultaneously, the YS fail to reach the higher yields. However, individually these components did not affect the yield.

Interestingly the YS sequencing results showed a SNV mutation in the *ptsG* gene. PtsG in *B. subtilis* is part of *PtsGHI* system that functions as glucose specific permease system[308]. It senses the glucose availability in the medium and the other part of the PTS then activates the carbon catabolic repression mechanism[309]. This glucose induced catabolic repression also acts on the oxidation of dicarboxylates that form part of the TCA cycle. Glucose grown cells experience long lag when shifting to the uptake of decarboxylases[310].

It is plausible that the observed mutation in *ptsG* in the YS results in impaired sensing of glucose affecting the catabolic repression and so the cells also utilize succinate and glutamate, resulting in the growth delay. Of course this hypothesis needs to be further confirmed by introducing the mutation in the wild type ancestral strain to check if there is an observed delay due to the observed mutation. Additionally, when the medium lacked glucose, even the ancestor and RS showed the similar initial delay in growth. It is therefore a possibility that the delay in YS is due to the utilization of other medium components along with glucose while the RS prefers glucose.

Glutamate acts as the link between nitrogen and carbon metabolisms in *B. subtilis*. The TCA intermediate, α- keto glutarate and glutamine both synthesize glutamate using enzyme glutamate synthase[311,312]. Both glutamate and succinate feed in to the TCA cycle constantly; making it an energetically promising and efficient strategy.

A collaborative project to identify the metabolic profiling of the medium components consumed over time and the metabolic profile of the strains is being performed currently.

Concluding remarks

This dissertation is a comprehensive study involving numerous elements and characteristics of *Bacillus subtilis* biofilms. The documentation of variation in the capabilities of biofilm formation capabilities exhibited by different laboratory strain variants puts forth a strong understanding on elements that govern biofilm formation- be it the proper sugar source (e.g. glucose) or certain genetic differences (e.g. point mutations in genes responsible for biofilm formation). Though the impact of metal ions on biofilm formation is extensively studied, the study highlighting the role of manganese also touches upon several other aspects of *B. subtilis* lifestyle such as submerged surface attachment, pellicle formation, antimicrobial production, sporulation and other Mn^{2+}-affected gene expressions. Previous studies on surfactin induced sliding mechanisms were studied on less viscous agar surfaces. The novel observation that surfactin and other secreted matrix components aid in escape of cells from the fully mature biofilm colony is an important step in understanding robust biofilm structures. Importantly, the presence of Ca2+ ions restricts this escape mechanism, as they form complexes with the surfactin molecules. In addition to the physical features that shape biofilms, intrinsic metabolic strategies also play an important role in biofilms. The tradeoff between growth rate and yield; and their coexistence in spatial structures marks the first empirical evidence of its kind.

References

References

1 Flemming, H. C. & Wingender, J. The biofilm matrix. *Nat Rev Microbiol* ***8***, 623-633 (2010).

2 Stoodley, P., Sauer, K., Davies, D. & Costerton, J. W. Biofilms as complex differentiated communities. *Annu Rev Microbiol* ***56***, 187-209 (2002).

3 Ben-Jacob, E. Bacterial self–organization: co–enhancement of complexification and adaptability in a dynamic environment. *Phil. Trans. R. Soc. A* ***361***, 1283-1312 (2003).

4 Abee, T., Kovacs, A. T., Kuipers, O. P. & van der Veen, S. Biofilm formation and dispersal in Gram-positive bacteria. *Curr Opin Biotechnol* ***22***, 172-179 (2011).

5 Castiblanco, L. F. & Sundin, G. W. New insights on molecular regulation of biofilm formation in plant-associated bacteria. *J Integr Plant Biol* ***58***, 362-372 (2016).

6 Hall-Stoodley, L., Costerton, J. W. & Stoodley, P. Bacterial biofilms: from the natural environment to infectious diseases. *Nat Rev Microbiol* ***2***, 95-108 (2004).

7 Oliveira, N. M. *et al.* Biofilm formation as a response to ecological competition. *PLoS Biol* ***13***, e1002191 (2015).

8 Lindsay, D. & Von Holy, A. Bacterial biofilms within the clinical setting: what healthcare professionals should know. *J Hosp Infect* ***64***, 313-325 (2006).

9 Costerton, J. W. *et al.* Bacterial biofilms in nature and disease. *Annu Rev Microbiol* ***41***, 435-464 (1987).

10 Høiby, N., Ciofu, O. & Bjarnsholt, T. *Pseudomonas aeruginosa* biofilms in cystic fibrosis. *Future Microbiol* ***5***, 1663-1674 (2010).

11 Lindback, T. *et al.* CodY, a pleiotropic regulator, influences multicellular behaviour and efficient production of virulence factors in *Bacillus cereus*. *Environ Microbiol* ***14***, 2233-2246 (2012).

12 Allen, B., Gore, J. & Nowak, M. A. Spatial dilemmas of diffusible public goods. *Elife* ***2***, e01169 (2013).

13 Bachmann, H., Bruggeman, F. J., Molenaar, D., Branco Dos Santos, F. & Teusink, B. Public goods and metabolic strategies. *Curr Opin Microbiol* ***31***, 109-115 (2016).

14 Morris, J. J., Lenski, R. E. & Zinser, E. R. The Black Queen Hypothesis: evolution of dependencies through adaptive gene loss. *mBio* ***3*** (2012).

15 Aguilar, C., Eichwald, C. & Eberl, L. Multicellularity in Bacteria: From Division of Labor to Biofilm Formation. *Adv Mar Genomics*, 79 (2015).

16 Smits, W. K., Kuipers, O. P. & Veening, J.-W. Phenotypic variation in bacteria: the role of feedback regulation. *Nat Rev Microbiol* ***4***, 259-271 (2006).

17 Waters, C. M. & Bassler, B. L. Quorum sensing: cell-to-cell communication in bacteria. *Annu. Rev. Cell Dev. Biol.* ***21***, 319-346 (2005).

18 Pesci, E. C. *et al.* Quinolone signaling in the cell-to-cell communication system of *Pseudomonas aeruginosa*. *Proc Natl Acad Sci U S A* ***96***, 11229-11234 (1999).

19 Kumar, S. & Engelberg-Kulka, H. Quorum sensing peptides mediating interspecies bacterial cell death as a novel class of antimicrobial agents. *Curr Opin Microbiol* ***21***, 22-27 (2014).

20 Nealson, K. H., Platt, T. & Hastings, J. W. Cellular control of the synthesis and activity of the bacterial luminescent system. *J Bacteriol* ***104***, 313-322 (1970).

21 Sio, C. F. *et al.* Quorum quenching by an N-acyl-homoserine lactone acylase from Pseudomonas aeruginosa PAO1. *Infect Immun* ***74***, 1673-1682 (2006).

22 Hamoen, L. W., Venema, G. & Kuipers, O. P. Controlling competence in *Bacillus subtilis:* shared use of regulators. *Microbiol* ***149***, 9-17 (2003).
23 Li, Y.-H. *et al.* A quorum-sensing signaling system essential for genetic competence in *Streptococcus mutans* is involved in biofilm formation. *J Bacteriol* ***184***, 2699-2708 (2002).
24 Mitri, S., Clarke, E. & Foster, K. R. Resource limitation drives spatial organization in microbial groups. *ISME J* ***10***, 1471-1482 (2016).
25 Momeni, B., Waite, A. J. & Shou, W. Spatial self-organization favors heterotypic cooperation over cheating. *Elife* ***2***, e00960 (2013).
26 Nadell, C. D., Drescher, K., Wingreen, N. S. & Bassler, B. L. Extracellular matrix structure governs invasion resistance in bacterial biofilms. *ISME J* ***9***, 1700-1709 (2015).
27 Pande, S. *et al.* Privatization of cooperative benefits stabilizes mutualistic cross-feeding interactions in spatially structured environments. *ISME J* ***10***, 1413-1423 (2016).
28 Van Dyken, J. D., Müller, M. J., Mack, K. M. & Desai, M. M. Spatial population expansion promotes the evolution of cooperation in an experimental prisoner's dilemma. *Curr Biol* ***23***, 919-923 (2013).
29 Dietrich, L. E., Teal, T. K., Price-Whelan, A. & Newman, D. K. Redox-active antibiotics control gene expression and community behavior in divergent bacteria. *Science* ***321***, 1203-1206 (2008).
30 Sun, S., Tay, Q. X. M., Kjelleberg, S., Rice, S. A. & McDougald, D. Quorum sensing-regulated chitin metabolism provides grazing resistance to *Vibrio cholerae* biofilms. *ISME J* ***9***, 1812-1820 (2015).
31 Ponciano, J. M., La, H. J., Joyce, P. & Forney, L. J. Evolution of diversity in spatially structured *Escherichia coli* populations. *Appl Environ Microbiol* ***75***, 6047-6054 (2009).
32 Stocker, R. Marine microbes see a sea of gradients. *Science* ***338***, 628-633 (2012).
33 Tilman, D. Resource competition between plankton algae: an experimental and theoretical approach. *Ecology* ***58***, 338-348 (1977).
34 Kassen, R. Toward a general theory of adaptive radiation. *Ann N Y Acad Sci* ***1168***, 3-22 (2009).
35 Harcombe, W. Novel cooperation experimentally evolved between species. *Evolution* ***64***, 2166-2172 (2010).
36 Beardmore, R. E., Gudelj, I., Lipson, D. A. & Hurst, L. D. Metabolic trade-offs and the maintenance of the fittest and the flattest. *Nature* ***472***, 342-346 (2011).
37 Ponomarova, O. & Patil, K. R. Metabolic interactions in microbial communities: untangling the Gordian knot. *Curr Opin Microbiol* ***27***, 37-44 (2015).
38 Craig MacLean, R. Adaptive radiation in microbial microcosms. *J Evol Biol* ***18***, 1376-1386 (2005).
39 Meyer, J. R., Gudelj, I. & Beardmore, R. Biophysical mechanisms that maintain biodiversity through trade-offs. *Nat Commun* ***6***, 6278 (2015).
40 Roller, B. R. & Schmidt, T. M. The physiology and ecological implications of efficient growth. *ISME J* ***9***, 1481-1487 (2015).
41 Stettner, A. I. & Segre, D. The cost of efficiency in energy metabolism. *Proc Natl Acad Sci U S A* ***110***, 9629-9630 (2013).
42 Molenaar, D., van Berlo, R., de Ridder, D. & Teusink, B. Shifts in growth strategies reflect tradeoffs in cellular economics. *Mol Syst Biol* ***5***, 323 (2009).

43 Flamholz, A., Noor, E., Bar-Even, A., Liebermeister, W. & Milo, R. Glycolytic strategy as a tradeoff between energy yield and protein cost. *Proc Natl Acad Sci U S A* ***110***, 10039-10044 (2013).
44 Dykhuizen, D. & Davies, M. An experimental model: bacterial specialists and generalists competing in chemostats. *Ecology* ***61***, 1213-1227 (1980).
45 Schuster, S., Pfeiffer, T. & Fell, D. A. Is maximization of molar yield in metabolic networks favoured by evolution? *J Theorl Biol* ***252***, 497-504 (2008).
46 Gudelj, I. *et al.* An integrative approach to understanding microbial diversity: from intracellular mechanisms to community structure. *Ecol Lett* ***13***, 1073-1084 (2010).
47 Lele, U. N. & Gwatve, M. Bacterial growth rate and growth yield: Is there a relationship? *Proc Natl Acad Sci U S A* ***80***, 537 (2014).
48 Pfeiffer, T., Schuster, S. & Bonhoeffer, S. Cooperation and competition in the evolution of ATP-producing pathways. *Science* ***292***, 504-507 (2001).
49 Merritt, J. & Kuehn, S. When communities collide. *Elife* ***5***, e18753 (2016).
50 Barrett, R. D., MacLean, R. C. & Bell, G. Experimental evolution of *Pseudomonas fluorescens* in simple and complex environments. *Am. Nat* ***166***, 470-480 (2005).
51 Esser, D. S., Leveau, J. H. & Meyer, K. M. Modeling microbial growth and dynamics. *Appl Microbiol Biotechnol* ***99***, 8831-8846 (2015).
52 Bachmann, H. *et al.* Availability of public goods shapes the evolution of competing metabolic strategies. *Proc Natl Acad Sci U S A* ***110***, 14302-14307 (2013).
53 Bachmann, H., Pronk, J. T., Kleerebezem, M. & Teusink, B. Evolutionary engineering to enhance starter culture performance in food fermentations. *Curr Opin Biotechnol* ***32***, 1-7 (2015).
54 Kreft, J. U. Biofilms promote altruism. *Microbiol* ***150***, 2751-2760 (2004).
55 Collins, S. Growth rate evolution in improved environments under Prodigal Son dynamics. *Evol Appl*, doi:10.1111/eva.12403 (2016).
56 Dmitriew, C. M. The evolution of growth trajectories: what limits growth rate? *Biol Rev* ***86***, 97-116 (2011).
57 Frick, T. & Schuster, S. An example of the prisoner's dilemma in biochemistry. *Die Naturwissenschaften* ***90***, 327-331 (2003).
58 Amado, A., Fernández, L., Huang, W., Ferreira, F. F. & Campos, P. R. Competing metabolic strategies in a multilevel selection model. *arXiv preprint arXiv:1602.04773* (2016).
59 Nowak, M. A. & May, R. M. Evolutionary games and spatial chaos. *Nature* ***359***, 826-829 (1992).
60 Wanner, O. & Reichert, P. Mathematical modeling of mixed‐culture biofilms. *Biotechnol Bioeng* ***49***, 172-184 (1996).
61 Wortel, M. T., Bosdriesz, E., Teusink, B. & Bruggeman, F. J. Evolutionary pressures on microbial metabolic strategies in the chemostat. *Sci Rep* ***6*** (2016).
62 Zarecki, R. *et al.* Maximal sum of metabolic exchange fluxes outperforms biomass yield as a predictor of growth rate of microorganisms. *PLoS One* ***9***, e98372 (2014).
63 Stanley, N. R. & Lazazzera, B. A. Defining the genetic differences between wild and domestic strains of *Bacillus subtilis* that affect poly-gamma-dl-glutamic acid production and biofilm formation. *Mol Microbiol* ***57***, 1143-1158 (2005).
64 Branda, S. S., Chu, F., Kearns, D. B., Losick, R. & Kolter, R. A major protein component of the *Bacillus subtilis* biofilm matrix. *Mol Microbiol* ***59***, 1229-1238 (2006).
65 Branda, S. S. *et al.* Genes involved in formation of structured multicellular communities by *Bacillus subtilis*. *J Bacteriol* ***186***, 3970-3979 (2004).

66 Hobley, L. *et al.* BslA is a self-assembling bacterial hydrophobin that coats the *Bacillus subtilis* biofilm. *Proc Natl Acad Sci U S A* ***110***, 13600-13605 (2013).
67 Kobayashi, K. & Iwano, M. BslA (YuaB) forms a hydrophobic layer on the surface of *Bacillus subtilis* biofilms. *Mol Microbiol* ***85***, 51-66 (2012).
68 Kovács, Á. T., van Gestel, J. & Kuipers, O. P. The protective layer of biofilm: a repellent function for a new class of amphiphilic proteins. *Mol Microbiol* ***85***, 8-11 (2012).
69 Romero, D., Aguilar, C., Losick, R. & Kolter, R. Amyloid fibers provide structural integrity to *Bacillus subtilis* biofilms. *Proc Natl Acad Sci U S A* ***107***, 2230-2234 (2010).
70 McLoon, A. L., Guttenplan, S. B., Kearns, D. B., Kolter, R. & Losick, R. Tracing the domestication of a biofilm-forming bacterium. *J Bacteriol* ***193***, 2027-2034 (2011).
71 Pollak, S., Bendori, S. O. & Eldar, A. A complex path for domestication of *B. subtilis* sociality. *Curr Gen* ***61***, 493-496 (2015).
72 Branda, S. S., Gonzalez-Pastor, J. E., Ben-Yehuda, S., Losick, R. & Kolter, R. Fruiting body formation by *Bacillus subtilis*. *Proc Natl Acad Sci U S A* ***98***, 11621-11626 (2001).
73 Kobayashi, K. Gradual activation of the response regulator DegU controls serial expression of genes for flagellum formation and biofilm formation in *Bacillus subtilis*. *Mol Microbiol* ***66***, 395-409 (2007).
74 Bais, H. P., Weir, T. L., Perry, L. G., Gilroy, S. & Vivanco, J. M. The role of root exudates in rhizosphere interactions with plants and other organisms. *Annu. Rev. Plant Biol.* ***57***, 233-266 (2006).
75 Vlamakis, H., Chai, Y., Beauregard, P., Losick, R. & Kolter, R. Sticking together: building a biofilm the *Bacillus subtilis* way. *Nat Rev Microbiol* ***11***, 157-168 (2013).
76 Patrick, J. E. & Kearns, D. B. Laboratory strains of *Bacillus subtilis* do not exhibit swarming motility. *J Bacteriol* ***191***, 7129-7133 (2009).
77 Jiang, M., Shao, W., Perego, M. & Hoch, J. A. Multiple histidine kinases regulate entry into stationary phase and sporulation in *Bacillus subtilis*. *Mol Microbiol* ***38***, 535-542 (2000).
78 Kolodkin-Gal, I. *et al.* Respiration control of multicellularity in *Bacillus subtilis* by a complex of the cytochrome chain with a membrane-embedded histidine kinase. *Genes Dev* ***27***, 887-899 (2013).
79 Straight, P. D., Willey, J. M. & Kolter, R. Interactions between *Streptomyces coelicolor* and *Bacillus subtilis*: Role of surfactants in raising aerial structures. *J Bacteriol* ***188***, 4918-4925 (2006).
80 Lopez, D., Fischbach, M. A., Chu, F., Losick, R. & Kolter, R. Structurally diverse natural products that cause potassium leakage trigger multicellularity in *Bacillus subtilis*. *Proc Natl Acad Sci U S A* ***106***, 280-285 (2009).
81 Lopez, D., Gontang, E. A. & Kolter, R. Potassium sensing histidine kinase in *Bacillus subtilis*. *Methods Enzymol* ***471***, 229-251 (2010).
82 Romero, D., Traxler, M. F., Lopez, D. & Kolter, R. Antibiotics as signal molecules. *Chem Rev* ***111***, 5492-5505 (2011).
83 Yepes, A. *et al.* The biofilm formation defect of a *Bacillus subtilis* flotillin‐defective mutant involves the protease FtsH. *Mol Microbiol* ***86***, 457-471 (2012).
84 Le, A. T. T. & Schumann, W. The Spo0E phosphatase of *Bacillus subtilis* is a substrate of the FtsH metalloprotease. *Microbiol* ***155***, 1122-1132 (2009).

85 Donovan, C. & Bramkamp, M. Characterization and subcellular localization of a bacterial flotillin homologue. *Microbiol* ***155***, 1786-1799 (2009).
86 Shemesh, M., Kolter, R. & Losick, R. The biocide chlorine dioxide stimulates biofilm formation in *Bacillus subtilis* by activation of the histidine kinase KinC. *J Bacteriol* ***192***, 6352-6356 (2010).
87 Shank, E. A. *et al.* Interspecies interactions that result in *Bacillus subtilis* forming biofilms are mediated mainly by members of its own genus. *Proc Natl Acad Sci U S A* ***108***, E1236-E1243 (2011).
88 Beauregard, P. B., Chai, Y., Vlamakis, H., Losick, R. & Kolter, R. *Bacillus subtilis* biofilm induction by plant polysaccharides. *Proc Natl Acad Sci U S A* ***110***, E1621-1630 (2013).
89 Chai, Y., Beauregard, P. B., Vlamakis, H., Losick, R. & Kolter, R. Galactose metabolism plays a crucial role in biofilm formation by *Bacillus subtilis*. *MBio* ***3***, e00184-00112 (2012).
90 Lopez, D. & Kolter, R. Functional microdomains in bacterial membranes. *Genes Dev* ***24***, 1893-1902 (2010).
91 Lopez, D., Vlamakis, H., Losick, R. & Kolter, R. Cannibalism enhances biofilm development in *Bacillus subtilis*. *Mol Microbiol* ***74***, 609-618 (2009).
92 Chen, Y. *et al.* A *Bacillus subtilis* sensor kinase involved in triggering biofilm formation on the roots of tomato plants. *Mol Microbiol* ***85***, 418-430 (2012).
93 Shemesh, M. & Chai, Y. A combination of glycerol and manganese promotes biofilm formation in *Bacillus subtilis* via histidine kinase KinD signaling. *J Bacteriol* ***195***, 2747-2754 (2013).
94 Pelchovich, G., Omer-Bendori, S. & Gophna, U. Menaquinone and iron are essential for complex colony development in *Bacillus subtilis*. *PloS one* ***8***, e79488 (2013).
95 Rubinstein, S. M. *et al.* Osmotic pressure can regulate matrix gene expression in *Bacillus subtilis*. *Mol Microbiol* ***86***, 426-436 (2012).
96 Wu, R. *et al.* Insight into the sporulation phosphorelay: crystal structure of the sensor domain of *Bacillus subtilis* histidine kinase, KinD. *Protein Sci* ***22***, 564-576 (2013).
97 Charney, J., Fisher, W. & Hegarty, C. Manganese as an essential element for sporulation in the genus Bacillus. *J Bacteriol* ***62***, 145 (1951).
98 Hoover, S. E., Xu, W., Xiao, W. & Burkholder, W. F. Changes in DnaA-dependent gene expression contribute to the transcriptional and developmental response of *Bacillus subtilis* to manganese limitation in Luria-Bertani medium. *J Bacteriol* ***192***, 3915-3924 (2010).
99 Mhatre, E. *et al.* The impact of manganese on biofilm development of *Bacillus subtilis*. *Microbiol* ***162***, 1468-1478 (2016).
100 Aguilar, C., Vlamakis, H., Guzman, A., Losick, R. & Kolter, R. KinD is a checkpoint protein linking spore formation to extracellular-matrix production in *Bacillus subtilis* biofilms. *MBio* ***1*** (2010).
101 Mhatre, E., Monterrosa, R. G. & Kovacs, A. T. From environmental signals to regulators: modulation of biofilm development in Gram-positive bacteria. *J Basic Microbiol* ***54***, 616-632 (2014).
102 Farrand, S. & Taber, H. Changes in menaquinone concentration during growth and early sporulation in *Bacillus subtilis*. *J Bacteriol* ***117***, 324-326 (1974).

103 Chubukov, V. & Sauer, U. Environmental dependence of stationary-phase metabolism in Bacillus subtilis and Escherichia coli. *Appl Environ. Microbiol* ***80***, 2901-2909 (2014).
104 Grau, R. R. *et al.* A duo of potassium-responsive histidine kinases govern the multicellular destiny of *Bacillus subtilis*. *mBio* ***6***, e00581-00515 (2015).
105 Kinsinger, R. F., Shirk, M. C. & Fall, R. Rapid surface motility in *Bacillus subtilis* is dependent on extracellular surfactin and potassium ion. *J Bacteriol* ***185***, 5627-5631 (2003).
106 van Gestel, J., Vlamakis, H. & Kolter, R. From cell differentiation to cell collectives: *Bacillus subtilis* uses division of labor to migrate. *PLoS Biol* ***13***, e1002141 (2015).
107 Fall, R., Kearns, D. B. & Nguyen, T. A defined medium to investigate sliding motility in a *Bacillus subtilis* flagella-less mutant. *BMC Microbiol* ***6***, 1 (2006).
108 Chai, Y., Chu, F., Kolter, R. & Losick, R. Bistability and biofilm formation in *Bacillus subtilis*. *Mol Microbiol* ***67***, 254-263 (2008).
109 Kearns, D. B., Chu, F., Branda, S. S., Kolter, R. & Losick, R. A master regulator for biofilm formation by *Bacillus subtilis*. *Mol Microbiol* ***55***, 739-749 (2005).
110 Lewis, R. J., Brannigana, J. A., Smith, I. & Wilkinson, A. J. Crystallisation of the *Bacillus subtilis* sporulation inhibitor SinR, complexed with its antagonist, Sinl. *FEBS Lett.* ***378***, 98-100 (1996).
111 Kobayashi, K. SlrR/SlrA controls the initiation of biofilm formation in *Bacillus subtilis*. *Mol Microbiol* ***69***, 1399-1410 (2008).
112 Chai, Y., Kolter, R. & Losick, R. Reversal of an epigenetic switch governing cell chaining in *Bacillus subtilis* by protein instability. *Mol Microbiol* ***78***, 218-229 (2010).
113 Chai, Y., Norman, T., Kolter, R. & Losick, R. An epigenetic switch governing daughter cell separation in *Bacillus subtilis*. *Genes Dev.* ***24***, 754-765 (2010).
114 Murray, E. J., Kiley, T. B. & Stanley-Wall, N. R. A pivotal role for the response regulator DegU in controlling multicellular behaviour. *Microbiol* ***155***, 1-8 (2009).
115 Hamoen, L. W., Van Werkhoven, A. F., Venema, G. & Dubnau, D. The pleiotropic response regulator DegU functions as a priming protein in competence development in *Bacillus subtilis*. *Proc Natl Acad Sci U S A* ***97***, 9246-9251 (2000).
116 Verhamme, D. T., Kiley, T. B. & Stanley-Wall, N. R. DegU co-ordinates multicellular behaviour exhibited by *Bacillus subtilis*. *Mol Microbiol* ***65***, 554-568 (2007).
117 Comella, N. & Grossman, A. D. Conservation of genes and processes controlled by the quorum response in bacteria: characterization of genes controlled by the quorum‐sensing transcription factor ComA in *Bacillus subtilis*. *Mol Microbiol* ***57***, 1159-1174 (2005).
118 Magnuson, R., Solomon, J. & Grossman, A. D. Biochemical and genetic characterization of a competence pheromone from *B. subtilis*. *Cell* ***77***, 207-216 (1994).
119 Kleerebezem, M., Quadri, L. E., Kuipers, O. P. & De Vos, W. M. Quorum sensing by peptide pheromones and two‐component signal transduction systems in Gram positive bacteria. *Mol Microbiol* ***24***, 895-904 (1997).
120 Ruzheinikov, S. *et al.* The 1.2 Å structure of a novel quorum-sensing protein, *Bacillus subtilis* LuxS. *J Mol Biol* ***313***, 111-122 (2001).
121 Stefanic, P. *et al.* The quorum sensing diversity within and between ecotypes of *Bacillus subtilis*. *Environ Microbiol* ***14***, 1378-1389 (2012).
122 Kearns, D. B. Division of labour during *Bacillus subtilis* biofilm formation. *Mol Microbiol* ***67***, 229-231 (2008).

123 Stefanic, P., Kraigher, B., Lyons, N. A., Kolter, R. & Mandic-Mulec, I. Kin discrimination between sympatric Bacillus subtilis isolates. *Proc Natl Acad Sci U S A* ***112***, 14042-14047 (2015).
124 Nandy, S. K., Bapat, P. M. & Venkatesh, K. Sporulating bacteria prefers predation to cannibalism in mixed cultures. *FEBS letters* ***581***, 151-156 (2007).
125 Claverys, J. P. & Håvarstein, L. S. Cannibalism and fratricide: mechanisms and raisons d'etre. *Nat Rev Microbiol* ***5***, 219-229 (2007).
126 Schuster, S., Kreft, J.-U., Schroeter, A. & Pfeiffer, T. Use of game-theoretical methods in biochemistry and biophysics. *J Biol Phys* ***34***, 1-17 (2008).
127 Dauner, M., Storni, T. & Sauer, U. *Bacillus subtilis* metabolism and energetics in carbon-limited and excess-carbon chemostat culture. *J Bacteriol* ***183***, 7308-7317 (2001).
128 Sonenshein, A. L. Control of key metabolic intersections in *Bacillus subtilis*. *Nat Rev Microbiol* ***5***, 917-927 (2007).
129 Chai, Y., Kolter, R. & Losick, R. A widely conserved gene cluster required for lactate utilization in *Bacillus subtilis* and its involvement in biofilm formation. *J Bacteriol* ***191***, 2423-2430 (2009).
130 Commichau, F. M. & Stülke, J. Trigger enzymes: bifunctional proteins active in metabolism and in controlling gene expression. *Mol Microbiol* ***67***, 692-702 (2008).
131 González-Cabaleiro, R., Ofi, tcedil, I. D., Lema, J. M. & Rodríguez, J. Microbial catabolic activities are naturally selected by metabolic energy harvest rate. *ISME J* ***9***, 2630-2641 (2015).
132 Liu, J. *et al.* Metabolic co-dependence gives rise to collective oscillations within biofilms. *Nature* ***523***, 550-554 (2015).
133 Earl, A. M., Losick, R. & Kolter, R. Ecology and genomics of *Bacillus subtilis*. *Trends Microbiol* ***16***, 269-275 (2008).
134 Shank, E. A. & Kolter, R. Extracellular signaling and multicellularity in *Bacillus subtilis*. *Curr Opin Microbiol* ***14***, 741-747 (2011).
135 Bjarnsholt, T. *et al.* The in vivo biofilm. *Trends Microbiol* ***21***, 466-474 (2013).
136 Valderrama, W. B. & Cutter, C. N. An ecological perspective of *Listeria monocytogenes* biofilms in food processing facilities. *Crit Rev Food Sci Nutr* ***53***, 801-817 (2013).
137 Bais, H. P., Fall, R. & Vivanco, J. M. Biocontrol of *Bacillus subtilis* against infection of Arabidopsis roots by *Pseudomonas syringae* is facilitated by biofilm formation and surfactin production. *Plant Physiol* ***134***, 307-319 (2004).
138 Mielich-Suss, B. & Lopez, D. Molecular mechanisms involved in *Bacillus subtilis* biofilm formation. *Environ Microbiol* ***17***, 555-565 (2015).
139 Burkholder, P. R. & Giles Jr, N. H. Induced biochemical mutations in *Bacillus subtilis*. *Am. J. Bot.*, 345-348 (1947).
140 Barbe, V. *et al.* From a consortium sequence to a unified sequence: the *Bacillus subtilis* 168 reference genome a decade later. *Microbiol* ***155***, 1758-1775 (2009).
141 Kunst, F. *et al.* The complete genome sequence of the gram-positive bacterium *Bacillus subtilis*. *Nature* ***390***, 249-256 (1997).
142 Zeigler, D. R. *et al.* The origins of 168, W23, and other *Bacillus subtilis* legacy strains. *J Bacteriol* ***190***, 6983-6995 (2008).
143 Cairns, L. S., Hobley, L. & Stanley‐Wall, N. R. Biofilm formation by *Bacillus subtilis*: new insights into regulatory strategies and assembly mechanisms. *Mol Microbiol* ***93***, 587-598 (2014).

144 Romero, D. Bacterial determinants of the social behavior of *Bacillus subtilis*. *Res Microbiol* ***164***, 788-798 (2013).
145 Pollak, S., Omer Bendori, S. & Eldar, A. A complex path for domestication of *B. subtilis* sociality. *Curr Genet* ***61***, 493-496 (2015).
146 Branda, S. S. *et al.* Genes involved in formation of structured multicellular communities by *Bacillus subtilis*. *J Bacteriol* ***186***, 3970-3979 (2004).
147 Jones, S. E., Paynich, M. L., Kearns, D. B. & Knight, K. L. Protection from intestinal inflammation by bacterial exopolysaccharides. *J Immunol* ***192***, 4813-4820 (2014).
148 Roux, D. *et al.* Identification of poly-N-acetylglucosamine as a major polysaccharide component of the *Bacillus subtilis* biofilm matrix. *J Biol Chem* ***290***, 19261-19272 (2015).
149 Kohlstedt, M. *et al.* Adaptation of *Bacillus subtilis* carbon core metabolism to simultaneous nutrient limitation and osmotic challenge: a multi-omics perspective. *Environ Microbiol* ***16***, 1898-1917 (2014).
150 Meyer, H. *et al.* A time resolved metabolomics study: the influence of different carbon sources during growth and starvation of *Bacillus subtilis*. *Mol Biosyst* ***10***, 1812-1823 (2014).
151 Kovacs, A. T. & Kuipers, O. P. Rok regulates yuaB expression during architecturally complex colony development of *Bacillus subtilis* 168. *J Bacteriol* ***193***, 998-1002 (2011).
152 Arabolaza, A. L. *et al.* Characterization of a novel inhibitory feedback of the anti‐anti‐sigma SpoIIAA on Spo0A activation during development in *Bacillus subtilis*. *Mol Microbiol* ***47***, 1251-1263 (2003).
153 González-Pastor, J. E., Hobbs, E. C. & Losick, R. Cannibalism by sporulating bacteria. *Science* ***301***, 510-513 (2003).
154 Kobayashi, K. *Bacillus subtilis* pellicle formation proceeds through genetically defined morphological changes. *J Bacteriol* ***189***, 4920-4931 (2007).
155 Chu, F., Kearns, D. B., Branda, S. S., Kolter, R. & Losick, R. Targets of the master regulator of biofilm formation in *Bacillus subtilis*. *Mol Microbiol* ***59***, 1216-1228 (2006).
156 Romero, D., Vlamakis, H., Losick, R. & Kolter, R. An accessory protein required for anchoring and assembly of amyloid fibres in *B. subtilis* biofilms. *Mol Microbiol* ***80***, 1155-1168 (2011).
157 Chen, Y. *et al.* Biocontrol of tomato wilt disease by *Bacillus subtilis* isolates from natural environments depends on conserved genes mediating biofilm formation. *Environ Microbiol* ***15***, 848-864 (2013).
158 Stanley, C. E. *et al.* Probing bacterial–fungal interactions at the single cell level. *Integr Biology* ***6***, 935-945 (2014).
159 Buescher, J. M. *et al.* Global network reorganization during dynamic adaptations of *Bacillus subtilis* metabolism. *Science* ***335***, 1099-1103 (2012).
160 Ozturk, S., Calik, P. & Ozdamar, T. H. Fed-batch biomolecule production by *Bacillus subtilis*: A state of the art review. *Trends Biotechnol* ***34***, 329-345 (2016).
161 Nicolas, P. *et al.* Condition-dependent transcriptome reveals high-level regulatory architecture in *Bacillus subtilis*. *Science* ***335***, 1103-1106 (2012).
162 Bajaj, I., Veiga, T., van Dissel, D., Pronk, J. T. & Daran, J.-M. Functional characterization of a *Penicillium chrysogenum* mutanase gene induced upon co-cultivation with *Bacillus subtilis*. *BMC Microbiol* ***14***, 1 (2014).

163 Benoit, I. *et al. Bacillus subtilis* attachment to Aspergillus niger hyphae results in mutually altered metabolism. *Environ Microbiol* ***17***, 2099-2113 (2015).
164 Powers, M. J., Sanabria-Valentin, E., Bowers, A. A. & Shank, E. A. Inhibition of cell differentiation in *Bacillus subtilis* by *Pseudomonas protegens*. *J Bacteriol* ***197***, 2129-2138 (2015).
165 Vargas-Bautista, C., Rahlwes, K. & Straight, P. Bacterial competition reveals differential regulation of the pks genes by *Bacillus subtilis*. *J Bacteriol* ***196***, 717-728 (2014).
166 Kearns, D. B. & Losick, R. Swarming motility in undomesticated *Bacillus subtilis*. *Mol Microbiol* ***49***, 581-590 (2004).
167 Asally, M. *et al.* Localized cell death focuses mechanical forces during 3D patterning in a biofilm. *Proc Natl Acad Sci U S A* ***109***, 18891-18896 (2012).
168 Wilking, J. N. *et al.* Liquid transport facilitated by channels in *Bacillus subtilis* biofilms. *Proc Natl Acad Sci U S A* ***110***, 848-852 (2013).
169 van Gestel, J., Weissing, F. J., Kuipers, O. P. & Kovacs, A. T. Density of founder cells affects spatial pattern formation and cooperation in *Bacillus subtilis* biofilms. *ISME J* ***8***, 2069-2079 (2014).
170 Harwood, C. R. & Cutting, S. M. *Molecular biological methods for Bacillus*. (Wiley, 1990).
171 Konkol, M. A., Blair, K. M. & Kearns, D. B. Plasmid-encoded ComI inhibits competence in the ancestral 3610 strain of *Bacillus subtilis*. *J Bacteriol* ***195***, 4085-4093 (2013).
172 Oslizlo, A. *et al.* Exploring ComQXPA quorum-sensing diversity and biocontrol potential of Bacillus spp. isolates from tomato rhizoplane. *Microb Biotechnol* ***8***, 527-540 (2015).
173 Seccareccia, I., Kovács, Á. T., Gallegos-Monterrosa, R. & Nett, M. Unraveling the predator-prey relationship of *Cupriavidus necator* and *Bacillus subtilis*. *Microbiol Res* ***192***, 231-238 (2016).
174 He, K. & Bauer, C. E. Chemosensory signaling systems that control bacterial survival. *Trends Microbiol* (2014).
175 Ng, W.-L. & Bassler, B. L. Bacterial quorum-sensing network architectures. *Annu Rev Genet* ***43***, 197-222 (2009).
176 Kaiser, D. in *Evolutionary Transitions to Multicellular Life* 469-485 (Springer, 2015).
177 Traxler, M. F. & Kolter, R. Natural products in soil microbe interactions and evolution. *Nat Prod Rep* (2015).
178 Lopez, D. & Kolter, R. Extracellular signals that define distinct and coexisting cell fates in *Bacillus subtilis*. *FEMS Microbiol Rev* ***34***, 134-149 (2010).
179 Hoch, J. A. Regulation of the phosphorelay and the initiation of sporulation in *Bacillus subtilis*. *Annu Rev Microbiol* ***47***, 441-465 (1993).
180 Grimshaw, C. E. *et al.* Synergistic kinetic interactions between components of the phosphorelay controlling sporulation in *Bacillus subtilis*. *Biochemistry* ***37***, 1365-1375 (1998).
181 Kovács, Á. T. Bacterial differentiation via gradual activation of global regulators. *Curr Genet*, 1-4 (2015).
182 Jakubovics, N. S. & Jenkinson, H. F. Out of the iron age: new insights into the critical role of manganese homeostasis in bacteria. *Microbiol* ***147***, 1709-1718 (2001).

183 Helmann, J. D. Specificity of metal sensing: iron and manganese homeostasis in *Bacillus subtilis*. *J Biol Chem* ***289***, 28112-28120 (2014).
184 Vasantha, N. & Freese, E. The role of manganese in growth and sporulation of *Bacillus subtilis*. *J Gen Microbiol* ***112***, 329 (1979).
185 Nozaka, S. *et al.* Manganese ion increases LAB-yeast mixed-species biofilm formation. *Biosci Microbiota Food Health* ***33***, 79-84 (2014).
186 Mironczuk, A. M., Manu, A., Kuipers, O. P. & Kovács, Á. T. Distinct roles of ComK1 and ComK2 in gene regulation in *Bacillus cereus*. *PLoS One* ***6***, e21859 (2011).
187 Webb, J. S. *et al.* Cell death in *Pseudomonas aeruginosa* biofilm development. *J Bacteriol* ***185***, 4585-4592 (2003).
188 Yudkin, M. Structure and function in a *Bacillus subtilis* sporulation-specific sigma factor: molecular nature of mutations in *spoIIAC*. *Microbiol* ***133***, 475-481 (1987).
189 Eichenberger, P. *et al.* The program of gene transcription for a single differentiating cell type during sporulation in *Bacillus subtilis*. *PLoS Biol* (2004).
190 Kuwana, R., Okumura, T., Takamatsu, H. & Watabe, K. The *ylbO* gene product of *Bacillus subtilis* is involved in the coat development and lysozyme resistance of spore. *FEMS Microbiol Lett* ***242***, 51-57 (2005).
191 Hamon, M. A. & Lazazzera, B. A. The sporulation transcription factor Spo0A is required for biofilm development in *Bacillus subtilis*. *Mol Microbiol* ***42***, 1199-1209 (2001).
192 Veening, J. W. *et al.* Transient heterogeneity in extracellular protease production by *Bacillus subtilis*. *Mol Syst Biol* ***4***, 184 (2008).
193 Lopez, D., Vlamakis, H., Losick, R. & Kolter, R. Paracrine signaling in a bacterium. *Genes Dev* ***23***, 1631-1638 (2009).
194 Veening, J. W., Hamoen, L. W. & Kuipers, O. P. Phosphatases modulate the bistable sporulation gene expression pattern in *Bacillus subtilis*. *Mol Microbiol* ***56***, 1481-1494 (2005).
195 Zheng, G., Yan, L. Z., Vederas, J. C. & Zuber, P. Genes of the *sbo-alb* Locus of *Bacillus subtilis* are required for production of the antilisterial Bacteriocin Subtilosin. *J Bacteriol* ***181***, 7346-7355 (1999).
196 Devi, S. N., Vishnoi, M., Kiehler, B., Haggett, L. & Fujita, M. In vivo functional characterization of the transmembrane histidine kinase KinC in *Bacillus subtilis*. *Microbiol* ***161***, 1092-1104 (2015).
197 Kobayashi, K. *et al.* Essential *Bacillus subtilis* genes. *Proc Natl Acad Sci U S A* ***100***, 4678-4683 (2003).
198 Fujita, M., González-Pastor, J. E. & Losick, R. High-and low-threshold genes in the Spo0A regulon of *Bacillus subtilis*. *J Bacteriol* ***187***, 1357-1368 (2005).
199 Cangiano, G. *et al.* Direct and indirect control of late sporulation genes by GerR of *Bacillus subtilis*. *J Bacteriol* ***192***, 3406-3413 (2010).
200 Anagnostopoulos, C. & Spizizen, J. Requirements for transformation in *Bacillus subtilis*. *J Bacteriol* ***81***, 741 (1961).
201 Veening, J.-W., Murray, H. & Errington, J. A mechanism for cell cycle regulation of sporulation initiation in *Bacillus subtilis*. *Genes Dev* ***23***, 1959-1970 (2009).
202 Hölscher, T. *et al.* Motility, chemotaxis and aerotaxis contribute to competitiveness during bacterial pellicle biofilm development. *J Mol Biol* (2015).
203 Van Hijum, S., De La Nava, J. G., Trelles, O., Kok, J. & Kuipers, O. P. MicroPreP: a cDNA microarray data pre-processing framework. *Appl. Bioinformatics* ***2***, 241-244 (2003).

204 Kuipers, O. P. *et al.* Transcriptome analysis and related databases of *Lactococcus lactis*. *Antonie Van Leeuwenhoek* ***82***, 113-122 (2002).
205 Baldi, P. & Long, A. D. A Bayesian framework for the analysis of microarray expression data: regularized t-test and statistical inferences of gene changes. *Bioinformatics* ***17***, 509-519 (2001).
206 Ireton, K., Gunther, N. t. & Grossman, A. D. *spo0J* is required for normal chromosome segregation as well as the initiation of sporulation in *Bacillus subtilis*. *J Bacteriol* ***176***, 5320-5329 (1994).
207 Kovács, Á. T. & Kuipers, O. P. Rok regulates *yuaB* expression during architecturally complex colony development of *Bacillus subtilis* 168. *J Bacteriol* ***193***, 998-1002 (2011).
208 Resnekov, O., Driks, A. & Losick, R. Identification and characterization of sporulation gene *spoVS* from *Bacillus subtilis*. *J Bacteriol* ***177***, 5628-5635 (1995).
209 Casadaban, M. J., Chou, J. & Cohen, S. N. In vitro gene fusions that join an enzymatically active beta-galactosidase segment to amino-terminal fragments of exogenous proteins: *Escherichia coli* plasmid vectors for the detection and cloning of translational initiation signals. *J Bacteriol* ***143***, 971-980 (1980).
210 Veening, J. W., Smits, W., Hamoen, L. & Kuipers, O. Single cell analysis of gene expression patterns of competence development and initiation of sporulation in *Bacillus subtilis* grown on chemically defined media. *J Appl Microbiol* ***101***, 531-541 (2006).
211 Shapiro, J. A. Thinking about bacterial populations as multicellular organisms. *Annu Rev Microbiol* ***52***, 81-104 (1998).
212 Hammar, M. r., Arnqvist, A., Bian, Z., Olsén, A. & Normark, S. Expression of two *csg* operons is required for production of fibronectin‐and Congo red‐binding curli polymers in *Escherichia coli* K‐12. *Mol Microbiol* ***18***, 661-670 (1995).
213 Seminara, A. *et al.* Osmotic spreading of *Bacillus subtilis* biofilms driven by an extracellular matrix. *Proc Natl Acad Sci U S A* ***109***, 1116-1121 (2012).
214 von Bodman, S. B., Willey, J. M. & Diggle, S. P. Cell-cell communication in bacteria: united we stand. *J Bacteriola* ***190***, 4377-4391 (2008).
215 Oppenheimer-Shaanan, Y. *et al.* Spatio-temporal assembly of functional mineral scaffolds within microbial biofilms. *npj Biofilms Microbiomes* ***2***, 15031 (2016).
216 Barabesi, C. *et al. Bacillus subtilis* gene cluster involved in calcium carbonate biomineralization. *J Bacteriol* ***189***, 228-235 (2007).
217 Kraas, F. I., Helmetag, V., Wittmann, M., Strieker, M. & Marahiel, M. A. Functional dissection of surfactin synthetase initiation module reveals insights into the mechanism of lipoinitiation. *Chem Biol* ***17***, 872-880 (2010).
218 Hölscher, T. *et al.* Monitoring spatial segregation in surface colonizing microbial populations. *J Vis Exp* (2016).
219 Herbaud, M.-L., Guiseppi, A., Denizot, F., Haiech, J. & Kilhoffer, M.-C. Calcium signalling in *Bacillus subtilis*. *Biochim. Biophys. Acta* ***1448***, 212-226 (1998).
220 Arutchelvi, J., Sangeetha, J., Philip, J. & Doble, M. Self-assembly of surfactin in aqueous solution: Role of divalent counterions. *Colloids Surf.,B* ***116***, 396-402 (2014).
221 Oknin, H., Steinberg, D. & Shemesh, M. Magnesium ions mitigate biofilm formation of Bacillus species via downregulation of matrix genes expression. *Front Microbiol* ***6*** (2015).
222 Zhang, W. *et al.* Surface indentation and fluid intake generated by the polymer matrix of *Bacillus subtilis* biofilms. *Soft matter* ***11***, 3612-3617 (2015).

223 Zhang, X., Wang, X., Nie, K., Li, M. & Sun, Q. Simulation of *Bacillus subtilis* biofilm growth on agar plate by diffusion–reaction based continuum model. *Phys Biol* ***13***, 046002 (2016).
224 Fletcher, M. Attachment of *Pseudomonas fluorescens* to glass and influence of electrolytes on bacterium-substratum separation distance. *J Bacteriol* ***170***, 2027-2030 (1988).
225 Malik, A. & Kakii, K. Intergeneric coaggregations among *Oligotropha carboxidovorans* and Acinetobacter species present in activated sludge. *FEMS Microbiol Lett* ***224***, 23-28 (2003).
226 Meng, Y. *et al.* Calcium regulates glutamate dehydrogenase and poly-γ-glutamic acid synthesis in *Bacillus natto*. *Biotechnol Lett* ***38***, 673-679 (2016).
227 Grau, A., Fernandez, J. C. G., Peypoux, F. & Ortiz, A. A study on the interactions of surfactin with phospholipid vesicles. *Biochim. Biophys. Acta* ***1418***, 307-319 (1999).
228 Ryder, C., Byrd, M. & Wozniak, D. J. Role of polysaccharides in *Pseudomonas aeruginosa* biofilm development. *Curr Opin Microbiol* ***10***, 644-648 (2007).
229 Oslizlo, A., Stefanic, P., Dogsa, I. & Mandic-Mulec, I. Private link between signal and response in *Bacillus subtilis* quorum sensing. *Proc Natl Acad Sci U S A* ***111***, 1586-1591 (2014).
230 Bohannan, B. J., Kerr, B., Jessup, C. M., Hughes, J. B. & Sandvik, G. Trade-offs and coexistence in microbial microcosms. *Antonie van Leeuwenhoek* ***81***, 107-115 (2002).
231 Michod, R. E. Evolution of individuality during the transition from unicellular to multicellular life. *Proc Natl Acad Sci U S A* ***104***, 8613-8618 (2007).
232 Brauner, A., Fridman, O., Gefen, O. & Balaban, N. Q. Distinguishing between resistance, tolerance and persistence to antibiotic treatment. *Nat. Rev. Microbiol.* ***14***, 320-330 (2016).
233 Veening, J. W., Smits, W. K. & Kuipers, O. P. Bistability, epigenetics, and bet-hedging in bacteria. *Annu. Rev. Microbiol.* ***62***, 193-210 (2008).
234 Smith, H. L. & Waltman, P. *The theory of the chemostat: dynamics of microbial competition*. Vol. 13 (Cambridge university press, 1995).
235 Gudelj, I., Beardmore, R., Arkin, S. & MacLean, R. Constraints on microbial metabolism drive evolutionary diversification in homogeneous environments. *J Evol Biol* ***20***, 1882-1889 (2007).
236 MacLean, R. The tragedy of the commons in microbial populations: insights from theoretical, comparative and experimental studies. *Heredity* ***100***, 471-477 (2008).
237 Novak, M., Pfeiffer, T., Lenski, R. E., Sauer, U. & Bonhoeffer, S. Experimental tests for an evolutionary trade‐off between growth rate and yield in *E. coli*. *Am Nat* ***168***, 242-251 (2006).
238 Lipson, D. A. The complex relationship between microbial growth rate and yield and its implications for ecosystem processes. *Front Microbiol* ***6*** (2015).
239 Pirt, S. J. The maintenance energy of bacteria in growing cultures. *Proc. R Soc. Lond. B Biol. Sci.* ***163***, 224-231 (1965).
240 Ibarra, R. U., Edwards, J. S. & Palsson, B. O. *Escherichia coli* K-12 undergoes adaptive evolution to achieve in silico predicted optimal growth. *Nature* ***420***, 186-189 (2002).
241 Andrews, J. H. & Harris, R. F. *r*- and *k*-selection and microbial ecology. *Adv Microbial Ecol* ***9***, 99-147 (1986).
242 D'Souza, G. *et al.* Less is more: selective advantages can explain the prevalent loss of biosynthetic genes in bacteria. *Evolution* ***68***, 2559-2570 (2014).

243 Kaeberlein, T., Lewis, K. & Epstein, S. S. Isolating" uncultivable" microorganisms in pure culture in a simulated natural environment. *Science* ***296***, 1127-1129 (2002).
244 Solopova, A. *et al.* Bet-hedging during bacterial diauxic shift. *Proc Natl Acad Sci U S A* ***111***, 7427-7432 (2014).
245 Harcombe, W. R. *et al.* Metabolic resource allocation in individual microbes determines ecosystem interactions and spatial dynamics. *Cell Rep* ***7***, 1104-1115 (2014).
246 Hellweger, F. L., Clegg, R. J., Clark, J. R., Plugge, C. M. & Kreft, J.-U. Advancing microbial sciences by individual-based modelling. *Nat Rev Microbiol* (2016).
247 Berger, B. J., English, S., Chan, G. & Knodel, M. H. Methionine regeneration and aminotransferases in *Bacillus subtilis*, B*acillus cereus*, and *Bacillus anthracis. J Bacteriol* ***185***, 2418-2431 (2003).
248 Brinsmade, S. R. *et al.* Hierarchical expression of genes controlled by the *Bacillus subtilis* global regulatory protein CodY. *Proc Natl Acad Sci U S A* ***111***, 8227-8232 (2014).
249 Ratzke, C. & Gore, J. Self-organized patchiness facilitates survival in a cooperatively growing *Bacillus subtilis* population. *Nat Microbiol* ***1***, 16022 (2016).
250 Poltak, S. R. & Cooper, V. S. Ecological succession in long-term experimentally evolved biofilms produces synergistic communities. *ISME J* ***5***, 369-378 (2011).
251 Hansen, S. K., Rainey, P. B., Haagensen, J. A. & Molin, S. Evolution of species interactions in a biofilm community. *Nature* ***445***, 533-536 (2007).
252 Martín, P. V., Hidalgo, J., de Casas, R. R. & Muñoz, M. A. Eco-evolutionary model of rapid phenotypic diversification in species-rich communities. *PLoS Comput Biol* ***12***, e1005139 (2016).
253 Bailey, S. F. & Kassen, R. Spatial structure of ecological opportunity drives adaptation in a bacterium. *Am Nat* ***180***, 270-283 (2012).
254 Steinmetz, M. & Richter, R. Plasmids designed to alter the antibiotic resistance expressed by insertion mutations in *Bacillus subtilis*, through in vivo recombination. *Gene* ***142***, 79-83 (1994).
255 Msadek, T. *et al.* Signal transduction pathway controlling synthesis of a class of degradative enzymes in *Bacillus subtilis*: expression of the regulatory genes and analysis of mutations in degS and degU. *J Bacteriol* ***172***, 824-834 (1990).
256 Paintdakhi, A. *et al.* Oufti: an integrated software package for high‐accuracy, high‐throughput quantitative microscopy analysis. *Mol Microbiol* ***99***, 767-777 (2016).
257 Heydorn, A. *et al.* Quantification of biofilm structures by the novel computer program COMSTAT. *Microbiol* ***146***, 2395-2407 (2000).
258 Boles, B. R., Thoendel, M. & Singh, P. K. Self-generated diversity produces “insurance effects” in biofilm communities. *Proc Natl Acad Sci U S A* ***101***, 16630-16635 (2004).
259 Lang, G. I. & Desai, M. M. The spectrum of adaptive mutations in experimental evolution. *Genomics* ***104***, 412-416 (2014).
260 Blount, Z. D., Borland, C. Z. & Lenski, R. E. Historical contingency and the evolution of a key innovation in an experimental population of *Escherichia coli*. *Proc Natl Acad Sci U S A* ***105***, 7899-7906 (2008).
261 Ferenci, T. & Maharjan, R. Mutational heterogeneity: A key ingredient of bet‐hedging and evolutionary divergence? *BioEssays* ***37***, 123-130 (2015).
262 Lind, P. A., Farr, A. D. & Rainey, P. B. Experimental evolution reveals hidden diversity in evolutionary pathways. *Elife* ***4***, e07074 (2015).

263 Freese, P. D., Korolev, K. S., Jimenez, J. I. & Chen, I. A. Genetic drift suppresses bacterial conjugation in spatially structured populations. *Biophys J* ***106***, 944-954 (2014).
264 Mars, R. A. *et al.* Small regulatory RNA-induced growth rate heterogeneity of *Bacillus subtilis*. *PLoS Genet* ***11***, e1005046 (2015).
265 Nester, E. W. & Lederberg, J. Linkage of genetic units of *Bacillus subtilis* in DNA transformation. *Proc Natl Acad Sci U S A* ***47***, 52-55 (1961).
266 Spizizen, J. Transformation of biochemically deficient strains of *Bacillus subtilis* by deoxyribonucleate. *Proc Natl Acad Sci U S A* ***44***, 1072-1078 (1958).
267 Thorne, C. B. Transduction in *Bacillus subtilis*. *J Bacteriol* ***83***, 106-111 (1962).
268 Yoshikawa, H. & Sueoka, N. Sequential replication of *Bacillus subtilis* chromosome, I. Comparison of marker frequencies in exponential and stationary growth phases. *Proc Natl Acad Sci U S A* ***49***, 559-566 (1963).
269 Youngman, P., Perkins, J. B. & Losick, R. Construction of a cloning site near one end of Tn917 into which foreign DNA may be inserted without affecting transposition in *Bacillus subtilis* or expression of the transposon-borne *erm* gene. *Plasmid* ***12***, 1-9 (1984).
270 Achtman, M. & Wagner, M. Microbial diversity and the genetic nature of microbial species. *Nat Rev Microbiol* ***6***, 431-440 (2008).
271 Cohan, F. M. What are bacterial species? *Annu Rev Microbiol* ***56***, 457-487 (2002).
272 Gallegos-Monterrosa, R., Mhatre, E. & T, K. A. Specific *Bacillus subtilis* 168 variants do form biofilms on nutrient rich medium. *Microbiol* (2016).
273 Morikawa, M. *et al.* Biofilm formation by a *Bacillus subtilis* strain that produces γ-polyglutamate. *Microbiol* ***152***, 2801-2807 (2006).
274 Van Loon, L. Plant responses to plant growth-promoting rhizobacteria. *Eur J Plant Pathol* ***119***, 243-254 (2007).
275 Brencic, A. & Winans, S. C. Detection of and response to signals involved in host-microbe interactions by plant-associated bacteria. *Microbiol. Mol. Biol. Rev.* ***69***, 155-194 (2005).
276 Hooper, L. V. & Gordon, J. I. Commensal host-bacterial relationships in the gut. *Science* ***292***, 1115-1118 (2001).
277 Bedran, T. B., Azelmat, J., Spolidorio, D. P. & Grenier, D. Fibrinogen-induced streptococcus mutans biofilm formation and adherence to endothelial cells. *Biomed Res Int* ***2013***, 431465 (2013).
278 Hoffman, L. R. *et al.* Aminoglycoside antibiotics induce bacterial biofilm formation. *Nature* ***436***, 1171-1175 (2005).
279 Linares, J. F., Gustafsson, I., Baquero, F. & Martinez, J. Antibiotics as intermicrobial signaling agents instead of weapons. *Proc Natl Acad Sci U S A* ***103***, 19484-19489 (2006).
280 Liu, Y. & Tay, J.-H. The essential role of hydrodynamic shear force in the formation of biofilm and granular sludge. *Water Res* ***36***, 1653-1665 (2002).
281 Gottschalk, G. *Bacterial metabolism*. (Springer Science & Business Media, 2012).
282 Toyofuku, M. *et al.* Environmental factors that shape biofilm formation. *Biosci Biotechnol Biochem* ***80***, 7-12 (2016).
283 Moreau-Marquis, S., Stanton, B. A. & O'Toole, G. A. *Pseudomonas aeruginosa* biofilm formation in the cystic fibrosis airway. *Pulm Pharmacol Ther* ***21***, 595-599 (2008).

284 Dubreuil, J. D., Del Giudice, G. & Rappuoli, R. *Helicobacter pylori* interactions with host serum and extracellular matrix proteins: potential role in the infectious process. *Microbiol Mol Biol Rev* ***66***, 617-629 (2002).
285 Oliveira, R., Melo, L., Oliveira, A. & Salgueiro, R. Polysaccharide production and biofilm formation by *Pseudomonas fluorescen*: effects of pH and surface material. *Colloids Surf B* ***2***, 41-46 (1994).
286 Herald, P. J., Zottola & A, E. Attachment of *Listeria monocytogenes* to stainless steel surfaces at various temperatures and pH values. *J Food Sci* ***53***, 1549-1562 (1988).
287 Kaplan, J. á. Biofilm dispersal: mechanisms, clinical implications, and potential therapeutic uses. *J Den Res* ***89***, 205-218 (2010).
288 Ingham, C. J., Kalisman, O., Finkelshtein, A. & Ben-Jacob, E. Mutually facilitated dispersal between the nonmotile fungus *Aspergillus fumigatus* and the swarming bacterium *Paenibacillus vortex*. *Proc Natl Acad Sci U S A* ***108***, 19731-19736 (2011).
289 Venturi, V., Bertani, I., Kerényi, Á., Netotea, S. & Pongor, S. Co-swarming and local collapse: quorum sensing conveys resilience to bacterial communities by localizing cheater mutants in *Pseudomonas aeruginosa*. *PLoS One* ***5***, e9998 (2010).
290 Pollitt, E. J., Crusz, S. A. & Diggle, S. P. *Staphylococcus aureus* forms spreading dendrites that have characteristics of active motility. *Sci Rep* ***5*** (2015).
291 Ke, W.-J., Hsueh, Y.-H., Cheng, Y.-C., Wu, C.-C. & Liu, S.-T. Water surface tension modulates the swarming mechanics of *Bacillus subtilis*. *Front Microbiol* ***6*** (2015).
292 Blair, K. M., Turner, L., Winkelman, J. T., Berg, H. C. & Kearns, D. B. A molecular clutch disables flagella in the *Bacillus subtilis* biofilm. *Science* ***320***, 1636 (2008).
293 Johnson, D. R., Goldschmidt, F., Lilja, E. E. & Ackermann, M. Metabolic specialization and the assembly of microbial communities. *ISME J* ***6***, 1985-1991 (2012).
294 Kreft, J.-U. & Bonhoeffer, S. The evolution of groups of cooperating bacteria and the growth rate versus yield trade-off. *Microbiol* ***151***, 637-641 (2005).
295 Amarasekare, P. Competitive coexistence in spatially structured environments: a synthesis. *Ecol Lett* ***6***, 1109-1122 (2003).
296 Feldgarden, M., Stoebel, D. M., Brisson, D. & Dykhuizen, D. E. Size doesn't matter: Microbial selection experiments address ecological phenomena. *Ecology* ***84***, 1679-1687 (2003).
297 Nadell, C., Ricaurte, D., Yan, J., Drescher, K. & Bassler, B. Flow environment and matrix structure interact to determine spatial competition in *Pseudomonas aeruginosa* biofilms. *bioRxiv*, 077354 (2016).
298 Nadell, C. D., Drescher, K. & Foster, K. R. Spatial structure, cooperation and competition in biofilms. *Nat Rev Microbiol* (2016).
299 Penterman, J. *et al.* Rapid evolution of culture-impaired bacteria during adaptation to biofilm growth. *Cell Rep* ***6***, 293-300 (2014).
300 Kim, H. J., Du, W. & Ismagilov, R. F. Complex function by design using spatially pre-structured synthetic microbial communities: degradation of pentachlorophenol in the presence of Hg (II). *Integr Biology* ***3***, 126-133 (2011).
301 Lindemann, S. R. *et al.* Engineering microbial consortia for controllable outputs. *ISME J* (2016).
302 Ernebjerg, M. & Kishony, R. Distinct growth strategies of soil bacteria as revealed by large-scale colony tracking. *Appl Environ Microbiol* ***78***, 1345-1352 (2012).
303 Nadell, C. D., Foster, K. R. & Xavier, J. B. Emergence of spatial structure in cell groups and the evolution of cooperation. *PLoS Comput Biol* ***6***, e1000716 (2010).

304 Bolten, C. J., Heinzle, E., Müller, R. & Wittmann, C. Investigation of the central carbon metabolism of *Sorangium cellulosum*: metabolic network reconstruction and quantification of pathway fluxes. *J Microbiol Biotechnol* ***19***, 23-36 (2009).
305 Kappler, O., Janssen, P. H., Kreft, J.-U. & Schink, B. Effects of alternative methyl group acceptors on the growth energetics of the O-demethylating anaerobe *Holophaga foetida*. *Microbiol* ***143***, 1105-1114 (1997).
306 Lipson, D. A., Monson, R. K., Schmidt, S. K. & Weintraub, M. N. The trade-off between growth rate and yield in microbial communities and the consequences for under-snow soil respiration in a high elevation coniferous forest. *Biogeochemistry* ***95***, 23-35 (2009).
307 Westerhoff, H. V., Hellingwerf, K. J. & Van Dam, K. Thermodynamic efficiency of microbial growth is low but optimal for maximal growth rate. *Proc Natl Acad Sci U S A* ***80***, 305-309 (1983).
308 Bachem, S. & Stülke, J. Regulation of the *Bacillus subtilis* GlcT antiterminator protein by components of the phosphotransferase system. *J Bacteriol* ***180***, 5319-5326 (1998).
309 Stülke, J. & Hillen, W. Carbon catabolite repression in bacteria. *Curr Opin Microbiol* ***2***, 195-201 (1999).
310 Zmijewski Jr, M. J. & MacQuillan, A. M. Dual effects of glucose on dicarboxylic acid transport in *Kluyveromyces lactis*. *Can J Microbiol* ***21***, 473-480 (1975).
311 Commichau, F. M., Herzberg, C., Tripal, P., Valerius, O. & Stülke, J. A regulatory protein–protein interaction governs glutamate biosynthesis in *Bacillus subtilis*: the glutamate dehydrogenase RocG moonlights in controlling the transcription factor GltC. *Mol Microbiol* ***65***, 642-654 (2007).
312 Commichau, F. M., Gunka, K., Landmann, J. J. & Stülke, J. Glutamate metabolism in *Bacillus subtilis*: gene expression and enzyme activities evolved to avoid futile cycles and to allow rapid responses to perturbations of the system. *J Bacteriol* ***190***, 3557-3564 (2008).

Supporting Information

Supporting information for Chapter 1

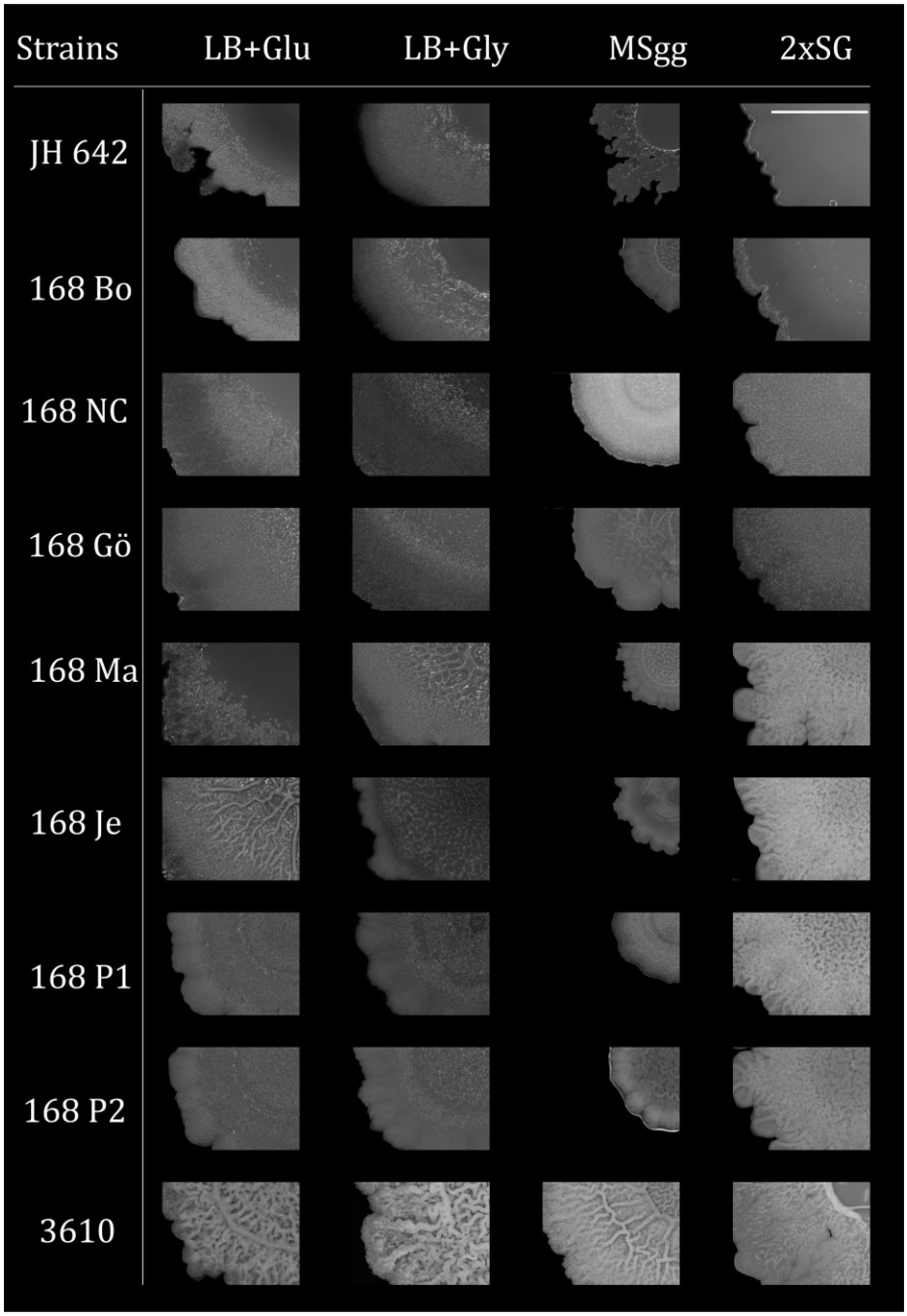

Figure 1*| *Magnified details of complex colonies of *B. subtilis* strain 3610 and 168 variants on different media after 72 hours of incubation, arranged by increasing colony wrinkleality on 2xSG medium. The scale bar shown at the top right represents 5 mm. Strain abbreviations are described in Table 1.

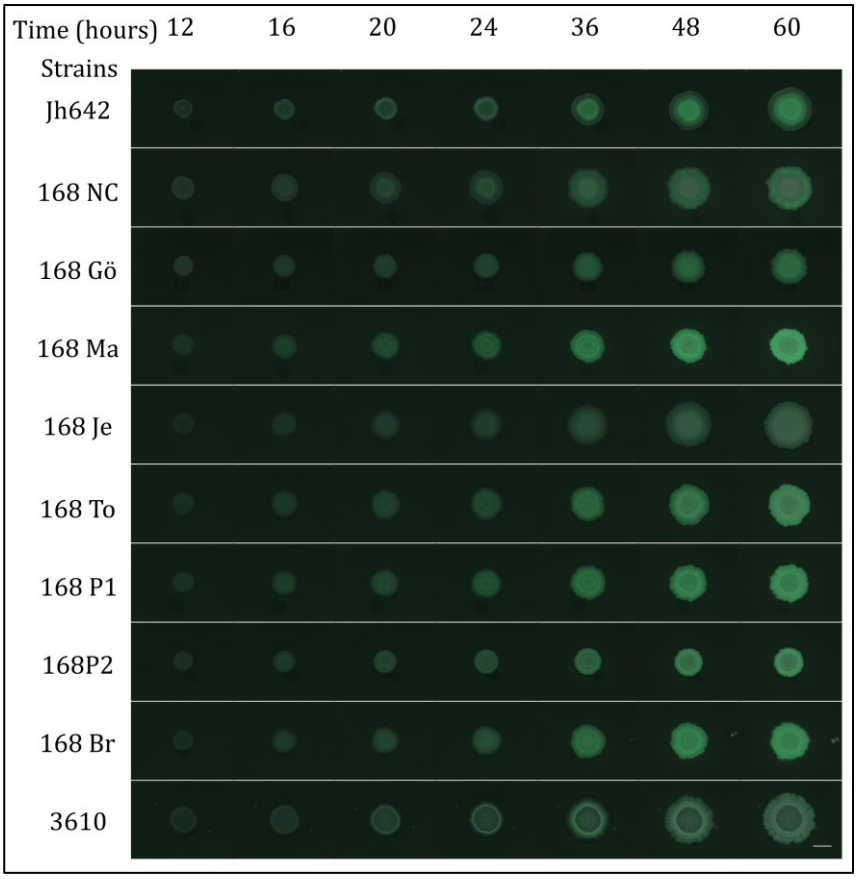

Figure 2 | Colonies of B. subtilis strain 3610 and 168 variants carrying a transcriptional P_{eps}-GFP fusion at different time points. Overlays of fluorescence (green) and transmitted light (gray) images are shown. The colonies are representative of the observed phenotype for each strain or variant. The scale bar at the bottom right is 5 mm.

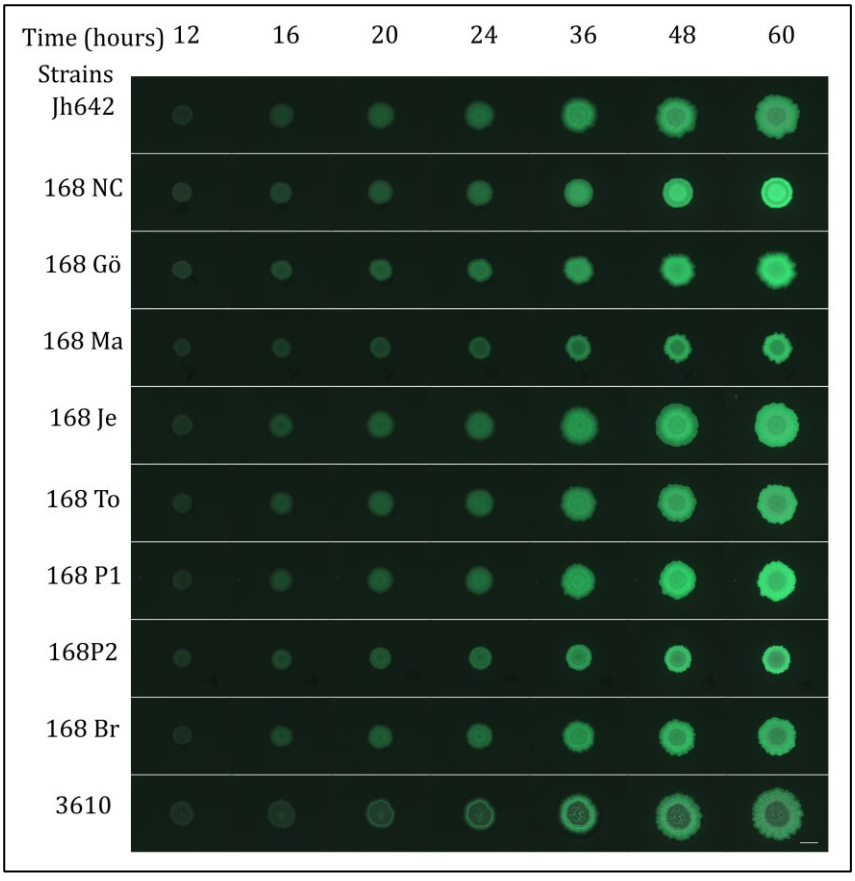

Figure 3 | Colonies of B. subtilis strain 3610 and 168 variants carrying a transcriptional P_{tapA}-GFP fusion at different time points. Overlays of fluorescence (green) and transmitted light (gray) images are shown. The colonies are representative of the observed phenotype for each strain or variant. The scale bar at the bottom right is 5 mm.

Supporting information for Chapter 2

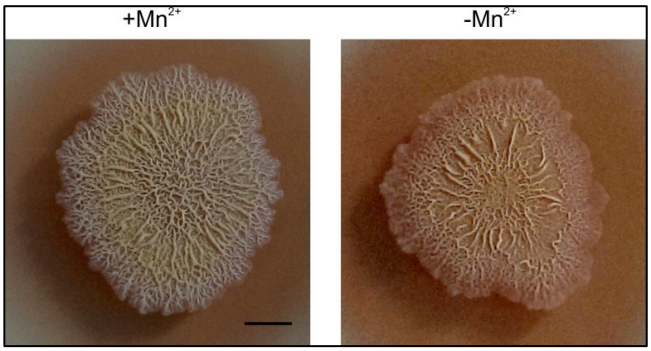

Figure 1 | Chalky patterns in the presence and pale colonies of NCIB 3610 in the absence of Mn^{2+} on the MSgg medium. The 3 days old colony images of NCIB 3610 on MSgg medium with and without Mn^{2+} are presented to notice the formation of white chalky patterns and their absence. These patterns are possibly attributed to the sporulation where Mn^{2+} plays an important role. These observations are in line with the experiments on WT168 that shows the down-regulation of biofilm-related genes in absence of Mn^{2+}. The scale bar in the image equals to 5mm.

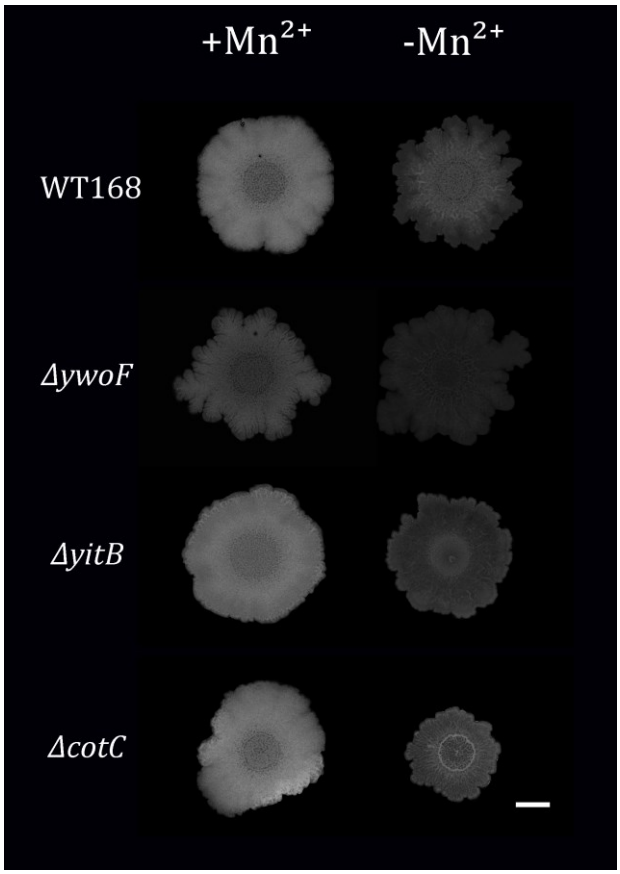

Figure 2 | Colony morphologies of selected gene mutants. Genes *ywoF* (unknown function), *yitB* (sulfate reduction), *cotC* (outer spore coat protein) that were found to be downregulated in the transcriptome analysis when Mn^{2+} was not supplemented, were tested for complex colony morphology on 2xSG agar medium. The scale bar at the lower right corner represents 5mm.

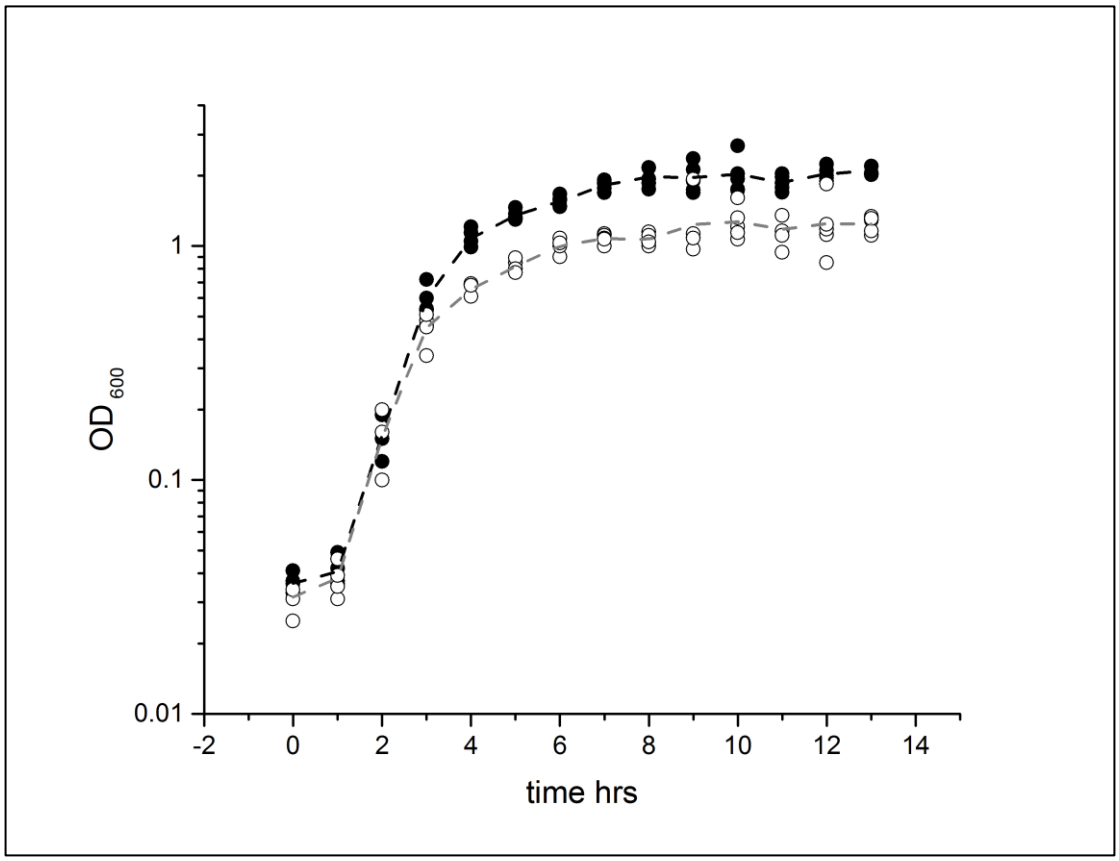

Figure 3 | Growth in presence and absence of Mn^{2+}. The overnight cultures of WT168 were inoculated (1:100) in 50 ml 2xSG and incubated at 37°C under shaken conditions. The optical density (OD) of the growing cultures was measured spectrophotometrically at 600nm every 2hrs for 12 hours. The ODs were plotted using OriginLab 2015 software. The experiments were done on two independent occasions each with 5 and 3 biological replicates, respectively. We observed no difference in growth rate of the cultures grown in presence or absence of added Mn^{2+}. However, the final yield in lack of Mn^{2+} is slightly lower.

Table 1. List of genes differentially regulated in colony biofilms is shown in the absence versus in the presence of manganese in the otherwise biofilm inducing 2xSG medium. List of significantly (p value $<10^{-4}$) up or downregulated *B. subtilis* genes (fold > 4 or < -4) are shown. The raw data is available in Gene Expression Omnibus database (Accession No. GSE61232).

Locus-tag	***Gene name***	***Predicted or putative function of coded proteins***	***Ratio***	***Bayes.p***
BSU08880	*rpsNB*	alternative ribosomal protein S14	30.4	10^{-14}
BSU33240	*oxdC*	oxalate decarboxylase	22.8	10^{-12}
BSU03340	*folEB*	GTP cyclohydrolase IB	21.1	10^{-12}
BSU08950	*yhbE*	unknown	20.2	10^{-10}
BSU32990	*mrgA*	iron storage protein, DNA-binding stress protein	19.9	10^{-11}
BSU38550	*ilvK*	branched-chain amino acid aminotransferase	18.1	10^{-5}
BSU08960	*yhbF*	unknown	17.0	10^{-11}
BSU08820	*katA*	vegetative catalase 1	15.3	10^{-11}
BSU35830	*ywtG*	general stress protein, similar to metabolite transport protein	15.3	10^{-8}
BSU38120	*rodA*	control of cell shape and elongation	13.8	10^{-7}
BSU06220	*ydjJ*	unknown	13.3	10^{-12}
BSU30770	*mntA*	manganese ABC transporter (membrane protein)	12.8	10^{-9}
BSU03350	*yciB*	zinc transporter	11.8	10^{-9}
BSU13850	*zosA*	zinc transporter	10.8	10^{-13}
BSU07610	*citM*	Mg^{2+}-citrate transporter	10.1	10^{-12}
BSU04360	*mntH*	manganese transporter (proton symport)	10.1	10^{-8}
BSU18730	*yoaS*	unknown	9.9	10^{-10}
BSU02830	*ycdF*	general stress protein, similar to glucose 1-dehydrogenase	8.9	10^{-11}
BSU00320	*yaaT*	control of the phosphorelay	8.9	10^{-10}
BSU08940	*yhbD*	unknown	7.5	10^{-11}
BSU06150	*gutB*	D-sorbitol dehydrogenase	7.4	10^{-9}
BSU30750	*mntC*	manganese ABC transporter (membrane protein)	7.3	10^{-8}
BSU38610	*yxzF*	general stress protein	7.2	10^{-6}
BSU17390	*nrdF*	ribonucleoside-diphosphate reductase (major subunit)	7.1	10^{-10}
BSU00330	*yabA*	tethers DnaA to the polymerase-clamp protein DnaN	7.1	10^{-10}
BSU17870	*yneB*	similar to resolvase	7.1	10^{-9}
BSU05630	*dinB*	nuclease inhibitor	7.0	10^{-10}
BSU27590	*dtd*	putative D-Tyr-tRNA(Tyr) deacylase	6.9	10^{-10}
BSU30760	*mntB*	manganese ABC transporter (ATP-binding protein)	6.9	10^{-8}
BSU09500	*yhdK*	anti-SigM protein	6.8	10^{-11}
BSU16780	*rnjB*	RNase J2	6.8	10^{-12}
BSU39690	*iolH*	unknown, may be involved in myo-inositol catabolism	6.8	10^{-5}
BSU09700	*yheJ*	unknown	6.8	10^{-10}
BSU35160	*uvrA*	excinuclease ABC (subunit A)	6.7	10^{-9}
BSU02850	*adcA*	ABC transporter for zinc (binding protein)	6.5	10^{-11}
BSU09530	*yhdN*	general stress protein, aldo/keto reductase	6.5	10^{-11}
BSU03010	*amhX*	amidohydrolase	6.5	10^{-10}
BSU17600	*xylA*	xylose isomerase	6.5	10^{-11}
BSU26558	*yrzM*	unknown, putative pseudogene	6.3	10^{-7}
BSU24750	*yqhB*	general stress protein, similar to hemolysin	6.2	10^{-9}
BSU27540	*yrvM*	similar to E. coli enzyme that catalyzes ATP-dependent dehydration of N6-threonylcarbamoyladenosine to form	6.2	10^{-10}

		cyclic N6-threonylcarbamoyladenosine		
BSU15600	*cysC*	adenylyl-sulfate kinase	6.1	10^{-9}
BSU38470	*ywaD*	double-zinc aminopeptidase	5.9	10^{-7}
BSU06230	*iolT*	major transporter for inositol	5.9	10^{-10}
BSU14850	*ftsW*	cell-division protein	5.9	10^{-9}
BSU04180	*ydaC*	unknown	5.9	10^{-8}
BSU32670	*sufB*	synthesis of Fe-S-clusters	5.8	10^{-8}
BSU38090	*vpr*	minor extracellular serine protease	5.8	10^{-5}
BSU34660	*yvdB*	putative anion transporter	5.7	10^{-8}
BSU18570	*yoaE*	formate dehydrogenase	5.7	10^{-8}
BSU30160	*ytcQ*	similar to ABC transporter (solute-binding lipoprotein)	5.7	10^{-5}
BSU17380	*nrdE*	ribonucleoside-diphosphate reductase (major subunit)	5.7	10^{-9}
BSU34670	*yvdA*	similar to carbonic anhydrase	5.6	10^{-9}
BSU15620	*sirB*	probable siroheme ferrochelatase	5.6	10^{-10}
BSU32060	*yuiD*	unknown	5.6	10^{-9}
BSU32240	*thrB*	homoserine kinase	5.5	10^{-9}
BSU30630	*ytkD*	error prevention oxidized guanine system	5.5	10^{-9}
BSU17860	*yneA*	inhibits cell division during SOS response	5.5	10^{-10}
BSU36670	*csbD*	general stress protein	5.4	10^{-8}
BSU02170	*ybfB*	unknown	5.4	10^{-10}
BSU38430	*gspA*	general stress protein	5.3	10^{-7}
BSU38480	*ywaC*	(p)ppGpp synthetase, small alarmone synthetase	5.3	10^{-7}
BSU15610	*sumT*	probable uroporphyrin-III C-methyltransferase	5.3	10^{-9}
BSU15630	*sirC*	probably precorrin-2 dehydrogenase	5.3	10^{-9}
BSU33230	*sigO*	RNA polymerase sigma factor YvrI	5.3	10^{-7}
BSU08730	*perR*	transcriptional repressor of the peroxide regulon	5.2	10^{-8}
BSU14860	*pycA*	pyruvate carboxylase	5.2	10^{-11}
BSU38960	*yxjG*	putative methionine synthase	5.2	10^{-5}
BSU21870	*ilvD*	dihydroxy-acid dehydratase	5.1	10^{-9}
BSU05620	*ydgF*	similar to amino acid ABC transporter (permease)	5.1	10^{-10}
BSU15590	*sat*	sulfate adenylyltransferase	5.1	10^{-9}
BSU08850	*ssuC*	epoxyqueuosine reductase	5.0	10^{-6}
BSU07220	*yetL*	transcriptional repressor of *yetM* and *yetL*	5.0	10^{-10}
BSU06070	*ydiP*	similar to DNA-3-methyladenine glycosidase II	5.0	10^{-10}
BSU27600	*relA*	GTP pyrophosphokinase (stringent response)	5.0	10^{-9}
BSU09330	*yhcZ*	two-component response regulator	5.0	10^{-10}
BSU33420	*nhaK*	cation/H+ antiporter	4.9	10^{-9}
BSU26530	*yrkF*	unknown	4.9	10^{-7}
BSU27160	*cypB*	similar to cytochrome P^{450} / NADPH-cytochrome P^{450} reductase	4.9	10^{-8}
BSU38360	*ywbD*	unknown	4.9	10^{-6}
BSU27860	*nadC*	nicotinate-nucleotide diphosphorylase	4.9	10^{-7}
BSU26540	*yrkE*	unknown	4.8	10^{-6}
BSU02840	*ycdG*	general stress protein, similar to oligo-1,6-glucosidase	4.8	10^{-9}
BSU17580	*xynB*	xylan beta-1,4-xylosidase	4.8	10^{-8}
BSU32690	*sufS*	cysteine desulfurase	4.7	10^{-8}
BSU12940	*dppC*	dipeptide ABC transporter (permease)	4.7	10^{-8}
BSU08870	*ygaN*	unknown	4.7	10^{-8}
BSU32680	*iscU*	iron-sulfur cluster scaffold protein, synthesis of Fe-S clusters	4.7	10^{-7}

BSU32090	*yuiA*	unknown	4.7	10^{-8}
BSU11880	*metC*	cystathionine beta-lyase	4.7	10^{-9}
BSU40100	*ahpF*	alkyl hydroperoxide reductase (large subunit) / NADH dehydrogenase	4.7	10^{-5}
BSU37770	*rocB*	involved in arginine and ornithine utilization	4.6	10^{-4}
BSU39710	*iolF*	inositol transport protein	4.6	10^{-5}
BSU36710	*fdhD*	putative subunit of an respiration oxidoreductase	4.6	10^{-7}
BSU29640	*ytsP*	unknown	4.6	10^{-8}
BSU11560	*yjbI*	truncated hemoglobin, NO protection	4.6	10^{-8}
BSU36700	*moaA*	molybdopterin precursor biosynthesis	4.5	10^{-7}
BSU32250	*thrC*	threonine synthase	4.5	10^{-8}
BSU37800	*yweA*	inhibitor of KinA autophosphorylation	4.4	10^{-7}
BSU02500	*ycbG*	transcription regulator of the glucarate/galactarate utilization operon	4.4	10^{-8}
BSU39810	*csbC*	general stress protein, putative sugar transporter	4.4	10^{-4}
BSU30170	*ytcP*	similar to ABC transporter (permease)	4.4	10^{-6}
BSU17570	*xynP*	beta-xyloside permease	4.4	10^{-7}
BSU09420	*lytE*	cell wall hydrolase (major autolysin),endopeptidase-type autolysin	4.4	10^{-10}
BSU00170	*yaaI*	general stress protein, similar to isochorismatase	4.3	10^{-9}
BSU37590	*ywgA*	unknown	4.3	10^{-6}
BSU18450	*gltA*	large subunit of glutamate synthase	4.3	10^{-9}
BSU34690	*yvcS*	ABC transporter for the export of lipid II-binding lantibiotics	4.3	10^{-7}
BSU37520	*ywhD*	unknown	4.3	10^{-7}
BSU39350	*hutH*	histidase	4.2	10^{-5}
BSU39720	*iolE*	2-keto-myo-inositol dehydratase	4.2	10^{-4}
BSU28170	*hemA*	glutamyl-tRNA reductase	4.2	10^{-8}
BSU34940	*yvpB*	unknown	4.2	10^{-7}
BSU13640	*spo0E*	Spo0A-P phosphatase, control of the phosphorelay	4.2	10^{-8}
BSU37740	*bacA*	bacilysin biosynthesis protein, prephenate decarboxylase	4.2	10^{-4}
BSU18740	*yozG*	similar to transcriptional regulator	4.1	10^{-8}
BSU18750	*yoaT*	unknown	4.1	10^{-9}
BSU36530	*bcrC*	undecaprenyl pyrophosphate phosphatase, bacitracin resistance	4.1	10^{-7}
BSU28300	*ilvH*	acetolactate synthase (small subunit)	4.1	10^{-8}
BSU39700	*iolG*	inositol 2-dehydrogenase	4.1	10^{-4}
BSU11500	*spxA*	Transcriptional regulator Spx, involved in regulation of many genes.	4.1	10^{-8}
BSU32700	*sufD*	synthesis of Fe-S-clusters	4.1	10^{-7}
BSU14310	*moaD*	molybdopterin synthase (small subunit)	4.1	10^{-11}
BSU32710	*sufC*	ABC transporter (ATP-binding protein), synthesis of Fe-S clusters	4.1	10^{-7}
BSU03360	*yciC*	putative metallochaperone	4.1	10^{-9}
BSU13740	*queE*	7-carboxy-7-deazaguanine synthase	4.1	10^{-8}
BSU09320	*yhcY*	two-component sensor kinase	4.1	10^{-8}
BSU17850	*lexA*	transcriptional repressor of the SOS regulon	4.0	10^{-10}
BSU09510	*yhdL*	anti-SigM protein	4.0	10^{-10}
BSU28310	*ilvB*	acetolactate synthase (large subunit)	4.0	10^{-8}
BSU21780	*yplP*	transcriptional activator (for SigL-dependent promoter)	4.0	10^{-8}
BSU35360	*hag*	flagellin protein	4.0	10^{-7}

BSU34040	*yvfW*	lactate catabolic enzyme	4.0	10^{-7}
BSU09770	*yheD*	spore coat protein	0.25	10^{-8}
BSU17780	*yndG*	unknown	0.25	10^{-10}
BSU28560	*lcfA*	long chain acyl-CoA synthetase	0.25	10^{-8}
BSU22730	*ndk*	nucleoside diphosphate kinase	0.25	10^{-8}
BSU32720	*yurZ*	unknown	0.25	10^{-8}
BSU14220	*ykuU*	similar to 2-cys peroxiredoxin	0.25	10^{-9}
BSU38980	*scoB*	probable succinyl CoA:3-oxoacid CoA-transferase (subunit B)	0.25	10^{-4}
BSU21470	*sunT*	sublancin lantibiotic ABC transporter	0.25	10^{-8}
BSU06600	*pcrB*	unknown	0.25	10^{-10}
BSU28100	*ysxE*	unknown	0.25	10^{-9}
BSU19280	*yocN*	similar to permease	0.24	10^{-8}
BSU31990	*dhbC*	isochorismate synthase	0.24	10^{-7}
BSU15090	*ylbO*	probably DNA-binding protein, regulates transcription of some spore coat genes	0.24	10^{-11}
BSU34470	*yveA*	aspartate/ glutamate transporter	0.24	10^{-8}
BSU28110	*spoVID*	spore coat morphogenetic protein, promotes encasement of the spore	0.24	10^{-8}
BSU11290	*yjaV*	SigE-dependent sporulation gene	0.24	10^{-9}
BSU17420	*spoVK*	required for spore maturation	0.24	10^{-9}
BSU09140	*yhcM*	general stress protein	0.24	10^{-8}
BSU32270	*yutH*	spore coat protein	0.24	10^{-9}
BSU38970	*yxjF*	similar to gluconate 5-dehydrogenase	0.24	10^{-4}
BSU18290	*yngL*	unknown	0.24	10^{-8}
BSU20590	*yoqL*	unknown	0.24	10^{-6}
BSU34310	*epsG*	extracellular polysaccharide synthesis	0.24	10^{-8}
BSU39950	*yxaJ*	unknown	0.24	10^{-4}
BSU19720	*yodR*	similar to butyrate-acetoacetate CoA-transferase	0.24	10^{-6}
BSU16825	*ymfD*	exporter for the siderophore bacillibactin	0.24	10^{-11}
BSU33540	*yvaB*	similar to NAD(P)H dehydrogenase (quinone)	0.24	10^{-8}
BSU33770	*spbC*	toxin, kills non-sporulating cells	0.24	10^{-8}
BSU35060	*cypX*	cytochrome P^{450}-like enzyme	0.24	10^{-7}
BSU03940	*ycnI*	unknown	0.23	10^{-9}
BSU23440	*spoVAA*	essential for the uptake of the 1:1 chelate of pyridine-2,6-dicarboxylic acid and Ca^{2+} into developing spores	0.23	10^{-7}
BSU14800	*ylaJ*	unknown	0.23	10^{-11}
BSU34290	*epsI*	extracellular polysaccharide synthesis	0.23	10^{-8}
BSU00160	*yaaH*	general stress protein, survival of ethanol stress	0.23	10^{-11}
BSU32610	*frlB*	fructoselysine-6-P-glycosidase	0.23	10^{-8}
BSU21480	*sunA*	sublancin lantibiotic antimicrobial precursor peptide	0.23	10^{-5}
BSU14250	*yknT*	spore coat protein	0.23	10^{-11}
BSU23970	*artQ*	high affinity arginine ABC transporter (permease)	0.23	10^{-9}
BSU34280	*epsJ*	similar to 1,4-galactosyltransferase	0.23	10^{-8}
BSU39000	*yxjC*	unknown	0.23	10^{-5}
BSU24230	*spoIVB*	serine protease, cleaves SpoIVFA	0.23	10^{-9}
BSU26950	*yraG*	forespore-specific sporulation protein	0.23	10^{-6}
BSU01970	*skfG*	unknown	0.23	10^{-10}
BSU19660	*yozD*	unknown	0.23	10^{-7}
BSU25770	*spoIVCA*	site-specific DNA recombinase required for creating the *sigK* gene	0.23	10^{-8}

BSU27440	*glnH*	glutamine ABC transporter (binding protein)	0.23	10^{-8}
BSU13380	*ykoS*	unknown	0.23	10^{-11}
BSU16790	*tepA*	sporulation protein, signal peptide peptidase required for efficient processing of pre-proteins	0.23	10^{-10}
BSU29570	*sspA*	small acid-soluble spore protein (major alpha-type SASP)	0.22	10^{-6}
BSU06890	*cotJA*	polypeptide composition of the spore coat	0.22	10^{-10}
BSU27260	*mccA*	O-acetylserine-thiol-lyase	0.22	10^{-7}
BSU24640	*yqxM*	TasA anchoring/assembly protein	0.22	10^{-4}
BSU14230	*ykuV*	thiol disulfide oxidoreductase	0.22	10^{-11}
BSU09780	*yheC*	unknown	0.22	10^{-9}
BSU41050	*rnpA*	protein component of RNase P	0.22	10^{-4}
BSU40270	*yycP*	unknown	0.22	10^{-4}
BSU10740	*yisJ*	unknown	0.22	10^{-7}
BSU29440	*argH*	argininosuccinate lyase	0.22	10^{-4}
BSU09180	*yhcQ*	unknown	0.22	10^{-8}
BSU30620	*ytlD*	similar to ABC transporter (permease)	0.22	10^{-8}
BSU30090	*yteU*	unknown	0.22	10^{-7}
BSU29260	*ytpI*	unknown	0.22	10^{-8}
BSU34260	*eps*	deleted	0.22	10^{-8}
BSU36460	*ywoF*	unknown	0.22	10^{-4}
BSU33750	*sdpA*	maybe involved in cannibalism of siblings	0.21	10^{-9}
BSU34320	*epsF*	similar to glycosyltransferase	0.21	10^{-8}
BSU18720	*yoaR*	unknown	0.21	10^{-9}
BSU03930	*gdh*	glucose 1-dehydrogenase (NAD)	0.21	10^{-10}
BSU24620	*tasA*	major component of biofilm matrix, forms amyloid fibers	0.21	10^{-6}
BSU30840	*yteA*	sporulation protein	0.21	10^{-8}
BSU32000	*dhbA*	2,3-dihydro-2,3-dihydroxybenzoate dehydrogenase	0.21	10^{-9}
BSU40660	*yybF*	similar to antibiotic resistance protein	0.21	10^{-6}
BSU40170	*yydG*	oxidoreductase, modification of YydF	0.21	10^{-5}
BSU12070	*yjdJ*	unknown	0.21	10^{-10}
BSU18210	*yngE*	methylcrotonoyl-CoA carboxylase, subunit	0.21	10^{-10}
BSU09750	*sspB*	small acid-soluble spore protein	0.21	10^{-8}
BSU00560	*spoVT*	transcription activator and repressor of SigG-dependent genes	0.21	10^{-8}
BSU36080	*ywrF*	unknown	0.20	10^{-8}
BSU33410	*yvgO*	general stress protein, survival of ethanol stress	0.20	10^{-8}
BSU05520	*ydzH*	unknown	0.20	10^{-9}
BSU21670	*ypqP*	similar to capsular polysaccharide biosynthesis, in *B. subtilis* 168 the gene is disrupted by the SP-beta prophage	0.20	10^{-4}
BSU26820	*yrpD*	unknown	0.20	10^{-8}
BSU25750	*nucB*	sporulation-specific extracellular nuclease	0.20	10^{-8}
BSU01980	*skfH*	unknown	0.20	10^{-11}
BSU31980	*dhbE*	2,3-dihydroxybenzoate-AMP	0.20	10^{-9}
BSU34230	*epsN*	extracellular polysaccharide synthesis	0.20	10^{-9}
BSU08660	*sspE*	small acid-soluble spore protein	0.20	10^{-6}
BSU23420	*spoVAC*	essential for the uptake of the 1:1 chelate of pyridine-2,6-dicarboxylic acid and Ca^{2+} into developing spores	0.20	10^{-9}
BSU22860	*yphA*	unknown	0.20	10^{-10}
BSU34250	*epsL*	similar to UDP-galactose phosphate transferase, extracellular polysaccharide synthesis	0.19	10^{-9}

BSU40280	*yycO*	unknown	0.19	10^{-6}
BSU12100	*yjeA*	peptidoglycan deacetylase C	0.19	10^{-7}
BSU03690	*yczF*	unknown	0.19	10^{-10}
BSU26990	*yraD*	forespore-specific sporulation protein, similar to spore coat protein	0.19	10^{-8}
BSU17820	*yndL*	similar to phage-related replication protein	0.19	10^{-11}
BSU00430	*yabG*	protease	0.19	10^{-10}
BSU37420	*albF*	antilisterial bacteriocin (subtilosin) production	0.19	10^{-4}
BSU31470	*kapD*	inhibitor of the KinA pathway to sporulation	0.19	10^{-7}
BSU03920	*glcU*	probable glucose uptake protein	0.19	10^{-10}
BSU15810	*spoVM*	required for normal spore cortex and coat synthesis, inhibits the proteolytic activity of FtsH	0.18	10^{-12}
BSU19710	*yodQ*	putative deacylase	0.18	10^{-9}
BSU24650	*yqzG*	unknown	0.18	10^{-9}
BSU08490	*yfhD*	general stress protein, survival of ethanol stress and low temperatures	0.18	10^{-9}
BSU21630	*yokD*	similar to aminoglycoside N3'-acetyltransferase	0.18	10^{-6}
BSU19690	*kamA*	lysine 2,3-aminomutase	0.18	10^{-8}
BSU06920	*yesJ*	unknown	0.18	10^{-11}
BSU18600	*yozQ*	unknown	0.17	10^{-11}
BSU17830	*yndM*	unknown	0.17	10^{-11}
BSU24120	*prpB*	methylisocitrate lyase	0.17	10^{-9}
BSU03400	*yckD*	unknown	0.17	10^{-9}
BSU32850	*fadM*	fatty acid degradation, similar to proline dehydrogenase	0.17	10^{-8}
BSU14200	*ykuS*	unknown	0.17	10^{-12}
BSU22920	*ypeB*	unknown	0.17	10^{-10}
BSU19840	*yotL*	unknown	0.17	10^{-6}
BSU19740	*yodT*	similar to adenosylmethionine-8-amino-7-oxononanoate aminotransferase	0.17	10^{-9}
BSU26970	*adhB*	forespore-specific protein, similar to alcohol dehydrogenase	0.17	10^{-8}
BSU11790	*yjcA*	unknown	0.17	10^{-10}
BSU04240	*ydzA*	unknown	0.17	10^{-10}
BSU20220	*yorX*	unknown	0.17	10^{-8}
BSU01920	*skfB*	thioether bond forming radical SAM enzyme, catalyzes the first step in the maturation of spore killing factor	0.16	10^{-11}
BSU23150	*resA*	extracytoplasmic thioredoxin, cytochrome c biogenesis, reduces disulfide bonds in apo-cytochrome prior to the attachment of heme	0.16	10^{-10}
BSU26960	*yraF*	forespore-specific sporulation protein, similar to spore coat protein	0.16	10^{-9}
BSU11990	*yjdB*	unknown	0.16	10^{-8}
BSU16720	*ymxH*	sporulation protein	0.16	10^{-12}
BSU01935	*skfC*	may be involved in spore killing	0.16	10^{-12}
BSU02600	*cwlJ*	cell wall hydrolase	0.16	10^{-11}
BSU25760	*spoIVCB*	sporulation-specific sigma factor (SigK) (N-terminal half)	0.16	10^{-8}
BSU04530	*ydbN*	Fur-regulated basic protein, acts as RNA chaperone for *fsrA*	0.16	10^{-10}
BSU12400	*yjnA*	unknown	0.15	10^{-11}
BSU26390	*spoIIIC*	RNA polymerase sporulation-specific sigma factor (SigK) (C-terminal half)	0.15	10^{-8}
BSU13780	*ykvP*	unknown	0.15	10^{-9}

BSU31380	*yuzA*	general stress protein	0.15	10^{-8}
BSU27570	*yrzK*	unknown	0.15	10^{-10}
BSU03680	*yclG*	unknown	0.15	10^{-10}
BSU11260	*yjzC*	unknown	0.15	10^{-10}
BSU24130	*prpD*	putative methyl-cis-aconitase	0.15	10^{-10}
BSU00450	*sspF*	small acid-soluble spore protein (minor)	0.15	10^{-12}
BSU23980	*artP*	high affinity arginine ABC transporter (ATP-binding protein)	0.15	10^{-5}
BSU37310	*fnr*	transcriptional regulator of anaerobic genes	0.15	10^{-9}
BSU22200	*cotD*	spore coat protein (inner)	0.15	10^{-8}
BSU39580	*yxeE*	spore coat protein	0.15	10^{-4}
BSU18260	*yngJ*	3-methylbutanoyl-CoA dehydrogenase	0.14	10^{-10}
BSU24160	*mmgB*	3-hydroxyacyl-CoA dehydrogenase (acetoacetyl-CoA)	0.14	10^{-8}
BSU15800	*thiN*	thiamine pyrophosphokinase	0.14	10^{-10}
BSU10280	*yhfM*	unknown	0.14	10^{-12}
BSU34330	*epsE*	similar to glycosyltransferase	0.14	10^{-10}
BSU18220	*yngF*	methylglutaconyl-CoA hydratase	0.14	10^{-10}
BSU37260	*narJ*	nitrate reductase (protein J)	0.14	10^{-8}
BSU06390	*yebD*	unknown	0.14	10^{-9}
BSU38230	*ywcB*	unknown	0.14	10^{-7}
BSU37280	*narG*	nitrate reductase (alpha subunit)	0.13	10^{-9}
BSU19820	*yotN*	unknown	0.13	10^{-8}
BSU36070	*cotG*	spore coat protein	0.13	10^{-4}
BSU26980	*yraE*	forespore-specific sporulation protein, similar to spore coat protein	0.13	10^{-9}
BSU11210	*argB*	N-acetylglutamate 5-phosphotransferase	0.13	10^{-12}
BSU24170	*mmgA*	degradative acetoacetyl-CoA thiolase	0.13	10^{-10}
BSU05530	*ydfR*	unknown	0.13	10^{-10}
BSU38990	*scoA*	probable succinyl CoA:3-oxoacid CoA-transferase (subunit A)	0.13	10^{-6}
BSU19110	*yobW*	sporulation membrane protein	0.13	10^{-10}
BSU18820	*yobB*	unknown	0.13	10^{-5}
BSU20580	*yoqM*	unknown	0.13	10^{-6}
BSU03960	*ycnK*	transcription repressor of the *ycnJ* gene	0.12	10^{-11}
BSU35080	*yvmB*	unknown	0.12	10^{-4}
BSU05550	*cotP*	probable spore coat protein	0.12	10^{-10}
BSU19700	*yodP*	beta-lysine acetyltransferase	0.12	10^{-10}
BSU32860	*yusN*	unknown	0.12	10^{-11}
BSU18230	*yngG*	3-hydroxy-3-methylglutaryl-coenzyme A (HMG-CoA) lyase	0.12	10^{-10}
BSU37820	*spsK*	dTDP-4-dehydrorhamnose reductase, spore coat polysaccharide synthesis	0.12	10^{-8}
BSU27830	*coxA*	spore cortex protein	0.12	10^{-11}
BSU24150	*mmgC*	acyl-CoA dehydrogenase	0.12	10^{-9}
BSU19670	*yodN*	unknown	0.12	10^{-9}
BSU30600	*ytlB*	none	0.12	10^{-8}
BSU11190	*argC*	N-acetyl-g-glutamyl-phosphate reductase	0.12	10^{-12}
BSU37830	*spsJ*	dTDP-glucose-4,6-dehydratase, spore coat polysaccharide synthesis	0.12	10^{-8}
BSU17320	*ymaF*	unknown	0.12	10^{-11}
BSU30850	*ytdA*	similar to UTP-glucose-1-phosphate uridylyltransferase	0.12	10^{-8}
BSU18250	*yngI*	aceto-acetate-CoA ligase	0.12	10^{-11}
BSU34520	*yvdP*	spore coat protein	0.11	10^{-10}

BSU25120	*yqfT*	unknown	0.11	10^{-10}
BSU24140	*mmgD*	2-methylcitrate synthase	0.11	10^{-9}
BSU37430	*albG*	subtilosin production	0.11	10^{-9}
BSU17670	*cotU*	spore coat protein	0.11	10^{-10}
BSU10680	*gerPE*	probable spore germination protein	0.11	10^{-10}
BSU29450	*argG*	argininosuccinate synthase, reversible	0.11	10^{-11}
BSU11250	*argF*	ornithine carbamoyltransferase	0.11	10^{-12}
BSU08550	*sspK*	small acid-soluble spore protein	0.11	10^{-12}
BSU37810	*spsL*	dTDP-4-dehydrorhamnose-3,5-epimerase, spore coat polysaccharide synthesis	0.11	10^{-8}
BSU34370	*epsA*	extracellular polysaccharide synthesis	0.11	10^{-10}
BSU10400	*yhxC*	similar to alcohol dehydrogenase	0.11	10^{-12}
BSU11220	*argD*	acetylornithine transaminase	0.11	10^{-12}
BSU18240	*yngHA*	methylcrotonoyl-CoA carboxylase	0.10	10^{-12}
BSU16880	*ymfJ*	unknown	0.10	10^{-12}
BSU37410	*albE*	subtilosin production	0.10	10^{-9}
BSU19950	*sspC*	small acid-soluble spore protein	0.10	10^{-10}
BSU09150	*yhcN*	forespore-specific gene	0.10	10^{-11}
BSU19730	*yodS*	similar to 3-oxoadipate CoA-transferase	0.10	10^{-6}
BSU28320	*ysnD*	spore coat protein	0.10	10^{-9}
BSU11200	*argJ*	N-acetylglutamate synthase	0.10	10^{-12}
BSU11230	*carA*	carbamoyl-phosphate transferase-arginine (subunit A)	0.10	10^{-12}
BSU24630	*sipW*	signal peptidase I involved in maturation of TasA protein	0.10	10^{-11}
BSU11240	*carB*	carbamoyl-phosphate transferase-arginine (subunit B)	0.10	10^{-12}
BSU18670	*yoaN*	oxalate decarboxylase, spore coat protein	0.10	10^{-10}
BSU13510	*ykzE*	unknown	0.10	10^{-13}
BSU09350	*yhdB*	unknown	0.10	10^{-12}
BSU10610	*yhjR*	spore coat protein	0.09	10^{-10}
BSU10690	*gerPD*	probable spore germination protein	0.09	10^{-10}
BSU37350	*sboA*	subtilosin A	0.09	10^{-6}
BSU21310	*yozP*	unknown	0.09	10^{-10}
BSU33340	*sspJ*	small acid-soluble spore protein	0.09	10^{-7}
BSU22250	*yppG*	unknown	0.09	10^{-10}
BSU37370	*albA*	radical S-adenosylmethionine enzyme, subtilosin production	0.09	10^{-8}
BSU37360	*sboX*	bacteriocin-like product	0.09	10^{-6}
BSU10710	*gerPB*	probable spore germination protein	0.09	10^{-11}
BSU09190	*yhcR*	extracellular non-specific endonuclease, RNase	0.09	10^{-13}
BSU12110	*yjfA*	unknown	0.08	10^{-13}
BSU37380	*albB*	subtilosin production	0.08	10^{-8}
BSU12050	*yjdH*	unknown	0.08	10^{-13}
BSU10950	*yitD*	unknown	0.08	10^{-10}
BSU14980	*ylbE*	unknown	0.08	10^{-13}
BSU37400	*albD*	ABC transporter (membrane protein), export of subtilosin	0.08	10^{-10}
BSU27470	*yrrD*	forespore-specific sporulation protein	0.08	10^{-11}
BSU30470	*ytzC*	unknown	0.08	10^{-10}
BSU11280	*yjaU*	unknown	0.08	10^{-12}
BSU30659	*ytzI*	unknown	0.08	10^{-11}
BSU10700	*gerPC*	probable spore germination protein	0.08	10^{-11}
BSU19490	*gerT*	spore coat protein, involved in germination	0.08	10^{-10}

BSU18030	*tlp*	thioredoxin-like protein	0.08	10^{-12}
BSU12080	*ctaO*	heme O synthase (minor enzyme)	0.08	10^{-13}
BSU35070	*yvmC*	unknown	0.08	10^{-11}
BSU25080	*yqfX*	unknown	0.08	10^{-11}
BSU30890	*ytxO*	spore coat protein	0.08	10^{-8}
BSU27100	*yrhP*	similar to efflux protein	0.08	10^{-9}
BSU19780	*cgeA*	spore coat protein, maturation of the outermost layer of the spore	0.08	10^{-5}
BSU14970	*ylbD*	unknown	0.08	10^{-13}
BSU39590	*yxeD*	unknown	0.07	10^{-7}
BSU07310	*yfnD*	unknown	0.07	10^{-13}
BSU10720	*gerPA*	probable spore germination protein	0.07	10^{-12}
BSU25820	*yqcI*	unknown	0.07	10^{-10}
BSU19600	*yodH*	unknown	0.07	10^{-8}
BSU37850	*spsG*	spore coat polysaccharide synthesis	0.07	10^{-9}
BSU13470	*sspD*	small acid-soluble spore protein	0.07	10^{-14}
BSU22290	*sspM*	small acid-soluble spore protein	0.07	10^{-12}
BSU05560	*ydgA*	unknown	0.07	10^{-10}
BSU17260	*aprX*	intracellular alkaline serine protease	0.07	10^{-12}
BSU11810	*spoVIF*	required for spore coat assembly and resistance	0.07	10^{-10}
BSU07300	*yfnE*	unknown	0.07	10^{-14}
BSU40570	*yybO*	similar to ABC transporter (permease)	0.07	10^{-5}
BSU18020	*sspN*	small acid-soluble spore protein (minor)	0.07	10^{-13}
BSU11750	*cotY*	spore coat protein (insoluble fraction)	0.07	10^{-12}
BSU27190	*yrzI*	unknown	0.07	10^{-11}
BSU10670	*gerPF*	probable spore germination protein	0.06	10^{-12}
BSU37910	*spsA*	spore coat polysaccharide synthesis	0.06	10^{-10}
BSU06300	*cotA*	laccase, bilirubin oxidase, spore coat protein (outer)	0.06	10^{-13}
BSU36060	*cotH*	spore coat protein (inner)	0.06	10^{-10}
BSU30860	*ytcA*	similar to to NDP-sugar dehydrogenase	0.06	10^{-10}
BSU37840	*spsI*	glucose-1-phosphate thymidylyltransferase, spore coat polysaccharide synthesis	0.06	10^{-8}
BSU37890	*spsC*	spore coat polysaccharide synthesis	0.06	10^{-9}
BSU19510	*yojB*	unknown	0.06	10^{-7}
BSU30880	*ytcC*	sporulation protein, similar to lipopolysaccharide N-acetylglucosaminyltransferase	0.06	10^{-9}
BSU37860	*spsF*	spore coat polysaccharide synthesis	0.06	10^{-9}
BSU17990	*sspO*	small acid-soluble spore protein (minor)	0.06	10^{-13}
BSU25150	*yqfQ*	late sporulation protein	0.06	10^{-8}
BSU37440	*ywhL*	unknown	0.06	10^{-10}
BSU11780	*cotV*	spore coat protein (insoluble fraction)	0.06	10^{-12}
BSU37870	*spsE*	spore coat polysaccharide synthesis	0.06	10^{-8}
BSU37880	*spsD*	spore coat polysaccharide synthesis	0.06	10^{-10}
BSU37900	*spsB*	spore coat polysaccharide synthesis	0.05	10^{-8}
BSU17980	*sspP*	probable small acid-soluble spore protein (minor)	0.05	10^{-14}
BSU36030	*ywrK*	similar to arsenical pump membrane protein	0.05	10^{-11}
BSU10920	*yitA*	sulfate adenylyltransferase	0.05	10^{-12}
BSU16740	*spoVFB*	dipicolinate synthase (subunit B)	0.05	10^{-11}
BSU16730	*spoVFA*	dipicolinate synthase (subunit A)	0.05	10^{-11}
BSU30870	*ytcB*	putative UDP-glucose epimerase	0.05	10^{-10}

BSU11760	*cotX*	spore coat protein (insoluble fraction)	0.05	10^{-12}
BSU10910	*yisZ*	adenylylsulfate kinase	0.05	10^{-11}
BSU23350	*ypzD*	unknown	0.05	10^{-9}
BSU10930	*yitB*	phospho-adenylylsulfate sulfotransferase	0.05	10^{-10}
BSU19760	*cgeD*	maturation of the outermost layer of the spore	0.05	10^{-8}
BSU11740	*cotZ*	spore coat protein (insoluble fraction)	0.05	10^{-13}
BSU30900	*cotS*	spore coat protein	0.04	10^{-10}
BSU34530	*cotR*	spore protein	0.04	10^{-10}
BSU17310	*ymaG*	spore coat protein	0.04	10^{-11}
BSU10940	*yitC*	mother cell-specific sporulation protein	0.04	10^{-11}
BSU05570	*ydgB*	unknown	0.04	10^{-12}
BSU06850	*yeeK*	spore coat protein	0.04	10^{-13}
BSU30920	*cotI*	spore coat protein	0.04	10^{-10}
BSU36050	*cotB*	spore coat protein (outer)	0.04	10^{-12}
BSU09240	*yhcW*	similar to phosphoglycolate phosphatase	0.04	10^{-13}
BSU32650	*yurS*	sporulation protein	0.04	10^{-8}
BSU17970	*cotM*	spore coat protein (outer)	0.04	10^{-13}
BSU11770	*cotW*	spore coat protein (insoluble fraction)	0.04	10^{-13}
BSU07280	*yfnG*	similar to CDP-glucose 4,6-dehydratase	0.03	10^{-12}
BSU30910	*cotSA*	spore coat protein	0.03	10^{-10}
BSU19610	*yodI*	unknown	0.03	10^{-12}
BSU20190	*yosA*	unknown	0.03	10^{-12}
BSU12090	*cotT*	spore coat protein (inner)	0.03	10^{-14}
BSU09165	*yhcO*	unknown	0.03	10^{-13}
BSU07290	*yfnF*	unknown	0.03	10^{-13}
BSU11809	*yjcZ*	unknown	0.03	10^{-13}
BSU07270	*yfnH*	similar to glucose-1-phosphate cytidylyltransferase	0.03	10^{-12}
BSU32640	*sspG*	small acid-soluble spore protein (minor)	0.02	10^{-14}
BSU28410	*gerE*	transcriptional regulator (repressor or activator) of a subset of sigma-K-dependent late spore coat genes	0.02	10^{-13}
BSU19770	*cgeC*	maturation of the outermost layer of the spore	0.02	10^{-11}
BSU19790	*cgeB*	maturation of the outermost layer of the spore	0.02	10^{-12}

Supporting Information for Chapter 3

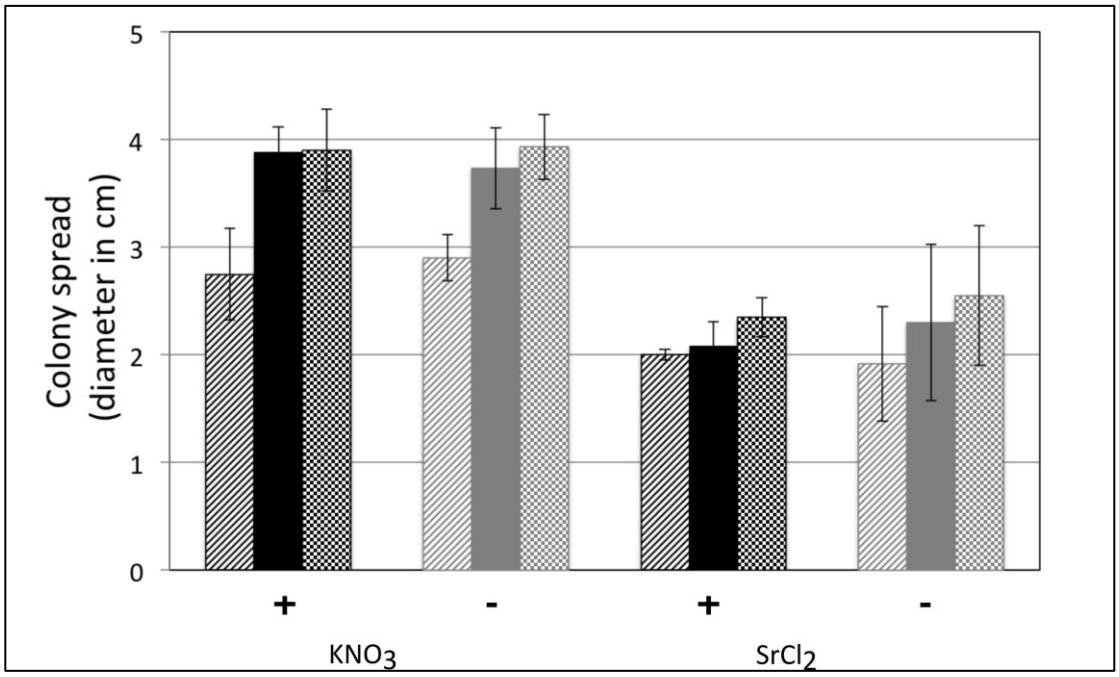

Figure 1| (A) Ca^{2+} specifically reduce colony escape. The colony expansion diameters of *B. subtilis* DK1042 are shown after 3 (striped), 5 (filled), and 7 (checked) days. Black bars present data in presence, while grey bars indicate in absence of KNO_3 and $SrCl_2$ in the 2×SG medium. KNO_3 was used to observe the impact of NO_3^-, while $SrCl_2$ was applied to assay the influence of another divalent cation. The error bars indicate 95% confidence intervals.

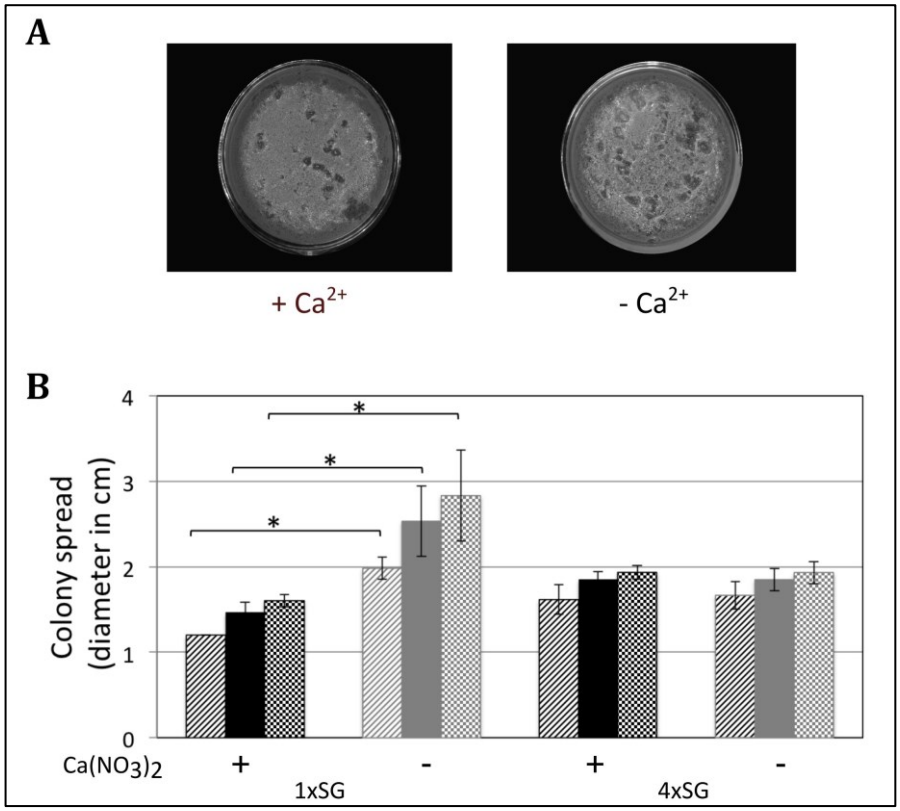

Figure 2 | (A) Pellicle formation of *B. subtilis* DK1042 on 2×SG medium in the presence (left) and absence (right) of Ca^{2+} supplementation after 3 days. (B) The colony expansion diameters of the *B. subtilis* DK1042 are shown on 1×SG and 4×SG media with 1.5% agar after 3 (striped), 5 (filled), and 7 (checked) days. The black bars present data in presence, while grey bars indicate in absence of Ca^{2+} supplementation in the media. The error bars indicate 95% confidence intervals. * denotes significant differences ($p<0.05$) analyzed with paired t-test.

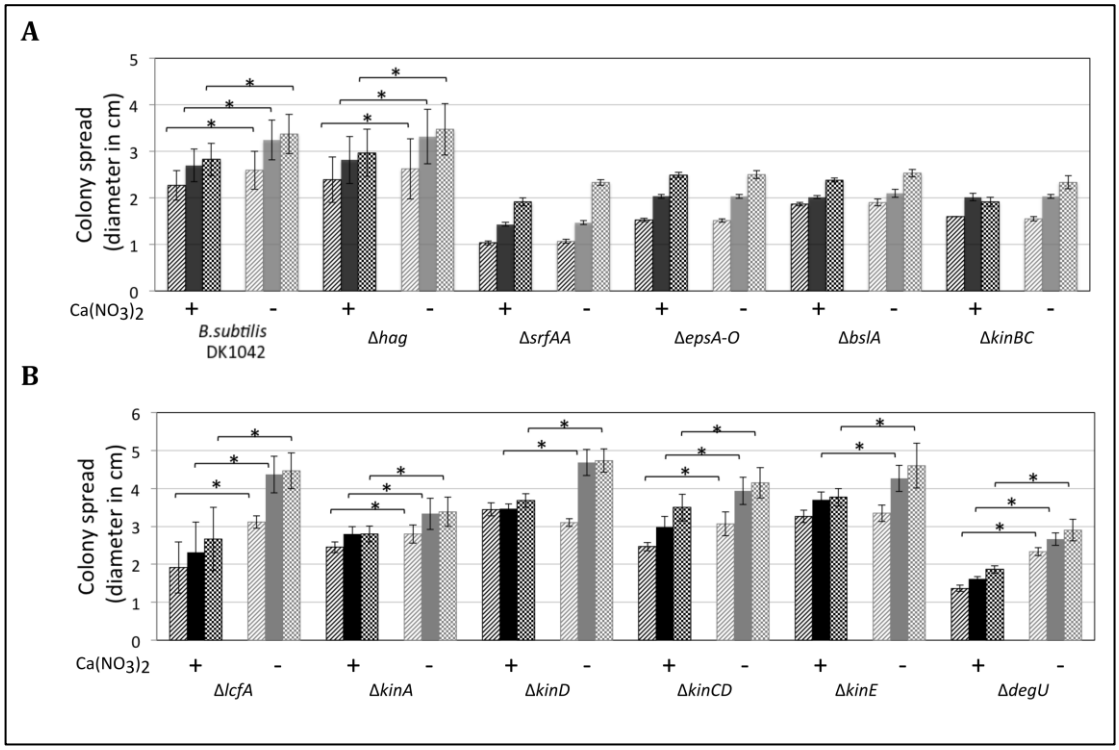

Figure 3 | Colony escape of various strains on MSgg (A) and 2×SG (B) medium. (A) The colony expansion diameters of the *B. subtilis* DK1042 and its derivatives, Δ*hag*, Δ*srfAA*, Δ*epsA-O*, Δ*bslA*, and Δ*kinB*Δ*kinC* are shown on MSgg medium after 4 (striped), 6 (filled), and 8 (checked) days. (B) The colony expansion diameters of the *B. subtilis* Δ*lcfA,* Δ*kinA*, Δ*kinD*, Δ*kinE*, Δ*kinC*Δ*kinD*, and Δ*degU* are shown on 2×SG medium after 3 (striped), 5 (filled), and 7 (checked) days. Black bars present data in presence, while grey bars indicate in absence of Ca^{2+} supplementation in the respective media in both panels. The error bars indicate 95% confidence intervals. * denotes significant differences ($p<0.05$) analyzed with paired t-test.

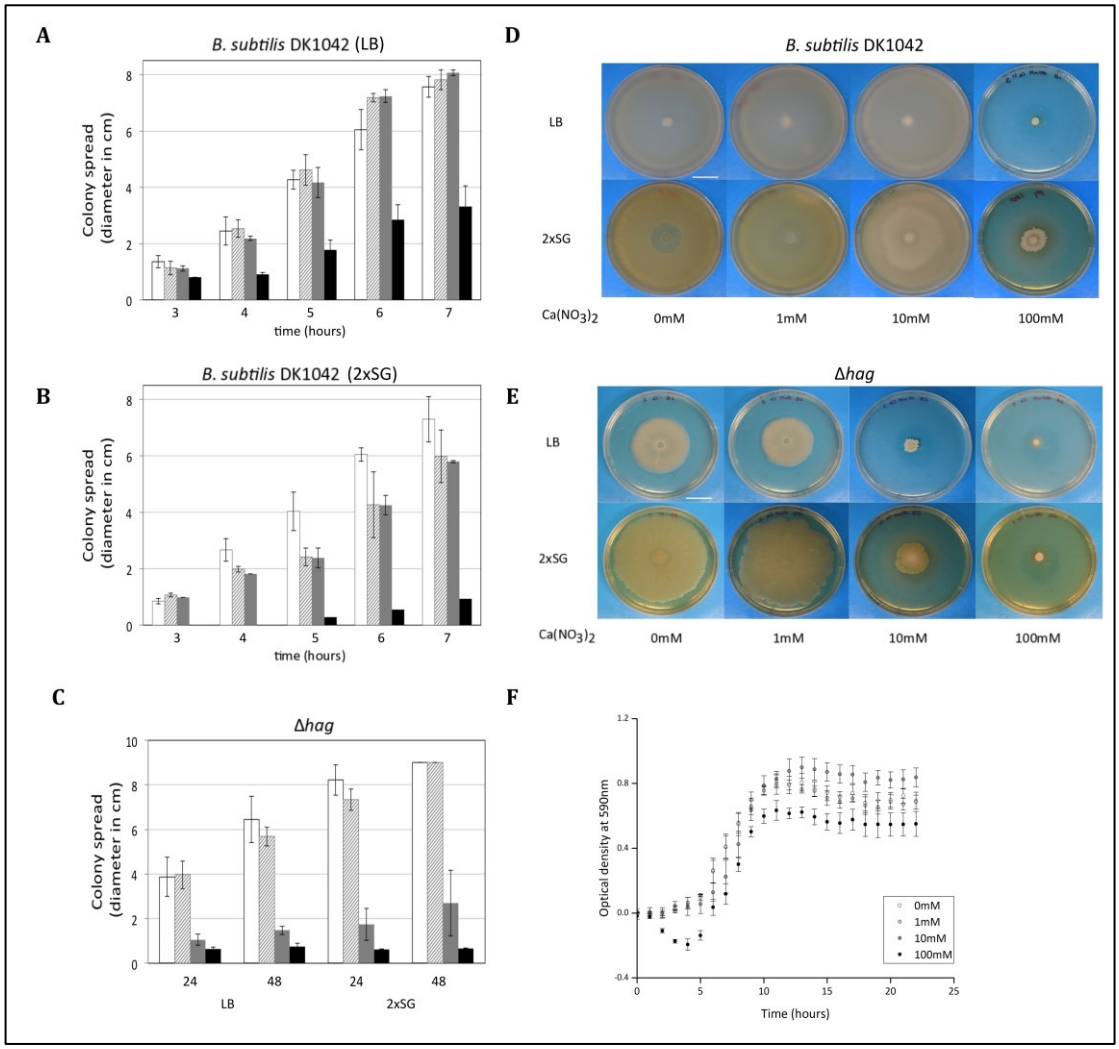

Figure 4 **/** Impact of the presence of Ca^{2+} on swarming and sliding mediated surface colonization of *B. subtilis* DK1042 and Δ*hag* strains, respectively, on LB and 2×SG medium. Swarming diameter of *B. subtilis* DK1042 strain after 3 to 7 hours on LB (A) and 2×SG (B) media with 0.7% agar without (white bars) or with 1 (stripped bars), 10 (grey bars), 100 mM (black bars) Ca^{2+} supplemented. Sliding diameter of *B. subtilis* Δ*hag* strain (C) after 24 and 48 hours on LB (left) and 2×SG (right) media supplemented with various amount of $Ca(NO_3)_2$ (labeling similar to S4A). Swarming (D) and sliding (E) disk of WT and Δ*hag* strains, respectively, 24 hours after inoculation on LB (above) and 2×SG (below) media with 0.7% agar in the absence or presence of various amount of Ca^{2+} supplementation. Scale bars indicate 2 cm. Growth properties of *B. subtilis* DK1042 (F) in 2×SG medium supplemented with different amount $Ca(NO_3)_2$ from 1mM to 100mM.

Supporting information for Chapter 4

Table 1| Strains used in this study.

No.	***Name***	***Description***	***Created***
B. subtilis			
1	JH642	*ΔtrpC2 ΔpheA1 citS642*, derived from Marburg strain.	Laboratory Stock (Grau, R., originally from Hoch, J.A.)
2	YS 1	Evolved yield strategist	This study
3	YS1.1	TBYS 1 $P_{hyperspank}$-*gfp::*Cm	This study
4	YS1.2	TBYS1 $P_{hyperspank}$-*gfp::cat*-Km-*cat*	This study
5	YS 1.3	TBYS 1 $P_{hyperspank}$-mKATE*::*Cm	This study
6	TB237	JH642 $P_{hyperspank}$-*gfp::*Cm	This study
7	TB236	JH642 $P_{hyperspank}$- mKATE*::*Cm	This study
8	RS 1	Evolved rate strategist (control)	This study
9	RS 1.1	TBRS 1 $P_{hyperspank}$-*gfp::*Cm	This study
10	RS 1.2	TBRS1 $P_{hyperspank}$-*gfp::cat*-Km-*cat*	This study
11	RS 1.3	TBRS 1 $P_{hyperspank}$-mKATE*::*Cm	This study
Plasmids			
1	pHy-GFP	$P_{hyperspank}$-*gfp::*Cm- *amyE*	[169]
2	pHy-mKATE	$P_{hyperspank}$- mKATE*::*Cm- *amyE*	[169]
3	pCm-Km	*cat: neo :cat*	This study

Supporting figures

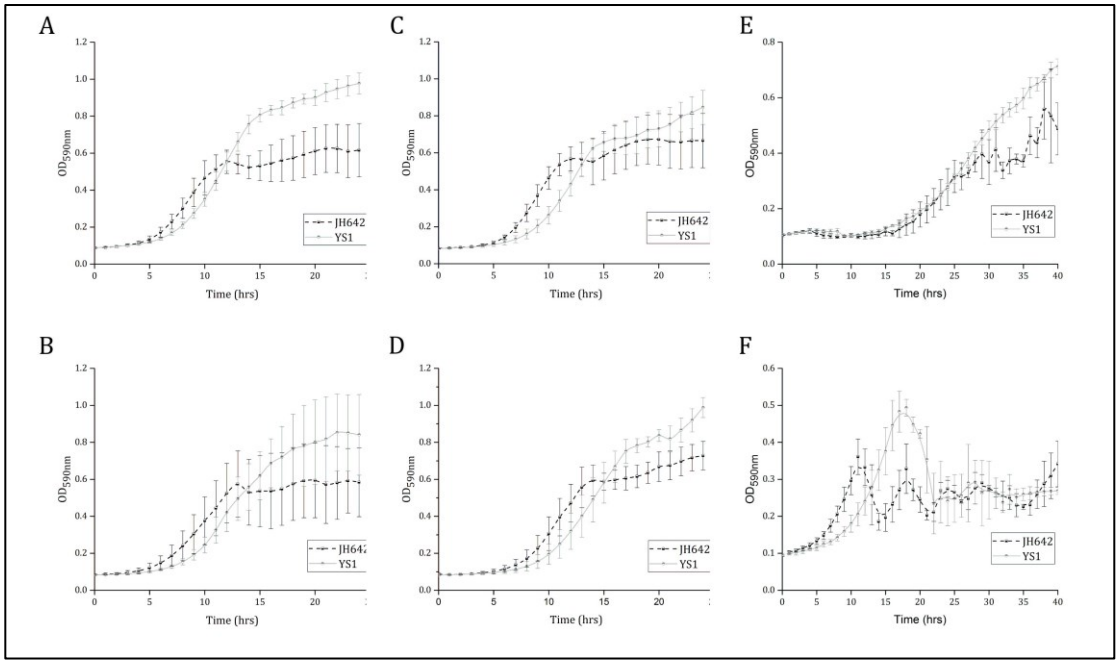

Figure 1 | Growth in CSE medium with different carbon sources. The growth kinetics of ancestor JH642 (black dotted lines) and YS1 (grey lines) are compared in medium containing (A) glucose, (B) malate, (C) fructose, and (D) glycerol. In all cases where glucose is replaced with another carbon source, the YS shows initial delayed growth but final higher yield. Since the typical CSE medium has glutamate, succinate and glucose as major nutrient sources, the medium conditions were modified to see the growth kinetics in different conditions. Medium devoid of glucose, (E) shows similar growth delay also in ancestor strain indicating the uptake of succinate and glutamate leading to the initial delay in YS1. Other condition where succinate and glutamate are absent, f, in the medium shows the higher yield compromised in YS1. This importantly highlights that metabolism dependent on uptake of succinate and glutamate has key role in higher yield.

Figure 2 | Characterization of YS1

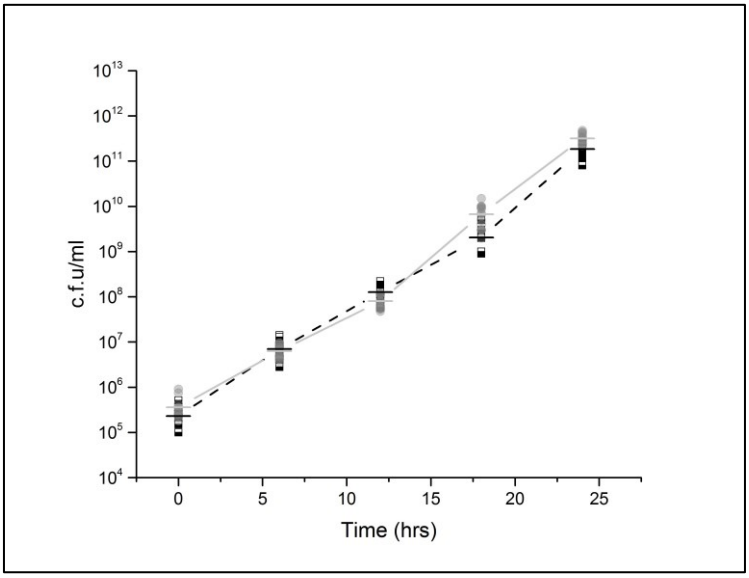

(A) ***Viable cell counts in CSE medium.*** The cell counts performed every 6 hours from the CSE medium growing cultures of ancestor JH642 and YS1 show the comparable patterns seen in the optical densities measured during growth curves. The YS1 cells are initially lower than JH642 until 12 hours, but increase in numbers at 18th and 24th hour.

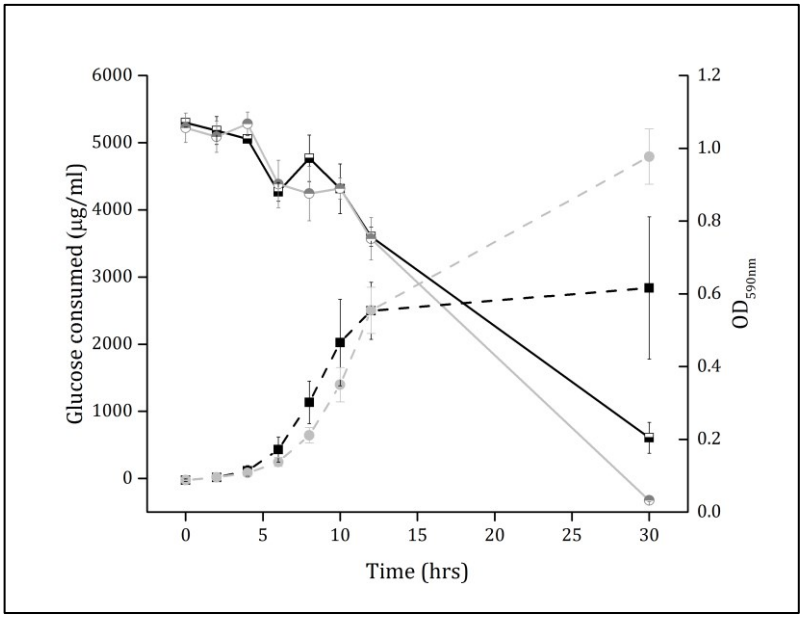

(B) ***Glucose utilized in the medium.*** The biochemical quantification of glucose in the medium is used to calculate the amount consumed by the ancestor and YS1. It can be noted that there is slight difference between the glucose uptake at 7th and 8th hour indicating the change in metabolic strategy in the medium.

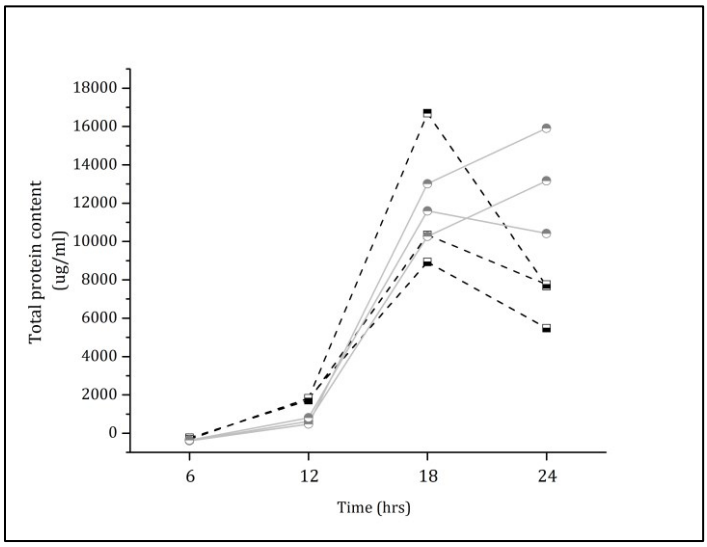

(C) ***Protein content***. The overall protein content in the growing cultures of JH642 and YS1 are calculated using the Bradford assay. Comparable to the growth kinetics and cell area measurements, the total protein content is higher in YS1 at 24 hours.

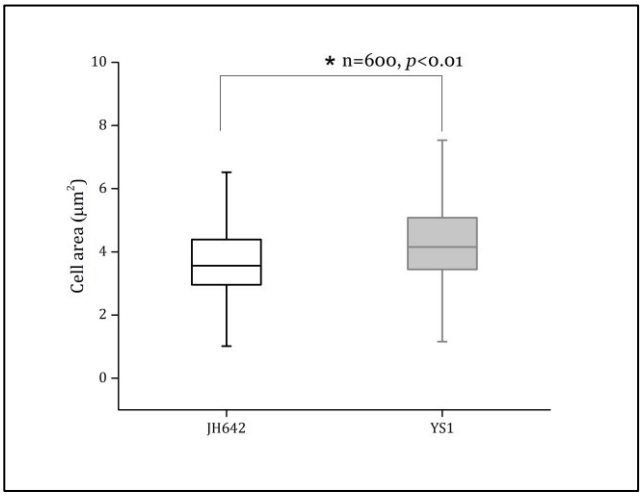

(D) ***Cell area.*** The ancestor JH642 and YS1 were grown for 6 hours in CSE medium in triplicates. The microscopic slides were prepared by putting 5ul of grown culture on the uniform agarose gel and then covered by coverslip. The phase contrast single cell images (100x magnification, oil immersion, phase contrast lens) were obtained using Axio plus fluorescent microscope. These images were the analyzed for the cell length and cell area measurements using Oufti application. The calculated cell area of YS1 is significantly higher than JH642 (*, s=0, p<0.01). The error bars in the box plot indicate the 95% confidence interval. The black scale bars on the left side bottom of the cell images are 10um.

Figure 3 | Biofilm characteristics

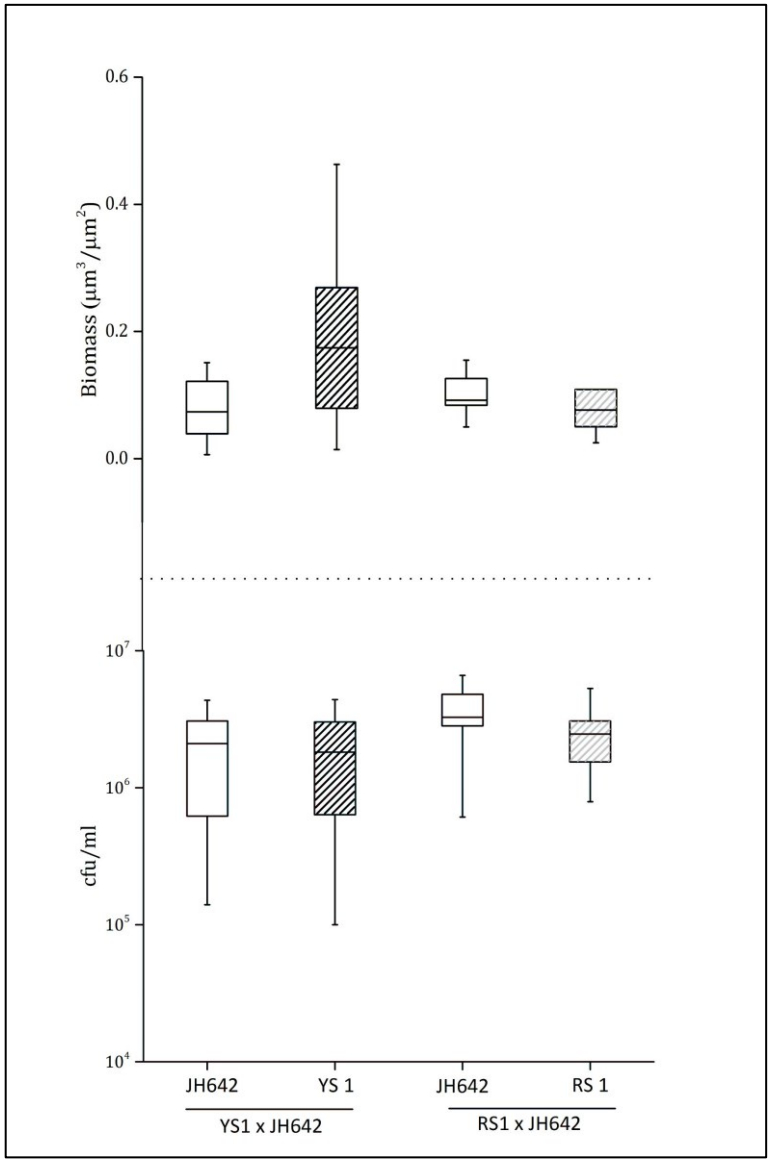

(A) ***Initial attachment.*** It is crucial to cross out the possibility that initial attachment has role in the resulting biofilms at 24 and 48 hours. This initial attachment is the cells attached to the submerged surface two hours after inoculation. Since supernatant medium is changed at this point, it is only the attached cells that further grow in the biofilm. We now know from the mono culture biomass that the growth strategies do not influence the biofilm characteristics of the ancestor and the derived cultures. To check if these two strains also attach equally, we performed microscopic studies as well as cell counts of the initial attached cells in mixed biofilms. We see that both the competing partners in all cases show equal attachment. The error bars indicate the 95% confidence interval.

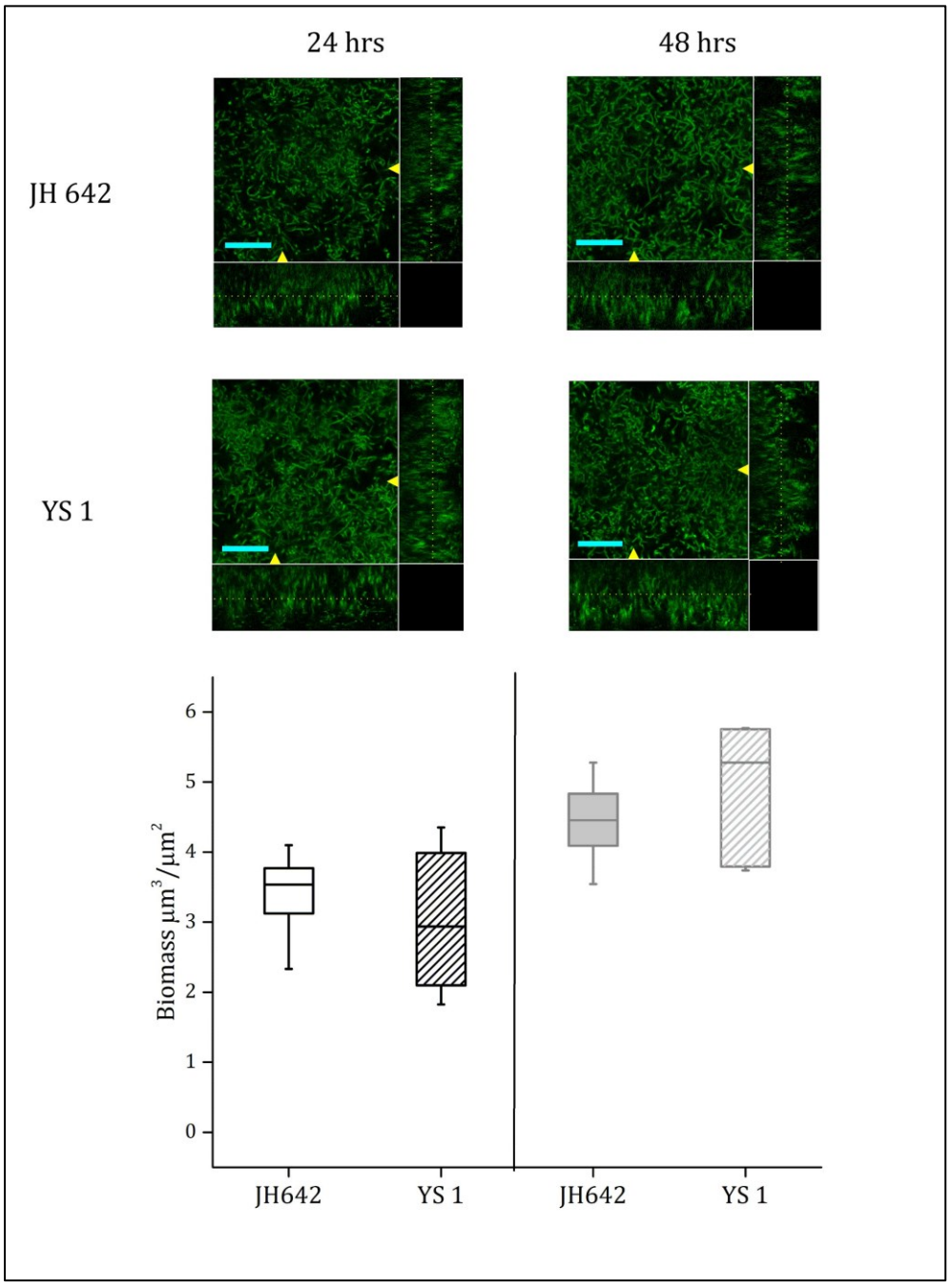

(B) ***Mono-culture biofilms of JH642 and YS1 show similar biomass.*** The biofilm forming properties of JH642 and YS1 are not dependent on the growth strategies. Both the cultures form robust biofilms at 24 and 48 hours. The biofilm pictures show the orthogonal views where the yellow arrows indicate the transverse and lateral cut points showing the x and y planes on the right and bottom. The dotted lines on these planes are the z-position that is seen in the main frame. The scale bar in blue is 30um. The biomass is calculated using Comstat for the images at 24 as well as 48 hours. The values of YS1 and JH642 show no significant difference (s_{24}= 0.198, s_{48}= 0.227, $p>0.05$). However, the biomass of YS1 varies to a large range.

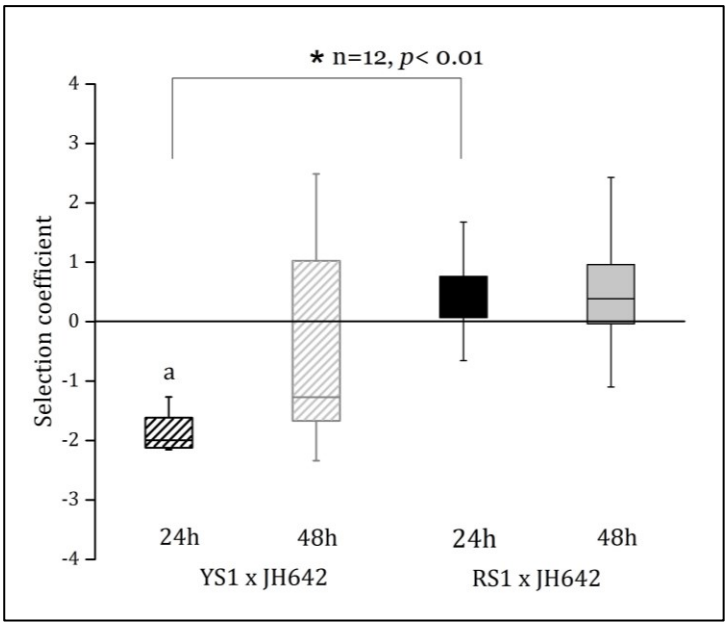

(C) ***Competition in submerged biofilms***. The competing cultures, similar to the competitions in shaken and droplet conditions, are mixed 1:1 in BGM medium. These are distributed as technical replicates in 3 96 well plates (12 biological replicates in each well). After two hours, when the medium is changed (see methods) attached biofilm from one plate is scrapped and cell counts are performed as initial count. In course of time, the 24th and 48th hour biofilms are also scrapped and cell counts are performed. The selection coefficient is calculated from the cell counts. The competition outcomes of YS are compared to RS at 24 hours (*, s= 0.004 , p<0.01, paired t test) and 48 hours (no significant difference). The error bars indicate the 95% confidence interval. (a=s= 0, p<0.01, one sample t-test).

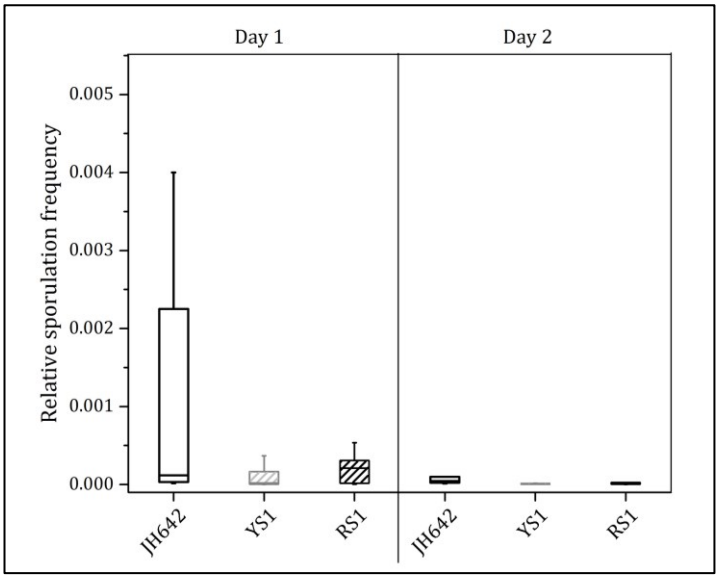

(D) ***Sporulation in submerged biofilms.*** The attached biofilms of JH642, YS and RS were scrapped as described above at 24 and 48 hours of growth and the cell counts were performed before and after the heat treatment (80 °C for 25 minutes). The frequency of sporulation was determined by dividing the colony forming units obtained after heat treatment by the total cell counts before the heat treatment. Sporulation in submerged biofilms is very low and this process does not affect the outcomes of the competition experiments. The error bars indicate 95% confidence interval.

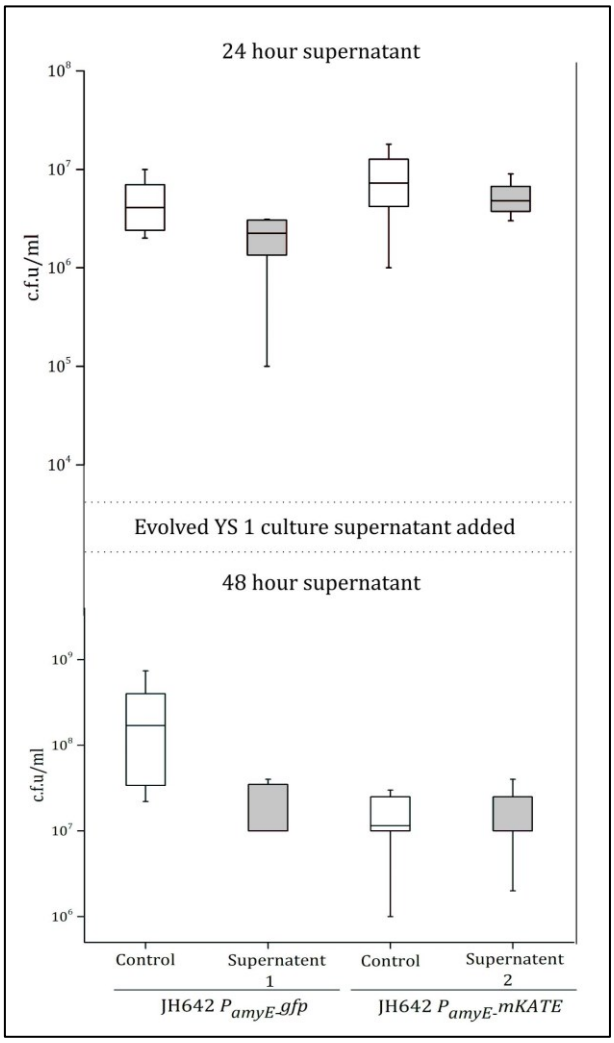

(E) ***Rate of dispersion.*** The biofilm model is so designed that the medium is changed every 12 hours in order to get rid of planktonic and the air liquid interface mat forming cells. Since the submerged biofilms show the emergence of YS1 at 48 hour, we asked the question if it modifies the dispersion of its competing partner that results in its emergence. In order to check this, we performed cell counts on the dispersed cells of JH642 (cells in the supernatant) at 24th hour where YS1 is present in low numbers and hence does not influence and at 48th hour where YS is present in influencing numbers. To mimic the 48th hour scenario, we added 1:50 diluted YS1 supernatant to the JH642 biofilms at 24 hour and also at 32 hour during the medium change. We used gfp labeled YS1's supernatant for JH642 P_{amyE}-*mKATE* and mKate labeled YS1's supernatant for JH642 P_{amyE}-*gfp*. We find that the differences between the dispersed c. f. u of control and the ones where supernatant added are not significant (s_1=0.071, s_2= 0.649, p>0.05, paired t-test). This indicates that the YS1 does not play a role in dispersing the JH642. It seems that the biofilms have constant rate of dispersion at a threshold and this additionally makes it spatial for the YS1 to emerge.

Figure 4| Mutations in YS

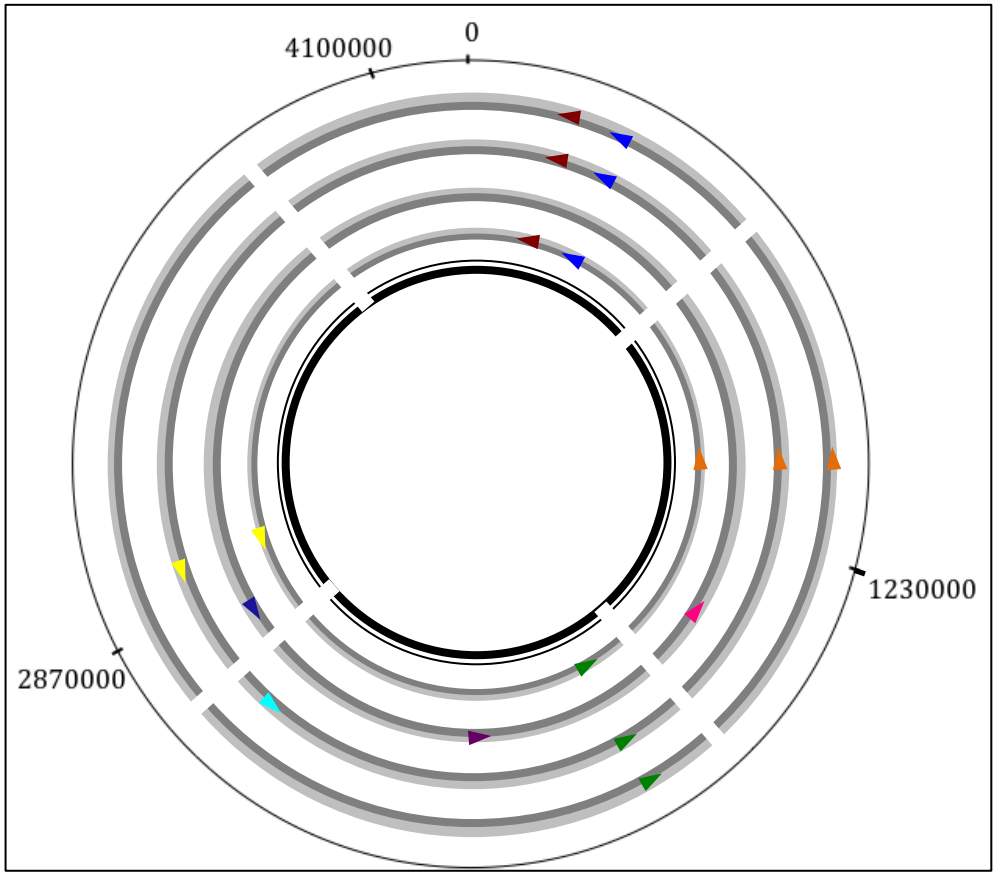

Symbol	Location	Gene	Mutation
◀	255376	*ptsG*	SNV
◀	259234	*ybgE*	Deletion
◀	1012546	*yhdL*	MNV
◀	1396650	*rsgI*	SNV
◀	1626764	*coaBC*	SNV
◀	1952019	*ppsA*	Deletion
◀	2607883	*gpr*	SNV
◀	2863975	*leuB*	SNV
◀	2965557	*dnaE*	SNV

The schematic representation of the genome maps indicating the location of mutations in 4 strains of YS (grey circles) compared to the ancestor JH642 (black circle). The different mutations are denoted by colored triangles and are represented in the table below left.

Acknowledgement

It is often said that you are, because of whom you meet.
I have been extremely lucky in life to meet and be around some crazy bunch of people that have always contributed to that even crazier self that I have turned out to be, influenced me and shaped me to be whatever I am now, been there for me in all the walks of life as a support, as companions, advisors or simply to make life as it is, awesome.
Coming this far with such interesting work with a 100 plus paged thesis to write about wasn't an easy task. I still don't believe at times that it is the time now when I am writing this to look back at when it all started. This acknowledgement is for all those pillars in my life that have helped me get this far. A big thank you and hugs.

I have to start with my research supervisor and advisor, Akos for nurturing my curious thoughts and always being there for me. I cannot thank you enough for putting up with me in my attempts to almost stick to the deadlines, to always be the positive influence when things didn't work the way they should and also to help me push my limits in achieving what ever I have so far.
Working in the lab, and indulging in other social activities has been a fun experience and I thank you once again for letting me be part and parcel of the amazing TeBi group.
I have to thanks all the present and past lab members that have contributed to the awesome time I had. Anna, to scientifically influence me to give my research curiosities another chance, to be there to discuss numerous possibilities and lab tricks, to encourage the drive to perform better and also for just being there always to talk about life and other adventures over wine or at some hill top in Jena.
Ramses, for being as awesome as he always is, for being that breathe of fresh thought when I am clogged with no solutions, to have ample discussions on lifehacks, politics, games and tv-series. Theresa for being there always as a ray of hope, a go to person and someone who is always there for me whenever needed. I admire your patience and aim to be more positive and down to earth person as you are
Mavic, for those awesome discussions on the parallel lifestyles in Asia and Europe. Anne, to make me curious about my love-hate relationships with cats, and to positively push me to learn some unique German words.
Ben and Pam, Felix, Tim, Sonja, Wieland, Jan and other past members of the lab that have contributed to the merry times spend and also significantly to the work produced.
The current lab members, Tino, Anand and Surabhi for contributing awesomely to the lab traditions of cakes and traditional sweets.

To Christian Kost for the enthralling discussions on evolution and social interaction in life, mentoring my scientific side and influencing me study microbial evolution.
To the past and present EEE members for great scientific influence, making *E.coli* awesome for me, and specially Daniel and Lisa for providing awesome kitchen to cook Indian dishes.

To many people that influenced and made fruitful suggestions to my work. Kevin Foster to always give the great inputs, Carey Nadel and Knut Dresher for the feedbacks on projects.
Jan Ulrich Kreft, Daniel Lopez and others for providing strains and methods for the study. Richard Lenski, for inducing the drive and hunger to study microbial evolution. Zachary, Vaughn and Will for the great feedback on the work.
To many collaborators that have influenced the outcomes of this work.
To Prof Kothe, for being the phenomenal woman to look up to and a scientific advisor. The Kothe department people, Christin, Reyna, Sophia, Elke, Micha, Katherin, to always being there and helping me out.
To Katja, for being very kind and helpful in administrative processes. Jan for awesome career advises and being one of the greatest JSMC managers. To Annika and other JSMC building mates for fun filled times.
To a bunch of fellow JSMC people, Sindy, Hella, Daniel and Ana (for scary movie nights), Sarahi, Ashish, Silvio for making social life in Jena amazing.
To the awesome Micom 2015 team- Tini, Daniel, Reyna, Sophia, Stefan, Joao (for that drunk night), Shraddha (for more of those drunk nights) and Karen for the crazy time we had putting up a great conference.
To Jena ke kaminey Indians for those lively movie, food and Diwali nights. To be that homely support system away from home.

To Glen for always being that charm, a great motivator, crazy lover, great friend, travel and food companion and the reason for what I have become today.
To Mansi Limbad and Manasi Mankatty for being the people to tell me always how great it feels to be me. To Ridhina and Renu for the great understanding and being the great friends for life. To Ninad, for the crazy ideas and love for food and Marathi that we share.

To my parents, Aai and Baba to always be behind me as a support system and to make me a responsible person. To influence me to take risks in life and to lead the life with love and compassion for others.
To the awesome people of Narmada Sadan for being a lovely, happy family together. In spite being this far always from home, distance doesn't seem much due to the great bond we share and the constant attempt to stay in touch.
And last but not the least, to that amazing strength and drive that keeps me curious, yet content with life.

Curriculum Vitae

EISHA MHATRE
Institute of Microbiology
Friedrich Schiller University of Jena
Neugasse 23, Jena 07743. DE

Phone: +49 176 72632605
Email: eisha.r.mhatre@gmail.com
Date of Birth: 7th August 1989

CURRENT POSITION (*since April 2013*)

Doctoral Researcher in Terrestrial Biofilms Group, Institute of Microbiology- FSU Jena, DE

EDUCATION

2012 M.Sc in Microbiology, The Maharaja Sayajirao University of Baroda, Vadodara

2010 B.Sc in Microbiology, Wilson College- Mumbai

2007 Junior College, Patkar College- Mumbai

RESEARCH EXPERIENCE

Doctoral research (*2013- present, anticipated 2016*)

Title: Extrinsic and intrinsic factors governing bacterial biofilms

Advisor: Dr. Akos T. Kovacs, Terrestrial Biofilms Group, Institute of Microbiology- FSU Jena, DE

Project Assistance (*2012-2013*)

Title: Influence of biofilm inducing genes on *Salmonella* pathogenesis

Advisor: Dr. Dipshikha Chakravortty, Department of Microbiology and Cell Biology, Indian Institute of Science, Bangalore, IN.

M.Sc Dissertation (*2011- 2012*)

Title: Characterization of mutants showing loss in bio emulsifier production in a newly isolated strain of *Solibacillus silvestris*.

Advisor: Dr.Anuradha Nerurkar, Department of Microbiology and Biotechnology Centre, Maharaja Sayajirao University of Baroda, IN.

PUBLICATIONS

Peer Reviewed and published

1. ***Mhatre E***, Gallegos Monterrosa R, Kovács ÁT (2014) From environmental signals to regulators: modulation of biofilm development in Gram-positive bacteria*. (J. Basic Microbiol.)* 54(7): 616-632

2. Grau R, de Oña P, Kunert M, Leñini C, Gallegos-Monterrosa R, ***Mhatre E***, Vileta D, Donato V, Hölscher T, Boland W, Kuipers OP, Kovács ÁT (2015) A duo of potassium-

responsive histidine kinases govern the multicellular destiny of *Bacillus subtilis*. *(mBio)* 6(4):e00581-15

3. Hölscher T, Dragoš A, Gallegos-Monterrosa R, Martin M, ***Mhatre E***, Richter A, Kovács AT (2016) Monitoring spatial segregation in surface colonizing microbial populations. *(JoVE)* e54752, http://dx.doi.org/10.3791/54752

4. ***Mhatre E***, Troszok A, Gallegos Monterrosa R, Lindstaedt S, Hölscher T, Kuipers OP, Kovács AT (2016) The impact of manganese on biofilm development of Bacillus subtilis. *(Microbiol)* 162(8):1468-1478

5. Raie DS, ***Mhatre E***, Thiele M, Labena AE, Al-Ghannam GA, Farahat LA, Youssef T, Fritzsche W, Kovács AT (2016) Application of quercetin and its bio-inspired nanoparticles as anti-adhesive agents against *Bacillus subtilis* attachment to surface, *(Mater. Sci. Eng., C)* http://dx.doi.org/10.1016/j.msec.2016.09.038

6. Gallegos-Monterrosa R, ***Mhatre E***, Kovács AT (2016) Specific *Bacillus subtilis* 168 variants do form biofilms on nutrient rich medium. *(Microbiol)* e01272-16. http://dx.doi.org/10.1128/genomeA.01272-16

7. Krawinkel J, Torres-Mapa ML, ***Mhatre E***, Kovács AT, Heisterkamp A (2016) Structural damage of *Bacillus subtilis* biofilms using pulsed laser interaction with gold thin films. *(J. Biophotonics)* http://dx.doi.org/10.1002/jbio.201600146

8. ***Mhatre E***, Sundaram A, Hölscher T, Mühlstädt M, Bossert J, Kovács AT (2016) Presence of calcium maintains rugose biofilm structure of *Bacillus subtilis*. *(Microorganisms)* 5(1):7

To be submitted

1. ***Mhatre E***, Bartels B, Boltz HH, Klumpp S, Kovács AT, Spatially structured environment facilitates the emergence of yield strategists. *(Nat. Commun.)*

2. ***Mhatre E***, Kovács AT, Taking the road less travelled: emergence of rare strategies and metabolic interactions in spatially structured environments *(NPJ Biofilms and Microbiomes)*

RESEARCH PRESENTATIONS

Talks

1. Spatial segregation allows the emergence of yield strategy phenotypes in *Bacillus subtilis (2nd ASM conference on Experimental Microbial Evolution)* 2016, Washington. DC

2. Spatial segregation allows the emergence of yield strategy phenotypes in *Bacillus subtilis (Vereinigung für Allgemeine und Angewandte Mikrobiologie- VAAM 2016)* 2016, Jena

3. Spatial segregation allows the emergence of yield strategy phenotypes in *Bacillus subtilis (Jena School of Microbial Communication symposium)* 2015, Jena

4. Manganese influences cellular processes in *Bacillus subtilis* biofilms *(Jena School of Microbial Communication symposium)* 2014, Jena

Posters

1. Spatial segregation allows the emergence of yield strategy phenotypes in *Bacillus subtilis (EMBO- New Approaches and Concepts in Microbiology)* 2015, Heidelberg

2. Evolving growth strategic phenotypes in *Bacillus subtilis (Vereinigung für Allgemeine und Angewandte Mikrobiologie- VAAM 2015)* 2015, Marburg

3. Evolving growth strategic phenotypes in *Bacillus subtilis (Microbial Communication- MiCom 2015)*, 2015, Jena

4. Manganese influences cellular processes in *Bacillus subtilis* biofilms *(Microbial Communication- MiCom 2014)* 2014, Jena

5. Manganese influences cellular processes in *Bacillus subtilis* biofilms *(Biofilm 6)* 2014, Vienna

6. Phenotypic heterogeneity in *Bacillus subtilis* biofilms *(Jena School of Microbial Communication Symposium)* 2013, Jena

GRANTS, AWARDS AND ACHIEVEMENTS

July 2016 - ASM travel grant for Conference

June 2016 - ProChance 2016 FSU-Jena travel grant

May 2016 - FEMS Meeting Attendance Grant

Jan 2016 - Three-month extension of funding fellowship of the doctorate

Nov 2015 - Jena School of Microbial Communication Conference travel grant

Oct 2015 - EMBL Advanced Training Centre Corporate Partnership Programme Fellowship

Mar 2015 - Student travel allowance. Annual Conference 2015 of the Association for General and Applied Microbiology ***(***VAAM***)***

May 2014 - Jena School of Microbial Communication Conference travel grant

Mar 2014 - BacFoodNet COST Action FA1202 (Short lab visit grant)

Apr 2013 - Jena School of Microbial Communication fellowship for doctoral research (2013-2016)

June 2010-The Vikrant Khanvilkar Memorial Prize for the highest score in B.Sc.Microbiology

ACTIVITIES AND SCIENTIFIC OUTREACH

1. Responsible for organization of the scientific program and public relations of the 5th International Student Conference on Microbial Communication – MiCom 2015 held in Jena in April 2015.

2. Co-ordinator of Biomosaic 2009, an Intercollegiate Event at Department of Microbiology, Wilson College.

3. Responsible for logistical and scientific organization of ADNIKA: A nature conservation exposition held in Mumbai in September 2008 in Wilson College, Mumbai. (Attended by 10,000 people).

4. Editor of FOOTPRINT, monthly newsletter of Wilson College Nature Club (2007-2009).

Declaration of Independent Assignment

I declare in accordance with the conferral of the degree of doctor from the Faculty of Biology and Pharmacy of the Friedrich-Schiller-University of Jena that the submitted thesis was written only with the assistance of the literature cited in the text.

People who assisted in experiments, data analysis and writing of the manuscripts are listed as co-authors of the respective manuscripts.

A consultant for doctorate theses did not assist me.

The thesis has not been previously submitted elsewhere, whether to the Friedrich-Schiller-University of Jena or to any other university.

Jena, 28th October, 2016 Eisha Mhatre

Eisha Mhatre